Investigation of sorption properties of carbon nanomaterials using packed columns and inverse liquid chromatography

Dissertation

zur Erlangung des akademischen Grades eines
Doktors der Naturwissenschaften
– Dr. rer. nat. –

vorgelegt von

Florian Metzelder

geboren in Essen

Lehrstuhl für Instrumentelle Analytische Chemie
der
Universität Duisburg-Essen

2018

Die vorliegende Arbeit wurde im Zeitraum von April 2014 bis April 2018 im Arbeitskreis von Prof. Dr. Torsten C. Schmidt am Institut für Instrumentelle Analytische Chemie der Universität Duisburg-Essen durchgeführt.

Tag der Disputation: 29.8.18

Gutachter:	Prof. Dr. Torsten C. Schmidt
	Prof. Dr. Stefan Panglisch
	Prof. Dr. Eckhard Worch
Vorsitzender:	Prof. Dr. Stephan Schulz

Danksagung

Mein besonderer Dank gilt Herrn Prof. Dr. Torsten C. Schmidt für die Möglichkeit diese Arbeit anzufertigen und die hervorragende Betreuung der Arbeit. Er gab mir die Möglichkeit meine eigenen Ideen umzusetzen und stand mir aber selbstverständlich bei Bedarf und Problemen immer mit Rat und Tat zur Seite. Des Weiteren möchte ich auch Herrn Prof. Dr. Stefan Panglisch für die Übernahme des Zweitgutachtens dieser Arbeit danken.

Ausdrücklich möchte ich mich bei Dr. Thorsten Hüffer bedanken, der nach der Betreuung meiner Master-Arbeit auch während der Promotion stehts zum Austausch zur Verfügung stand. Der mehrwöchige Forschungsaufenthalt in Wien, in seiner derzeitigen Arbeitsgruppe (Department für Geowissenschaften von Herrn Prof. Dr. Thilo Hofmann), war so eine großartige Gelegenheit das Wissen aus meiner Arbeit mit seiner Arbeit zu kombinieren. In meiner Zeit dort habe ich sehr willkommen gefühlt und die Zusammenarbeit mit ihm und allen dortigen Mitarbeitern sehr genossen. Dank gebührt an dieser Stelle auch Herrn Titus Breski, Herrn Matin Funck und Herrn Julios A. Kontchou, die meine Arbeit durch Praktika und Abschlussarbeiten unterstützt haben und deren Betreuung ich übernehmen durfte. Sie alle haben Beiträge zu dieser Arbeit geleistet, die wichtig für den Fortschritt waren.

Den aktuellen und ebenso ehemaligen Mitarbeitern des Lehrstuhls für Instrumentelle Analytische Chemie an der Universität Duisburg-Essen möchte ich für die produktive und sich gegenseitig unterstützende Zusammenarbeit danken. Außerhalb der Arbeitszeit, konnte man aber auch gemeinsam Spaß haben (AOP-Ausflüge, Feuerzangenbowle, …), die eine gute Abwechslung zum Arbeitsalltag dargestellt haben.

Einen besonderen Dank gebührt an dieser Stelle auch der Prof. Werdelmann-Stiftung, die meinen Antrag auf Förderung meines Promotionsvorhabens bewilligte, mich 3 ½ Jahre unterstützte und so die finanzielle Unterstützung für diese Arbeit bereitstellte. So war auch der mehrwöchige Aufenthalt im Ausland möglich, der es mir erlaubt hat, viele neue Eindrücke abseits des gewohnten Umfelds zu gewinnen.

Abschließend möchte ich natürlich und ganz besonders meiner Familie und Freunden und natürlich Laura danken, die mich über den gesamten Zeitraum unterstützt und mir in schwierigen / anstrengenden Phasen der Arbeit beigestanden haben.

Summary

Sorption studies on carbon-based materials and carbon-based nanomaterials (CNMs) like multiwalled carbon nanotubes (MWCNTs) are typically conducted using batch experiments. This experimental approach is simple to perform and gives reliable results for most sorbates. However, weakly sorbing compounds may be challenging due to a limited sorbent to solution ratio. Here, column chromatography using sorbent packed columns for the determination of sorption data like distribution coefficients (K_d) can be a promising complementary approach offering significantly higher sorbent to solution ratios enabling the analysis of weakly sorbing compounds. This approach was already used for sorption studies on soils. Mandatory for this experimental approach is a non-retarded tracer, showing no interaction with the sorbent material as this is necessary as reference point for the calculation of K_d values. Furthermore, reversible sorption using pulse injection of the investigated sorbates is mandatory as otherwise no sorption data could be calculated. To this end, this thesis aims at the investigation of the suitability of column chromatography for sorption studies on CNMs and especially MWCNTs for weakly sorbing compounds.

Adaptation and modification of a method from literature originally developed for soil materials allowed the reproducible packing of stable columns. Main characteristics of packed columns like porosity and bulk density varied by less than 3 % relative standard deviation. Heavy water (D_2O) could be identified as only suitable non-retarded tracer after typically used tracers like inorganic anions (e.g. nitrite) showed significant sorption depending on applied eluent conditions regarding ionic strength. The influence of a broad range of environmental conditions (pH, ionic strength, and temperature) was successfully studied on sorption of inorganic compounds (initially expected to be useful non-retarded tracers) and organic compounds to MWCNTs. Heterocyclic organic compounds like pyrazole were hardly studied in literature and weak sorption was expected from prediction models. It could be shown that environmental conditions can strongly influence sorption. Sorption reduced with increasing temperature indicating an exothermic process and the contribution of H-bonding to overall sorption. Ionic strength strongly affected sorption of inorganic anions while the effect on organic sorbates was lower. Sorption of for example iodide was reduced by 90 % or completely suppressed for bromide and nitrite when increasing NaCl concentration from 1 to 100 mM. A key factor in sorption of inorganic and organic sorbates was the pH value as it was previously shown in literature for selected compounds using batch experiments. Electrostatic attraction of negatively charged inorganic anions to the oppositely charged

sorbent surface at pH 3 increased sorption about factor ten compared to electrostatic repulsion conditions at pH 9. For ionizable organic compounds of this study (e.g. pyridine or imidazole) electrostatic repulsion was observed at pH 3 due to the similar positive charges of sorbent and sorbate reducing sorption by 80 % compared to pH 9 where the sorbates were not charged. Therefore, electrostatic interactions can increase or reduce, but not prevent sorption. Other sorbent materials than MWCNTs like functionalized MWCNTs, graphene, graphite, and activated carbon could also be studied and compared regarding their sorption properties using the developed column chromatography method allowing the comparison of sorbent materials and effects of for example the surface modification of MWCNTs comparable to batch experiments with strongly reduced sorbent demand.

Consequently, this thesis demonstrates that column chromatography is suitable as complementary technique in sorption studies for carbon-based materials and nanomaterials to study sorption of weakly sorbing compounds and the influence of environmental conditions on their sorption as well as the comparison of different sorbent materials. Relationships and trends regarding the influence of environmental conditions or material modifications observed using batch experiments could also be confirmed using column chromatography and extended to other sorbates. Using column chromatography, time and sorbent material demand for isotherm determination could be reduced and the automation potential increased showing the benefits of this methodology compared to batch experiments. In future, column chromatography and its benefits can be used for example in studies using plastic materials as sorbent material investigating the influence of these materials on sorption in soils and the aqueous environment.

Zusammenfassung

Untersuchung der Sorptionseigenschaften von Kohlenstoffnanomaterialen mittels gepackter Säulen und inverser Flüssigkeitschromatographie

Sorptionsuntersuchungen an kohlenstoffbasierten Materialien sowie an kohlenstoffbasierten Nanomaterialien (CNMs) wie mehrwandige Kohlenstoffnanoröhren (MWCNTs) werden typischerweise in Batchversuchen durchgeführt. Dieser experimentelle Ansatz ist einfach durchführbar und es können verlässliche Ergebnisse für viele Sorbate erzielt werden. Bei diesem experimentellen Ansatz können schwach sorbierende Verbindungen eine Herausforderung darstellen, da das Sorbens zu Lösungsverhältnis begrenzt ist. In diesen Fällen kann die Säulenchromatographie bzw. inverse Flüssigkeitschromatographie einen ergänzenden Ansatz darstellen, bei der mit dem zu untersuchenden Sorbens gepackte Säulen für die Bestimmung von Sorptionsdaten wie Verteilungskoeffizienten (K_d) genutzt werden. Durch deutlich höhere Sorbens zu Lösungsverhältnisse können so auch schwach sorbierende Verbindungen untersucht werden, was für Sorptionsuntersuchungen an Böden bereits genutzt wurde. Grundvoraussetzung ist für diesen experimentellen Ansatz ein nicht-sorbierender Tracer, für den keine Sorption am zu untersuchenden Sorbensmaterial beobachtet wird und als Referenzpunkt für die Berechnung von K_d Werten herangezogen wird. Des Weiteren ist eine reversible Sorption des Sorbates am Sorbens eine Voraussetzung, wenn ein Puls des zu untersuchenden Sorbates in die Säule injiziert wird, da sonst keine Sorptionsdaten berechnet werden können. Deshalb ist das Ziel dieser Arbeit die Säulenchromatographie auf ihre Anwendbarkeit für Sorptionsuntersuchungen an CNMs und im Besonderen MWCNTs für schwach sorbierende Verbindungen zu untersuchen.

Eine Methode aus der Literatur, die ursprünglich für Bodenmaterialien und zum Packen stabiler Säulen erfolgreich eingesetzt wurde, wurde in dieser Arbeit adaptiert und modifiziert. Wichtige Charakteristika der mit der modifizierten Methode gepackten Säulen wie Porosität und Schüttdichte hatten eine Standardabweichung von weniger als 3 %, was eine gute Reproduzierbarkeit der Packmethode aufzeigt. Als nicht-sorbierender Tracer wurde schweres Wasser (D_2O) identifiziert, nachdem andere typischerweise in der Literatur genutzte Tracer wie Nitrit je nach vorliegenden Umweltbedingungen eine deutliche Sorption an MWCNTs aufwiesen. Heterozyklische organische Verbindungen wie Pyrazol wurden bisher wenig auf ihre Sorption an CNMs bzw. MWCNTs untersucht, was auch an einer schwachen zu erwartenden Sorption liegen kann. Die Umweltbedingungen (pH, Ionenstärke, Temperatur) beeinflussten die Sorption von anorganischen und organischen Verbindungen an MWCNTs

stark. Die Sorption verringerte sich mit steigender Temperatur, was auf einen exothermen Prozess und die Beteiligung von Wasserstoffbrücken hindeutete. Die Ionenstärke beeinflusste die Sorption anorganischer Verbindungen stark, während der Einfluss bei organischen Verbindungen geringer war. Die Sorption von Iodid wurde um 90 % reduziert oder für Bromid und Nitrit komplett unterdrückt, wenn die Konzentration von NaCl im Eluenten von 1 auf 100 mM erhöht wurde. Ein wichtiger Faktor für die Sorption anorganischer und organischer Verbindungen war der pH-Wert, wie es in Batchversuchen in der Literatur für bestimmte Verbindungen bereits gezeigt wurde. Elektrostatische Anziehung von anorganischen Anionen zur gegensätzlich geladenen Oberfläche des Sorbens bei pH 3 erhöhte die Sorption um eine Größenordnung im Vergleich zu elektrostatischen Abstoßung bei pH 9. Für ionisierbare organische Verbindungen (z.B. Pyridin oder Imidazol) wurde durch elektrostatische Abstoßung bei pH 3 durch gleiche Ladung von Sorbat und Sorbens die Sorption um 80 % im Vergleich zu pH 9, bei dem die Sorbate ungeladen vorlagen, reduziert. Somit können elektrostatische Wechselwirkungen die Sorption verstärken oder verringern aber im untersuchten Bereich nicht komplett unterdrücken. Andere Sorbentien wie funktionalisierte MWCNTs, Graphen, Graphit oder Aktivkohle können ebenfalls mit der erarbeiteten Methode untersucht und hinsichtlich ihrer Sorptionseigenschaften verglichen werden. So konnte zum Beispiel der Effekt einer Oberflächenmodifikation von MWCNTs mit deutlich verringertem Sorbensbedarf aufgezeigt und vergleichbare Ergebnisse zu Ergebnissen aus Batchversuchen erzielt werden.

Zusammenfassend konnte durch diese Arbeit gezeigt werden, dass die Säulenchromatographie als ergänzender Ansatz zu Batchversuchen für Sorptionsuntersuchungen auch für kohlenstoffbasierte Materialien und CNMs bezüglich schwach sorbierender Verbindungen einsetzbar ist, der Einfluss von Umweltbedingungen auf die Sorption aufgezeigt werden kann und der Vergleich von kohlenstoffbasierten Sorbentien möglich ist. Zusammenhänge und Trends bezüglich des Einflusses von Umweltbedingungen oder Veränderung der Sorbensoberfläche aus Batchversuchen in der Literatur konnten auch mit der Säulenchromatographie bestätigt und um weitere, bisher wenig bis kaum untersuchte Sorbate erweitert werden. Der Zeitaufwand und Sorbensbedarf zur Bestimmung von Sorptionsisothermen können durch die Säulenchromatographie reduziert werden und auch die Automatisierbarkeit erhöht werden, was die Vorteile dieses experimentellen Ansatzes im Vergleich zu Batchversuchen aufzeigt. In der Zukunft können diese Vorteile z. B. in Sorptionsuntersuchungen an Plastikmaterialien als Sorbens genutzt und der Einfluss dieser Materialien auf die Sorption in Böden und der aquatischen Umwelt untersucht werden.

Table of contents

Chapter 1 - General Introduction

1.1 Carbon-based nanomaterials (CNMs)

1.1.1 General information

Carbon-based nanomaterials (CNMs) are a diverse class of materials that can be subdivided in materials of natural or anthropogenic / engineered origin. Natural materials may include soot particles from natural fires, but soot may also originate from anthropogenic sources like combustion processes. Engineered materials include for example carbon nano diamonds, carbon onions, graphene, graphite, fullerenes (C_{60}) and carbon nanotubes (CNTs) (figure 1.1). CNTs may be the most studied and applied material of this class. CNTs occur in two main forms: singlewalled carbon nanotubes (SWCNTs) consisting of a single cylindrically rolled graphene layer (figure 1.1 f) and multiwalled carbon nanotubes (MWCNTs) consisting of several rolled layers arranged concentrically around each other (figure 1.1 g).

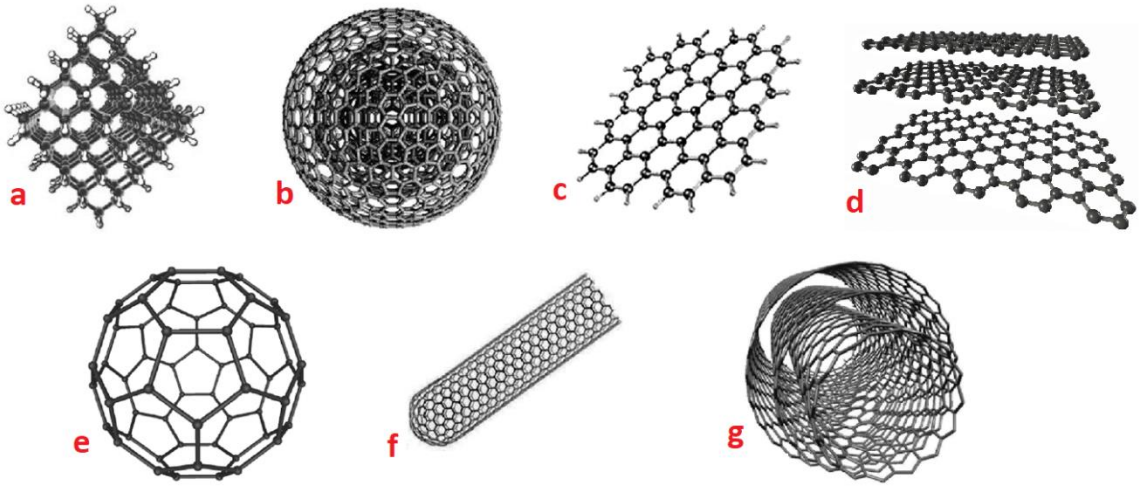

Figure 1.1: Schematic representation of different carbon nanomaterials (CNMs). a: nano diamond; b: carbon onion; c: graphene; d: graphite; e: fullerene (C60); f: singlewalled carbon nanotube (SWCNT); g: multiwalled carbon nanotube (MWCNT) (adapted from literature[1] with exception of d, which is from another reference[2]).

1.1.2 Production of CNTs

Since the first occurrence of CNTs in an arc discharge process in 1991,[3] different production processes were developed yielding CNTs with different characteristics. These processes are for example modifications of the arc discharge process,[4, 5] flame synthesis,[6, 7] electrolysis,[8] synthesis from bulk polymer structures,[9] laser ablation,[10] synthesis in liquid organic phases[11] or chemical vapor deposition (CVD).[12-15]

Production of only small batches of CNTs connected with high costs and a non-constant product quality were characteristics of early CVD processes.[16] This limited applications based on CNTs and cheaper alternatives like carbon black were used. Carbon black offers relatively similar properties and a constant quality with lesser costs.[17] After the scale up of production processes for CNTs, costs were reduced and a more constant product quality could be achieved.[17] Bayer Technology Services was one of the first companies investing in upscaled processes and placed their product under the brand Baytubes® on the market in 2007.[17] The aim was an annual production of up to 200 tons per year. Demand of CNTs did not increase as expected and consequently, Bayer sold their plant in 2013.[18] Despite this, there are today still other manufacturers available that produce CNTs in large amounts and enable an application of those as part of products. CNT suppliers may use different production, purification and functionalization processes with the consequence that CNTs may have different characteristics regarding e.g. purity, type, length, diameter, and functionalization. With known and constant quality of CNTs, potential applications of CNTs in products were investigated in different disciplines of science due to their unique properties including, among others, optical activity, electrical conductivity, and an enhanced mechanical strength.

1.1.3 Applications, products and environmental implications of CNTs

Trying to take advantage of these properties, CNTs were tested for example in the fields of material science, physics / electronics, medicine, and chemistry. In material science they were tested as additive to polymers, which may represent one of the most important application for CNTs. The addition of CNTs results in an increased electrical conductivity[17] and enhanced mechanical properties.[19] Stiffness and strength of polymers increased with the amount of CNTs added while the electrical resistivity decreased.[20] In physics and electronics, CNTs and also other CNMs were tested as sensors,[21] storage materials[22] and field effect transistors.[23] In medicine, CNTs were used as drug delivery vehicle in cancer treatment.[24] Tumor growth was reduced in *in-vivo* studies in mice and, according to the author, a transition to clinical medicine is in principal possible.[24] The utilization of CNTs as drug delivery device uses the sorption properties of CNTs, which are the primary focus in chemistry. They were used for the removal of NOM from water,[25] solid-phase extraction of organic compounds from water[26-29] and inorganic compounds like metals from different matrices.[30-32] A high sorption capacity and also quantitative desorption is a prerequisite for these applications. In comparison to other typical sorbent phases, CNTs have enhanced sorption characteristics for certain analytes.[26]

Arising from these small and laboratory scale applications in science and connected with more constant material characteristics and properties, also larger scale products containing CNTs are placed on the market. For example, the Nanocomp Technologies, Inc. (Merrimack, New Hampshire, USA) produces sheets, tape, yarn or dispersed additives under the brand Miralon®.[33] These materials should potentially be used in heaters, conductors, smart textiles, composites, cable shielding, filtration, and environmental protection in terms of e.g. corrosion.[33] Advantages are the reduced weight, high strength, as well as increased chemical and environmental resistance.[33] Furthermore, CNTs were added to epoxy composites, which are a building block of surfboards, skis, and hockey sticks to enhance their properties.[20]

Large scale production and applications in industrial products rather than small scale applications in science make a release of CNTs to the environment more likely.[1, 34] The release of CNTs from these products is possible in all phases of its lifecycle (manufacturing, processing, use, disposal, and recycling).[35] Precise data on annual production and release of CNTs and other CNMs to the environment are not available and are often estimated using models.[36-38] Values are estimated by models and strongly deviate from each other. Consequently, a direct measurement of CNM concentrations in the environment would ensure more precise data. First measurement techniques / protocols to determine CNTs in the environment were developed in recent years. Petersen *et al.*[39] summarized in a review already developed techniques and concluded that most methods involve uncommon equipment, uncommon expertise and are often vulnerable to modifications on CNTs due to environmental influences. Modifications on CNMs occurring in the environment may include changes in the colloidal stability due to pH,[40] ion strength[40] or natural organic matter (NOM).[41, 42] Furthermore, more standardization, alternative extraction techniques, and reference samples to compare different techniques are required.[39] As CNTs exhibit strong sorption properties, an interaction with various compounds after release to the environment is highly likely. Thus, CNTs may also influence the transport of compounds including pollutants in the environment by sorption and desorption.[43, 44] On the one hand, the bioavailability may be reduced by permanent sorption to them or, on the other hand, the concentration would be even increased if sorption was only temporary leading to peaking concentrations at certain locations and times. Consequently, a precise knowledge about sorption and desorption processes is necessary for understanding and accessing of the environmental impact and behavior of CNTs.

1.2 Theory of sorption and desorption

In general, sorption describes the distribution of a compound, the so-called sorbate between two phases,[45] while desorption describes the reverse process. Sorption can be further divided in two separate processes. Firstly, the *ad*sorption, describing the accumulation of a compound, also called sorbate, at the surface of a solid phase, also called sorbent, from a liquid or gaseous phase.[45] Secondly, the *ab*sorption, describing the penetration of the sorbate from one phase into a three-dimensional matrix of the second phase.[45] This matrix may be liquid, gaseous or even solid like in case of some polymers, where absorption was shown to be the dominant sorption mode.[46]

At equilibrium conditions, no change in the concentration of the sorbate in the liquid phase ($c_{w,eq}$) and the sorbed concentration in the second phase ($c_{s,eq}$) can be determined as the sorption and desorption rates are the same. The ratio of both concentrations is defined as the distribution coefficient (K_d) in equation 1.1.[45]

$$K_d = c_{s,eq} / c_{w,eq} \quad (1.1)$$

Sorption isotherms can be derived from equilibrium sorption data. In the easiest case, sorption is linear and K_d is independent of the concentration range investigated. This observation is commonly made in case of two liquid phases as in case of liquid extraction of organic compounds from aqueous solutions using organic solvents.

In natural systems or technical processes utilizing sorption like for example drinking water treatment using activated carbon as sorbent, linear sorption over a broad concentration range is less common and nonlinear sorption is often observed.[47] If the observed concentration range is sufficiently small, also linear sorption may be observed. K_d is not constant in case of nonlinear sorption when comparing different concentrations and sorption cannot be described using a single coefficient like K_d. Consequently, other models are necessary to describe nonlinear sorption isotherms. Different models were developed in literature, of which the most prominent for sorption in aqueous systems will briefly be discussed in the following paragraphs. One of the most frequently applied sorption models is the Freundlich model (equation 1.2). It is an empirically derived relationship, which assumes various types of sorption sites with different sorption energies, but does not include a maximum loading or limited sorption capacity.[45] Multiple layers of the sorbate may be formed on the sorbate surface.

$$c_{s,eq} = K_f \times c_{w,eq}^{n} \quad (1.2)$$

K_f represents the Freundlich coefficient while n is the Freundlich exponent. Three different sorption isotherms can be distinguished and described with this model (figure 1.2).

Firstly, for n = 1, the sorption isotherm becomes linear and K_f equals K_d and the energy distribution of sorption sites diminishes (figure 1.2a).[45] Secondly, for n > 1, sorption energy increases with increasing sorbate concentration and the isotherm gets a convex shape (figure 1.2b).[45] Finally, for n < 1, sorption energy decreases with increasing concentration of the sorbate and the isotherm is characterized by a concave shape (figure 1.2c).[45]

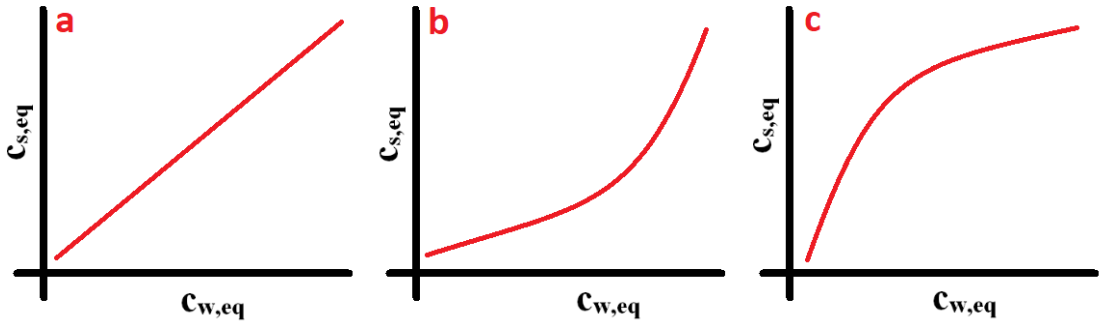

Figure 1.2: Schematic representation of a linear isotherm with Freundlich exponent (n) = 1 (a), a convex isotherm with n > 1 (b) and a concave isotherm with n < 1 (c).

The Langmuir model (equation 1.3) assumes, contrary to the Freundlich model, a maximum loading of the surface i.e. a limited sorption capacity by the formation of a monolayer on the sorbent surface.[45] Consequently, $c_{s,eq}$ cannot increase indefinitely. Furthermore, all sorption sites on the surface are energetically homogenous.[45]

$$c_{s,eq} = (Q_{max} \times K_L \times c_{w,eq}) / (1 + K_L \times c_{w,eq}) \quad (1.3)$$

K_L represents the Langmuir affinity coefficient while Q_{max} is the maximum sorption capacity. As the capacity is also a function of the size of the sorbate, Q_{max} may differ strongly between different sorbates.[45]

Besides these sorption models also many other models are used in literature for different sorbent and sorbate combinations to describe the determined sorption isotherms. This involves natural sorbents like biochar,[48] soils,[49] or sediments[50] as well as engineered sorbents like activated carbon[51, 52] or CNMs[43, 52-55] with sorbates from different compound classes.

1.3 Sorption to CNMs

Sorption studies to investigate the sorption properties of CNMs are frequently done in literature. Different types of CNMs are applied using various sorbates. Sorption studies were done with sorbates having different characteristics like polarity or size. Data are mostly

available for organic compounds like polycyclic aromatic hydrocarbons (PAHs), polychlorinated biphenyls (PCBs), phenols, aromatic amines, or differently substituted aliphatic compounds (selected examples from literature in table 1.1). However, sorption data for more polar organic compounds like small heterocyclic compounds[56, 57] (e.g. pyridine, pyrazole) and also inorganic compounds[58, 59] are only hardly available in literature so that there are certain gaps in the data availability concerning the sorbate diversity.

Nonlinear sorption is commonly found for CNMs in literature.[52, 55, 60-71] Only in very rare cases, like for sorption of very low concentrations of PAHs to MWCNTs in a relatively small concentration range, linear sorption was observed, which also became nonlinear when extending the concentration range to higher concentrations.[72] The linearity may in this case be related to the occupation of high-energy sorption sites exhibiting similar sorption energies at low concentrations while at higher concentrations also less favorable sorption sites yielding a lower sorption energy are used.[53] High-energy sorption sites are for example surface defects,[73] functional groups,[74] and locations in gaps or caves of CNM bundles.[75] Furthermore, condensation on the sorbent surface or in capillaries may be possible.[76-78] Different sorption models were used to fit the experimental data, all yielding good results. Sorption models include the already described Langmuir[61] and Freundlich,[60] but also other models like the Polyani potential theory,[55, 66] dual-mode models[72] or the Brunauer-Emmett-Teller (BET) model[79] were used. Consequently, application of a single sorption coefficient like K_d assuming a linear sorption behavior to describe or predict sorption would result in significant deviations as K_d can change strongly with the investigated concentration range.

Table 1.1: Summary of different sorbate and sorbent combinations used in literature to study sorption to CNMs.

sorbate	sorbent	reference
phenol, naphthylamine, naphthol	MWCNTs	[61]
naphthalene, phenanthrene, lindane, atrazine	MWCNTs	[80]
perchlorate	MWCNTs	[58]
different organophosphate esters	MWCNTs	[63]
17 different PCB congeners	MWCNTs	[64]
phenol and aniline derivates with chloro- or nitroso functional groups	MWCNTs	[55]
aliphatic (e.g. alcohols, ethers) and aromatic compounds (phenol derivates, PAHs) with various polarities	MWCNTs	[60]
phenanthrene	SWCNTs	[76]
atrazine	SWCNTs	[65]
PAHs, benzene derivates, alkene derivates, atrazine	SWCNTs	[52]
ibuprofen, triclosan	SWCNTs	[66]
different phthalates	SWCNTs	[67]
PAHs	fullerenes	[43]
bisphenol A, 17α-ethinyl estradiol	fullerenes	[68]
naphthalene and benzene derivates	graphite	[81]
tetracycline	graphite	[69]
phenanthrene, biphenyl	graphene nanosheets	[70]
sulfamethoxazole, ciprofloxacin	graphene oxide	[71]

Sorption to the surface of CNTs and CNMs in general is related to different sorption mechanisms. Initially, only non-specific interactions like van-der-Waals (vdW) interactions were thought to be the dominant factor for sorption.[82] This assumption could not be supported as the prediction of K_d values with hydrophobic parameters like the octanol / water partition coefficient (K_{OW}) or the hexadecane / water partition coefficients (K_{HW}) was not possible and no general correlation could be found.[53, 83] Consequently, other interactions have to contribute to the overall sorption process. This includes, first, specific interactions between aromatic systems located on the CNT surface and sorbates containing C-C double bonds or aromatic

systems, second, hydrogen bonds between functional groups of sorbates as well as those located on the CNT surface, or third, electrostatic interactions between charged sorbates and the charged sorbent surface.[53, 54, 84]

Properties of the sorbent can strongly influence sorption. CNMs tend to occur in aggregates, which may also influence sorption. The external surface of aggregates is always available for sorption without size restrictions related to the sorbate size, while intestinal regions of aggregates may be inaccessible due to size restrictions (figure 1.3). Pores of aggregates may be too small to be reached by sorbates of a certain size. On the one hand, this was shown for SWCNTs with pores in tubes with an outer diameter smaller than 0.85 nm (inner diameter is smaller, but no precise value was mentioned), which were discussed to be too small to be penetrated by naphthalene with a minimal size of 0.75 nm.[85] On the other hand, pores of CNTs with 3 – 5 nm diameter were accessible for large molecules like enzymes.[86] Additionally, pores may be blocked by amorphous carbon, functional groups or residual metal catalyst particles.[87] This may result in inaccessible pores that would normally be large enough for sorbates. Also, properties of the sorbate may influence sorption. For example, sorption of amines and phenols decreased when molecules were mainly present as their charged species.[55] In this case, the pH is the dominant factor that influences both, the speciation of the sorbate and the sorbent. The sorbent surface may change its charge when changing the pH of the solution leading to electrostatic attraction or repulsion between sorbent and sorbate.

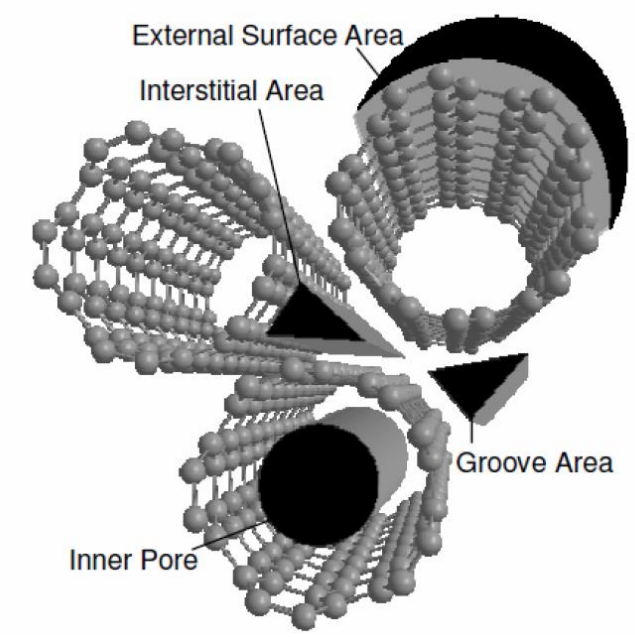

Figure 1.3: Schematic representation of possible sorption sites in or at CNT bundles.[53]

Consequently, the contribution of the different sorption mechanisms to overall sorption depends on characteristics of CNTs (e.g. morphology or functionalization), characteristics of the sorbate (e.g. charges or presence of aromatic systems), and environmental conditions (e.g. temperature or pH). A precise knowledge about interactions between CNTs and sorbates and the contribution of the different mechanisms to overall sorption is necessary to be able to predict sorption. Therefore, sorption studies to investigate these interactions and sorption properties of CNMs are typically performed using batch experiments.[60-62, 64-66, 68, 70, 71, 87]

1.3.1 Batch experiments as classical experimental approach

For the batch approach, a known mass of the sorbent is placed together with a known volume of liquid or gaseous phase in a lockable vessel. This liquid or gaseous phase is spiked with a likewise known initial mass of the sorbate (m_0). The vessel is afterwards incubated at constant temperature and defined matrix conditions regarding pH or ionic strength and continuously mixed till the sorption equilibrium is reached. In case of CNTs, sorption experiments are predominantly done using an aqueous phase with adjusted and known properties regarding pH and ionic strength. After equilibration, both phases need to be separated and the remaining concentration of the sorbate in the aqueous phase in equilibrium is determined ($c_{w,eq}$). Phase separation can be done using centrifugation,[60] sedimentation,[83] filtration,[66] or combinations of these techniques.[88] Using m_0 and $c_{w,eq}$, the concentration of the sorbate in the solid phase ($c_{s,eq}$) can be calculated using a mass balance (equation 1.4).

$$m_0 = m_w + m_s = c_{w,eq} \times V_w + c_{s,eq} \times m_{sorbent} \quad (1.4)$$

m_w and m_s are the mass of the sorbate in the liquid and solid phase in equilibrium, respectively. Those can be calculated from the respective concentration in both phases using the volume of liquid phase (V_w) and the mass of sorbent ($m_{sorbent}$). As $c_{w,eq}$ is determined and m_0 as well as $m_{sorbent}$ are known, $c_{s,eq}$ can be calculated by rearranging equation 1.4. Sorption isotherms are determined using multiple vessels with different initial concentrations of the sorbate keeping the amount of sorbent constant or vice versa. Both approaches are used in literature. Afterwards, different sorption models are used to fit sorption data determined in experiments.

Batch experiments are simple and reliable to perform, which may explain the wide spread use of this methodology in literature. However, they are also accompanied by several drawbacks limiting their applicability. First, the long equilibration time from hours[89] up to

several weeks[72, 83] applied in literature for sorption of organic compounds to CNTs makes experiments time intensive. This especially increases the time expenses to study the influence of environmental conditions on sorption, because each variation of environmental conditions (e.g. pH or ionic strength) will require the complete equilibration time. Here, one can argue that this drawback may be overestimated, as experiments can be performed simultaneously for different conditions. However, too weak or strong sorption leading to inconclusive results due to changed environmental conditions will require the repetition of this experiment and consequently, require the complete equilibration time again. The high time demand of sorption experiments and high number of different organic compounds led to the development of models like polyparameter linear free-energy relationships (ppLFERs) to predict K_d values,[60, 90, 91] but these are only valid for one set of environmental conditions and non-charged sorbate molecules. Thus, they are not useful to predict sorption for changed environmental conditions or charged sorbate speciation like deprotonated phenols or charged amines. Second, for weakly sorbing compounds it may be challenging to obtain reliable sorption data in batch experiments because of the limited sorbent to solution ratio.[92] In this case, $c_{s,eq}$ in equilibrium will be very small so that the difference between the initial concentration (c_0) and $c_{w,eq}$ will be small, which may not be quantifiable or result in large errors as reported in literature.[93, 94] Third, phase separation of very fine materials from the water phase may be a critical step, where techniques like centrifugation, sedimentation or filtration can be insufficient.[72] Finally, the manual workload is high. Weighing of sorbent into various vessels, spiking of those with the sorbate and final phase separation after equilibration are steps that are mainly done manually, which makes the whole procedure time intensive.

1.3.2 Column experiments as alternative experimental approach

As alternative to batch experiments, dynamic column experiments can be used to study sorption. For this experimental approach, the sorbent material is packed in a column and the column is implemented in a liquid chromatography system. Column packing can be done using different techniques, but the procedure must yield columns that are homogenous, stable and reproducible. Dry packing followed by the direct execution of sorption experiments[95], dry packing followed by compression with either a manual compression[96] or using a flow of liquid phase[92, 97, 98] or pumping the sorbent suspended in a liquid[99] were already described in literature. Column packing without additional compression can result in broad peaks with shifting retention times for the tracer, which is the consequence of void volume at the column

inlet.[100] Void volume may be generated from slow compression of the sorbent material[100] also resulting in changing retention time and changes in packing density[101], which can be better prevented using a preliminary compression in a liquid stream during packing[92, 100, 102]. Applying this methodology, a precolumn is used as sorbent reservoir during packing ensuring that the column used for sorption experiments is filled with sorbent material and no further compression will occur during sorption experiments. This results in significantly sharper peaks and stable retention times for hundreds of injections.[92, 100, 102]

An important prerequisite, despite the reproducible packing of columns, is a non-retarded tracer. The tracer should be transported through the column without any or only negligible interactions with the sorbent material. The peak of the tracer should be symmetrical and stable in retention time.[100] In literature different types of tracers were used for different types of sorbents ranging from inorganic anions[103, 104] to organic compounds[105, 106] (examples given in table 1.2). Not every tracer is suitable for every sorbent. The application of charged tracers can result in pore exclusion due to electrostatic repulsion or electrostatic attraction to the sorbent leading to retention inside the column.[100] Non-charged tracers may penetrate all pores, but undergo vdW or specific interactions like H-bonds. The ideal tracer in water-based systems would be for example deuterated or tritiated water,[107] but it is not detectable with commonly applied UV-detectors and needs detectors like a refractive index detector. Consequently, the tracer selection must be done with care and investigations on their suitability for a certain sorbent must be performed in preliminary experiments. Additionally, the tracer selection must be adjusted to the instrumental equipment available in the laboratory.

Table 1.2: Tracers applied in column chromatography for determination of sorption data.

tracer	sorbent
thiourea	soil[92, 98, 102], minerals[97, 105], soot[106]
nitrite	soil[103]
nitrate	soil[108], minerals[99]
bromide	soil[104], minerals[99]
tritiated water	soil[93, 107]
fluorescein	soil[109]
sulfaflavine	minerals[99]

Advantages of the column-based method compared to batch experiments are a higher sorbent to solution ratio that enables the analysis of weakly sorbing compounds without the

need of large amounts of sorbent and studies on generally weakly sorbing sorbent materials. This is especially interesting for expensive sorbents or those with limited availability. Furthermore, environmental conditions can be changed much easier than in batch experiments by changing the eluent or regulating the column temperature using a column thermostat. The automation potential is higher compared to batch experiments as measurements can be done using an autosampler. No manual steps are necessary after column packing and preparation of sorbate solutions. Phase separation as critical step in batch experiments can be excluded in this case, as the sorbent should stay fixed in the column using sieves at the column outlet having pores smaller than the sorbent particle size.

However, column experiments may also have disadvantages. Column clogging and too strong sorption can be serious problems, which lead to very high backpressure or cause long retention times and deterioration of the signal by peak broadening, respectively. Concomitant, backpressure and sorption can both be reduced by the dilution of the sorbent material with inert material like quartz[92, 102] or silicium carbide[95], which should not show any interaction with the sorbate and tracer, which has to be checked in additional experiments. Dilution with inert material to avoid clogging should be preferred compared to sieving out smaller particles, which are a potential reason for clogging. Sieving out smaller particles may result, especially in case soils, in changed properties of the soil as for example the carbon content is heterogeneously distributed along different particle sizes.[107] An important disadvantage, potentially preventing the applicability of column experiments, is sorption hysteresis. Sorption hysteresis describes the incomplete desorption of a sorbate from the sorbent. Using a Dirac input (i.e. injection of a sorbate pulse instead of a continuous sorbate input) desorption is a prerequisite in column experiments, because otherwise no signal can be recorded. If sorbate molecules remain sorbed to the surface, changed interactions between the sorbent surface and sorbate molecules will be the consequence in consecutive measurements and this will result in potentially misleading sorption data. For the measurement of breakthrough curves, sorption hysteresis is less problematic, but each column could only be used for one compound and one investigated concentration. For further consecutive measurements, the sorbent surface would not be pristine as sorbate molecules remain sorbed on the surface. Incomplete desorption from CNMs has already been shown for some organic compounds in batch experiments[110-112] indicated by differences between the sorption and desorption isotherm.

For sorption experiments, the column is equilibrated with an aqueous phase of desired pH and ionic strength and heated to a certain temperature. Injection of the sorbate in the

stream of the aqueous phase can be done using an injection loop valve. Retention of the sorbate in the column can be monitored using different detection techniques like a UV detector. Calculation of sorption data represented by K_d values is done by relating the retention time of the sorbate inside the column (t_R) in the first step to that of the non-retarded tracer (t_0) to determine the retardation factor (R) according to equation 1.5.

$$R = (t_R - t') / (t_0 - t') \quad (1.5)$$

t´ is the time of sorbate and tracer inside the system without column installed in the system. There are different ways in literature to determine the retention time of an eluting peak. First, the definition of the retention time using the apex point of the peak, which can be easily derived from the chromatogram without further calculations. Second, the calculation of the retention time can be done using the complete peak based on the first moment.[113] For this approach, the peak data are weighted and the retention time gives the center of gravity. The tailing of the peak has to be recorded completely, but in case of long tailing this may not be possible and a significant amount lacks and is not recorded, because the quantification limit of the detector may be reached.[100] Consequently, the peak limits will not be determined correctly, which will affect the determined retention time.[100] The first-moment approach is also affected by baseline drift, incomplete resolution and insufficient sampling frequency.[100] All these factors result in a potentially high uncertainty associated with this method.[100] Finally, the calculation of the retention time using the half-mass point is possible. At this point, the peak area is divided into two equally sized parts and accounts for non-equilibrium sorption effects.[114] This approach is less frequently used in literature, but it offers advantages. It is less affected by baseline drift and variations in peak limits as the first moment approach.[100] This is especially important in case of very long measurements. The signal drift may influence results as shown by Bi *et al.*[100]. For ideal and completely symmetrical peaks, all three methods will give the same results. The more the peak shape deviates from the ideal Gaussian shape, the larger the differences will become.

The retardation factor from equation 1.5 can be transferred to a K_d value using equation 1.6. θ is the porosity and ρ_b the bulk density of the column. These are determined using the non-retarded tracer and repeated measurements with and without column for column validation. During sorption experiments, the tracer is measured repeatedly to monitor column stability.

$$R = 1 + \rho_b/\theta \times K_d \quad (1.6)$$

K_d can only be defined as equilibrium coefficient, if sorption is at or at least close to equilibrium, which may be difficult to be achieved in column experiments.[100] Equilibration

time in column experiments can be reduced by particle grinding, as the particle size is important.[94] Model calculations showed that a decrease in particle size of factor ten reduces the equilibration time by factor 100.[94] However, changes to the native material like increased surface area might occur, that must be kept in mind. Also properties of the sorbate influence the equilibration time as the more hydrophobic the sorbate, the longer the time to reach sorption equilibrium.[115] Consequently, sorption equilibrium can be achieved faster for polar compounds as indicated by column measurements[100] and batch experiments.[116] Nonequilibrium may include diffusion through intraparticle pores or through matrices of for example natural organic matter.[117] Equilibrium state in column experiments can be determined by performing measurements at least two different flow rates.[100, 118] Reducing the flow rate increases contact time of the sorbate with the sorbent inside the column. If sorption is at or close to equilibrium, determined R and K_d values will show no or only slight dependence on the flow rate. R and K_d will increase with decreasing flow rate, if sorption is not at equilibrium because of the increased contact time.[100] Alternatively, also stopped-flow experiments can be performed completely avoiding flow effects,[119] but this approach is less convenient compared to measurements at different flow rates[100] and needs, depending on the time with stopped-flow, much more measurement time. Additionally, the stopped-flow period must be started with the whole sorbate injection volume inside the column. This requires precise knowledge of dead volumes of the system and its capillaries.

Injecting different concentrations of the sorbate can also give information about sorption linearity as K_d will change in case of nonlinear sorption or stay constant in case of linear sorption. Using the chromatograms also isotherms can be derived from column measurements as it was already done in literature.[95, 99, 120] The approaches applied to derive these isotherms are quite different. For example, the approach presented by Schenzel *et al.*[95] derives isotherms from chromatograms of several injected concentrations. Another approach by Bürgisser *et al.*[99] derives the isotherm from the tail in the chromatogram of one concentration.

The column approach is less frequently used in literature for sorption studies than the batch approach, but has been demonstrated successfully nevertheless. Sorption studies of PAHs[106] and PCBs to soot particles[120] were done, but water with addition of methanol was necessary as sorption to soot was too strong and was extrapolated to pure water conditions. Because of the addition of methanol and extrapolation to pure water conditions, deviations to measurements really using pure water are likely. Additionally, various organic compounds ranging from small polar heterocyclic compounds to larger molecules like toxins or hormones

to soils[92, 95, 96, 98, 102, 104, 105, 121-124] or chlorinated benzenes and PAHs to mineral surfaces[97, 125] were carried out without the addition of methanol. The influence of environmental conditions like temperature and pH on sorption was also investigated and highlighted again the advantage of easily changeable conditions. The comparability of sorption data from batch and column experiments was also evaluated in literature without a general tendency. Well comparable results were reported for sorption of naphthalene to aquifer materials[93] or lead to soils,[126] while deviations were reported for sorption of 1-methylnaphthalene and 1,2-dichlorobenzene to aquifer materials[127] as well as sorption of benzene and dimethyl phthalate to soils.[128] Consequently, the comparability has to be evaluated for new sorbent materials to enable conclusions.

Applications of column chromatography for CNMs like CNTs are hardly found. An application of a column-based method in sorption studies was found in literature,[129] but this was not focused on the determination of K_d values or isotherms, but for the determination of the affinity of PAHs to CNTs using silica particles coated with CNTs.[129] Tetrahydrofuran was used as eluent so that information on the interaction in water based systems cannot be directly deduced from these experiments. Additionally, CNMs were applied in stationary phases, but also in these cases no determination of sorption data was done.[130, 131] Because of the advantages of the column method mentioned previously, column experiments represent a promising complementary approach to well-known batch experiments also for CNMs.

1.4 References

1. Mauter, M. S.; Elimelech, M. Environmental applications of carbon-based nanomaterials. *Environmental Science & Technology* **2008,** 42 (16), 5843-5859.
2. National Infromal Stem Education Network: Scientific Image - Graphite models. http://nisenet.org/catalog/scientific-image-graphite-models (Accessed on 15.11.2017),
3. Iijima, S. Helical microtubules of graphitic carbon. *Nature* **1991,** 354 (6348), 56-58.
4. Iijima, S.; Ichihashi, T. Single-shell carbon nanotubes of 1-nm diameter. *Nature* **1993,** 363 (6430), 603-605.
5. Charinpanitkul, T.; Tanthapanichakoon, W.; Sano, N. Carbon nanostructures synthesized by arc discharge between carbon and iron electrodes in liquid nitrogen. *Current Applied Physics* **2009,** 9 (3), 629-632.
6. Xu, F. S.; Liu, X. F.; Tse, S. D. Synthesis of carbon nanotubes on metal alloy substrates with voltage bias in methane inverse diffusion flames. *Carbon* **2006,** 44 (3), 570-577.
7. Liu, Y. L.; Fu, Q.; Pan, C. X. Synthesis of carbon nanotubes on pulse plated Ni nanocrystalline substrate in ethanol flames. *Carbon* **2005,** 43 (11), 2264-2271.
8. Hsu, W. K.; Hare, J. P.; Terrones, M.; Kroto, H. W.; Walton, D. R. M.; Harris, P. J. F. Condensed-phase nanotubes. *Nature* **1995,** 377 (6551), 687-687.

9. Cho, W. S.; Hamada, E.; Kondo, Y.; Takayanagi, K. Synthesis of carbon nanotubes from bulk polymer. *Applied Physics Letters* **1996,** 69 (2), 278-279.
10. Guo, T.; Nikolaev, P.; Thess, A.; Colbert, D. T.; Smalley, R. E. Catalytic growth of single-walled nanotubes by laser vaporization. *Chemical Physics Letters* **1995,** 243 (1-2), 49-54.
11. Zhang, Y. F.; Gamo, M. N.; Xiao, C. Y.; Ando, T. Liquid phase synthesis of carbon nanotubes. *Physica B-Condensed Matter* **2002,** 323 (1-4), 293-295.
12. Bondi, S. N.; Lackey, W. J.; Johnson, R. W.; Wang, X.; Wang, Z. L. Laser assisted chemical vapor deposition synthesis of carbon nanotubes and their characterization. *Carbon* **2006,** 44 (8), 1393-1403.
13. Li, W. Z.; Xie, S. S.; Qian, L. X.; Chang, B. H.; Zou, B. S.; Zhou, W. Y.; Zhao, R. A.; Wang, G. Large-scale synthesis of aligned carbon nanotubes. *Science* **1996,** 274 (5293), 1701-1703.
14. Rajarao, R.; Bhat, B. R. Large-scale synthesis of high purity carbon nanotubes by novel catalytic route. *Synthesis and Reactivity in Inorganic Metal-Organic and Nano-Metal Chemistry* **2013,** 43 (10), 1418-1422.
15. Wang, Y.; Wei, F.; Luo, G. H.; Yu, H.; Gu, G. S. The large-scale production of carbon nanotubes in a nano-agglomerate fluidized-bed reactor. *Chemical Physics Letters* **2002,** 364 (5-6), 568-572.
16. See, C. H.; Harris, A. T. A review of carbon nanotube synthesis via fluidized-bed chemical vapor deposition. *Industrial & Engineering Chemistry Research* **2007,** 46 (4), 997-1012.
17. Bierdel, M.; Buchholz, S.; Michele, V.; Mleczko, L.; Rudolf, R.; Voetz, M.; Wolf, A. Industrial production of multiwalled carbon nanotubes. *Physica Status Solidi B-Basic solid state physics* **2007,** 244 (11), 3939-3943.
18. Chemistry World. https://www.chemistryworld.com/news/carbon-nanotubes-not-commercially-viable-for-bayer/6154.article (Accessed at 15.11.2017),
19. Cadek, M.; Coleman, J. N.; Ryan, K. P.; Nicolosi, V.; Bister, G.; Fonseca, A.; Nagy, J. B.; Szostak, K.; Beguin, F.; Blau, W. J. Reinforcement of polymers with carbon nanotubes: The role of nanotube surface area. *Nano Letters* **2004,** 4 (2), 353-356.
20. Schmid, M. Tiny tubes with a huge impact. *Kunststoffe International* **2007,** 97 (8), 96-98.
21. Wong, S. S.; Joselevich, E.; Woolley, A. T.; Cheung, C. L.; Lieber, C. M. Covalently functionalized nanotubes as nanometre-sized probes in chemistry and biology. *Nature* **1998,** 394 (6688), 52-55.
22. Ye, Y.; Ahn, C. C.; Witham, C.; Fultz, B.; Liu, J.; Rinzler, A. G.; Colbert, D.; Smith, K. A.; Smalley, R. E. Hydrogen adsorption and cohesive energy of single-walled carbon nanotubes. *Applied Physics Letters* **1999,** 74 (16), 2307-2309.
23. Avouris, P.; Appenzeller, J.; Martel, R.; Wind, S. J. Carbon nanotube electronics. *Proceedings of the Ieee* **2003,** 91 (11), 1772-1784.
24. Liu, Z.; Chen, K.; Davis, C.; Sherlock, S.; Cao, Q. Z.; Chen, X. Y.; Dai, H. J. Drug delivery with carbon nanotubes for in vivo cancer treatment. *Cancer Research* **2008,** 68 (16), 6652-6660.
25. Yang, X. S.; Lee, J.; Yuan, L. X.; Chae, S. R.; Peterson, V. K.; Minett, A. I.; Yin, Y. B.; Harris, A. T. Removal of natural organic matter in water using functionalised carbon nanotube buckypaper. *Carbon* **2013,** 59, 160-166.
26. Cai, Y. Q.; Jiang, G. B.; Liu, J. F.; Zhou, Q. X. Multiwalled carbon nanotubes as a solid-phase extraction adsorbent for the determination of bisphenol a, 4-n-nonylphenol, and 4-tert-octylphenol. *Analytical Chemistry* **2003,** 75 (10), 2517-2521.

27. Cai, Y. Q.; Cai, Y. E.; Mou, S. F.; Lu, Y. Q. Multi-walled carbon nanotubes as a solid-phase extraction adsorbent for the determination of chlorophenols in environmental water samples. *Journal of Chromatography A* **2005,** 1081 (2), 245-247.
28. Fang, G. Z.; He, J. X.; Wang, S. Multiwalled carbon nanotubes as sorbent for on-line coupling of solid-phase extraction to high-performance liquid chromatography for simultaneous determination of 10 sulfonamides in eggs and pork. *Journal of Chromatography A* **2006,** 1127 (1-2), 12-17.
29. Hüffer, T.; Osorio, X. L.; Jochmann, M. A.; Schilling, B.; Schmidt, T. C. Multi-walled carbon nanotubes as sorptive material for solventless in-tube microextraction (ITEX2) - a factorial design study. *Analytical and Bioanalytical Chemistry* **2013,** 405 (26), 8387-8395.
30. Gil, R. A.; Goyanes, S. N.; Polla, G.; Smichowski, P.; Olsina, R. A.; Martinez, L. D. Application of multi-walled carbon nanotubes as substrate for the on-line preconcentration, speciation and determination of vanadium by ETAAS. *Journal of Analytical Atomic Spectrometry* **2007,** 22 (10), 1290-1295.
31. Duran, A.; Tuzen, M.; Soylak, M. Preconcentration of some trace elements via using multiwalled carbon nanotubes as solid phase extraction adsorbent. *Journal of Hazardous materials* **2009,** 169 (1-3), 466-471.
32. Behbahani, M.; Bagheri, A.; Amini, M. M.; Sadeghi, O.; Salarian, M.; Najafi, F.; Taghizadeh, M. Application of multiwalled carbon nanotubes modified by diphenylcarbazide for selective solid phase extraction of ultra traces Cd(II) in water samples and food products. *Food Chemistry* **2013,** 141 (1), 48-53.
33. Nanocomp Technologies Incorporation. http://www.nanocomptech.com/sheet/tape (Accessed on 15.11.2017),
34. Nowack, B.; Bucheli, T. D. Occurrence, behavior and effects of nanoparticles in the environment. *Environmental Pollution* **2007,** 150 (1), 5-22.
35. Petersen, E. J.; Zhang, L. W.; Mattison, N. T.; O'Carroll, D. M.; Whelton, A. J.; Uddin, N.; Nguyen, T.; Huang, Q. G.; Henry, T. B.; Holbrook, R. D.; Chen, K. L. Potential release pathways, environmental fate, and ecological risks of carbon nanotubes. *Environmental Science & Technology* **2011,** 45 (23), 9837-9856.
36. Gottschalk, F.; Sonderer, T.; Scholz, R. W.; Nowack, B. Modeled environmental concentrations of engineered nanomaterials (TiO_2, ZnO, Ag, CNT, fullerenes) for different regions. *Environmental Science & Technology* **2009,** 43 (24), 9216-9222.
37. Gottschalk, F.; Sun, T. Y.; Nowack, B. Environmental concentrations of engineered nanomaterials: Review of modeling and analytical studies. *Environmental Pollution* **2013,** 181, 287-300.
38. Koelmans, A. A.; Nowack, B.; Wiesner, M. R. Comparison of manufactured and black carbon nanoparticle concentrations in aquatic sediments. *Environmental Pollution* **2009,** 157 (4), 1110-1116.
39. Petersen, E. J.; Flores-Cervantes, D. X.; Bucheli, T. D.; Elliott, L. C. C.; Fagan, J. A.; Gogos, A.; Hanna, S.; Kagi, R.; Mansfield, E.; Bustos, A. R. M.; Plata, D. L.; Reipa, V.; Westerhoff, P.; Winchester, M. R. Quantification of carbon nanotubes in environmental matrices: current capabilities, case studies, and future prospects. *Environmental Science & Technology* **2016,** 50 (9), 4587-4605.
40. Saleh, N. B.; Pfefferle, L. D.; Elimelech, M. Aggregation kinetics of multiwalled carbon nanotubes in aquatic systems: measurements and environmental implications. *Environmental Science & Technology* **2008,** 42 (21), 7963-7969.
41. Hyung, H.; Kim, J. H. Natural organic matter (NOM) adsorption to multi-walled carbon nanotubes: Effect of NOM characteristics and water quality parameters. *Environmental Science & Technology* **2008,** 42 (12), 4416-4421.

42. Zhou, X. Z.; Shu, L.; Zhao, H. B.; Guo, X. Y.; Wang, X. L.; Tao, S.; Xing, B. S. Suspending multi-walled carbon nanotubes by humic acids from a peat soil. *Environmental Science & Technology* **2012,** 46 (7), 3891-3897.
43. Yang, K.; Xing, B. S. Desorption of polycyclic aromatic hydrocarbons from carbon nanomaterials in water. *Environmental Pollution* **2007,** 145 (2), 529-537.
44. Ferguson, P. L.; Chandler, G. T.; Templeton, R. C.; Demarco, A.; Scrivens, W. A.; Englehart, B. A. Influence of sediment-amendment with single-walled carbon nanotubes and diesel soot on bioaccumulation of hydrophobic organic contaminants by benthic invertebrates. *Environmental Science & Technology* **2008,** 42 (10), 3879-3885.
45. Schwarzenbach, R. P.; Gschwend, P. M.; Imboden, D. M., *Environmental Organic Chemistry*. John Wiley and Sons: Hoboken, NJ, USA, 2003.
46. Hüffer, T.; Hofmann, T. Sorption of non-polar organic compounds by micro-sized plastic particles in aqueous solution. *Environmental Pollution* **2016,** 214, 194-201.
47. Arafat, H. A.; Franz, M.; Pinto, N. G. Effect of salt on the mechanism of adsorption of aromatics on activated carbon. *Langmuir* **1999,** 15 (18), 5997-6003.
48. Sigmund, G.; Sun, H. C.; Hofmann, T.; Kah, M. Predicting the sorption of aromatic acids to noncarbonized and carbonized sorbents. *Environmental Science & Technology* **2016,** 50 (7), 3641-3648.
49. Xing, B. S.; Pignatello, J. J.; Gigliotti, B. Competitive sorption between atrazine and other organic compounds in soils and model sorbents. *Environmental Science & Technology* **1996,** 30 (8), 2432-2440.
50. Radovic, T. T.; Grujic, S. D.; Kovacevic, S. R.; Lausevic, M. D.; Dimkic, M. A. Sorption of selected pharmaceuticals and pesticides on different river sediments. *Environmental Science and Pollution Research* **2016,** 23 (24), 25232-25244.
51. Nam, S. W.; Choi, D. J.; Kim, S. K.; Her, N.; Zoh, K. D. Adsorption characteristics of selected hydrophilic and hydrophobic micropollutants in water using activated carbon. *Journal of Hazardous materials* **2014,** 270, 144-152.
52. Brooks, A. J.; Lim, H. N.; Kilduff, J. E. Adsorption uptake of synthetic organic chemicals by carbon nanotubes and activated carbons. *Nanotechnology* **2012,** 23 (29), 13.
53. Pan, B.; Xing, B. S. Adsorption mechanisms of organic chemicals on carbon nanotubes. *Environmental Science & Technology* **2008,** 42 (24), 9005-9013.
54. Chen, W.; Duan, L.; Wang, L. L.; Zhu, D. Q. Adsorption of hydroxyl- and amino-substituted aromatics to carbon nanotubes. *Environmental Science & Technology* **2008,** 42 (18), 6862-6868.
55. Yang, K.; Wu, W. H.; Jing, Q. F.; Zhu, L. Z. Aqueous adsorption of aniline, phenol, and their substitutes by multi-walled carbon nanotubes. *Environmental Science & Technology* **2008,** 42 (21), 7931-7936.
56. Diaz-Flores, P. E.; Arcibar-Orozco, J. A.; Perez-Aguilar, N. V.; Rangel-Mendez, J. R.; Medina, V. M. O.; Alcala-Jauegui, J. A. Adsorption of organic compounds onto multiwall and nitrogen-doped carbon nanotubes: Insights into the adsorption mechanisms. *Water Air and Soil Pollution* **2017,** 228 (4), 13.
57. Wang, L. L.; Zhu, D. Q.; Duan, L.; Chen, W. Adsorption of single-ringed N- and S-heterocyclic aromatics on carbon nanotubes. *Carbon* **2010,** 48 (13), 3906-3915.
58. Fang, Q. L.; Chen, B. L. Adsorption of perchlorate onto raw and oxidized carbon nanotubes in aqueous solution. *Carbon* **2012,** 50 (6), 2209-2219.
59. Ansari, M.; Kazemipour, M.; Dehghani, M. The defluoridation of drinking water using multi-walled carbon nanotubes. *Journal of Fluorine Chemistry* **2011,** 132 (8), 516-520.
60. Hüffer, T.; Endo, S.; Metzelder, F.; Schroth, S.; Schmidt, T. C. Prediction of sorption of aromatic and aliphatic organic compounds by carbon nanotubes using poly-parameter linear free-energy relationships. *Water Research* **2014,** 59, 295-303.

61. Sheng, G. D.; Shao, D. D.; Ren, X. M.; Wang, X. Q.; Li, J. X.; Chen, Y. X.; Wang, X. K. Kinetics and thermodynamics of adsorption of ionizable aromatic compounds from aqueous solutions by as-prepared and oxidized multiwalled carbon nanotubes. *Journal of Hazardous materials* **2010,** 178 (1-3), 505-516.
62. Pan, B.; Zhang, D.; Li, H.; Wu, M.; Wang, Z. Y.; Xing, B. S. Increased adsorption of sulfamethoxazole on suspended carbon nanotubes by dissolved humic acid. *Environmental Science & Technology* **2013,** 47 (14), 7722-7728.
63. Yan, W.; Yan, L.; Duan, J. M.; Jing, C. Y. Sorption of organophosphate esters by carbon nanotubes. *Journal of Hazardous materials* **2014,** 273, 53-60.
64. Velzeboer, I.; Kwadijk, C.; Koelmans, A. A. Strong sorption of PCBs to nanoplastics, microplastics, carbon nanotubes, and fullerenes. *Environmental Science & Technology* **2014,** 48 (9), 4869-4876.
65. Yan, X. M.; Shi, B. Y.; Lu, J. J.; Feng, C. H.; Wang, D. S.; Tang, H. X. Adsorption and desorption of atrazine on carbon nanotubes. *Journal of Colloid and Interface Science* **2008,** 321 (1), 30-38.
66. Cho, H. H.; Huang, H.; Schwab, K. Effects of solution chemistry on the adsorption of ibuprofen and triclosan onto carbon nanotubes. *Langmuir* **2011,** 27 (21), 12960-12967.
67. Wang, F.; Yao, J.; Sun, K.; Xing, B. S. Adsorption of dialkyl phthalate esters on carbon nanotubes. *Environmental Science & Technology* **2010,** 44 (18), 6985-6991.
68. Pan, B.; Lin, D. H.; Mashayekhi, H.; Xing, B. S. Adsorption and hysteresis of bisphenol A and 17 alpha-ethinyl estradiol on carbon nanomaterials. *Environmental Science & Technology* **2008,** 42 (15), 5480-5485.
69. Ji, L. L.; Chen, W.; Bi, J.; Zheng, S. R.; Xu, Z. Y.; Zhu, D. Q.; Alvarez, P. J. Adsorption of tetracycline on single-walled and multi-walled carbon nanotubes as affected by aqueous solution chemistry. *Environmental Toxicology and Chemistry* **2010,** 29 (12), 2713-2719.
70. Apul, O. G.; Wang, Q. L.; Zhou, Y.; Karanfil, T. Adsorption of aromatic organic contaminants by graphene nanosheets: Comparison with carbon nanotubes and activated carbon. *Water Research* **2013,** 47 (4), 1648-1654.
71. Chen, H.; Gao, B.; Li, H. Removal of sulfamethoxazole and ciprofloxacin from aqueous solutions by graphene oxide. *Journal of Hazardous materials* **2015,** 282, 201-207.
72. Kah, M.; Zhang, X. R.; Jonker, M. T. O.; Hofmann, T. Measuring and modelling adsorption of PAHs to carbon nanotubes over a six order of magnitude wide concentration range. *Environmental Science & Technology* **2011,** 45 (14), 6011-6017.
73. Shih, Y. H.; Li, M. S. Adsorption of selected volatile organic vapors on multiwall carbon nanotubes. *Journal of Hazardous materials* **2008,** 154 (1-3), 21-28.
74. Fagan, S. B.; Souza, A. G.; Lima, J. O. G.; Mendes, J.; Ferreira, O. P.; Mazali, I. O.; Alves, O. L.; Dresselhaus, M. S. 1,2-dichlorobenzene interacting with carbon nanotubes. *Nano Letters* **2004,** 4 (7), 1285-1288.
75. Zhao, J. J.; Buldum, A.; Han, J.; Lu, J. P. Gas molecule adsorption in carbon nanotubes and nanotube bundles. *Nanotechnology* **2002,** 13 (2), 195-200.
76. Gotovac, S.; Hattori, Y.; Noguchi, D.; Miyamoto, J.; Kanamaru, M.; Utsumi, S.; Kanoh, H.; Kaneko, K. Phenanthrene adsorption from solution on single wall carbon nanotubes. *Journal of Physical Chemistry B* **2006,** 110 (33), 16219-16224.
77. Lee, J. W.; Kang, H. C.; Shim, W. G.; Kim, C.; Moon, H. Methane adsorption on multi-walled carbon nanotube at (303.15, 313.15, and 323.15) K. *Journal of Chemical and Engineering Data* **2006,** 51 (3), 963-967.
78. Yudasaka, M.; Fan, J.; Miyawaki, J.; Iijima, S. Studies on the adsorption of organic materials inside thick carbon nanotubes. *Journal of Physical Chemistry B* **2005,** 109 (18), 8909-8913.

79. Hilding, J.; Grulke, E. A.; Sinnott, S. B.; Qian, D. L.; Andrews, R.; Jagtoyen, M. Sorption of butane on carbon multiwall nanotubes at room temperature. *Langmuir* **2001,** 17 (24), 7540-7544.
80. Shen, X. F.; Wang, X. L.; Tao, S.; Xing, B. S. Displacement and competitive sorption of organic pollutants on multiwalled carbon nanotubes. *Environmental Science and Pollution Research* **2014,** 21 (20), 11979-11986.
81. Chen, J. Y.; Chen, W.; Zhu, D. Adsorption of nonionic aromatic compounds to single-walled carbon nanotubes: Effects of aqueous solution chemistry. *Environmental Science & Technology* **2008,** 42 (19), 7225-7230.
82. Pyrzynska, K.; Stafiej, A.; Biesaga, M. Sorption behavior of acidic herbicides on carbon nanotubes. *Microchimica Acta* **2007,** 159 (3-4), 293-298.
83. Chen, W.; Duan, L.; Zhu, D. Q. Adsorption of polar and nonpolar organic chemicals to carbon nanotubes. *Environmental Science & Technology* **2007,** 41 (24), 8295-8300.
84. Lin, D. H.; Xing, B. S. Adsorption of phenolic compounds by carbon nanotubes: Role of aromaticity and substitution of hydroxyl groups. *Environmental Science & Technology* **2008,** 42 (19), 7254-7259.
85. Gotovac, S.; Song, L.; Kanoh, H.; Kaneko, K. Assembly structure control of single wall carbon nanotubes with liquid phase naphthalene adsorption. *Colloids and Surfaces a-Physicochemical and Engineering Aspects* **2007,** 300 (1-2), 117-121.
86. Davis, J. J.; Green, M. L. H.; Hill, H. A. O.; Leung, Y. C.; Sadler, P. J.; Sloan, J.; Xavier, A. V.; Tsang, S. C. The immobilisation of proteins in carbon nanotubes. *Inorganica Chimica Acta* **1998,** 272 (1-2), 261-266.
87. Yang, K.; Zhu, L. Z.; Xing, B. S. Adsorption of polycyclic aromatic hydrocarbons by carbon nanomaterials. *Environmental Science & Technology* **2006,** 40 (6), 1855-1861.
88. Hu, J. L.; Tong, Z. L.; Hu, Z. H.; Chen, G. W.; Chen, T. H. Adsorption of roxarsone from aqueous solution by multi-walled carbon nanotubes. *Journal of Colloid and Interface Science* **2012,** 377, 355-361.
89. Yu, F.; Ma, J.; Wu, Y. Q. Adsorption of toluene, ethylbenzene and m-xylene on multi-walled carbon nanotubes with different oxygen contents from aqueous solutions. *Journal of Hazardous materials* **2011,** 192 (3), 1370-1379.
90. Apul, O. G.; Wang, Q. L.; Shao, T.; Rieck, J. R.; Karanfil, T. Predictive model development for adsorption of aromatic contaminants by multi-walled carbon nanotubes. *Environmental Science & Technology* **2013,** 47 (5), 2295-2303.
91. Xia, X. R.; Monteiro-Riviere, N. A.; Riviere, J. E. An index for characterization of nanomaterials in biological systems. *Nature Nanotechnology* **2010,** 5 (9), 671-675.
92. Bi, E.; Schmidt, T. C.; Haderlein, S. B. Sorption of heterocyclic organic compounds to reference soils: Column studies for process identification. *Environmental Science & Technology* **2006,** 40 (19), 5962-5970.
93. Macintyre, W. G.; Stauffer, T. B.; Antworth, C. P. A comparison of sorption coefficients determined by batch, column and box methods on a low organic-carbon aquifer material. *Ground Water* **1991,** 29 (6), 908-913.
94. Worch, E., *Adsorption technology in water treatment- Fundamentals, processes, and modelling* Walter de Gruyter GmbH & Co. KG: Berlin/Boston, 2012.
95. Schenzel, J.; Goss, K. U.; Schwarzenbach, R. P.; Bucheli, T. D.; Droge, S. T. J. Experimentally determined soil organic matter-water sorption coefficients for different classes of natural toxins and comparison with estimated numbers. *Environmental Science & Technology* **2012,** 46 (11), 6118-6126.
96. Jolin, W. C.; Sullivan, J.; Vasudevan, D.; MacKay, A. K. Column chromatography to obtain organic cation sorption isotherms. *Environmental Science & Technology* **2016,** 50 (15), 8196-8204.

97. Qian, Y. Sorption of hydrophobic organic compounds (HOCs) to inorganic surfaces in aqueous solutions. Ph.D. disserstation, University Duisburg-Essen, Essen, Germany, 2010.
98. Li, B. H.; Qian, Y. A.; Bi, E. P.; Chen, H. H.; Schmidt, T. C. Sorption behavior of phthalic acid esters on reference soils evaluated by soil column chromatography. *Clean-Soil Air Water* **2010,** 38 (5-6), 425-429.
99. Bürgisser, C. S.; Cernik, M.; Borkovec, M.; Sticher, H. Determination of nonlinear adsorption-isotherms from column experiments - an alternative to batch studies. *Environmental Science & Technology* **1993,** 27 (5), 943-948.
100. Bi, E. P.; Schmidt, T. C.; Haderlein, S. B. Practical issues relating to soil column chromatography for sorption parameter determination. *Chemosphere* **2010,** 80 (7), 787-793.
101. Kromidas, S., *Practical Problem Solving in HPLC*. Wiley-VCH: Weinheim, 2000.
102. Bi, E.; Schmidt, T. C.; Haderlein, S. B. Environmental factors influencing sorption of heterocyclic aromatic compounds to soil. *Environmental Science & Technology* **2007,** 41 (9), 3172-3178.
103. Guo, R. B.; Liang, X. M.; Chen, J. P.; Wu, W. Z.; Zhang, Q.; Martens, D.; Kettrup, A. Prediction of soil organic carbon partition coefficients by soil column liquid chromatography. *Journal of Chromatography A* **2004,** 1035 (1), 31-36.
104. Das, B. S.; Lee, L. S.; Rao, P. S. C.; Hultgren, R. P. Sorption and degradation of steroid hormones in soils during transport: Column studies and model evaluation. *Environmental Science & Technology* **2004,** 38 (5), 1460-1470.
105. Fesch, C.; Simon, W.; Haderlein, S. B.; Reichert, P.; Schwarzenbach, R. P. Nonlinear sorption and nonequilibrium solute transport in aggregated porous media: Experiments, process identification and modeling. *Journal of Contaminant Hydrology* **1998,** 31 (3-4), 373-407.
106. Bucheli, T. D.; Gustafsson, O. Quantification of the soot-water distribution coefficient of PAHs provides mechanistic basis for enhanced sorption observations. *Environmental Science & Technology* **2000,** 34 (24), 5144-5151.
107. Culver, T. B.; Brown, R. A.; Smith, J. A. Rate-limited sorption and desorption of 1,2-dichlorobenzene to a natural sand soil column. *Environmental Science & Technology* **2000,** 34 (12), 2446-2452.
108. Bronner, G.; Goss, K. U. Sorption of organic chemicals to soil organic matter: influence of soil variability and pH dependence. *Environmental Science & Technology* **2011,** 45 (4), 1307-1312.
109. Ptak, T.; Piepenbrink, M.; Martac, E. Tracer tests for the investigation of heterogeneous porous media and stochastic modelling of flow and transport - a review of some recent developments. *Journal of Hydrology* **2004,** 294 (1-3), 122-163.
110. Wu, W. H.; Jiang, W.; Zhang, W. D.; Lin, D. H.; Yang, K. Influence of functional groups on desorption of organic compounds from carbon nanotubes into water: Insight into desorption hysteresis. *Environmental Science & Technology* **2013,** 47 (15), 8373-8382.
111. Li, H. B.; Zhang, D.; Han, X. Z.; Xing, B. S. Adsorption of antibiotic ciprofloxacin on carbon nanotubes: pH dependence and thermodynamics. *Chemosphere* **2014,** 95, 150-155.
112. Wang, Z. Y.; Yu, X. D.; Pan, B.; Xing, B. S. Norfloxacin sorption and its thermodynamics on surface-modified carbon nanotubes. *Environmental Science & Technology* **2010,** 44 (3), 978-984.
113. Young, D. F.; Ball, W. P. Column experimental design requirements for estimating model parameters from temporal moments under nonequilibrium conditions. *Advances in Water Resources* **2000,** 23 (5), 449-460.
114. Thomsen, A. B.; Henriksen, K.; Gron, C.; Moldrup, P. Sorption, transport, and degradation of quinoline in unsaturated soil. *Environmental Science & Technology* **1999,** 33 (17), 2891-2898.

115. Brusseau, M. L.; Rao, P. S. C. The influence of sorbate-organic matter interactions on sorption nonequilibrium. *Chemosphere* **1989,** 18 (9-10), 1691-1706.
116. Turin, H. J.; Bowman, R. S. Sorption behavior and competition of bromacil, napropamide, and prometryn. *Journal of Environmental Quality* **1997,** 26 (5), 1282-1287.
117. Pignatello, J. J.; Xing, B. S. Mechanisms of slow sorption of organic chemicals to natural particles. *Environmental Science & Technology* **1996,** 30 (1), 1-11.
118. Brusseau, M. L. Cooperative sorption of organic-chemicals in systems composed of low organic-carbon aquifer materials. *Environmental Science & Technology* **1991,** 25 (10), 1747-1752.
119. Brusseau, M. L.; Rao, P. S. C.; Jessup, R. E.; Davidson, J. M. Flow interruption: A method for investigating sorption nonequilibrium. *Journal of Contaminant Hydrology* **1989,** 4 (3), 223-240.
120. Bucheli, T. D.; Gustafsson, O. Soot sorption of non-ortho and ortho substituted PCBs. *Chemosphere* **2003,** 53 (5), 515-522.
121. Droge, S.; Goss, K. U. Effect of sodium and calcium cations on the ion-exchange affinity of organic cations for soil organic matter. *Environmental Science & Technology* **2012,** 46 (11), 5894-5901.
122. Altfelder, S.; Streck, T.; Maraqa, M. A.; Voice, T. C. Nonequilibrium sorption of dimethylphthalate - Compatibility of batch and column techniques. *Soil Science Society of America Journal* **2001,** 65 (1), 102-111.
123. Lee, L. S.; Rao, P. S. C.; Brusseau, M. L. Nonequilibrium sorption and transport of neutral and ionized chlorophenols. *Environmental Science & Technology* **1991,** 25 (4), 722-729.
124. Tülp, H. C.; Fenner, K.; Schwarzenbach, R. P.; Goss, K. U. pH-dependent sorption of acidic organic chemicals to soil organic matter. *Environmental Science & Technology* **2009,** 43 (24), 9189-9195.
125. Mader, B. T.; Goss, K. U.; Eisenreich, S. J. Sorption of nonionic, hydrophobic organic chemicals to mineral surfaces. *Environmental Science & Technology* **1997,** 31 (4), 1079-1086.
126. Plassard, F.; Winiarski, T.; Petit-Ramel, M. Retention and distribution of three heavy metals in a carbonated soil: comparison between batch and unsaturated column studies. *Journal of Contaminant Hydrology* **2000,** 42 (2-4), 99-111.
127. Macintyre, W. G.; Stauffer, T. B. Liquid-chromatography applications to determination of sorption on aquifer materials. *Chemosphere* **1988,** 17 (11), 2161-2173.
128. Maraqa, M. A.; Zhao, X.; Wallace, R. B.; Voice, T. C. Retardation coefficients of nonionic organic compounds determined by batch and column techniques. *Soil Science Society of America Journal* **1998,** 62 (1), 142-152.
129. Yoo, J.; Ozawa, H.; Fujigaya, T.; Nakashima, N. Evaluation of affinity of molecules for carbon nanotubes. *Nanoscale* **2011,** 3 (6), 2517-2522.
130. Chang, Y. X.; Zhou, L. L.; Li, G. X.; Li, L.; Yuan, L. M. Single-wall carbon nanotubes used as stationary phase in HPLC. *Journal of Liquid Chromatography & Related Technologies* **2007,** 30 (19), 2953-2958.
131. Li, Y.; Chen, Y.; Xiang, R.; Ciuparu, D.; Pfefferle, L. D.; Horwath, C.; Wilkins, J. A. Incorporation of single-wall carbon nanotubes into an organic polymer monolithic stationary phase for mu-HPLC and capillary electrochromatography. *Analytical Chemistry* **2005,** 77 (5), 1398-1406.

Chapter 2 - Scope and Aim

According to the literature review, column chromatography represents a promising complementary technique to batch experiments offering several advantages in sorption studies. Applications for carbon nanomaterials (CNMs) with the aim to determine sorption data utilizing these advantages are not yet found in literature. Consequently, the motivation of this study was to evaluate the applicability of column chromatography as complementary technique in the determination of sorption data to CNMs and other carbon-based materials and the identification of the influence of environmental conditions on sorption for weakly sorbing compounds without the need of large sorbent amounts. Four work packages (WP) were defined as schematically shown in figure 2.1 to systematically evaluate the applicability.

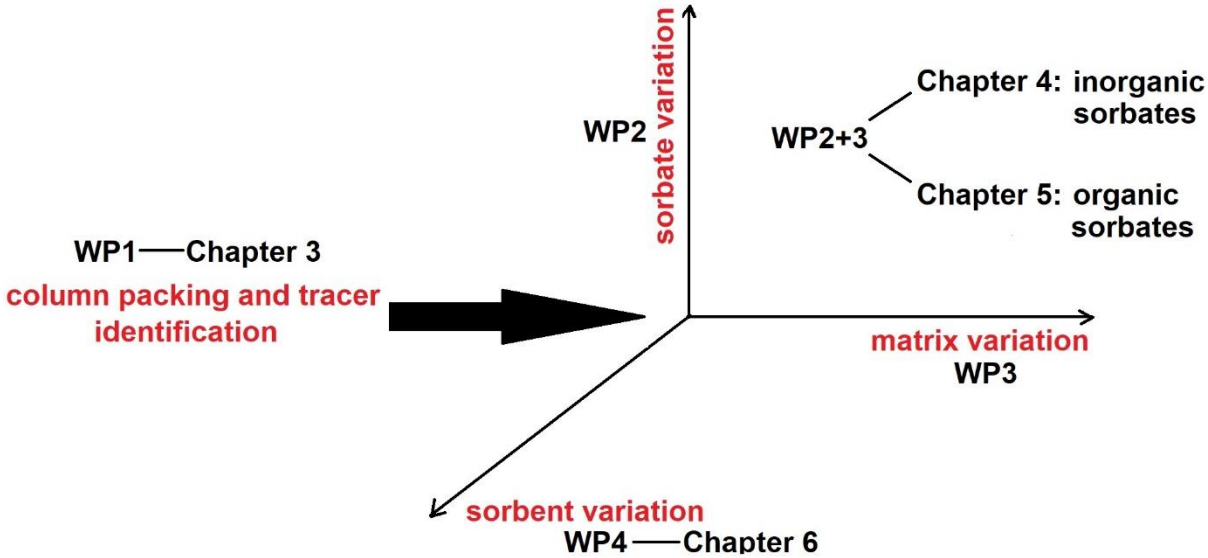

Figure 2.1: Graphical overview of the scope of this thesis.

Application of column chromatography needs as prerequisites a stable and reproducible column packing method and a non-retarded tracer. Thus, **Chapter 3** investigates the requirements for reproducible and stable column packing and identification of a suitable non-retarded tracer for multiwalled carbon nanotubes (MWCNTs). Steps in optimization of the packing procedure originally used for soils and mineral materials are presented. Reproducible column packing is evaluated on basis of the column characteristics like porosity (θ) and bulk density (ρ_b), but also based on determined distribution coefficients (K_d) for an organic and inorganic sorbate as representatives. Finally, column derived sorption data are compared to batch derived sorption data to demonstrate the comparability of both sorption study approaches.

The results of **Chapter 3** showed that inorganic anions initially thought to be suitable tracers showed substantial sorption to MWCNTs. Therefore, **Chapter 4** deals with the determination of sorption isotherms as well as the identification of the influence of

environmental conditions on sorption for different inorganic anions to MWCNTs. Environmental conditions were varied by changing the composition of the eluent regarding pH and ionic strength while the influence of temperature was studied using the column thermostat. Additionally, the surface characteristics of MWCNTs were studied and linked to the influence of environmental conditions on sorption to MWCNTs.

Since the study of inorganic sorbates was very successful in **Chapter 4** using column chromatography, **Chapter 5** deals with organic compounds as sorbates and the influence of environmental conditions. Furthermore, sorption of organic compounds to CNMs and the influence of environmental conditions on sorption are of great interest as sorption to CNMs present in the environment may be affected and consequently, also the transport of environmental contaminants. Heterocyclic organic compounds were chosen as organic sorbates as sorption data of these compounds to CNMs are very limited in literature mainly due to weak sorption, which is indicated by model predictions. Especially, these weakly sorbing compounds are suitable to be analyzed for their sorption behavior using column chromatography.

As **Chapters 3 – 5** showed the general applicability of column chromatography to MWCNTs as one representative of CNMs in general, other CNMs like functionalized MWCNTs (fMWCNTs) and graphene platelets as well as other carbon-based materials like graphite, biochar, and commercially available activated carbons were also investigated using column chromatography in **Chapter 6**. Sorption data derived with the column method are compared to batch derived data from literature to identify the suitability of the column method for material comparison.

Finally, in **Chapter 7** the main results of this study are summarized and combined to an outlook on further research needs arising from this thesis.

Chapter 3 - Column Packing and Validation

3.1 Abstract

Column chromatography requires well packed columns to obtain reliable and reproducible sorption data. Different methods were developed in literature to pack columns with sorbent materials, but applications for carbon nanomaterials (CNMs) were not reported. Consequently, adjustments may be necessary using CNMs as packing material. Additionally, a non-retarded tracer must be identified for column validation and as reference compound for calculation of sorption data.

Thus, the aim of this study was to adjust a method from literature originally used for packing of columns with reference soils to CNMs as packing material. Multiwalled carbon nanotubes (MWCNTs) were chosen as one representative of CNMs and a non-retarded tracer should be found. Furthermore, columns were validated and compared regarding reproducibility of column packing, sorption properties, and comparability to batch experiments.

For CNMs as packing material, adjustments of the packing procedure were necessary, which included avoidance of tapping the column wall and standardized steps in increase of flow rate. Adjustments resulted in a method able to finally yield reproducible and well packed columns of different lengths. Heavy water (D_2O) was identified as non-retarded tracer for MWCNTs in contrast to tracers used in literature for other sorbent materials. Column characteristics like porosity and bulk density varied by less than 5 % and determined sorption data like distribution coefficients for inorganic and organic sorbates varied by less than 10 % between columns indicating the good reproducibility of column packing. Sorption equilibrium could be achieved in columns and sorption isotherms were derived from measurements. However, sorption isotherms determined for different sorbates showed deviations to isotherms determined in batch experiments previously determined for MWCNTs. Deviations were related to differences in the experimental approaches of batch experiments and column chromatography. Despite these deviations, column chromatography can be used as fast determination method for sorption properties of CNMs requiring less time than classical batch experiments. Especially for those sorbates showing weak sorption, column chromatography represents a promising complementary approach as classical batch experiments may be unsuitable.

3.2 Introduction

For sorption studies using column experiments, stable, reproducible, and homogenous columns after column packing are very important to get reliable and comparable data. Well packed columns are characterized by stable retention times of the non-retarded tracer for multiple injections.[1, 2] Furthermore, the peak of the tracer should be symmetrical and sharp in intensity and no sinking of packing material should be observed resulting in dead volume at the column head.[1, 2] For poorly packed columns, the peak shape of the tracer would be broad and eluting later from the column as consequence of dead volume at the column head.[1] Additionally, radial heterogeneity in the packing bed may result in peak tailing[3] or changes of packing density during measurements will result in changing retention times comparing multiple measurements of the tracer.[4] Consequently, a method yielding well packed columns is an important prerequisite in column chromatography.

In literature, different methods were described to pack columns for sorption studies. In the simplest case the packing material is packed dry into the column and the density increased by tapping the wall of the column.[5] This method is simple and does not require additional equipment, but is labor intensive and less reproducible. Additionally, layers can be formed inside the column resulting in different properties like porosity and density and these characteristics may also change in course of the experiments when the packing materials are compressed by pressure applied to the packing bed during sorption experiments due to the eluent flow. Dead volume would be formed resulting in broader and less reproducible results.[1] A method able to produce columns with better reproducibility requires additional equipment.[6] A special device is necessary for this column packing procedure reducing the applicability of the method. However, the risk of changing porosity and packing density by compression of the packing material during experiments is reduced. A method relinquishing almost completely additional equipment, but yielding columns with good reproducibility and stability using predominantly available devices, was presented in literature for soils.[2, 7] A typical HPLC device can be used for column packing. The method combines dry packing with a liquid compression phase prior to sorption experiments. Column packing is done using a precolumn attached to the column later used for sorption experiments as reservoir for packing material. Due to this reservoir, no dead volume is formed during compression and the column will be completely filled. For new sorbent materials, existing methods developed for other sorbent materials can potentially be transferred directly, but it may also require changes in the methodology. Additionally, direct application of methods from literature may be challenging

as details for the packing procedure are not precisely mentioned or only mentioned with approximate values.

For the evaluation of the stability and reproducibility of column packing as well as the determination of sorption data in following experiments, a non-retarded tracer is necessary. A suitable non-retarded tracer must be found showing no or only negligible interactions with sorbent and inert material. Without this, no sorption experiments are possible. Typical non-retarded tracers were already shown in table 1.2 (chapter 1), that were used for materials like soils, minerals, or soot. However, for new material classes like carbon nanomaterials (CNMs) used as sorbent materials, the suitability of a tracer must be evaluated, because sorption to these materials may occur conversely to other materials. This was shown comparing quartz and alumina. While nitrite, already used as non-retarded tracer, showed no interaction with quartz, strong retardation was observed using alumina due to electrostatic interactions.[1, 2]

In this chapter, the adaption of a column packing procedure previously used for soils[2] is shown to enable the packing of columns containing multiwalled carbon nanotubes (MWCNTs) as one representative of CNMs. Additionally, the identification of a non-retarded tracer, evaluation of column reproducibility and the direct comparison of batch and column experiments will be discussed.

3.3 Materials and Methods

3.3.1 Chemicals and Packing Materials

Chemicals used during this study were calcium chloride ($CaCl_2$) ($CaCl_2 \times 2\ H_2O$, (≥99.5 %, AppliChem Panreac), sodium chloride (NaCl) (≥99.5 %, Bernd Kraft GmbH), sodium bromide (NaBr) (≥99 %, Fluka), sodium nitrite ($NaNO_2$) (≥99 %, Sigma-Aldrich), sodium nitrate ($NaNO_3$) (≥99.5 %, Riedel-de Häen), sodium iodide (NaI) (≥99.5 %, Sigma-Aldrich Chemicals), thiourea (THS) (99 %, Riedel-de Häen), heavy water (D_2O) (≥99.9 atom-%, Sigma-Aldrich), pyrazole (98 %, Aldrich Chemicals), anisole (≥99 %, Fluka), benzene (>99 %, Aldrich Chemicals), 2-chlorophenol (≥99 %, Sigma-Aldrich), and indole (>99 %, Aldrich Chemicals). Ultrapure water for preparation of stock solutions and eluents was derived from an ELGA system (18.2 MΩ cm^{-1} resistance, PURELAB Ultra, ELGA LabWater, Celle, Germany). Stock solutions prepared with these chemicals were stored at 4 °C in the dark when not used for measurements.

Sorbents used were quartz in a particle size <63 µm (≥99.7 %, Fluka) and MWCNTs (C150HP, Bayer Material Science, Leverkusen, Germany). General properties of MWCNTs used are given elsewhere.[8] MWCNTs were heated to 350 °C for 1 h to remove amorphous carbon according to literature.[9] Removal of amorphous carbon by this treatment was confirmed previously using transmission electron microscopy.[9] MWCNTs were ground to a particle size <63 µm equal to the quartz material using pestle and mortar. Particle size was controlled by sieving analysis. Grounding had negligible influence on the material properties like the surface area (table S3.1 in chapter 3.6).

3.3.2 Devices

Empty HPLC-columns (length: 14, 30, or 53 mm; diameter: 3 mm) and supplementary equipment used for column packing (precolumns, connecting nuts, stainless steel sieves (3 µm pore size), glass fiber filters and polytetrafluoroethylene (PTFE) seals) were purchased from Bischoff Chromatography (Bischoff Analysentechnik u. –geräte GmbH, Leonberg, Germany).

Column-based measurements were done using two different HPLC systems. The first device was a Shimadzu HPLC system consisting of following parts: System controller (SCL-$10A_{VP}$), HPLC-pump (LC-$10AT_{VP}$), degasser (DGU-$20A_{SR}$), solvent organizer (FCV-$10AL_{VP}$), autosampler (SIL-$10AD_{VP}$), and diode array detector (DAD) (SPD-$M10A_{VP}$). The software of the system was LabSolution (Version 1.25 SP4). The other instrument was a Knauer HPLC system having besides the DAD also a refractive index detector (RID), which were both connected in series connection passing first the DAD. In total it consisted of following parts: HPLC-pump (K-1001), a degasser, an autosampler (Triathlon Spark Holland), column oven (Jetstream 2 Plus), DAD with deuterium lamp (K-2700 and K-2701), and a RID (K-2301). The software of the system was ChromGate (Version 2.8, Build 861). A general sketch of the instrumental setup of the Knauer HPLC-system is shown in figure S3.1 in chapter 3.6. The RID was mandatory for the detection of D_2O. Dirac input of analyte solutions was done by an injection-loop-valve using 5 µL injection volume. The detection cell volumes of the DAD and RI-detector were 10 and 15 µL, respectively. Connecting capillaries were kept as short as possible and had a diameter of 0.13 mm to keep dead volume as low as possible. The UV spectrophotometer used for determination of UV calibrations for isotherm calculations was a Shimadzu UV-1650PC (Shimadzu Europe GmbH, Duisburg, Germany).

3.3.3 Column packing

The procedure used for column packing was adapted from literature. A method developed to pack columns with reference soils was adapted,[2] which was later used in several publications.[10, 11] This method and necessary preparation steps were used as starting point in the present study and therefore shall be briefly described in the following. At the beginning, the analytical column used for sorption experiments is connected with a connecting nut to a precolumn (figure S3.2 in chapter 3.6). This assembly is then filled with the dry packing material. The packing materials are ground with pestle and mortar to a particle size <63 µm, which is checked by sieving analysis. The material is added carefully to the column using a spatula. During addition of further material, the walls are tapped with a screwdriver to increase the packing density. After complete filling and no further compression by tapping, the assembly of analytical column and precolumn is connected to a HPLC pump. It is started with a low flow rate (e.g. 0.010 mL min^{-1}) to remove entrapped air and saturate all pores inside the column with water. The flow is gradually increased when the backpressure is stable until a high backpressure is finally reached (e.g. 450 bar). In case of low backpressure, the maximum flow rate of the pump of for example 1 mL min^{-1} can be used. In case of high backpressure at low flow rates, column clogging can be a problem and a dilution with inert material like quartz must be done. The highest flow rate is then held for 30 minutes or longer with a stable backpressure and then the precolumn is removed. Finally, the head of the analytical column is cleaned with a spatula and then closed with sieves, filters, and a seal.

Columns were packed according to the method described before[2] initially with quartz that was available in large quantities and consequently, ideal to adapt and further optimize the method in course of this thesis. Steps in optimization will be shown and discussed in the results and discussion section (3.4.1). No precise values were given in literature[2] for the steps in flow increase, the maximum flow rate and time at maximum flow rate. Initially, the flow rate was increased in self-selected steps, when the backpressure was stable, which was typically after 1 – 2 minutes, to following flow rates: 0.05, 0.1, 0.2, 0.4, 0.6, 0.8, 1.0, and finally 1.25 mL min^{-1}. The maximum flow rate of 1.25 mL min^{-1} corresponded to a backpressure of e.g. 265 bar for columns with 53 mm length and 3 mm diameter. This flow rate was held for 45 minutes with stable backpressure, which was longer than the at least 30 minutes mentioned previously.[2] The optimized procedure of columns packed with quartz was then transferred first to columns containing MWCNTs, which was the main sorbent in this thesis. Dilution with quartz as inert material was done in case of too strong sorption or clogging problems.

Non-retarded tracers used for quartz columns were thiourea (THS) and nitrite (NO_2^-), which were already used as non-retarded tracers in column-based measurements also using quartz as packing or inert material.[1, 2] Concentration of THS was 30 mg L^{-1} while that of NO_2^- was 20 mg L^{-1} in ultrapure water. For columns containing also MWCNTs, these compounds and other inorganic anions (bromide (Br^-), nitrate (NO_3^-), and iodide (I^-)) as well as D_2O were tested. Concentration was 20 mg L^{-1} of the respective anion and 10 vol.-% for D_2O in ultrapure water. Detection wavelengths were 200 nm (Br^- and NO_3^-), 210 nm (NO_2^-), 226 nm (I^-), and 236 nm (THS). D_2O was detected using the RID. The flow rate of the eluent was in all measurements of this chapter 0.1 mL min^{-1} with an injection volume of 5 µL.

3.3.4 Reproducibility of column characteristics and sorption properties

Columns packed with a mixture of MWCNTs and quartz are compared in this section to show the method reproducibility. Column characteristics bulk density (ρ_b) and porosity (θ) were determined using D_2O (10 vol.-% in ultrapure water). θ was calculated according to equation 3.1. This equation relates the pore volume of the packed column to the total volume of the empty column without packing material.

$$\theta = (v^* \times (t_{R,wc} - t_{R,woc})) / (\pi \times r^2 \times h) \quad (3.1)$$

v^* is the flow rate used for measurements with and without column, which was in both cases 0.1 mL min^{-1} with an injection volume of 5 µL. Ten replicates were measured for this purpose with and without column to keep uncertainties as low as possible. $t_{R,wc}$ is the retention time according to the determined half-mass point of D_2O with column, while $t_{R,woc}$ is related to the retention time of D_2O without column. r is the radius of the column used, h is the respective column length. The half-mass point was already explained in chapter 1.3.2.

ρ_b of each column was calculated according to equation 3.2. The mass of packing material inside the column after packing is related to the total volume of the empty column.

$$\rho_b = (m_{col,tot} - m_{water} - m_{col,equip}) / (\pi \times r^2 \times h) \quad (3.2)$$

$m_{col,tot}$ is the mass of the column after packing with all pores filled with water, m_{water} is the mass of water inside the column calculated by multiplying the pore volume of the column with the density of water at 25 °C (0.997 g mL^{-1}), and $m_{col,equip}$ is the mass of the empty column including supplementary equipment used for closure of the column (sieves, filters, and PTFE sealings) to finally have just the weight of the packing material inside the column after packing related to the volume of the empty column.

Comparison of sorption properties of identically packed columns was done using Br^- as inorganic reference sorbate und pyrazole as organic reference sorbate. Distribution coefficients (K_d) were calculated according to equations 3.3 and 3.4 using also the retardation

factor (R). Equation 3.3 is an adapted version of equation 1.5 from the general introduction (chapter 1) as two different retention times for measurements without column were necessary for sorbates (Br^- and pyrazole) and non-retarded tracer (D_2O). The sorbates were detected using the DAD while the tracer was detected using the RID yielding two different retention times for tracers and sorbates without column when using both detectors in series connection.

$$R = (t_{R,sorb} - t_{0,sorb}) / (t_{R,tracer} - t_{0,tracer}) \quad (3.3)$$

$$R = 1 + \rho_b / \theta \times K_d \quad (3.4)$$

$t_{R,sorb}$ is the retention time of the sorbate with column while $t_{0,sorb}$ is the retention time of the sorbate without column. $t_{R,tracer}$ is the retention time of the tracer with column while $t_{0,tracer}$ is the retention time of the tracer without column installed. The concentration of Br^- was 63 mg L^{-1} while pyrazole was used with a concentration of 470 mg L^{-1}. The flow rate of the eluent was 0.1 mL min^{-1} and the injection volume was 5 µL. Three replicates were done. Detection wavelength for pyrazole was 210 nm. Eluent for Br^- measurements was 1 mM NaCl and 10 mM $CaCl_2$ for pyrazole both with a pH value of 6 at a temperature of 25 °C. Different eluents were chosen as reproducible measurements were possible for inorganic anions already with 1 mM NaCl. Higher concentrations were not tested at that time. 10 mM $CaCl_2$ with pH 6 was the eluent for organic compounds as this matrix composition was already used in a previous study for batch experiments using MWCNTs as sorbent for organic sorbates.[12]

3.3.5 Determination of local equilibrium

The determination of local equilibrium was done using measurements at different flow rates. If the determined R value shows no dependence on the flow rate, local equilibrium in the column can be assumed. In case of non-equilibrium conditions, R would increase with reducing flow rate. Measurements at different flow rates were done for all sorbates tested in this thesis, but will only be shown here for Br^- as inorganic reference compound and pyrazole as organic reference compound with MWCNTs as reference sorbent. Flow rates tested were 0.025, 0.050, 0.075 and 0.100 mL min^{-1} in case of Br^- and 0.010, 0.025, 0.050 and 0.100 mL min^{-1} pyrazole. D_2O was used as non-retarded tracer. R was calculated according to equation 3.3 using the half-mass point. Injected concentrations were 20 mg L^{-1} for Br^- and 470 mg L^{-1} for pyrazole. The injection volume was 5 µL and measurements were carried out in triplicates. For other sorbates that are not shown here, also triplicate measurements were done. Only in case of very long measurement times (>90 minutes at the highest flow rate of

0.100 mL min^{-1}) triplicates were reduced to duplicates to limit the necessary measurement time. As variations between repeated injections were generally very low, duplicate measurements in rare cases (e.g. equilibration of pyridine used in chapter 5) were not problematic.

3.3.6 Comparison of batch and column experiments

Column and batch experiments were investigated for their comparability. Batch experiments for small heterocyclic organic compounds like pyrazole or imidazole as well as inorganic anions were not successful in this study because of too weak sorption. Consequently, stronger sorbing compounds from a previous study were used.[12] Anisole, benzene, 2-chlorophenol, and indole were chosen as sorbates for direct comparison. Columns used for measurements contained just 0.5 % (wt/wt) MWCNTs diluted with quartz as columns with a higher content of MWCNTs resulted in too high measurement times. Triplicate measurements of each injected concentration were done. Nine different concentrations of each sorbate were injected with increasing concentration. The flow rate of the eluent was 0.1 mL min^{-1} and the injection volume was 5 µL. All injected concentrations are summarized in table 3.1. Wavelengths used for detection were 218 nm (anisole), 202 nm (benzene), 200 nm (2-chlorophenol), and 214 nm (indole).

Table 3.1: Injected concentrations of the different sorbates (anisole, benzene, 2-chlorophenol and indole) in column experiments used for the direct comparison of batch and column experiments.

sorbate	injected concentration [mg L^{-1}]
anisole	200, 300, 400, 600, 800, 1000, 1250, 1500
benzene	40, 60, 80, 100, 150, 200, 300, 400, 500
2-chlorophenol	150, 200, 300, 500, 600, 750, 1000, 1500, 2000
indole	100, 200, 300, 400, 500, 600, 800, 1000, 1200

Different approaches have been used in literature to construct sorption isotherms from column studies.[13-15] In this study, two different approaches were used and compared for their suitability.

At first, the approach used by Schenzel *et al.*[13] was adapted. Nine solutions with different concentrations of the sorbate were separately injected. Concentrations of these solutions are given in table 3.1. Using an external calibration on a spectrophotometer

measured for each sorbate, the absorption in the chromatogram at the half-mass point was converted into the representative dissolved concentration at equilibrium ($c_{w,eq}$). Calibrations of each sorbate used for isotherm calculation are given in table S3.2. In a second step, $c_{w,eq}$ was multiplied with the corresponding K_d value of the half-mass point to finally yield the corresponding sorbed concentration at equilibrium ($c_{s,eq}$). This approach is referred as the "classical approach".

Secondly, the approach by Schenzel *et al.*[13] was adapted and combined with the approach by Bürgisser *et al.*[16] to yield an alternative evaluation approach. Bürgisser *et al.*[16] derived the sorption isotherm directly from the chromatogram from the desorption curve. The tailing of the peak in the chromatogram was used to construct the sorption isotherm. Consequently, only one injected concentration of each sorbate instead of nine different concentrations was necessary. The highest injected concentration of each sorbate used for the classical approach was used. Using again the external calibration, the absorption in the chromatogram was transferred into $c_{w,eq}$ starting at the determined half-mass point in the chromatogram. A K_d value corresponding to each data point following the half-mass point was calculated using equations 3.3 and 3.4, which was multiplied with the corresponding $c_{w,eq}$ in order to yield $c_{s,eq}$. This approach is referred as the "alternative approach". Both approaches are summarized stepwise in figures S3.3 and S3.4 in chapter 3.6.

The Freundlich model was used for isotherm generation with both evaluation approaches, because it was also used in the previous study supplying the batch data to fit sorption data.[12]

3.4 Results and Discussion

3.4.1 Optimization of column packing and tracer selection

Packing of columns with exclusively quartz applying the initial procedure yielded asymmetrical peaks for both tracers (THS and NO_2^-). Chromatograms showed broad peaks with pronounced tailing or fronting with in some cases even a formation of a shoulder besides the peak maximum (example shown in figure 3.1). An unstable packing bed in the final column was not the reason, because repeated measurements of both tracers showed no changes in the peak shape and retention time. Especially a changing retention time for repeated injections would be found in case of changes in packing density during measurements.[4] The observed peak shape may be the consequence of an inhomogeneity in the packing bed. The flow rate was increased after the backpressure was stable, which was

typically after 1 – 2 minutes. Stable backpressure is only an indicator for a stable packing bed. Thus, during column packing and while increasing the flow rate, the packing bed was maybe not stable contributing to the detected tailing. Furthermore, the tapping at the column wall with a screwdriver might have yielded a radial heterogeneity. A radial heterogeneity, which leads to different flow rates, when comparing wall and center regions of the column, may cause fronting or tailing of peaks.[3, 17]

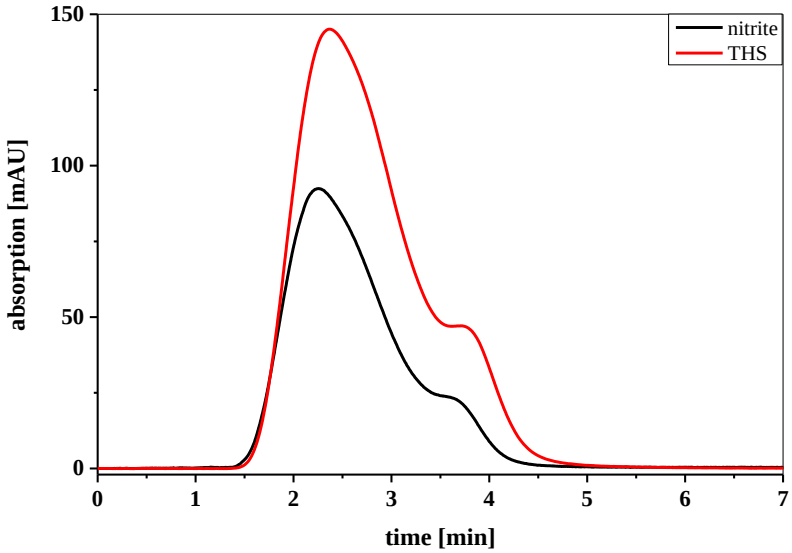

Figure 3.1: Chromatograms of nitrite and THS in a column packed with exclusively quartz applying the original method from literature (length: 5.3 cm, diameter: 0.3 cm, flow rate: 0.1 mL min^{-1}, eluent: ultrapure water with pH 6, injection volume: 5 µL).

Consequently, the packing procedure was more standardized during packing with defined times at each flow rate and increased time at maximum flow to allow a better stabilization of the bed. Additionally, tapping column walls was almost completely avoided to avoid a radial heterogeneity. Just very few taps at the head of the precolumn were used to transfer material from the plateau at the column head inside the column during dry packing. The column was just tapped with the lower end on the laboratory bench to increase packing density in the dry packing phase. Each flow rate was held for 15 minutes and the steps in increase of the flow rate mentioned in chapter 3.3.3 were slightly changed. The maximum flow rate was finally held for four hours for final stabilization of the bed. An example for the finally selected flow rates and observed pressures is shown in table 3.2 for a 5.3 cm column containing exclusively quartz as packing material. For shorter columns (1.4 and 3.0 cm) the maximum flow rate could be chosen higher (up to 3.5 mL min^{-1}) due to a lower backpressure. After finishing the packing procedure, the precolumn was removed and the column head cleaned as fast as possible to avoid relaxation of the compressed packing bed when the pressure was removed. This was described by Kirkland and DeStefano[18] for packing of

chromatographic columns for separation purposes. To decrease the time necessary for cleaning the column head, a stainless steel tool was self-prepared (figure 3.2). It fitted well in the column head without the risk to reach the small diameter part of the column and cause disturbances in the freshly packed column bed. Both sides of the tool were used for cleaning. The angled side was used to clean the edges of the column head. The blunt end was used to generate a smooth shaped finish of the packing bed between column head and analytical part of the column with the reduced diameter. Previously the column head was cleaned with a spatula, which needed 3 – 4 minutes. With the tool, this time could be reduced to 1 minute until sieves, filters and the PTFE seal could be introduced, and the column could be closed.

Table 3.2: Applied flow rates and times at each flow rate for a column packed with exclusively quartz (length: 5.3 cm, diameter: 0.3 cm).

flow rate [mL min^{-1}]	backpressure [bar]	time [min]
0.01	8	60
0.05	13	15
0.1	17	15
0.2	28	15
0.3	38	15
0.45	55	15
0.7	83	15
1.0	116	15
1.5	173	240

Figure 3.2: Self-made tool made of stainless steel used for fast cleaning of the column head after finishing the liquid packing procedure and removal of the precolumn.

The chromatograms of both tracers measured with a column packed with the optimized procedure with quartz as packing material are shown in figure 3.3. The peak shape could be significantly improved. The peak was more symmetrical, and the peak width could be reduced resulting in a much sharper peak. The pronounced tailing or fronting with shoulder could be removed. Only slight tailing or fronting could be observed (asymmetry factor at 10 % of the maximum intensity 0.9 for NO_2^- and 1.3 for THS) and repeated measurement gave a stable retention time for both tracers. Applying the procedure to several columns packed with quartz, retention times and peak shape were well comparable (figure S3.5 in chapter 3.6). Furthermore, shorter columns with a length of 1.4 cm and 3.0 cm could be packed with a symmetrical and sharp peak (figure S3.6 in chapter 3.6). NO_2^- was eluted slightly earlier than THS, which is most likely related to a pore exclusion as reported in literature.[1] Quartz is negatively charged at the experimental conditions (pH 6, ultrapure water, 25 °C) as the pH corresponding to a net neutral charge of the sorbent is typically at about 2. At higher pH values, the surface charge becomes negative and, consequently, negatively charged NO_2^- may be excluded from pores yielding a shorter retention time compared to the non-charged THS. This was proved using ultrapure water with increased ionic strength by the addition of salt (100 mM NaCl) as eluent. Retention time of NO_2^- was similar to THS using this eluent, because electrostatic exclusion from pores was prevented at increased ionic strength shielding charges and making all pores accessible also for charged NO_2^- (data not shown).

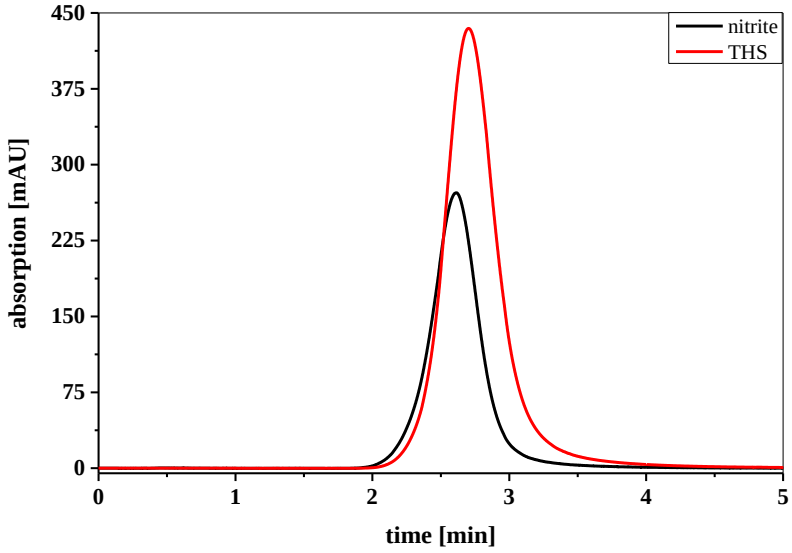

Figure 3.3: Chromatograms of nitrite and THS in a column packed with exclusively quartz applying the optimized method (length: 5.3 cm, diameter: 0.3 cm, flow rate: 0.1 mL min^{-1}, eluent: ultrapure water with pH 6, injection volume: 5 µL).

The primary interest of this work was the application of the column-based method to CNMs and other carbon-based sorbents. MWCNTs were chosen as starting sorbent as they are the most studied CNMs. Initially it was tested to pack columns with exclusively MWCNTs, but already at low flow rates of 0.5 – 1.0 mL min^{-1} with a corresponding pressure of about 30 – 35 bar column clogging became a problem. The aggregates of MWCNTs seem to burst at a backpressure of >30 – 35 bar and completely clog the sieves at the column outlet leading to a backpressure >300 bar, which stopped the HPLC pump. Dilution with quartz helped to overcome this problem. Columns containing for example 5 or 10 % (wt/wt) MWCNTs were successfully packed without clogging problems. The pressure could be increased above 200 bar using a flow rate of up to 3.5 mL min^{-1} and no clogging was observed. Quartz seems to stabilize the whole packing bed containing also MWCNTs and avoid the clogging of sieves. Measurements using THS and NO_2^- to evaluate the packing bed inside the column showed that both tracers were not suitable for columns containing MWCNTs (figure 3.4). THS showed a pronounced tailing after a sharp increase, while measurements of NO_2^- showed a very broad and relatively symmetrical peak using ultrapure water as eluent in a column containing only 5 % MWCNTs with a length of 1.4 cm. The peak shape of non-retarded tracers should be symmetrical and sharp,[1] which was not the case for both compounds. Additionally, determined half-mass points using THS and NO_2^- resulted for both compounds in a calculated pore volume much higher than the volume of the empty column without packing material. As this is not possible, a retardation inside the column caused by MWCNTs must be the reason. Maximum expected retention time in case of an

empty column without retention by the packing material would be approximately two minutes using the Shimadzu HPLC system. Additionally, repeated injections of NO_2^- showed deviations regarding the peak shape and retention time when changing the batch of ultrapure water, although it was derived from the same source (figure 3.5). Furthermore, stronger retention inside the column was observed using only 5 % MWCNTs instead of 10 % MWCNTs (data not shown). Stronger retention with reduced sorbent content could not be expected as a reduced sorbent content should result in a reduced retention inside the column. Consequently, only ultrapure water without further additives (e.g. salts) as eluent was unsuitable using NO_2^- as potential non-retarded tracer.

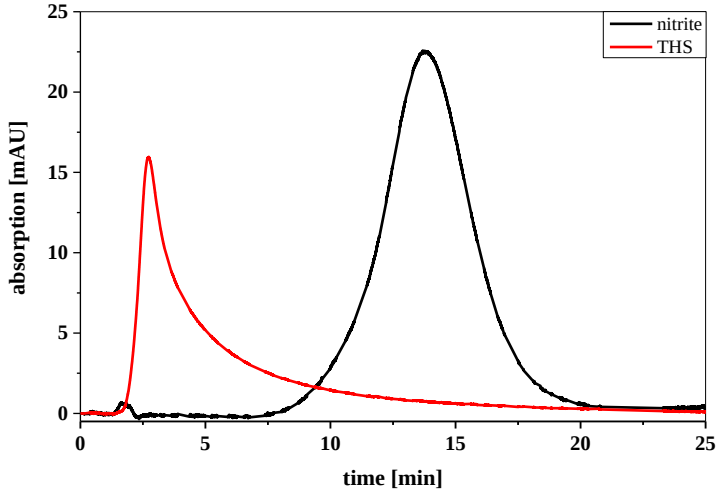

Figure 3.4: Chromatograms of nitrite and THS in a column containing 5 % MWCNTs and 95 % quartz packed with the optimized procedure (length: 1.4 cm, diameter: 0.3 cm, flow rate: 0.1 mL min^{-1}, eluent: ultrapure water with pH 6, injection volume: 5 µL).

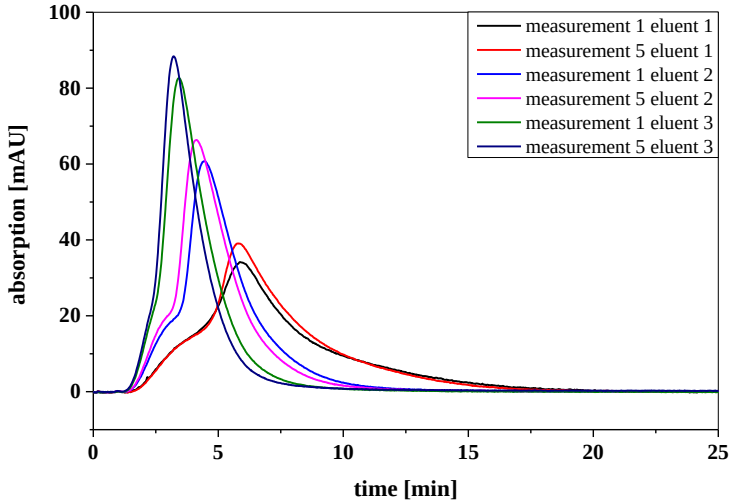

Figure 3.5: Chromatograms of repeated measurements of nitrite in a column containing 5 % MWCNTs and 95 % quartz packed with the optimized procedure, but three different batches of ultrapure water were used (length: 1.4 cm, diameter: 0.3 cm, flow rate: 0.1 mL min^{-1}, eluent: ultrapure water with pH 6, injection volume: 5 µL).

Other inorganic anions (Br^-, I^-, NO_3^-) were also tested for their applicability as they are easily detectable using an UV detector. Br^-[16, 19] and NO_3^-[16, 20] were also used in other studies as non-retarded tracers for other sorbents. No interaction with quartz was observed (data not shown), but also these compounds were retarded in columns containing MWCNTs (figure 3.6). As for NO_2^-, peaks were very broad, which is not typical for non-retarded tracers. Consequently, all these compounds were not suitable as non-retarded tracers. An interesting observation was that all inorganic anions tested as non-retarded tracers showed a different retention inside the column using ultrapure water as eluent (figure 3.6), but repeated injections showed again changing retention times and changes in peak shape using ultrapure water as eluent (data not shown). The addition of 1 mM NaCl to the eluent helped to overcome these problems. The peak shape became narrower and reproducible for repeated injections (data not shown). Retention times were reduced strongly, but differences in retention times between the anions remained (figure 3.7). Chloride anions seem to compete with the other tested anions for sorption sites while in ultrapure water with negligible concentrations of competing anions, consequently, retention inside the column was stronger. Additionally, because of the negligible amounts of ions present, small variations in the ultrapure water may occur although the quality was always good. This might be the reason for deviations observed using different reservoir bottles containing different charges of ultrapure water from the same source. The determined half-mass point using 1 mM NaCl in ultrapure water led to a pore volume still higher than the volume of the empty column. So even with the addition of small concentrations of salt to the eluent, the tested inorganic anions were not suitable as non-retarded tracers. Recovery of all inorganic anions was quantitative (between 80 – 120 %) using ultrapure water and 1 mM NaCl as eluent when comparing the peak area of injections with and without column. Consequently, sorption of those anions was reversible. Using ultrapure water as eluent, recoveries were in some cases higher than 100 % resulting maybe from baseline noise and the high peak width. Sorption of the tested anions could be expected to a certain extent as a very limited number of previous studies used MWCNTs as sorbent for other inorganic anions like perchlorate,[21] fluoride,[22] and phosphate.[23] Consequently, inorganic anions will be studied as sorbates in chapter 4 using the column-based method. The influence of environmental conditions on sorption of these compounds will be studied as it was already shown that the ionic strength can strongly influence sorption. Additionally, the influence of temperature and pH will help to investigate the underlying mechanisms and characteristics in sorption of these sorbates.

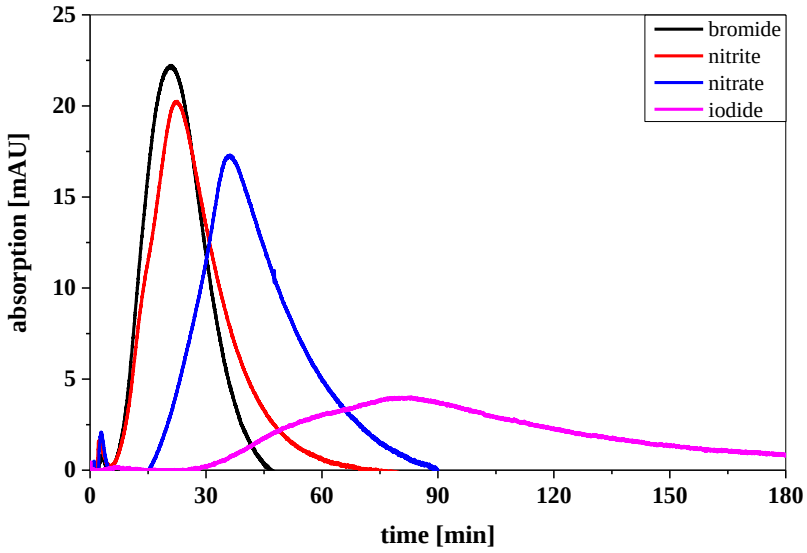

Figure 3.6: Chromatograms of inorganic anions (bromide, nitrite, nitrate, iodide) in a column containing 5 % MWCNTs and 95 % quartz (length: 1.4 cm, diameter: 0.3 cm, flow rate: 0.1 mL min^{-1}, eluent: ultrapure water with pH 6, injection volume: 5 µL).

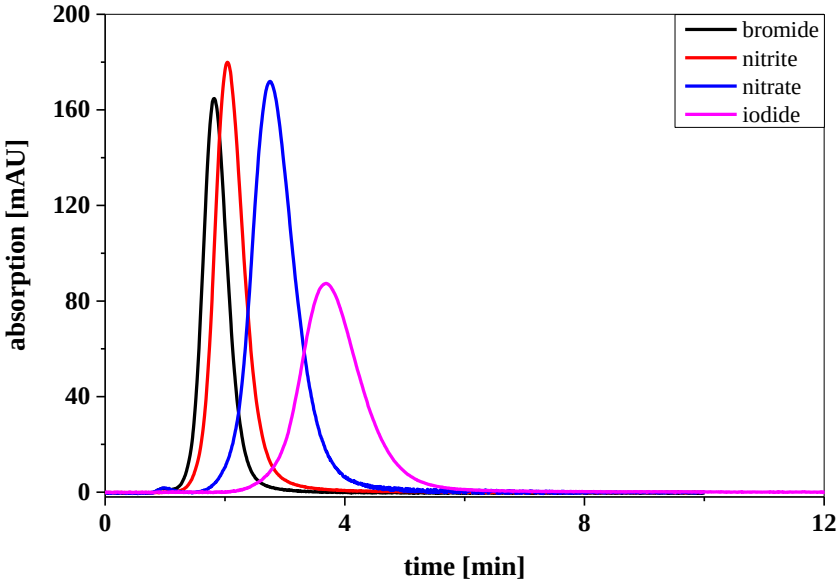

Figure 3.7: Chromatograms of inorganic anions (bromide, nitrite, nitrate, iodide) in a column containing 5 % MWCNTs and 95 % quartz (length: 1.4 cm, diameter: 0.3 cm, flow rate: 0.1 mL min^{-1}, 1 mM NaCl as eluent, injection volume: 5 µL).

Another compound had to be identified that could be used as non-retarded tracer. Organic compounds used as tracers for other sorbents (like fluorescein and others mentioned in table 1.2 in chapter 1.3.2) cannot be used because of the sorptive properties of MWCNTs towards organic compounds. As also inorganic anions were unsuitable, D_2O was tested as non-retarded tracer, but an additional detector was necessary. D_2O is not detectable using a DAD so that a RID was used, which can detect D_2O, because of the difference in the refractive index between D_2O and water (H_2O). D_2O showed no interaction with quartz as the

retention time inside a column packed with exclusively quartz was equal to THS, which was previously shown to be suitable for those columns (data not shown).

In columns containing besides quartz also MWCNTs, D_2O was also suitable as non-retarded tracer in contrast to all other compounds tested before. The peak was sharp, almost symmetrical and reproducible in retention time and peak shape (figure 3.8). The addition of 1 mM NaCl did not influence the determined retention time as it was found for the inorganic anions (data not shown). The asymmetry factor of 1.3 – 1.5 indicated only slight tailing, which is also found for injections without column. Recovery of D_2O was quantitative comparing the peak area of injections with and without column. Another important information using D_2O was that columns containing MWCNTs can be packed applying the optimized method developed with quartz as test material because of the sharp and symmetrical peak. Several columns produced using the procedure showed almost the same retention time for D_2O (figure S3.7 in chapter 3.6). Additionally, the determined pore volume determined using D_2O was lower as the volume of the empty column, which further supported the suitability of D_2O as non-retarded tracer. The method could also be transferred without changes to columns with different MWCNT content and column length from 1.4 to 5.3 cm with almost symmetrical peaks for D_2O (figure S3.8 in chapter 3.6).

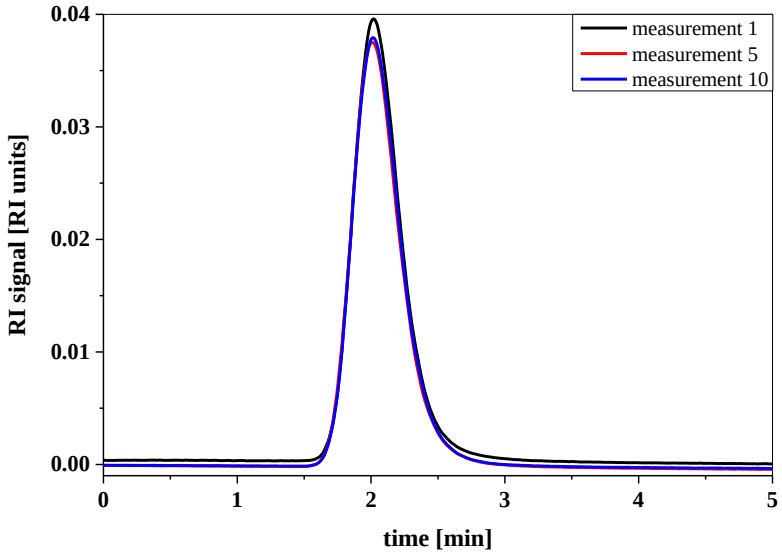

Figure 3.8: Chromatograms of repeated injections of D_2O using a column containing 5 % MWCNTs and 95 % quartz (length: 1.4 cm, diameter: 0.3 cm, flow rate: 0.1 mL min^{-1}, eluent: ultrapure water, injection volume: 5 µL).

After optimization and standardization of the packing procedure, it was possible to pack columns with quartz and a mixture of MWCNTs and quartz and to identify D_2O as non-retarded tracer for MWCNT columns. The reproducibility of column packing for those containing MWCNTs will be discussed in the following section.

3.4.2 Reproducibility of characteristics and sorption properties of columns containing MWCNTs

Several columns were packed with a mixture of quartz and MWCNTs to identify the comparability of their characteristics (θ and ρ_b) as well as the sorption data represented by K_d derived for inorganic and organic compounds.

The comparison of ρ_b and θ is shown in figure 3.9 for ten columns containing 5 % MWCNTs. ρ_b varied only slightly between the columns with a mean value of 1.31 kg L^{-1} connected with relative standard deviation of less than 3 %. A similar observation was made for θ with a mean value of 0.61 and a relative standard deviation of less than 2 %. Consequently, applying the optimized packing procedure, reproducible column packing was possible yielding columns with very similar characteristics.

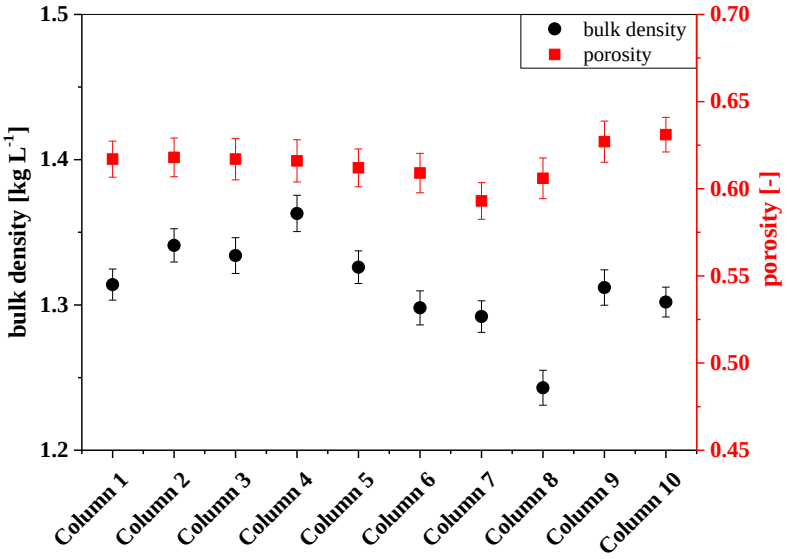

Figure 3.9: Comparison of bulk density and porosity of ten columns packed using the optimized procedure containing 5 % MWCNTs and calculated using D_2O as non-retarded tracer (length: 1.4 cm, diameter: 0.3 cm, eluent: ultrapure water, injected concentration of D_2O: 10 vol.-%, injection volume: 5 µL). Error bars represent the maximum error determined via error propagation from the retention times of repeated measurements (n=10) of sorbates as well as the tracer according to the half-mass point.

The sorption characteristics of columns containing 5 % MWCNTs for Br^- as inorganic reference anion and pyrazole as organic reference compound are shown in figures 3.10 and 3.11, respectively. K_d is used for comparison of the sorption properties of the different columns. It must be noted here that columns used for Br^- and pyrazole were not identical although the numbers in the figures may implicate this. Recovery of pyrazole was quantitative (90 – 110 %) like it was observed for Br^- although the peak of pyrazole was broader with a pronounced tailing instead of the sharp almost symmetrical peak of Br^-. Thus, sorption was reversible. The variation of K_d determined with Br^- and pyrazole for different columns was

small. On average K_d values of 13.3 ± 1.4 L kg^{-1} and 29.6 ± 1.8 L kg^{-1} were determined for Br^- and pyrazole, respectively. The relative standard deviation between columns was about 10 % in case of Br^- and about 6 % in case of pyrazole, which are acceptable deviations for self-packed columns. The content of MWCNTs in those columns was only 5 %. This dilution of MWCNTs was necessary to enable a measurement of pyrazole in a reasonable time. For a higher content of MWCNTs, measurement time would be long (>100 minutes) for complete sampling of the tailing. For Br^- a higher content of MWCNTs would have been possible, but 5 % was still sufficient for sorption measurements. Variations in the content of MWCNTs in the packing material between columns may be responsible for deviations in K_d between columns. Sorbent materials were mixed manually, which may result in small variations in the content of MWCNTs.

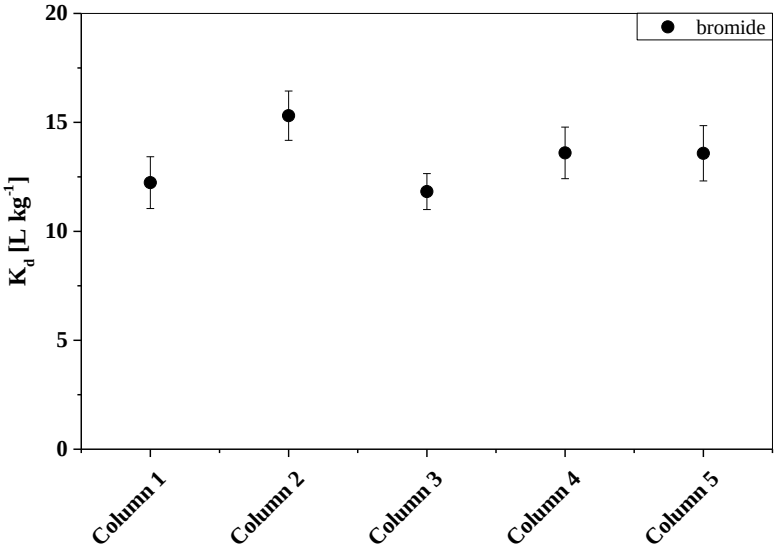

Figure 3.10: Comparison of K_d values determined injecting bromide in five columns packed using the optimized procedure containing 5 % MWCNTs and calculated using D_2O as non-retarded tracer (length: 1.4 cm, diameter: 0.3 cm, eluent: 1 mM NaCl with pH 6 at 25 °C, injected concentration of bromide: 63 mg L^{-1}, injected concentration of D_2O: 10 vol.-%, injection volume: 5 µL). Error bars represent the maximum error determined via error propagation from the retention times of repeated measurements of sorbates (n=5) as well as tracer (n=10) according to the half-mass point.

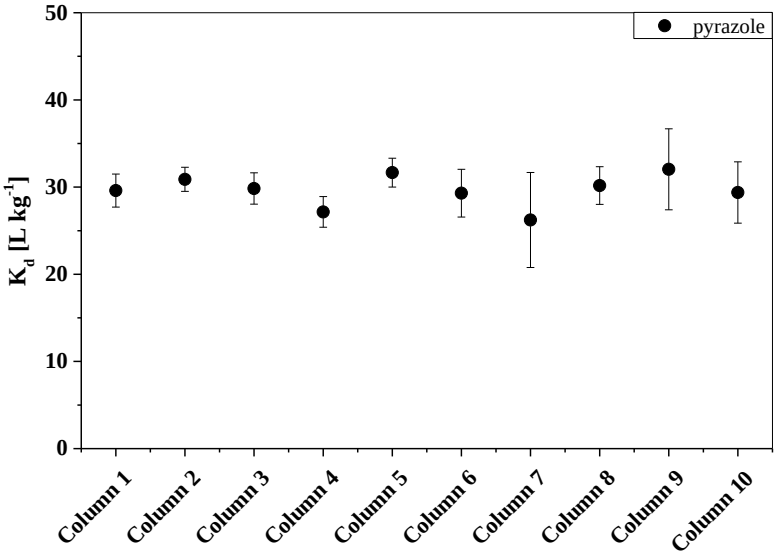

Figure 3.11: Comparison of K_d values determined injecting pyrazole in ten columns packed using the optimized procedure containing 5 % MWCNTs and calculated using D_2O as non-retarded tracer (length: 1.4 cm, diameter: 0.3 cm, eluent: 10 mM $CaCl_2$ with pH 6 at 25 °C, injected concentration of pyrazole: 470 mg L^{-1}, injected concentration of D_2O: 10 vol.-%, injection volume: 5 µL). Error bars represent the maximum error determined via error propagation from the retention times of repeated measurements of sorbates (n=5) as well as tracer (n=10) according to the half-mass point.

Variations in the sorbent content also influence determined K_d values. The more the sorbent is diluted, the stronger can these variations influence in the sorbent content the finally determined K_d values. For this reason, the deviations between columns for Br^- and pyrazole are acceptable and show the general suitability of the optimized method to finally yield columns with well reproducible sorption data using MWCNTs as sorbent.

3.4.3 Determination of local equilibrium in column experiments

To ensure that K_d really describes the equilibrium, measurements using different flow rates were performed. Pyrazole and Br^- are shown here again as reference compounds, but these measurements were done for all compounds presented over the course of this thesis. The dependence of the applied flow rate on the calculated R values for Br^- and pyrazole is shown in figure 3.12.

For both sorbates no dependence of the determined R value on the applied flow rate was observed. R remained almost constant and there was no increase when reaching lower flow rates. Consequently, local equilibrium inside the column could be assumed for both sorbates. That the equilibrium was reached also at the highest tested flow rate of 0.1 mL min^{-1} shows the advantage of the column-based method. One measurement needed in total for

detection of the complete peak including the tailing 30 minutes in case of pyrazole and 10 minutes in case of Br^-. Using the batch approach organic compounds were equilibrated for hours[24] up to weeks[25, 26] depending on the sorbate in literature. For inorganic compounds, equilibrium was reached in 1 hour, but 24 hours were chosen as the equilibration time in case of perchlorate.[21] But even with one hour equilibration time, the column-based method reduces the equilibration time strongly. Additionally, the sorbent demand is reduced strongly as the column can be used several times for different concentrations, while for batch experiments sorbent material is needed for each concentration point to determine an isotherm.

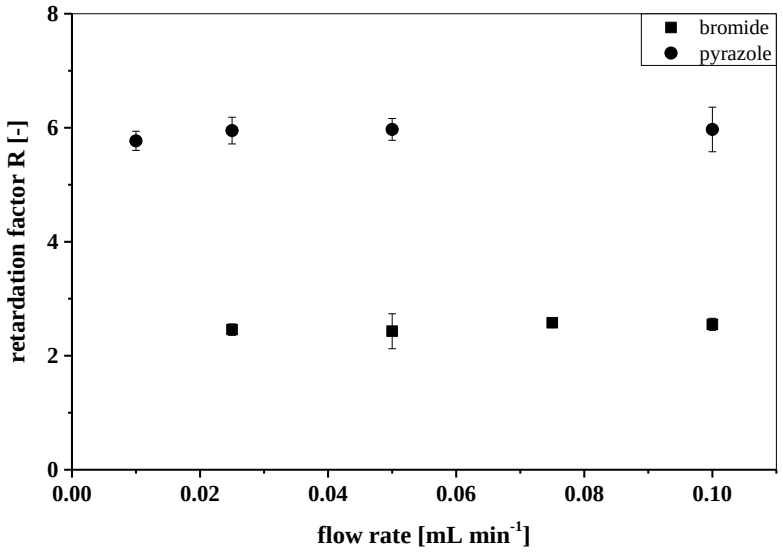

Figure 3.12: Determined retardation factors (R) for pyrazole and bromide for different flow rates using D_2O as non-retarded tracer (length: 1.4 cm, diameter: 0.3 cm, eluent: 10 mM $CaCl_2$ with pH 6 at 25 °C (pyrazole) or 1 mM NaCl with pH 6 at 25 °C (bromide), flow rate: 0.1 mL min^{-1}, injected concentration: 470 mg L^{-1} (pyrazole) and 63 mg L^{-1} (bromide), injection volume: 5 µL). Error bars represent the maximum error determined via error propagation from the retention times of repeated measurements of sorbates (n=5) as well as tracer (n=10) according to the half-mass point.

3.4.5 Comparison of batch and column experiments

Sorption isotherms were derived from column-based measurements for four organic compounds already used in batch experiments using the same sorbent and experimental conditions.[12] Chromatograms recorded for different injected concentrations of 2-chlorophenol are shown in figure 3.13. Measurement time per run was high and the peak showed a pronounced tailing for all injected concentrations. The apex point increased in intensity with increasing injected concentration, but the retention time belonging to the apex point reduced strongly. The same was observed for the retention time belonging to the determined half-mass

point. Similar observations regarding the peak shape and determined half-mass points were made also for the other sorbates (data not shown). This is a clear indication for non-linear sorption as the flow rate had no influence on the determined R value like it was shown in the previous section. Additionally, the Freundlich coefficient (K_f) and Freundlich exponent (n) determined from chromatograms at different flow rates and the same injected concentration using the alternative approach (explained in chapter 3.3.6) showed no dependence on the flow rate (table 3.3 exemplarily for 2-chlorophenol). The Freundlich model was well suitable to describe sorption isotherms as the correlation coefficient (R^2) was >0.99. Only the alternative approach was used here as measurements at different flow rates were only done with one injected concentration. The classical approach would have required several concentrations, which would have increased the necessary time strongly. Consequently, non-equilibrium sorption cannot be the reason for the decreasing retention time and peak tailing because of the almost constant R, K_f, and n values and only non-linear sorption was the reason.

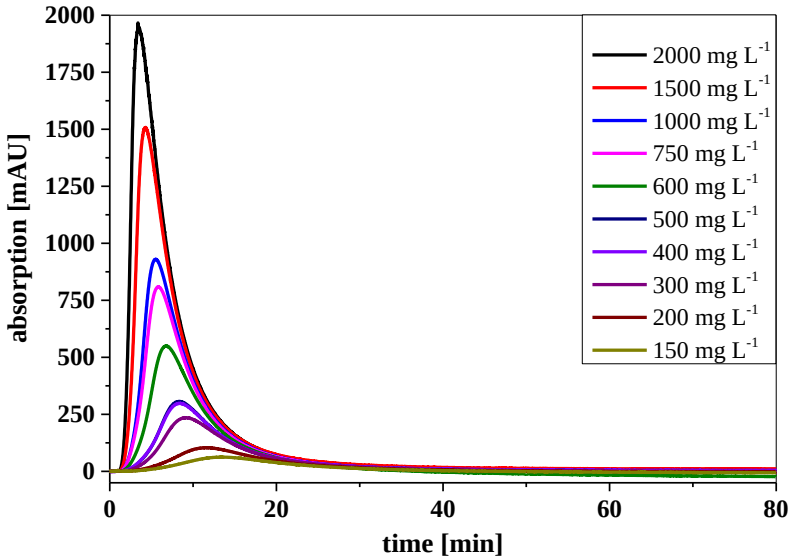

Figure 3.13: Chromatograms of 2-chlorophenol measurements in a column containing 0.5 % MWCNTs (length: 1.4 cm, diameter: 0.3 cm, eluent: 10 mM $CaCl_2$ with pH 6 at 25 °C, flow rate: 0.1 mL min^{-1}, injection volume: 5 µL).

Table 3.3: Freundlich coefficient (K_f) [(mg kg^{-1}) (mg L^{-1})$^{-n}$] and Freundlich exponent (n) [-] derived from chromatograms of 2-chlorophenol at different flow rates using the alternative evaluation approach. Mean values of K_f and n of triplicate measurements are shown with the corresponding standard deviation. The correlation coefficients (R^2) are not shown as they were in all cases > 0.98 indicating the good suitability of the Freundlich model.

flow rate [mL min^{-1}]	K_f	n
0.015 mL min^{-1}	$(1.85 \pm 0.06) \times 10^3$	0.60 ± 0.01
0.025 mL min^{-1}	$(1.89 \pm 0.05) \times 10^3$	0.62 ± 0.02
0.050 mL min^{-1}	$(1.79 \pm 0.03) \times 10^3$	0.57 ± 0.04
0.100 mL min^{-1}	$(1.84 \pm 0.01) \times 10^3$	0.62 ± 0.03

K_f and n for sorption isotherms of the different sorbates according to the classical and alternative approach are shown in table 3.4 in comparison to those values derived in previous batch experiments.[12] R^2 is not shown here, because it was >0.98 showing the suitability of the Freundlich model to describe sorption isotherms derived from chromatograms using both evaluation approaches. K_f and n were derived with the highest flow rate of 0.1 mL min^{-1}. Determined K_f values were for all sorbates larger using the alternative evaluation approach. The deviation to the classical approach is with maximum 30 % relatively small. K_f values from batch experiments are in all cases much higher (up to one order of magnitude) than those from column measurements. The sorption linearity expressed by n is for both evaluation approaches smaller than unity indicating non-linear sorption. The values are also with exception of benzene very similar. For benzene the value corresponding to the alternative approach is with 0.54 much smaller than the value of the classical approach with 0.65. In contrast, n values in batch experiments were much smaller than those from column experiments, while for K_f the opposite was observed. Thus, a much stronger non-linearity was found in batch experiments. It can be concluded that both evaluation approaches for column experiments yield almost the same results, while comparison of batch and column experiments showed larger deviations.

Table 3.4: Freundlich coefficient (K_f) [(mg kg^{-1}) (mg $L^{-1})^{-n}$] and Freundlich exponent (n) [-] derived from chromatograms using classical and the alternative evaluation approach in comparison to those values from batch sorption experiments from literature.[12] The correlation coefficients (R^2) is not shown as they were in all cases > 0.98 indicating the good suitability of the Freundlich model.

sorbate	column classical approach		column alternative approach		batch approach	
	K_f	n	K_f	n	K_f	n
anisole	(1.15 ± 0.01) × 10^3	0.64 ± 0.01	(1.30 ± 0.01) × 10^3	0.62 ± 0.01	(3.70 ± 0.05) × 10^3	0.32 ± 0.02
benzene	(2.71 ± 0.01) × 10^2	0.65 ± 0.01	(3.66 ± 0.01) × 10^2	0.54 ± 0.01	(1.82 ± 0.04) × 10^3	0.51 ± 0.02
2-chlorophenol	(1.38 ± 0.01) × 10^3	0.65 ± 0.02	(1.70 ± 0.01) × 10^3	0.58 ± 0.01	(1.13 ± 0.03) × 10^4	0.38 ± 0.01
indole	(5.18 ± 0.02) × 10^3	0.63 ± 0.02	(6.18 ± 0.02) × 10^3	0.58 ± 0.01	(8.47 ± 0.02) × 10^3	0.26 ± 0.02

The small deviation between both evaluation approaches of the column method can also be seen when comparing K_d values calculated for different aqueous concentrations in equilibrium ($c_{w,eq}$) ranging between 1 % and 0.01 % of the maximum solubility of the sorbate in water based on K_f and n (maximum solubility in water: anisole 1040 mg L^{-1}, benzene 1790 mg L^{-1}, 2-chlorophenol 11300 mg L^{-1}, indole 3560 mg L^{-1}). This is shown in figure 3.14 for 1 % of the maximum solubility in water while 0.1 % and 0.01 % are shown in figures S3.9 and S3.10, respectively, in chapter 3.6. K_d values of the classical and alternative approach were at all three concentration levels within 0.2 log units deviation, which is less than a factor of two and an acceptable deviation. Deviations to batch data were bigger. While for anisole the deviation was also less than 0.2 log units at 1 %, the deviation was bigger for the other compounds with a maximum of about 0.7 log units for benzene. With decreasing relative concentration, deviation increased for anisole and 2-chlorophenol. For benzene, deviation stayed almost the same for all three concentration levels. For anisole, benzene, and 2-chlorophenol, column derived K_d values were always smaller than those from batch experiments. For indole a different relationship was observed. While column derived K_d values were bigger than those of batch experiments at 1 %, they were smaller than batch derived data at 0.01 %. At 0.1 % values from batch and column experiments were very similar with less than 0.1 log unit deviation. Reason for this behavior is the different linearity of the

isotherms resulting in an intersection of the isotherms (figure S3.11 in chapter 3.6). At and very close to the intersection of the different isotherms, K_d values calculated using these isotherms will be similar as it was found here for 0.1 %. Consequently, there was no general trend in the comparability and deviation of K_d values derived from batch and column experiments.

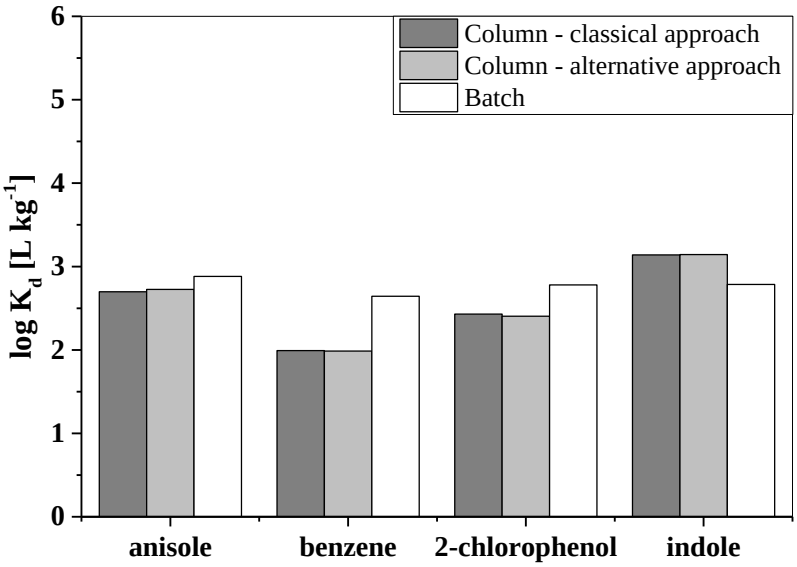

Figure 3.14: Comparison of K_d values calculated using the isotherms mentioned in table 3.4 for 1 % of the maximum solubility of the sorbate in water.

Deviations between batch and column sorption data are often reported in literature for different sorbents,[27-30] but also good agreement between both methods was reported.[27, 31] Consequently, there is also in literature no conclusive trend available. Reasons for deviations between batch and column methods mentioned in literature are manifold. For batch and column experiments non-equilibrium was mentioned to be a possible reason for deviations between both techniques.[31] However, reduced sorption in column measurements might be the consequence of no local equilibrium inside the column. As no such observation could be made in this study using measurements at different flow rates it is not likely to be the main reason. Furthermore, loss of sorbent material from the column may be responsible for lower values in column experiments.[30, 31] Particles of the sorbents were larger than the sieves at the column outlet so that the sorbent should stay fixed in the column. In the effluent of the column during packing no MWCNTs could be detected using the absorbance at 800 nm[32] so that a loss of sorbent is unlikely. Channeling and preferential flow regions at the column wall also lead to reduced sorption,[27, 31] but as particle size was smaller than 1/30 of the column diameter these phenomena should not be relevant.[33] Larger particles may lead to differences in the effective porosity and generate channels or the so-called wall effects. Another reason for reduced sorption in column experiments may be the absence of a non-retarded tracer. This

would lead to reduced sorption data as already the tracer would be retarded by the sorbent.[30] Consequently, a real "blank" value would be missing. This is very unlikely in this study as the porosity and peak characteristics of D_2O are in a possible range for a non-retarded tracer. Deviations in sorption data between batch and column like for example observed for benzene in this study were so big that it is very unlikely to originate just from a potentially retarded tracer. Also, a too high detection limit of the detector leading to an incomplete recovery of the tailing was mentioned as potential reason for reduced sorption in column experiments. As the recovery was quantitative in comparison to injections without column (recovery > 80 %) a strong influence of incomplete tailing recovery is unlikely.

The most likely reasons for differences between batch and column experiments are the very different sorbent to solution ratios, the investigated concentrations, and differences in the available surface area. The sorbent to solution ratio in column and batch techniques was strongly different, which was also mentioned in literature as potential reason for deviations.[34] While in batch experiments of a previous study the concentration of MWCNTs was between 100 and 500 mg L^{-1},[12] it was about 12500 mg L^{-1} in column experiments with approximately 0.75 mg MWCNTs present in one column (0.5 % MWCNTs in about 150 mg of packing material present in one column) being in contact with approximately 60 µL of solution. This large deviation may result in differences in total sorption observed during sorption experiments. Although the total concentration of sorbent is higher for the column experiments, sorption may be lower because of a high concentration of the sorbate moving through the column after the injection. The sorbate is inside the column not directly in contact with the whole sorbent amount present in the column and the injected concentration in column experiments was much higher than the initial concentration in batch experiments. The injected concentration was in case of 2-chlorophenol up to 2000 mg L^{-1}, while the initial concentration was only 50 mg L^{-1} in batch experiments. Due to the larger concentration in column experiments, competition for sorption sites while moving along the column may be bigger as well, leading to lower sorption derived from column experiments. Furthermore, the available surface area may be lower in column experiments as the direct contact between particles inside the column may block sorption sites.[35] In batch experiments, sorption sites are not blocked due to direct particle contact as the system is continuously mixed. This complete mixing of the sorbent with the sorbate in batch experiments and the completely different mixing in column experiments was also mentioned as potential reason for differences previously.[36]

Overall, after optimization of the packing procedure it was possible to reproducibly pack columns containing only quartz or a mixture of quartz and MWCNTs as the main sorbent of this study. Regular increases in flow rate, avoidance of tapping the column walls and a long time at the maximum flow are very important to pack homogenous columns as indicated by symmetrical peaks for the tracer. Dilution with quartz was necessary for columns containing MWCNTs as sorbent to avoid column clogging. D_2O could be identified as only compound tested in this study suitable as non-retarded tracer for columns containing also MWCNTs, while for quartz columns also other compounds can be used recognizing possible pore exclusion of charged tracers due to electrostatic repulsion or exclusion from pores. Although large deviations were determined between the column and batch technique for selected compounds due to the different methodology, it is still suitable for the fast determination of parameters influencing sorption as it was shown for the influence of ionic strength on sorption of inorganic anions. The influence of environmental conditions on sorption will be shown more in detail in **Chapters 4 and 5** for inorganic and organic sorbates, respectively. Time for sorption experiments and potentially also the sorbent demand can be reduced strongly applying the column-based method and the alternative evaluation approach. Three repeated injections need approximately four hours of strongly sorbing organic compound like 2-chlorophenol in the column approach, while isotherm determination using the batch approach needed approximately eight days including preparation, equilibration and measurement.[12] Knowing about the deviations between batch and column experiments for some compounds, values derived from column experiments can still be used as fast approximation when no sorption data are available like in case of polar heterocyclic organic compounds, which are used as sorbates in **Chapter 5**. The method optimized for non-functionalized MWCNTs will also be transferred to other CNMs like functionalized MWCNTs, graphene nanosheets and classical sorbents like activated carbons, which will be shown in **Chapter 6**.

3.5 References

1. Bi, E. P.; Schmidt, T. C.; Haderlein, S. B. Practical issues relating to soil column chromatography for sorption parameter determination. *Chemosphere* **2010,** 80 (7), 787-793.
2. Bi, E. Sorption and transport of heterocyclic aromatic compounds in soils. Tübingen University, Tübingen, Germany, 2006.
3. Miyabe, K.; Guiochon, G. Peak tailing and column radial heterogeneity in linear chromatography. *Journal of Chromatography A* **1999,** 830 (2), 263-274.
4. Kromidas, S., *Practical Problem Solving in HPLC*. Wiley-VCH: Weinheim, Germany, 2000.
5. Fesch, C.; Simon, W.; Haderlein, S. B.; Reichert, P.; Schwarzenbach, R. P. Nonlinear sorption and nonequilibrium solute transport in aggregated porous media: Experiments, process identification and modeling. *Journal of Contaminant Hydrology* **1998,** 31 (3-4), 373-407.
6. Yaron, B.; Bresler, E.; Shalhevet, J. A method for uniform packing of soil columns. *Soil Science* **1966,** 101 (3), 205-209.
7. Bi, E.; Schmidt, T. C.; Haderlein, S. B. Sorption of heterocyclic organic compounds to reference soils: Column studies for process identification. *Environmental Science & Technology* **2006,** 40 (19), 5962-5970.
8. Hüffer, T.; Osorio, X. L.; Jochmann, M. A.; Schilling, B.; Schmidt, T. C. Multi-walled carbon nanotubes as sorptive material for solventless in-tube microextraction (ITEX2) - a factorial design study. *Analytical and Bioanalytical Chemistry* **2013,** 405 (26), 8387-8395.
9. Lu, C. Y.; Chiu, H. S. Adsorption of zinc(II) from water with purified carbon nanotubes. *Chemical Engineering Science* **2006,** 61 (4), 1138-1145.
10. Bi, E.; Schmidt, T. C.; Haderlein, S. B. Environmental factors influencing sorption of heterocyclic aromatic compounds to soil. *Environmental Science & Technology* **2007,** 41 (9), 3172-3178.
11. Li, B. H.; Qian, Y. A.; Bi, E. P.; Chen, H. H.; Schmidt, T. C. Sorption behavior of phthalic acid esters on reference soils evaluated by soil column chromatography. *Clean-Soil Air Water* **2010,** 38 (5-6), 425-429.
12. Hüffer, T.; Endo, S.; Metzelder, F.; Schroth, S.; Schmidt, T. C. Prediction of sorption of aromatic and aliphatic organic compounds by carbon nanotubes using poly-parameter linear free-energy relationships. *Water Research* **2014,** 59, 295-303.
13. Schenzel, J.; Goss, K. U.; Schwarzenbach, R. P.; Bucheli, T. D.; Droge, S. T. J. Experimentally determined soil organic matter-water sorption coefficients for different classes of natural toxins and comparison with estimated numbers. *Environmental Science & Technology* **2012,** 46 (11), 6118-6126.
14. Droge, S.; Goss, K. U. Effect of sodium and calcium cations on the ion-exchange affinity of organic cations for soil organic matter. *Environmental Science & Technology* **2012,** 46 (11), 5894-5901.
15. Bucheli, T. D.; Gustafsson, O. Soot sorption of non-ortho and ortho substituted PCBs. *Chemosphere* **2003,** 53 (5), 515-522.
16. Bürgisser, C. S.; Cernik, M.; Borkovec, M.; Sticher, H. Determination of nonlinear adsorption-isotherms from column experiments - an alternative to batch studies. *Environmental Science & Technology* **1993,** 27 (5), 943-948.
17. Miyabe, K.; Guiochon, G. Influence of column radial heterogeneity on peak fronting in linear chromatography. *Journal of Chromatography A* **1999,** 857 (1-2), 69-87.
18. Kirkland, J. J.; DeStefano, J. J. The art and science of forming packed analytical high-performance liquid chromatography columns. *Journal of Chromatography A* **2006,** 1126 (1-2), 50-57.

19. Das, B. S.; Lee, L. S.; Rao, P. S. C.; Hultgren, R. P. Sorption and degradation of steroid hormones in soils during transport: Column studies and model evaluation. *Environmental Science & Technology* **2004,** 38 (5), 1460-1470.
20. Bronner, G.; Goss, K. U. Sorption of organic chemicals to soil organic matter: influence of soil variability and pH dependence. *Environmental Science & Technology* **2011,** 45 (4), 1307-1312.
21. Fang, Q. L.; Chen, B. L. Adsorption of perchlorate onto raw and oxidized carbon nanotubes in aqueous solution. *Carbon* **2012,** 50 (6), 2209-2219.
22. Ansari, M.; Kazemipour, M.; Dehghani, M. The defluoridation of drinking water using multi-walled carbon nanotubes. *Journal of Fluorine Chemistry* **2011,** 132 (8), 516-520.
23. Zong, E. M.; Wei, D.; Huan, Z. K.; Peng, D.; Wan, H. Q.; Zheng, S. R.; Xu, Z. Y. Adsorption of phosphate by zirconia functionalized multi-walled carbon nanotubes. *Chinese Journal of Inorganic Chemistry* **2013,** 29 (5), 965-972.
24. Yu, F.; Ma, J.; Wu, Y. Q. Adsorption of toluene, ethylbenzene and m-xylene on multi-walled carbon nanotubes with different oxygen contents from aqueous solutions. *Journal of Hazardous materials* **2011,** 192 (3), 1370-1379.
25. Kah, M.; Zhang, X. R.; Jonker, M. T. O.; Hofmann, T. Measuring and modelling adsorption of PAHs to carbon nanotubes over a six order of magnitude wide concentration range. *Environmental Science & Technology* **2011,** 45 (14), 6011-6017.
26. Chen, W.; Duan, L.; Zhu, D. Q. Adsorption of polar and nonpolar organic chemicals to carbon nanotubes. *Environmental Science & Technology* **2007,** 41 (24), 8295-8300.
27. Plassard, F.; Winiarski, T.; Petit-Ramel, M. Retention and distribution of three heavy metals in a carbonated soil: comparison between batch and unsaturated column studies. *Journal of Contaminant Hydrology* **2000,** 42 (2-4), 99-111.
28. Maraqa, M. A.; Zhao, X.; Wallace, R. B.; Voice, T. C. Retardation coefficients of nonionic organic compounds determined by batch and column techniques. *Soil Science Society of America Journal* **1998,** 62 (1), 142-152.
29. Goel, J.; Kadirvelu, K.; Rajagopal, C.; Garg, V. K. Removal of lead(II) by adsorption using treated granular activated carbon: Batch and column studies. *Journal of Hazardous materials* **2005,** 125 (1-3), 211-220.
30. Macintyre, W. G.; Stauffer, T. B. Liquid-chromatography applications to determination of sorption on aquifer materials. *Chemosphere* **1988,** 17 (11), 2161-2173.
31. Macintyre, W. G.; Stauffer, T. B.; Antworth, C. P. A comparison of sorption coefficients determined by batch, column and box methods on a low organic-carbon aquifer material. *Ground Water* **1991,** 29 (6), 908-913.
32. Kah, M.; Zhang, X. R.; Hofmann, T. Sorption behavior of carbon nanotubes: Changes induced by functionalization, sonication and natural organic matter. *Science of the Total Environment* **2014,** 497, 133-138.
33. Relyea, J. F. Theoretical and experimental considerations for the use of the column method for determining retardation factors. *Radioact. Waste Manage. Nucl. Fuel Cycle* **1982,** 3 (2), 151-166.
34. Karickhoff, S. W.; Morris, K. R. Sorption dynamics of hydrophobic pollutants in sediment suspensions. *Environmental Toxicology and Chemistry* **1985,** 4 (4), 469-479.
35. Celorie, J. A.; Woods, S. L.; Vinson, T. S.; Istok, J. D. A comparison of sorption equilibrium distribution coefficients using batch and entrifugation methods. *Journal of Environmental Quality* **1989,** 18 (3), 307-313.
36. Schweich, D.; Sardin, M.; Gaudet, J. P. Measurements of a cation-exchange isotherm from elution curves obtained in a soil column - preliminary-results. *Soil Science Society of America Journal* **1983,** 47 (1), 32-37.

3.6 Appendix to Chapter 3

Table S3.1: Determined properties of the pristine and ground MWCNTs.

	native material	ground material
specific surface area [m^2 g^{-1}][1]	211	228
C−C content [%][2]	75.23	74.91
C−O- content [%][2]	10.40	10.66
C=O content [%][2]	0.97	0.97
COOH content [%][2]	5.23	5.43
π-π* content [%][2]	8.17	8.03

[1)] determined using BET-measurements; [2)] relative content of functional groups under the C1s-peak were determined by XPS-measurements.

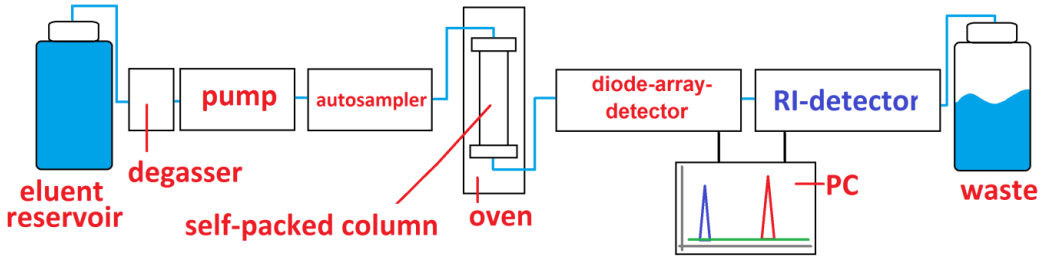

Figure S3.1: Schematic representation of the HPLC-system used in sorption studies.

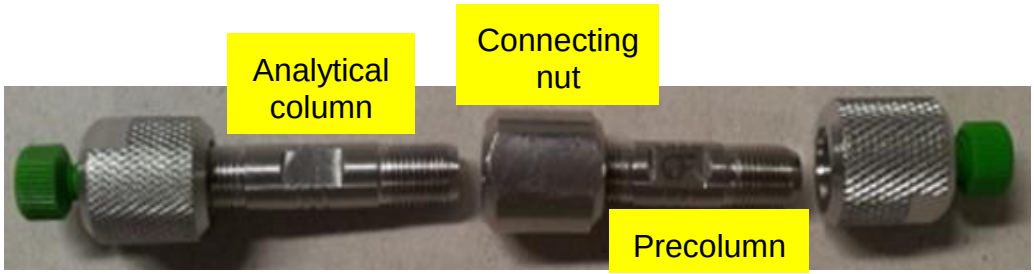

Figure S3.2: Assembly of column and precolumn used for column packing connected with the connecting nut.

Table S3.2: Calibrations of different sorbates used in this study (anisole, benzene, 2-chlorophenol, and indole) to calculate dissolved liquid concentration in equilibrium ($c_{w,eq}$) for isotherm calculation (10 mM $CaCl_2$, pH 6).

compound name	slope [mAU L mg^{-1}]	y-intercept [mAU]	R^2 [-]
anisole	58.2	5.2	0.9996
benzene	85.2	-1.2	0.9994
2-chlorophenol	173.2	4.0	0.9998
indole	299.5	2.0	0.9999

Figure S3.3 shows stepwise the procedure used for isotherm construction according to the classical approach adapted from Schenzel *et al.*[1]

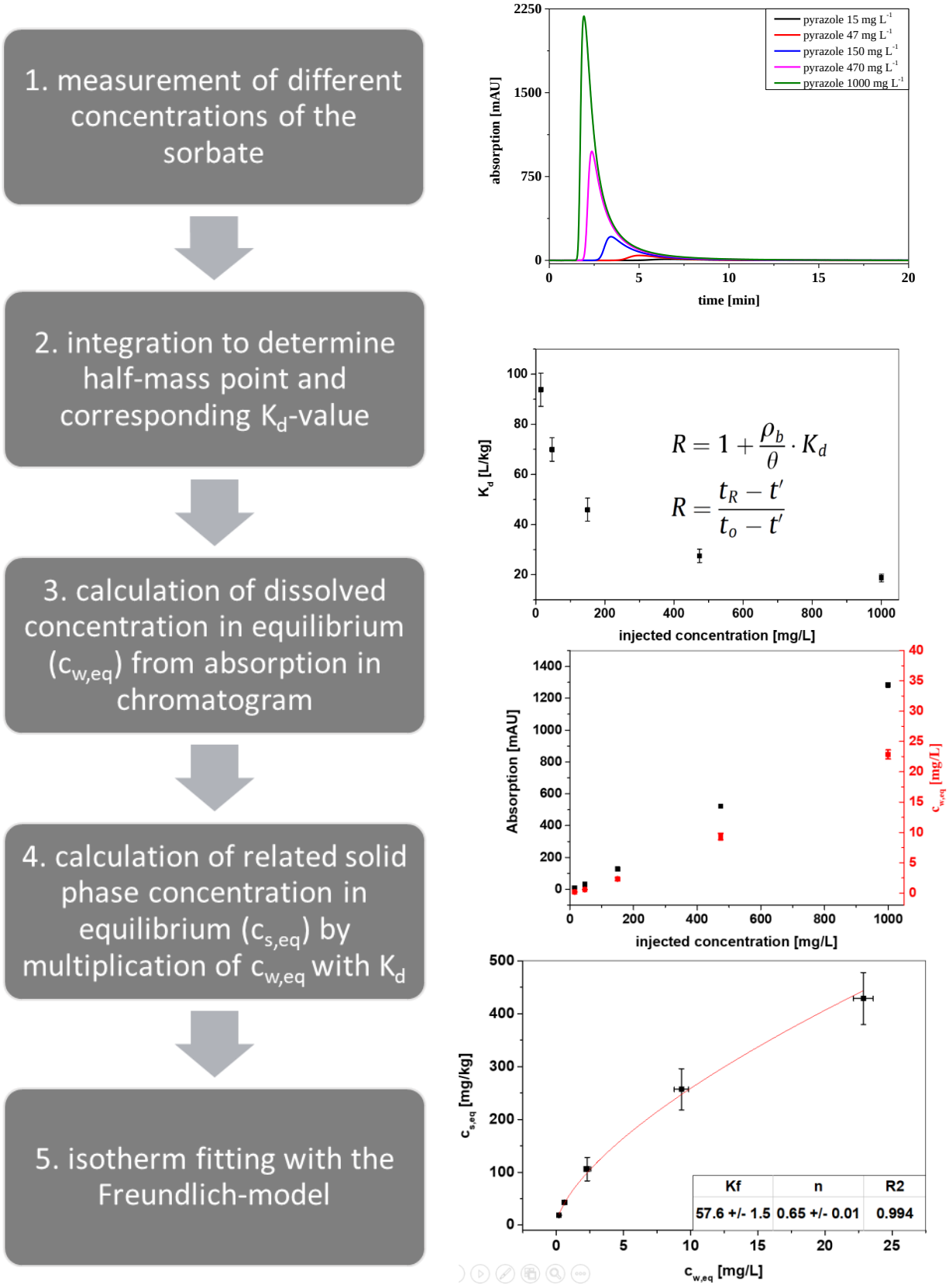

Figure S3.3: Schematic stepwise representation used for isotherm generation according to the classical approach adapted from Schenzel *et al.*[1]

Figure S3.4 shows stepwise the procedure used for isotherm construction according to the alternative approach adapted from Bürgisser *et al.*[2]

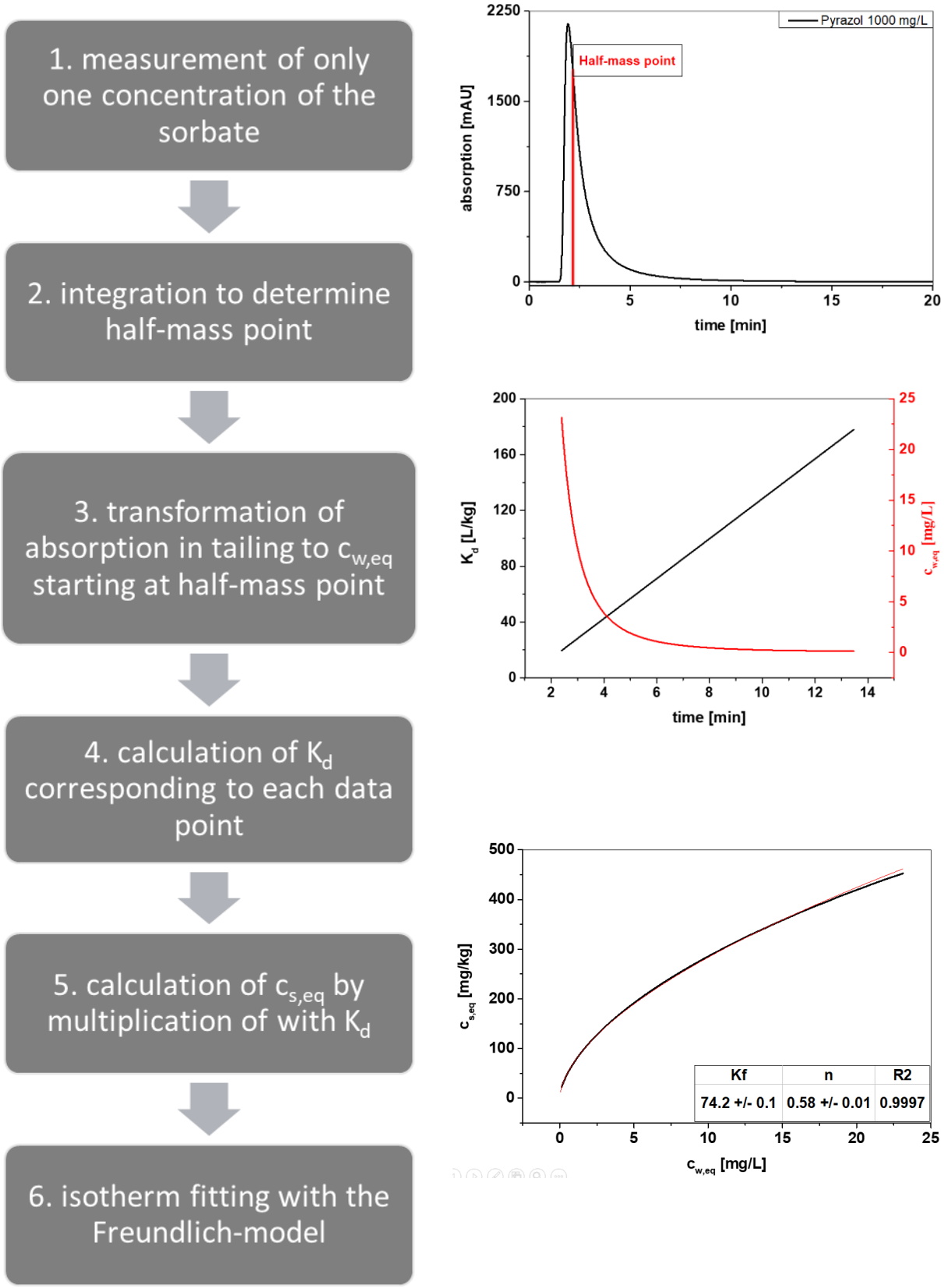

Figure S3.4: Schematic stepwise representation used for isotherm generation according to the alternative approach adapted from Bürgisser *et al.*[2]

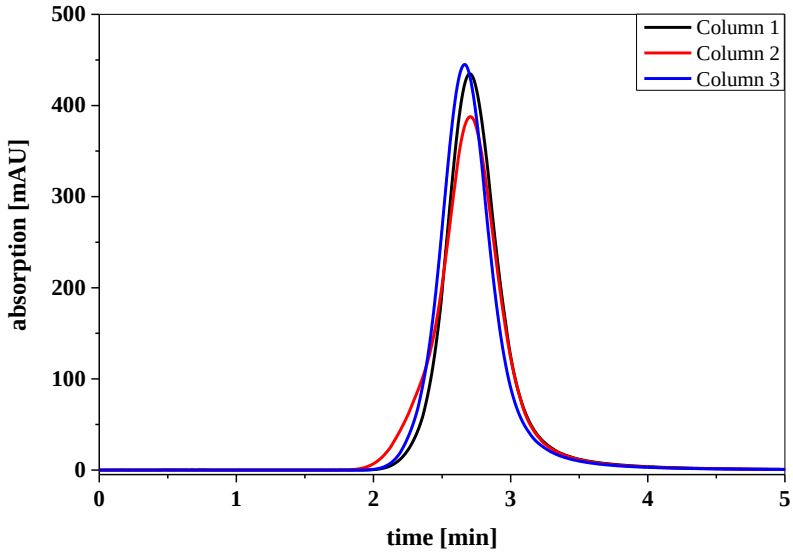

Figure S3.5: Chromatograms of THS in columns packed with exclusively quartz applying the optimized method (length: 5.3 cm, diameter: 0.3 cm, flow rate: 0.1 mL min^{-1}, eluent: ultrapure water with pH 6, injected concentration of THS: 30 mg L^{-1}, injection volume: 5 µL).

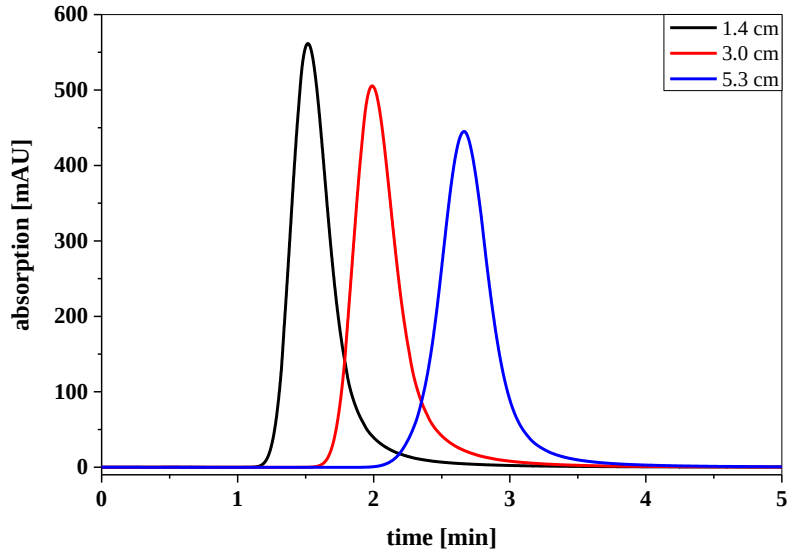

Figure S3.6: Chromatograms of THS in columns packed with exclusively quartz applying the optimized method (length: 1.4, 3.0, or 5.3 cm, diameter: 0.3 cm, flow rate: 0.1 mL min^{-1}, eluent: ultrapure water with pH 6, injected concentration of THS: 30 mg L^{-1}, injection volume: 5 µL).

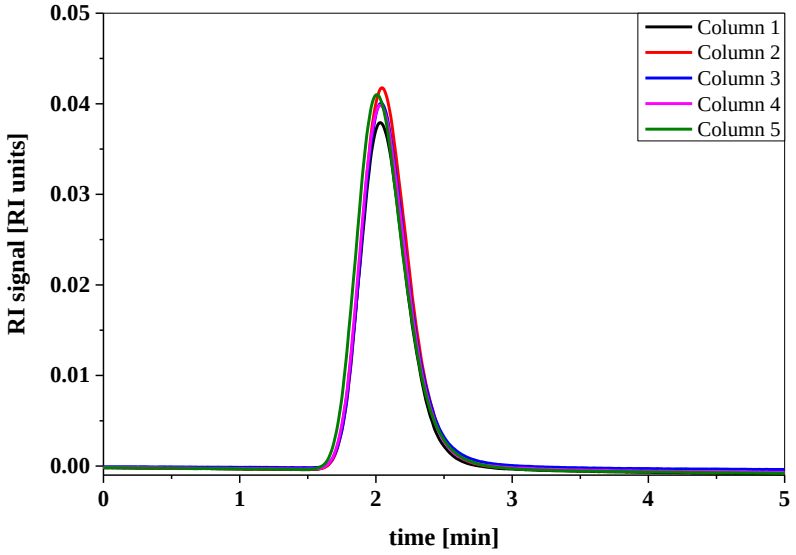

Figure S3.7: Chromatograms of D_2O in columns packed with 5 % MWCNTs and 95 % quartz applying the optimized method (length: 1.4 cm, diameter: 0.3 cm, flow rate: 0.1 mL min^{-1}, eluent: ultrapure water with pH 6, injected concentration of D_2O: 10 vol.-%, injection volume: 5 µL).

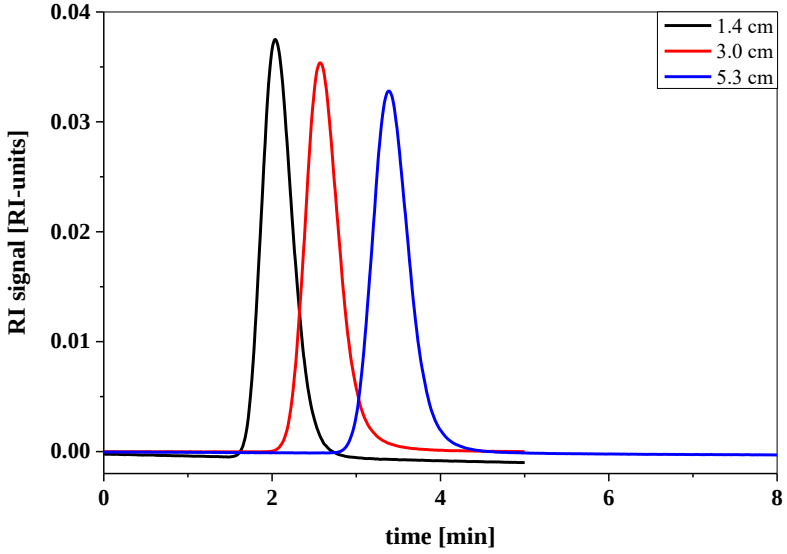

Figure S3.8: Chromatograms of D_2O in columns packed with 5 % MWCNTs and 95 % quartz applying the optimized method (length: 1.4, 3.0, or 5.3 cm, diameter: 0.3 cm, flow rate: 0.1 mL min^{-1}, eluent: ultrapure water with pH 6, injected concentration of D_2O: 10 vol.-%, injection volume: 5 µL).

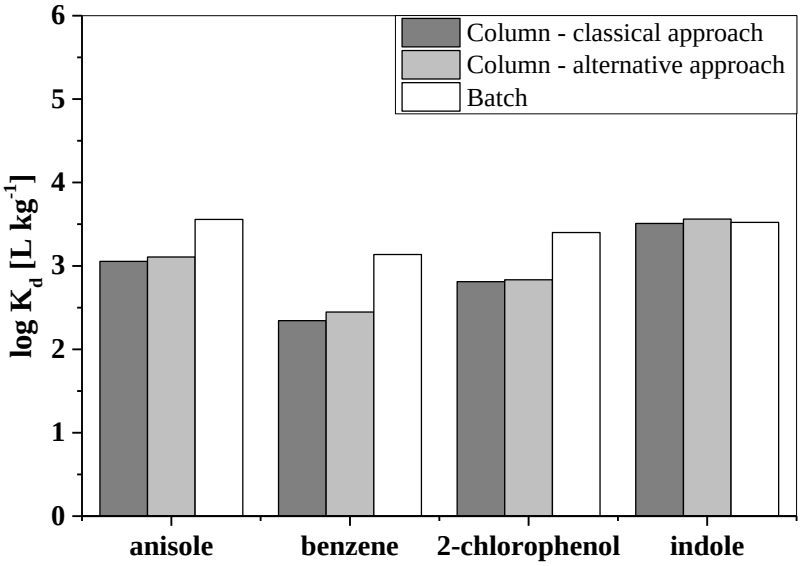

Figure S3.9: Comparison of K_d values calculated using the isotherms mentioned in table 3.4 for 0.1 % of the maximum solubility of the sorbate in water.

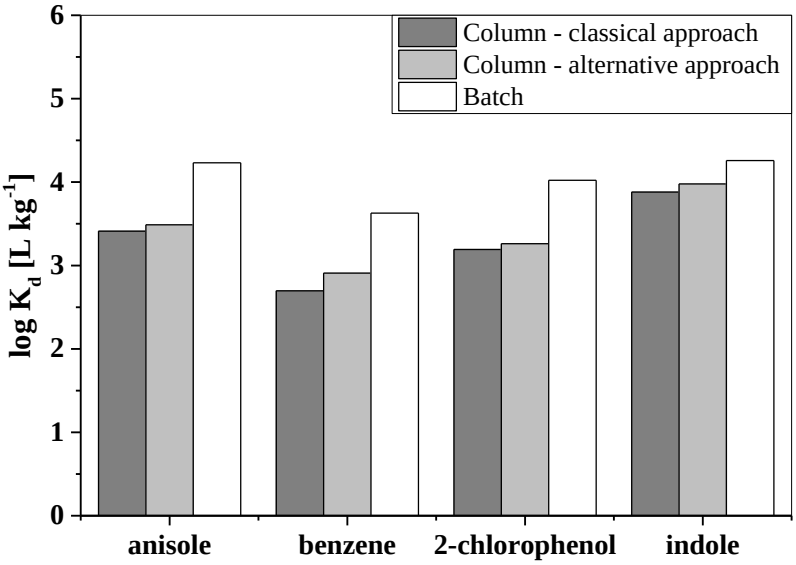

Figure S3.10: Comparison of K_d values calculated using the isotherms mentioned in table 3.4 for 0.01 % of the maximum solubility of the sorbate in water.

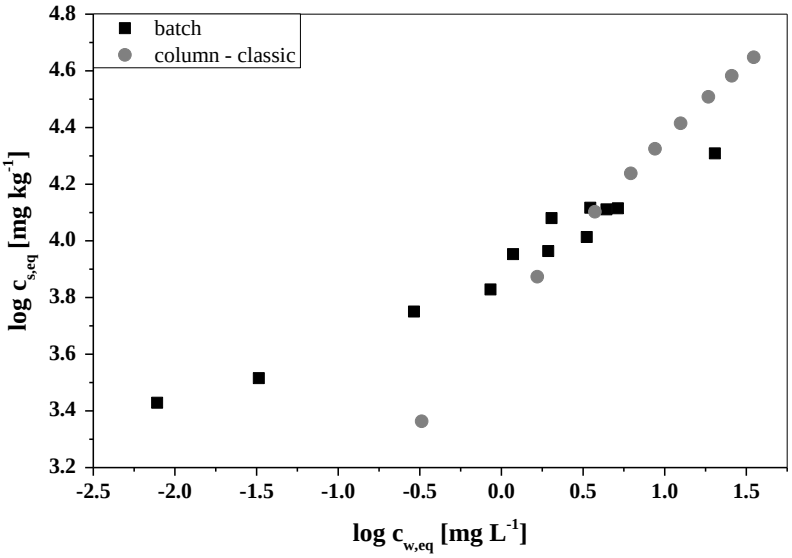

Figure S3.11: Comparison of an isotherm of indole derived with the classical approach from column experiments to an isotherm of indole from batch experiments.[3]

References Appendix to Chapter 3

1. Schenzel, J.; Goss, K. U.; Schwarzenbach, R. P.; Bucheli, T. D.; Droge, S. T. J. Experimentally determined soil organic matter-water sorption coefficients for different classes of natural toxins and comparison with estimated numbers. *Environmental Science & Technology* **2012,** 46 (11), 6118-6126.
2. Bürgisser, C. S.; Cernik, M.; Borkovec, M.; Sticher, H. Determination of nonlinear adsorption-isotherms from column experiments - an alternative to batch studies. *Environmental Science & Technology* **1993,** 27 (5), 943-948.
3. Hüffer, T.; Endo, S.; Metzelder, F.; Schroth, S.; Schmidt, T. C. Prediction of sorption of aromatic and aliphatic organic compounds by carbon nanotubes using poly-parameter linear free-energy relationships. *Water Research* **2014,** 59, 295-303.

Chapter 4 - Influence of environmental conditions on sorption of inorganic anions

Adapted from: Metzelder, F.; Schmidt, T.C. Environmental conditions influencing sorption of inorganic anions to multiwalled carbon nanotubes studied by column chromatography. *Environmental Science & Technology*, **2017**, 51(9), 2928 – 2935.

4.1 Abstract

Sorption to carbon-based nanomaterials is typically studied in batch experiments. An alternative method offering advantages to study sorption is column chromatography. Sorbent packed columns are used and sorption data are determined by relating sorbate retention to that of a non-retarded tracer.

In this study, column chromatography is applied for the first time to study the influence of environmental conditions on sorption of inorganic anions (bromide, nitrite, nitrate and iodide) to multiwalled carbon nanotubes. Deuterium oxide was used as non-retarded tracer.

Sorption isotherms were best described by the Freundlich model. Sorption increased in the order bromide < nitrite < nitrate < iodide. Increasing ionic strength from 1 mM to 100 mM sodium chloride significantly reduced or completely suppressed sorption (bromide, nitrite) due to competition with chloride. pH strongly affected sorption as negatively charged analytes were attracted by the positively charged surface at pH 3. At pH > 4.5 the surface charge was negative, but sorption was still detectable at pH 6 and 9. Consequently, other forces than electrostatic attraction contributed to sorption. These forces may include H-bonding as indicated by sorption enthalpy determined by variation of column temperature. Overall, column chromatography represents a promising complement in sorption studies to reveal sorbent properties.

4.2 Introduction

Since the discovery of carbon-based nanomaterials (CNMs), research in different areas has explored their properties and potential applications. Carbon nanotubes (CNTs) as one class of CNMs have been tested in medicine,[1] physics,[2] material sciences[3, 4] and chemistry.[5-7] In chemistry, research is focused on sorption properties of these materials, because they exhibit strong sorption for different compound classes. Multiwalled carbon nanotubes (MWCNTs) have been used as solid phase extraction material for organic[5] and inorganic compounds.[6, 7] Sorption properties of MWCNTs have already been characterized allowing a prediction of sorption strength of these materials for organic compounds,[8, 9] but these models are only valid for one setup of environmental conditions. Environmental parameters like pH, ionic strength and temperature influence sorption properties of CNMs and sorbates[10] so that these models may be insufficient to predict sorption at different environmental conditions.

Sorption studies on CNMs are typically conducted in batch experiments for organic[11-17] and inorganic compounds.[18-22] Different equilibration times have been applied in literature varying from hours[23] to weeks[11, 12] in case of organic compounds. This increases the time expenses to study the influence of environmental conditions on sorption. Additionally, for weakly sorbing and highly soluble compounds like inorganic anions, it may be difficult to obtain reliable sorption data in batch experiments, because of the limited sorbent to solution ratio.[24] As the price of CNMs can be very high, the application of high amounts should be avoided, which may be necessary in case of those compounds. Furthermore, phase separation of CNMs from the water phase may be a critical step, especially in case of dispersed materials[25, 26] where classical techniques like sedimentation or filtration can be insufficient.[11]

Alternatively, column experiments can be used to study sorption and determine distribution coefficients (K_d) using the retardation of the sorbate in relation to a non-retarded tracer in a column packed with the sorbent. Chromatographic columns have been successfully used for sorption studies to soot particles,[27] soils[24, 28-35] or mineral surfaces,[36, 37] but applications for sorption studies on CNMs have not been reported so far. Column experiments offer the advantage of higher sorbent to solution ratios enabling the analysis of weakly sorbing and highly soluble compounds without the need of large amounts of sorbent material. The influence of environmental conditions can be analyzed by changing the composition of the mobile phase regarding ionic strength, type of ions and pH or by changing the temperature using a column thermostat. As the sorbent is fixed in the column, additional equipment like centrifuges can be avoided. Disadvantages may be column clogging leading to very high

backpressure and destruction of the column or too strong sorption causing long retention times and deterioration of the signal by peak broadening. These disadvantages have been suppressed by the addition of inert material like quartz[24, 32] or silicium carbide,[29] which do not show any interaction with the sorbates. Additionally, use of inert material reduces the sorbent demand, which is interesting in case of expensive or limited sorbent materials. Concomitant, column stability is increased and retention times are reduced.

Sorption hysteresis may hinder the application of column chromatography to CNMs. Incomplete desorption from CNMs has already been shown for some organic analytes in batch experiments[38-40] indicated by differences between the sorption and desorption isotherm. Desorption is a prerequisite in column experiments using Dirac input (i.e. injection of a pulse of the sorbate instead of a continuous input), because no signal can be recorded in the chromatogram without desorption. In case of incomplete desorption, material properties may be altered due to molecules permanently bound to the surface changing interactions between sorbent surface and sorbate molecules. For breakthrough curves instead of Dirac input, sorption hysteresis presents a minor problem, but each column could only be used for one compound and one concentration, because the sorbent surface would not be pristine for a second consecutive measurement as sorbate molecules remain sorbed onto the surface.

Thus, the aim of this study was to investigate sorption to MWCNTs as one representative class of CNMs for the first time using column chromatography and to identify the influence of environmental conditions like temperature, ionic strength, and pH on sorption of inorganic anions as test compounds. Inorganic anions were chosen as they have been shown in literature to be hardly sorbing to CNTs in batch experiments demanding larger amounts of CNMs.[18]

4.3 Materials and Methods

4.3.1 Chemicals and Packing Materials

Chemicals used in this study were hydrochloric acid (HCl) (37 %, analytical grade, Fisher Scientific), perchloric acid (70 %, analytical grade, AppliChem Panreac), sodium chloride (NaCl) (≥ 99.5 %, Bernd Kraft GmbH), calcium chloride ($CaCl_2 \times 2\ H_2O$) (≥ 99.5 %, AppliChem Panreac), sodium bromide (NaBr) (≥ 99 %, Fluka), sodium iodide (NaI) (≥ 99.5 %, Sigma-Aldrich), sodium nitrite ($NaNO_2$) (≥ 99 %, Sigma-Aldrich), sodium nitrate ($NaNO_3$) (≥ 99.5 %, Riedel-de Häen) and deuterium oxide (D_2O) (≥ 99.9 atom-%, Sigma-Aldrich). Eluents for high performance liquid chromatography (HPLC) were prepared with

ultrapure water and addition of appropriate amounts of salts, acid or base to reach the desired concentrations or pH-value (18.2 MΩ cm^{-1} resistance, PURELAB Ultra, ELGA LabWater, Celle, Germany). Individual stock solutions of each analyte (bromide (Br^-), nitrite (NO_2^-), nitrate (NO_3^-), iodide (I^-)) containing 2 g L^{-1} and dilutions were prepared in the respective eluent used for measurements and stored at 4 °C in the dark.

Detailed information on the packing materials used in this chapter (MWCNTs and quartz) are mentioned in chapter 3.3.1.

4.3.2 Material characterization

Specific surface area was determined by Brunauer-Emmett-Teller N_2 method using a pore size analyzer (SA Coulter 3100, Beckman Coulter GmbH, Krefeld, Germany). Zeta potential measurements of MWCNTs were conducted using a Zeta potential/particle Sizer (NICOMP 380 ZLS, PSS-NICOMP Particle sizing systems, Santa Barbara (California), USA) by dispersing MWCNTs using ultrasonication in ultrapure water adjusted with HCl or NaOH to the desired pH value. VersoProbe II (Ulvac-Phi Inc., Kanagawa, Japan) equipped with a monochromatic Al-k(alpha) source in an angle of 45° between probe and analyzer was used to perform X-ray photoelectron spectroscopy (XPS)-measurements. Measurements were done at room temperature. Data evaluation was done using CasaXPS.

4.3.3 Apparatus

Detailed information on empty HPLC-columns and additional equipment used for column packing is mentioned in chapter 3.3.2. All experiments were conducted using the Knauer HPLC-system described also in chapter 3.3.2.

4.3.4 Column chromatography

Columns were packed with the procedure developed in chapter 3.4.1, which is summarized with the final workflow in chapter 4.6 (section SI4.1). Characteristics of the columns prepared und used in this chapter are given in chapter 4.6 (table S4.2). MWCNTs were diluted with quartz as inert material by a factor of 20, i.e. a MWCNT content of 5 % (wt/wt), which increased the stability of the packing material inside the column and reduced the backpressure. Other inert materials like polymeric particles were not considered,

because the method should perspectively be suitable for organic sorbates, which might show interactions with those particles.

D_2O diluted 1:9 with the respective eluent (vol.-%/vol.-%) was used as conservative tracer to determine the dead time ($t_{R,tracer}$) with the refractive index detector (RID). An UV-detector is not able to detect D_2O, consequently, the RID was mandatory. Generally, the half-mass point, i.e. the point at which the peak area is divided in two equal parts, was used to determine the mean retention time of the sorbates ($t_{R,sorb}$) and tracer in order to account for non-equilibrium sorption effects.[41] There are other methods to determine the retention time, like the apex point of the eluting peak or the first moment approach,[28, 29] which yields the center of gravity of the peak.[42, 43] The half-mass approach though is less affected by the peak shape, tailing, noise, baseline drift, inaccurate peak integration, incomplete resolution or insufficient sampling frequency than the first moment method.[44] The half-mass method has previously shown its applicability in sorption studies on soil and minerals.[24, 31, 32, 36] However, when comparing all three methods mentioned before, the results presented in this study agreed rather well as peaks of sorbates were almost symmetrical and did not suffer from strong tailing (data shown in section SI4.2 in chapter 4.6), which would have increased deviations between the different methods. Asymmetry factors determined at 10 % of the maximum intensity ranged between 1.3 and 1.8 indicating only a slight tailing. The retardation factor (R) of each analyte was calculated according to equation 4.1 and transferred into a distribution coefficient (K_d) using equation 4.2,

$$R = (t_{R,sorb} - t_{0,sorb}) / (t_{R,tracer} - t_{0,tracer}) \quad (4.1)$$

$$R = 1 + \rho_b / \theta \times K_d \quad (4.2)$$

where $t_{0,sorb}$ is the traveling time through injector and capillaries between autosampler and DAD without column, $t_{0,tracer}$ is the traveling time from autosampler to the RID or without column. Different corrections for the retention time of sorbate ($t_{R,sorb}$) and tracer ($t_{R,tracer}$) were necessary, as both detectors were connected in serial connection to the autosampler and dead volume between injector and each detector was different. All retention times are reported in minutes. θ [-] and ρ_b [kg L^{-1}] are the porosity and the bulk density of the column used calculated according to equations 3.1 and 3.2 in chapter 3 of this thesis. They were determined using repeated measurements of D_2O with and without column (n = 10). Determined column characteristics for column used in this chapter are summarized in chapter 4.6 (section SI4.1). Recovery of D_2O ranged from 95 to 105 %. Repeated measurements during sorption studies showed no significant shift of the retention time of D_2O for more than 300 injections (data not shown).

Columns were equilibrated with each eluent until a stable retention time for Br^- was reached. To test the degree of non-equilibrium in the experiments, measurements were performed at all tested environmental conditions using different flowrates / pore water velocities. The results show that sorption was at or very close to equilibrium, because determined R values varied only slightly with maximum 5 % at different flowrates / velocities ranging from 25 – 100 µL min^{-1} or 0.5 – 2.2 cm min^{-1}, respectively. As the variations were low, the highest tested flowrate of 100 µL min^{-1} was used for measurements. In batch experiments sorption equilibrium of inorganic anions has been achieved in less than one hour[18]. Consequently, it is likely that equilibrium is achieved also in column experiments very fast. Results determined with columns of 14 mm length were also checked with longer columns of 30 mm and 53 mm length packed with the same packing material composition with similar results (data not shown). Consequently, shorter columns were used as the measurement time was decreased.

Analytes were injected separately with three replicates. Sorption isotherms of sorbates investigated in this chapter were derived using the classical approach described in chapter 3.3.6 of this thesis. Instead of nine different solution with different concentrations only five concentrations were injected, which covered two orders of magnitude in concentration of the sorbates. The alternative approach was not used here as measurement times for the inorganic sorbates investigated in this chapter were much lower compared to organic sorbates investigated in chapter 3 and the benefit of the alternative approach was lower. Different sorption models (linear, Freundlich) were used to fit the data. A comparison is shown in section SI4.3 in chapter 4.6. Sorption data were fitted better by the Freundlich model. Consequently, all sorption isotherms were evaluated using the Freundlich model. Error bars given in diagrams represent the maximum error, which was derived from the standard deviation of the retention times of sorbate and tracer with and without column via error propagation.

Sorbate interaction with quartz as inert material was checked for all analytes at the different environmental conditions in a column packed with quartz (Q1) and was in all cases negligible ($R < 1.02$). A protonation of quartz was not expected in the investigated pH range as typical pH values of a net neutral surface charge (pH_{pzc}) for quartz are about 2. This is supported by no change in retention time in quartz columns comparing pH 3 to pH 6 and 9. Analytes were detected using a DAD with $\lambda = 200$ nm for Br^- and NO_3^-, $\lambda = 210$ nm for NO_2^- and $\lambda = 226$ nm for I^-. Mass recovery of analytes was evaluated comparing the peak area of each analyte from a CNT-column with that from a quartz column or measurements without

column. Recoveries generally were between 80 and 110 % for all analytes with some exceptions for very low injected concentrations (0.6 mg L^{-1}). The intensity in the chromatogram was very low and baseline noise became important due to peak broadening.

4.3.5 Variation of environmental conditions

1) *Ionic strength:* Column CNT1; flowrate of 100 µL min^{-1}; 25°C; pH 6; 1, 10 or 100 mM NaCl in the mobile phase. Injected concentrations of all analytes ranged between 0.6 – 63 mg L^{-1}.
2) *Cation type:* Column CNT2; flowrate of 100 µL min^{-1}; 25°C; pH 6; 1 mM NaCl or 0.5 mM $CaCl_2$ in the mobile phase. Injected concentrations ranged between 0.6 – 63 mg L^{-1}.
3) *Anion type:* Comparison of Br^- and chloride: Column CNT2; flowrate of 100 µL min^{-1}; 25 °C; pH 6; 1 mM NaCl or 1 mM NaBr in the mobile phase. Injected concentrations ranged between 0.6 –63 mg L^{-1} for I^-.

   Comparison of chloride and perchlorate (ClO_4^-): Column CNT5; flowrate of 100 µL min^{-1}; 25 °C; pH 3; 1 mM HCl or 1 mM $HClO_4$ in the mobile phase. Injected concentrations ranged between 0.6 – 63 mg L^{-1} for I^-.
4) *pH value:* Column CNT3; flowrate of 100 µL min^{-1}; 25 °C; pH 3, 6 or 9 at a constant ionic strength of 0.001 mol L^{-1} using NaCl at pH 6 and 9. NaOH was used to change the pH to 9, but the amount necessary increased the ionic strength by less than 1 %. At pH 3, only 1 mM HCl was used to reach the desired pH-value and ionic strength. Injected concentrations ranged between 0.6 – 63 mg L^{-1}.

   Variation of ionic strength at pH 3: Column CNT5; flowrate of 100 µL min^{-1}; 25 °C; pH 3; 1 mM HCl, 1 mM HCl + 9 mM NaCl or 1 mM HCl + 99 mM NaCl in the mobile phase. Injected concentrations ranged between 2 – 200 mg L^{-1} for I^-.
5) *Temperature:* Column CNT4; flowrate of 100 µL min^{-1}; 1 mM NaCl at pH 6 or 1 mM HCl at pH 3; concentration of 63 mg L^{-1} for all analytes at temperatures of 25, 40 and 55 °C.

4.4 Results and Discussion

4.4.1 Influence of ionic strength

The influence of ionic strength on sorption is shown in figure 4.1 for an injected concentration of 63 mg L^{-1} of each analyte at pH 6 and 25 °C. The results show that retardation inside the column / sorption to MWCNTs differed between the analytes. Determined distribution coefficients (K_d) for all tested conditions followed the order $I^- > NO_3^- > NO_2^- > Br^-$. With increasing ionic strength of the eluent, K_d was significantly reduced. While at 1 mM NaCl the determined distribution coefficients ranged between 15 and 45 L kg^{-1}, they reduced to 2 – 8 L kg^{-1} at 10 mM NaCl. At 100 mM NaCl only for NO_3^- and I^- retardation was observed with K_d values of 0.6 and 1.0 L kg^{-1}, respectively. Sorption of Br^- and NO_2^- was completely suppressed at 100 mM NaCl (K_d < 0.2 L kg^{-1}). This observation indicates that Cl^- acts as competitor for sorption sites and the excess of Cl^- at high concentrations of NaCl reduces or completely suppresses sorption of other inorganic anions. Measurements using ultrapure water without NaCl addition were also conducted and are shown in chapter 4.6 (section SI4.4). Reproducibility of the retention times of each analyte was poor using ultrapure water as eluent. No stable retention time was achieved for the analytes and peak width was extremely high leading to low intensities and difficulties to determine peak delimiters, especially, in case of I^-. The retardation using ultrapure water as eluent was higher than with NaCl containing ultrapure water and, consequently, followed the tendency described before. With background electrolyte, retention times were stable for repeated injections and peaks became substantially sharper with respect to the peak width leading to the rather small error bars shown in figure 4.1.

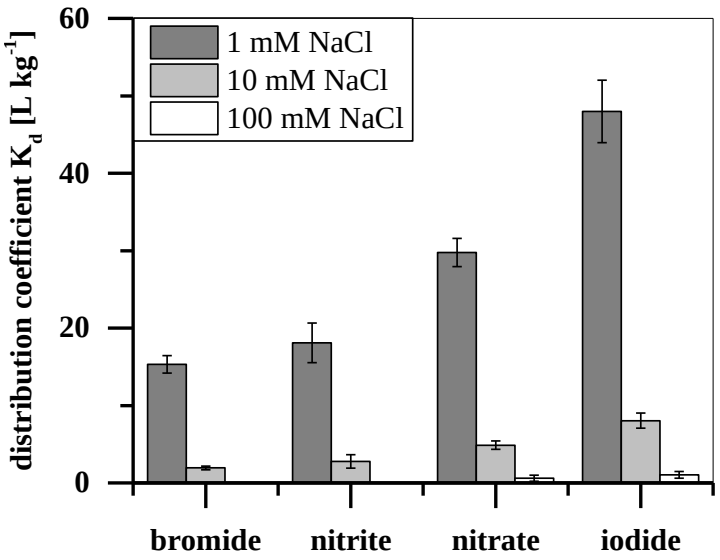

Figure 4.1: Determined distribution coefficients (K_d) for Br^-, NO_2^-, NO_3^-, and I^- at different concentrations of NaCl in the eluent ranging from 1 mM to 100 mM NaCl for an injected concentration of 63 mg L^{-1} of each analyte (pH 6; 25 °C).

Sorption of ClO_4^- to different types of CNTs was reduced in the presence of increasing concentrations of competing anions in solution at pH 6.5.[18] Similar results were derived for phosphate (PO_4^{3-}) by zirconia modified MWCNTs at pH 6[20] or fluoride (F^-) by unmodified MWCNTs at pH 5.5.[21] A direct comparison of measurements with ClO_4^-, F^-, or PO_4^{3-} in this study was not possible, because the UV-absorbance in the investigated concentration range was too low. Decreasing sorption of ClO_4^- with increasing concentration of competing anions to other carbon-based materials like activated carbon or biopolymers was also shown in literature and matches the tendencies observed in this study.[45-48] Data for the analytes of this study are not available in literature to the best of our knowledge so that the data presented here extend the knowledge about sorption of inorganic anions to MWCNTs.

Decreasing the injected concentration resulted in slightly increasing K_d values. Increase of K_d was with 5 – 25 % in most cases small. The only exception was detected for I^- at 100 mM NaCl where the increase was about 140 % when decreasing the injected concentration from 63 to 0.6 mg L^{-1}. Increasing K_d values with decreasing sorbate concentration are an indicator for non-linear sorption. The slight non-linearity of sorption isotherms is reflected by the better description of sorption isotherms of all analytes by the Freundlich model in comparison to a linear sorption model (Chapter 4.6 section SI4.3). Sorption isotherms for different NaCl concentrations in the eluent calculated from the retention data are shown exemplarily for I^- in figure 4.2. Sorption isotherms covered approximately two orders of magnitude in the equilibrium liquid phase concentration ($c_{w,eq}$) and decreased with increasing NaCl concentration. Sorption isotherms and determined

Freundlich parameters of the other analytes are shown in chapter 4.6 (section SI4.5). Sorption isotherms showed good agreement with the Freundlich model as indicated by the high determination coefficients (R^2) > 0.997. The slope of the isotherms in the double-logarithmic plot (equaling the Freundlich exponent (n)) varied between 0.94 and 0.99 indicating an almost linear sorption according to the Freundlich model. The only exception was I^- with 100 mM NaCl in the eluent. Here, the slope was only 0.87 and the non-linearity increased, which was already indicated by the strong increase in K_d with decreasing injected concentration.

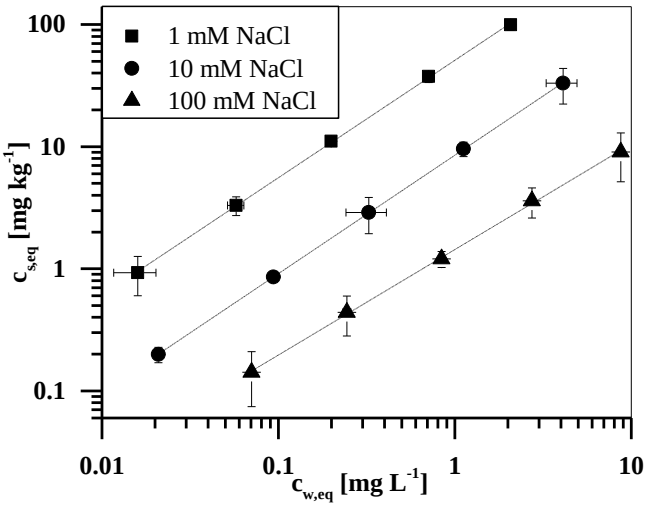

Figure 4.2: Sorption isotherms of I^- determined with different concentrations of NaCl in the eluent ranging from 1 to 100 mM NaCl (pH 6; 25 °C). Calculated equilibrium liquid phase concentration ($c_{w,eq}$) is plotted against the corresponding equilibrium solid phase concentration ($c_{s,eq}$). Dotted lines indicate the linear fit used to determine Freundlich parameters. Error bars represent the errors estimated from measurements.

Almost linear sorption of inorganic anions by MWCNTs was so far not reported in literature. A sorption isotherm of ClO_4^- to MWCNTs fitted with the Freundlich model had a slope of 0.784.[18] Sorption of F^-[21] or PO_4^{3-}[20] to CNTs was also found to be non-linear. Also for other types of materials (e.g. activated carbon or biopolymers) sorption of inorganic anions was non-linear.[46-50] Influence of ionic strength on isotherm shape in these studies can be neglected, because ionic strength of the liquid phase was in some cases adjusted using different salts and was approximately constant and not significantly changed by an increased analyte concentration. The most likely reason is the different sorbent to solution ratio present in batch and column experiments. In column experiments, the pore volume of about 60 µL inside the column was in contact with approximately 6 mg of MWCNTs (sorbent to solution ratio of 100 mg mL^{-1}), while in batch experiments performed for example by Fang and Chen,[18] 37 mg CNTs were added to 12 mL solution (sorbent to solution ratio of 3.1 mg mL^{-1}). This may lead to a stronger competition for sorption sites in batch experiments and a decreased sorption at a higher concentration of the analyte leading to non-linear sorption

isotherms. Sorption of polycyclic aromatic hydrocarbons (PAHs) to MWCNTs was shown to be linear in the low concentration range, while in the higher concentration range isotherms became non-linear.[11] The non-linearity was attributed to the heterogeneous energy distribution of sorption sites becoming relevant when reaching higher concentrations. At low concentrations only high energy sorption sites like defects or functional groups are occupied, while at higher concentrations also sorption sites exhibiting a lower energy get occupied and sorption affinity decreases.[10] Although these observations were made for organic compounds in batch experiments, sorption of inorganic compounds follows the same principles and the concentration range investigated in this study may not be high enough to reach the non-linear isotherm part for the MWCNTs used.

4.4.2 Influence of cation/anion type

Changing the cation from Na^+ to Ca^{2+}, while keeping the concentration of Cl^- constant, slightly reduced sorption of all analytes. K_d values determined using Ca^{2+} were lower than those determined with Na^+ (figure 4.3). Sorption isotherms still showed an almost linear behavior with a slope > 0.95. Sorption isotherms at 1 mM NaCl and 0.5 mM $CaCl_2$ are shown in chapter 4.6 (section SI4.6). This indicates that besides the concentration of the anion also the total ionic strength of the eluent is important. In case of 1 mM NaCl ionic strength is 0.001, while for 0.5 mM $CaCl_2$ ionic strength is 0.0015. Plotting the determined distribution coefficients against the corresponding ionic strength of the eluent (figure S4.6 in chapter 4.6) showed that K_d values determined with $CaCl_2$ fitted well to the trend observed with different concentrations of NaCl in the eluent.

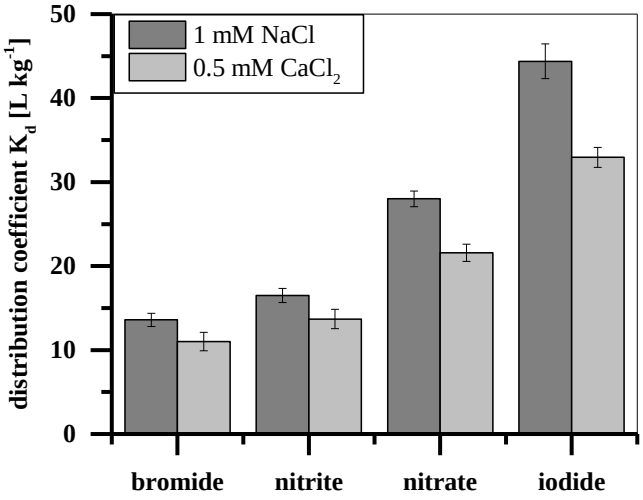

Figure 4.3: Determined distribution coefficients (K_d) of Br^-, NO_2^-, NO_3^-, and I^- using 1 mM NaCl and 0.5 mM $CaCl_2$ as eluent for an injected concentration of 63 mg L^{-1} for all analytes (pH 6; 25 °C).

The effect of a changed anion from Cl^- to Br^- in the eluent is shown for I^- in figure 4.4. The other analytes were not tested as Br^- significantly increased UV-absorption of the eluent and reduced the sensitivity of the detector in the range of 200 – 210 nm. I^- was analyzed at 226 nm and could be sufficiently quantified, because absorption was outside the strongly affected range. As the trends observed at different environmental conditions were similar for all compounds, it could be assumed that the trends would be similar also in this situation for NO_2^- and NO_3^-. Determined K_d values of I^- were not influenced by Cl^- to Br^- present in the eluent at pH 6. Consequently, a further anion was chosen to further investigate the influence of the anion. For this purpose, ClO_4^- was compared to Cl^-, as ClO_4^- was shown to be strongly sorbing to CNTs[18]. $HClO_4$ and HCl were used for comparison as $NaClO_4$ is highly hygroscopic and deviations in concentration could be avoided by using the corresponding acid. Sorption of I^- was strongly reduced using an eluent containing 1 mM $HClO_4$ instead of 1 mM HCl at pH 3 (figure 4.4). Sorption isotherms still showed an almost linear behavior with a slope > 0.95. Sorption isotherms of all conditions are shown in chapter 4.6 (section SI4.7). This indicates that the anion present in the eluent has an influence on sorption that was not observed comparing Cl^- to Br^-. That no effect was observed for Cl^- to Br^-, may be associated with a very similar behavior of both anions regarding their sorption strength to MWCNTs as Br^- was only slightly retained and the difference to Cl^- may be too small. In literature it has been shown that the type of anion had an influence on sorption to CNTs[18, 21] and activated carbon.[45] Cl^-, NO_3^- and SO_4^{2-} had a different influence on sorption of ClO_4^- to CNTs.[18] Consequently, the effect of the anion can also be investigated using the column method. Comparing K_d values of I^- at 1 mM HCl (pH 3) and 1 mM NaCl (pH 6) in the presence of 1 mM Cl^-, sorption was much stronger at pH 3 although the ionic strength was constant. This effect will be further discussed in the next section.

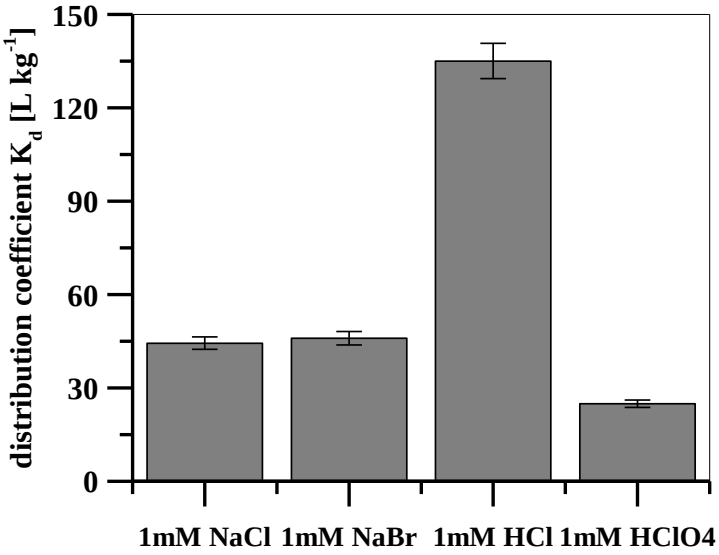

Figure 4.4: Determined distribution coefficients (K_d) of I^- using 1 mM NaCl (pH 6), 1 mM NaBr (pH 6), 1 mM HCl (pH 3) or 1 mM $HClO_4$ (pH 3) as eluent for an injected concentration of 63 mg L^{-1} for I^- (25 °C).

4.4.3 Influence of pH

The pH value of the eluent had a strong influence on sorption affinity to MWCNTs while keeping the ionic strength constant. NO_2^- at pH 3 was omitted as the formation of nitrous gases is possible at pH < pK_a of nitrous acid (pK_a = 3.3). Additionally, speciation of NO_2^- would be changed with the consequence that NO_2^- would also be present in the non-charged species. With increasing pH, K_d reduced strongly as shown in figure 4.5, but pH had no influence on sorption linearity, which was still close to linear. Sorption isotherms at different pH values are shown in chapter 4.6 (section SI4.8). Especially between pH 3 and 6 sorption increased significantly. The pH determines the surface charge of MWCNTs, which was tested using Zeta-potential measurements. At pH 3 the surface charge of MWCNTs was positive, while at pH 6 to 9 surface charge was negative (figure S4.11 in chapter 4.6). The pH_{pzc} was about 4.5. In literature, values of 6.5,[18] 4.3[51] and 3.5[22] were determined showing strong differences between CNTs, which may depend on the production process. Consequently, stronger sorption at pH 3 is related to electrostatic attraction between the positively charged surface of MWCNTs and negatively charged analytes. This could be confirmed as retention of I^- was significantly reduced increasing the ionic strength at pH 3 by the addition of NaCl (shown in section SI4.8 in chapter 4.6). Sorption isotherms at pH 3 were characterized by higher Freundlich coefficients (K_f) compared to pH 6 at similar ionic strength, which may still be related to the positive charge of MWCNTs (comparing tables S4.5 and S4.9 in chapter 4.6). At higher pH, sorption was reduced because of electrostatic repulsion between the negatively charged surface of MWCNTs and negatively charged

analytes, but sorption was not completely suppressed. Consequently, other interactions than nonspecific electrostatic forces must contribute to overall sorption. These interactions may include H-bonding with non-dissociated functional groups. These interactions are also reduced at pH 6 at elevated ionic strength due to competition of sorbates with chloride.

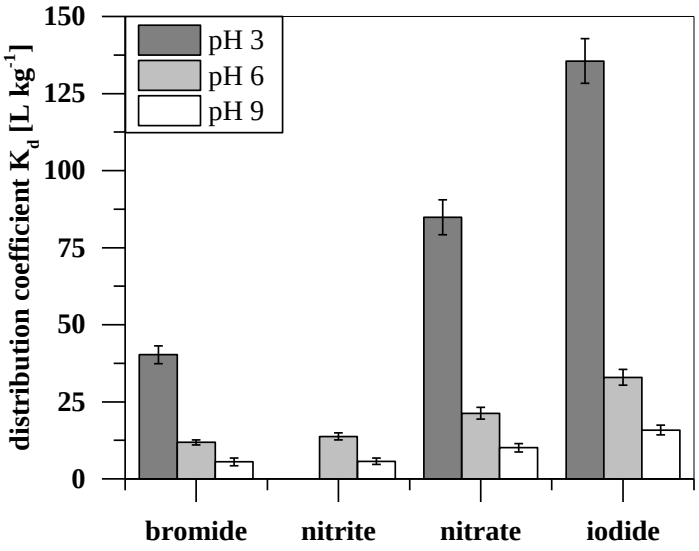

Figure 4.5: Determined K_d values of the analytes at the different pH values tested for an injected concentration of 63 mg L^{-1} (25 °C, 1 mM Cl^-).

The positive surface charge at low pH is most likely associated with protonation of functional groups located on the sorbent surface. Surface functional groups were determined using XPS-measurements. XPS-results for ground MWCNTs are shown in figure S4.12 in chapter 4.6. There was no difference between the ground and unground MWCNTs so that only the results for ground MWCNTs are shown. Deconvolution of the signal showed a main peak at 284.8 eV, which is attributed to the graphitic structure of MWCNTs.[52] Additional peaks at 286.2, 287.7 and 288.8 eV were assigned to C−OH, C=O, and COOH-groups, respectively, present on the sorbent surface. Finally, there was the π-π* transition loss peak at 291.7 eV. 81.9 % of the carbon atoms showed a graphitic structure, but also considerable amounts of surface carbon atoms were present in C−OH-groups (11.3 %) and COOH-groups (5.7 %). C=O-groups were of minor importance (1.1 %). Additional functional groups containing for example nitrogen could not be detected using XPS-measurements. The presence of nitrogen could also not be observed using an elemental analyzer. Fang and Chen (2012)[18] proposed a protonation of C−OH-groups forms C−OH_2^+-groups, which may be responsible for the positive charge at low pH leading to an electrostatic attraction of negatively charged analytes. Deprotonation of C−OH and COOH-groups is responsible for the negative surface charge at high pH.

The pH dependency presented here shows a similar relationship than those determined for CNTs[20] and other carbon-based sorbents,[47, 49, 50, 53] but differs from that presented for doublewalled carbon nanotubes (DWCNTs).[18] Fang and Chen[18] reported that sorption of ClO_4^- was highest at approximately neutral pH (6 – 7). Sorption decreased strongly at pH > 7. At lower pH values, sorption also decreased compared to pH 6 – 7, but stayed almost constant between pH 2 – 5 and then decreased further. The reason for highest sorption at neutral pH may be the very low ionic strength at this pH, because no acid/base was added to the solution and ionic strength was only governed by the analyte. The ionic strength was not constant while changing the pH in those experiments in contrast to the study presented here. This hypothesis is supported by the findings presented in this study and also for DWCNTs[18] as an increased ionic strength resulted in reduced sorption, which also occurs when changing the pH by addition of acid or base. Reduced negative surface charge and even more a positively charged surface increases sorption, while an increased ionic strength due to the addition of HCl reduces sorption. These two opposite effects may be the reason for the plateau in sorption strength observed in the pH range 2 – 5. At some point the increasing positive charge of the surface due to protonation cannot compensate for the higher concentration of Cl^- at very low pH leading to strongly reduced sorption at very low pH values (pH ≤ 2). Strongly decreased sorption has also been observed for other carbon-based sorbents and has been attributed to the excess of Cl^- from HCl addition.[47, 49, 53] The influence of pH and ionic strength on sorption of Br^- and NO_3^- was also observed in a column study on sorption to immobilized artificial membranes by Droge[54]. Sorption of Br^- and NO_3^- was increased strongly at pH < 5, but decreased when increasing the ionic strength at a constant pH-value. The observations were assigned to changes in surface charge of the particles used. Below pH 5, the surface charge is shifted to positive values and this results in electrostatic attraction. With increasing ionic strength of the mobile phase the positive surface potential is decreased resulting in reduced retention / sorption. At pH > 5 and ionic strength < 0.15 M both compounds were eluted before the dead time measured by the injection of ultrapure water. This may be related to the negative surface charge and electrostatic repulsion resulting in pore exclusion and a faster elution from the column compared to water than expected. These results, although made with another sorbent phase, are comparable to the results presented in this study.

4.4.4 Influence of temperature

The influence of temperature on the sorption is shown in figure 4.6. Sorption coefficients decreased with increasing temperature for all analytes. The enthalpy change (ΔH)

was calculated using the van´t Hoff equation from the slope of the regression line in figure 4.6 according to equation 4.3.

$$\ln K_d = \Delta S/R_{const} - \Delta H/R_{const} \times 1/T \quad (4.3)$$

Where ΔH is the enthalpy change [kJ mol^{-1}], ΔS the entropy change [kJ mol^{-1} K^{-1}], R_{const} is the gas constant [8.3145 × 10^{-3} kJ mol^{-1} K^{-1}] and T the temperature [K].

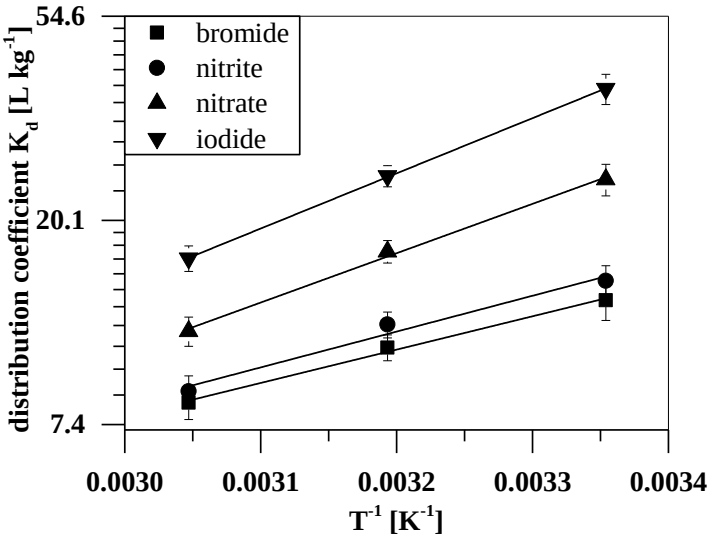

Figure 4.6: Determined K_d value of the analytes plotted against the reciprocal temperature at 1 mM NaCl in the eluent at pH 6 for an injected concentration of 63 mg L^{-1} (1 mM NaCl, pH 6). Scale of K_d in the ordinate is set to the natural logarithm.

The determined values for ΔH ranged between -13.5 and -22.5 kJ mol^{-1} and increased in the order $Br^- < NO_2^- < NO_3^- < I^-$. Consequently, sorption is an exothermic process. For PO_4^{3-}, sorption to CNTs was endothermic,[19] while sorption of NO_3^- onto a modified zeolite was exothermic.[55] Thus, there is no general tendency observed in sorption of anions to different sorbents. The surface charge at pH 6 was negative so that electrostatic attraction was not present. The small values for ΔH show the absence of covalent bonding like in case of chemisorption, which typically gives ΔH in the range from -60 to -80 kJ mol^{-1} for organic compounds.[56] Further support for the absence of chemisorption is shown by the fully reversible sorption for all analytes indicated by quantitative recovery. H-bonding (10 – 40 kJ mol^{-1}) with functional groups on the MWCNTs surface might be responsible for interactions between the analytes and sorbent.[57] At pH 3 using 1 mM HCl as eluent the temperature effect was less pronounced. Values for ΔH ranged between -7.4 and -19.7 kJ mol^{-1} increasing in the same order than before. This fitted well to the tendency of sorption of organic compounds to be less temperature dependent in case of ionic interactions contributing to sorption.[56]

Overall, column chromatography was used successfully for the first time to study sorption to MWCNTs and effects of environmental conditions on sorption of inorganic anions. Ionic strength, pH and type of ions present played an important role in sorption of inorganic anions, while the effect of temperature was lower. Applying column chromatography, it was possible to significantly reduce the sorbent demand, which was below 100 mg and, consequently, much lower than in studies using batch experiments. This method is directly applicable for UV-active anions, but it may also be transferred to other inorganic anions as well as cations (e.g. metals) or organic ions. Other detection techniques (e.g. conductivity detectors or inductively coupled plasma mass spectrometry (ICP-MS)) would increase the application range also to analytes with insufficient UV activity and could facilitate the direct comparison of batch data from literature with column data from this study. The applicability of the method for organic molecules, which are relevant sorbates in the environment, and other types of carbon-based sorbents will be investigated in the next chapters. The effect of environmental conditions on sorption of organic compounds will be investigated as well.

4.5 References

1. Liu, Z.; Chen, K.; Davis, C.; Sherlock, S.; Cao, Q. Z.; Chen, X. Y.; Dai, H. J. Drug delivery with carbon nanotubes for in vivo cancer treatment. *Cancer Research* **2008,** 68 (16), 6652-6660.
2. Avouris, P.; Appenzeller, J.; Martel, R.; Wind, S. J. Carbon nanotube electronics. *Proceedings of the Ieee* **2003,** 91 (11), 1772-1784.
3. Andrews, R.; Jacques, D.; Qian, D. L.; Rantell, T. Multiwall carbon nanotubes: Synthesis and application. *Accounts of Chemical Research* **2002,** 35 (12), 1008-1017.
4. Bierdel, M.; Buchholz, S.; Michele, V.; Mleczko, L.; Rudolf, R.; Voetz, M.; Wolf, A. Industrial production of multiwalled carbon nanotubes. *Physica Status Solidi B-Basic solid state physics* **2007,** 244 (11), 3939-3943.
5. Hüffer, T.; Osorio, X. L.; Jochmann, M. A.; Schilling, B.; Schmidt, T. C. Multi-walled carbon nanotubes as sorptive material for solventless in-tube microextraction (ITEX2) - a factorial design study. *Analytical and Bioanalytical Chemistry* **2013,** 405 (26), 8387-8395.
6. Duran, A.; Tuzen, M.; Soylak, M. Preconcentration of some trace elements via using multiwalled carbon nanotubes as solid phase extraction adsorbent. *Journal of Hazardous materials* **2009,** 169 (1-3), 466-471.
7. Gil, R. A.; Goyanes, S. N.; Polla, G.; Smichowski, P.; Olsina, R. A.; Martinez, L. D. Application of multi-walled carbon nanotubes as substrate for the on-line preconcentration, speciation and determination of vanadium by ETAAS. *Journal of Analytical Atomic Spectrometry* **2007,** 22 (10), 1290-1295.
8. Hüffer, T.; Endo, S.; Metzelder, F.; Schroth, S.; Schmidt, T. C. Prediction of sorption of aromatic and aliphatic organic compounds by carbon nanotubes using poly-parameter linear free-energy relationships. *Water Research* **2014,** 59, 295-303.

9. Apul, O. G.; Wang, Q. L.; Shao, T.; Rieck, J. R.; Karanfil, T. Predictive model development for adsorption of aromatic contaminants by multi-walled carbon nanotubes. *Environmental Science & Technology* **2013,** 47 (5), 2295-2303.
10. Pan, B.; Xing, B. S. Adsorption mechanisms of organic chemicals on carbon nanotubes. *Environmental Science & Technology* **2008,** 42 (24), 9005-9013.
11. Kah, M.; Zhang, X. R.; Jonker, M. T. O.; Hofmann, T. Measuring and modelling adsorption of PAHs to carbon nanotubes over a six order of magnitude wide concentration range. *Environmental Science & Technology* **2011,** 45 (14), 6011-6017.
12. Chen, W.; Duan, L.; Zhu, D. Q. Adsorption of polar and nonpolar organic chemicals to carbon nanotubes. *Environmental Science & Technology* **2007,** 41 (24), 8295-8300.
13. Li, X. N.; Zhao, H. M.; Quan, X.; Chen, S. O.; Zhang, Y. B.; Yu, H. T. Adsorption of ionizable organic contaminants on multi-walled carbon nanotubes with different oxygen contents. *Journal of Hazardous materials* **2011,** 186 (1), 407-415.
14. Chen, J. Y.; Chen, W.; Zhu, D. Adsorption of nonionic aromatic compounds to single-walled carbon nanotubes: Effects of aqueous solution chemistry. *Environmental Science & Technology* **2008,** 42 (19), 7225-7230.
15. Chen, W.; Duan, L.; Wang, L. L.; Zhu, D. Q. Adsorption of hydroxyl- and amino-substituted aromatics to carbon nanotubes. *Environmental Science & Technology* **2008,** 42 (18), 6862-6868.
16. Tóth, A.; Torocsik, A.; Tombacz, E.; Olah, E.; Heggen, M.; Li, C. L.; Klumpp, E.; Geissler, E.; Laszlo, K. Interaction of phenol and dopamine with commercial MWCNTs. *Journal of Colloid and Interface Science* **2011,** 364 (2), 469-475.
17. Tóth, A.; Torocsik, A.; Tombacz, E.; Laszlo, K. Competitive adsorption of phenol and 3-chlorophenol on purified MWCNTs. *Journal of Colloid and Interface Science* **2012,** 387, 244-249.
18. Fang, Q. L.; Chen, B. L. Adsorption of perchlorate onto raw and oxidized carbon nanotubes in aqueous solution. *Carbon* **2012,** 50 (6), 2209-2219.
19. Mahdavi, S.; Akhzari, D. The removal of phosphate from aqueous solutions using two nano-structures: copper oxide and carbon tubes. *Clean Technologies and Environmental Policy* **2016,** 18 (3), 817-827.
20. Zong, E. M.; Wei, D.; Huan, Z. K.; Peng, D.; Wan, H. Q.; Zheng, S. R.; Xu, Z. Y. Adsorption of phosphate by zirconia functionalized multi-walled carbon nanotubes. *Chinese Journal of Inorganic Chemistry* **2013,** 29 (5), 965-972.
21. Ansari, M.; Kazemipour, M.; Dehghani, M. The defluoridation of drinking water using multi-walled carbon nanotubes. *Journal of Fluorine Chemistry* **2011,** 132 (8), 516-520.
22. Chen, P. H.; Hsu, C. F.; Tsai, D. D. W.; Lu, Y. M.; Huang, W. J. Adsorption of mercury from water by modified multi-walled carbon nanotubes: adsorption behaviour and interference resistance by coexisting anions. *Environmental Technology* **2014,** 35 (15), 1935-1944.
23. Yu, F.; Ma, J.; Wu, Y. Q. Adsorption of toluene, ethylbenzene and m-xylene on multi-walled carbon nanotubes with different oxygen contents from aqueous solutions. *Journal of Hazardous materials* **2011,** 192 (3), 1370-1379.
24. Bi, E.; Schmidt, T. C.; Haderlein, S. B. Sorption of heterocyclic organic compounds to reference soils: Column studies for process identification. *Environmental Science & Technology* **2006,** 40 (19), 5962-5970.
25. Hyung, H.; Kim, J. H. Natural organic matter (NOM) adsorption to multi-walled carbon nanotubes: Effect of NOM characteristics and water quality parameters. *Environmental Science & Technology* **2008,** 42 (12), 4416-4421.
26. Lin, D. H.; Liu, N.; Yang, K.; Xing, B. S.; Wu, F. C. Different stabilities of multiwalled carbon nanotubes in fresh surface water samples. *Environmental Pollution* **2010,** 158 (5), 1270-1274.

27. Bucheli, T. D.; Gustafsson, O. Soot sorption of non-ortho and ortho substituted PCBs. *Chemosphere* **2003,** 53 (5), 515-522.
28. Droge, S.; Goss, K. U. Effect of sodium and calcium cations on the ion-exchange affinity of organic cations for soil organic matter. *Environmental Science & Technology* **2012,** 46 (11), 5894-5901.
29. Schenzel, J.; Goss, K. U.; Schwarzenbach, R. P.; Bucheli, T. D.; Droge, S. T. J. Experimentally determined soil organic matter-water sorption coefficients for different classes of natural toxins and comparison with estimated numbers. *Environmental Science & Technology* **2012,** 46 (11), 6118-6126.
30. Altfelder, S.; Streck, T.; Maraqa, M. A.; Voice, T. C. Nonequilibrium sorption of dimethylphthalate - Compatibility of batch and column techniques. *Soil Science Society of America Journal* **2001,** 65 (1), 102-111.
31. Li, B. H.; Qian, Y. A.; Bi, E. P.; Chen, H. H.; Schmidt, T. C. Sorption behavior of phthalic acid esters on reference soils evaluated by soil column chromatography. *Clean-Soil Air Water* **2010,** 38 (5-6), 425-429.
32. Bi, E.; Schmidt, T. C.; Haderlein, S. B. Environmental factors influencing sorption of heterocyclic aromatic compounds to soil. *Environmental Science & Technology* **2007,** 41 (9), 3172-3178.
33. Das, B. S.; Lee, L. S.; Rao, P. S. C.; Hultgren, R. P. Sorption and degradation of steroid hormones in soils during transport: Column studies and model evaluation. *Environmental Science & Technology* **2004,** 38 (5), 1460-1470.
34. Fesch, C.; Simon, W.; Haderlein, S. B.; Reichert, P.; Schwarzenbach, R. P. Nonlinear sorption and nonequilibrium solute transport in aggregated porous media: Experiments, process identification and modeling. *Journal of Contaminant Hydrology* **1998,** 31 (3-4), 373-407.
35. Lee, L. S.; Rao, P. S. C.; Brusseau, M. L. Nonequilibrium sorption and transport of neutral and ionized chlorophenols. *Environmental Science & Technology* **1991,** 25 (4), 722-729.
36. Qian, Y. Sorption of hydrophobic organic compounds (HOCs) to inorganic surfaces in aqueous solutions. Ph.D. disserstation, University Duisburg-Essen, Essen, Germany, 2010.
37. Mader, B. T.; Goss, K. U.; Eisenreich, S. J. Sorption of nonionic, hydrophobic organic chemicals to mineral surfaces. *Environmental Science & Technology* **1997,** 31 (4), 1079-1086.
38. Wu, W. H.; Jiang, W.; Zhang, W. D.; Lin, D. H.; Yang, K. Influence of functional groups on desorption of organic compounds from carbon nanotubes into water: Insight into desorption hysteresis. *Environmental Science & Technology* **2013,** 47 (15), 8373-8382.
39. Li, H. B.; Zhang, D.; Han, X. Z.; Xing, B. S. Adsorption of antibiotic ciprofloxacin on carbon nanotubes: pH dependence and thermodynamics. *Chemosphere* **2014,** 95, 150-155.
40. Wang, Z. Y.; Yu, X. D.; Pan, B.; Xing, B. S. Norfloxacin sorption and its thermodynamics on surface-modified carbon nanotubes. *Environmental Science & Technology* **2010,** 44 (3), 978-984.
41. Thomsen, A. B.; Henriksen, K.; Gron, C.; Moldrup, P. Sorption, transport, and degradation of quinoline in unsaturated soil. *Environmental Science & Technology* **1999,** 33 (17), 2891-2898.
42. Valocchi, A. J. Validity of the local equilibrium assumption for modeling sorbing solute transport through homogeneous soils. *Water Resources Research* **1985,** 21 (6), 808-820.
43. Young, D. F.; Ball, W. P. Column experimental design requirements for estimating model parameters from temporal moments under nonequilibrium conditions. *Advances in Water Resources* **2000,** 23 (5), 449-460.

44. Bi, E. P.; Schmidt, T. C.; Haderlein, S. B. Practical issues relating to soil column chromatography for sorption parameter determination. *Chemosphere* **2010,** 80 (7), 787-793.
45. Mahmudov, R.; Huang, C. P. Selective adsorption of oxyanions on activated carbon exemplified by Filtrasorb 400 (F400). *Separation and Purification Technology* **2011,** 77 (3), 294-300.
46. Xu, J. H.; Gao, N. Y.; Deng, Y.; Sui, M. H.; Tang, Y. L. Perchlorate removal by granular activated carbon coated with cetyltrimethyl ammonium bromide. *Journal of Colloid and Interface Science* **2011,** 357 (2), 474-479.
47. Yoon, I. H.; Meng, X. G.; Wang, C.; Kim, K. W.; Bang, S.; Choe, E.; Lippincott, L. Perchlorate adsorption and desorption on activated carbon and anion exchange resin. *Journal of Hazardous materials* **2009,** 164 (1), 87-94.
48. Jang, M.; Cannon, F. S.; Parette, R. B.; Yoon, S. J.; Chen, W. F. Combined hydrous ferric oxide and quaternary ammonium surfactant tailoring of granular activated carbon for concurrent arsenate and perchlorate removal. *Water Research* **2009,** 43 (12), 3133-3143.
49. Mahmudov, R.; Huang, C. P. Perchlorate removal by activated carbon adsorption. *Separation and Purification Technology* **2010,** 70 (3), 329-337.
50. Ito, K.; Akiba, K. Adsorption of pertechnetate ion on active-carbon from acids and their salt-solutions. *Journal of Radioanalytical and Nuclear Chemistry-Articles* **1991,** 152 (2), 381-390.
51. Kumar, A. S. K.; Jiang, S. J.; Tseng, W. L. Effective adsorption of chromium(VI)/Cr(III) from aqueous solution using ionic liquid functionalized multiwalled carbon nanotubes as a super sorbent. *Journal of Materials Chemistry A* **2015,** 3 (13), 7044-7057.
52. Datsyuk, V.; Kalyva, M.; Papagelis, K.; Parthenios, J.; Tasis, D.; Siokou, A.; Kallitsis, I.; Galiotis, C. Chemical oxidation of multiwalled carbon nanotubes. *Carbon* **2008,** 46 (6), 833-840.
53. Xie, Y. H.; Li, S. Y.; Wang, F.; Liu, G. L. Removal of perchlorate from aqueous solution using protonated cross-linked chitosan. *Chemical Engineering Journal* **2010,** 156 (1), 56-63.
54. Droge, S. T. J. Dealing with Confounding pH-Dependent Surface Charges in Immobilized Artificial Membrane HPLC Columns. *Analytical Chemistry* **2016,** 88 (1), 960-967.
55. Zhan, Y. H.; Lin, J. W.; Zhu, Z. L. Removal of nitrate from aqueous solution using cetylpyridinium bromide (CPB) modified zeolite as adsorbent. *Journal of Hazardous materials* **2011,** 186 (2-3), 1972-1978.
56. Delle Site, A. Factors affecting sorption of organic compounds in natural sorbent/water systems and sorption coefficients for selected pollutants. A review. *Journal of Physical and Chemical Reference Data* **2001,** 30 (1), 187-439.
57. Boutboul, A.; Lenfant, F.; Giampaoli, P.; Feigenbaum, A.; Ducruet, V. Use of inverse gas chromatography to determine thermodynamic parameters of aroma-starch interactions. *Journal of Chromatography A* **2002,** 969 (1-2), 9-16.

4.6 Appendix to Chapter 4

SI4.1 Column packing procedure

The following section describes in detail the procedure used for column packing. It was adapted from a previous study[1] and adjusted to the actual materials. First, MWCNTs were ground manually by pestle and mortar to a particle size less than 63 µm, which was checked by sieving analysis. Material properties of MWCNTs were not altered significantly by grinding as shown in table S4.1. In the beginning an empty HPLC-column was connected to an also empty precolumn using a connecting nut. The column outlet was closed as follows: one stainless steel sieve, three glass fiber filters, one stainless steel sieve and a PTFE seal. The packing materials were premixed in the respective ratio and carefully filled in the combination of column and pre-column using a stainless steel spatula. During transfer of packing material, the column was slightly tapped with its outlet on the laboratory bench to increase the density of the packing inside the column. When column and precolumn were filled completely and tapping did not result in further compression of the packing bed, the column was encased and connected to the HPLC-pump for the liquid compression process. The precolumn was used to ensure that after liquid compression the column used for sorption experiments was completely filled with the packing material without unnecessary void volume at the column head caused by compression while packing. Ultrapure water was used as packing solvent. It was started with a low flowrate (10 µL min^{-1}) to get rid of any air entrapped between the particles inside the column and evenly saturate the column with water. The flowrate was increased gradually to a high backpressure (max. 25 MPa) in steps of 15 min for each flowrate. The maximum flowrate (max. 3.5 mL min^{-1}) was held for 4 h with a stable backpressure to ensure complete compression of the material and avoid changes in the packing bed in sorption experiments. In sorption experiments the flowrate was several times lower so that changes in the packing bed could be excluded. Afterwards, the precolumn was removed and the column head cleaned immediately using the self prepared tool (figure 3.2 in chapter 3) to avoid relaxation of the packing material. After cleaning the column head, the column was closed using filters, sieves, PTFE seal as described above.

Table S4.1: Determined properties of the pristine and ground MWCNTs.

	native material	ground material
specific surface area [m^2 g^{-1}][1]	211	228.07
C−C content [%][2]	75.23	74.91
C−O- content [%][2]	10.40	10.66
C=O content [%][2]	0.97	0.97
COOH content [%][2]	5.23	5.43
π-π* content [%][2]	8.17	8.03

[1)] determined using BET-measurements; [2)] relative content of functional groups under the C1s-peak were determined by XPS-measurements.

Table S4.2: Summary of columns used in this study with their dimensions, packing material composition, bulk density and porosity.

column	dimension (L × ID) [mm]	packing material [w.-%]	bulk density ρ_b [kg L^{-1}]	porosity θ [-]
Q1	53 × 3	100 % quartz	1.55	0.45
CNT1	14 × 3	95% quartz / 5 % MWCNTs	1.34	0.63
CNT2	14 × 3	95 % quartz / 5 % MWCNTs	1.44	0.61
CNT3	14 × 3	95 % quartz / 5 % MWCNTs	1.44	0.60
CNT4	14 × 3	95 % quartz / 5 % MWCNTs	1.33	0.59
CNT5	14 × 3	95 % quartz / 5 % MWCNTs	1.29	0.59

SI4.2 Comparison of evaluation methods (Apex, Half-mass, First-moment)

Determined distribution coefficients (K_d) for three different evaluation methods to determine the retention time (Apex, Half-mass, First-moment) are presented in table S4.3 at an injected concentration of 63 mg L^{-1} with 1 mM NaCl as eluent. Determined K_d values agreed rather well for all three evaluation methods, but determined values increased in the order K_d Apex < K_d Half-mass < K_d First moment. Nevertheless, the overall trend observed in previous studies for tailing peaks is confirmed [1]. This increase in K_d is connected to the slight tailing of peaks recorded for the different analytes. For symmetrical peaks without tailing or fronting all three methods would yield the same result. Determined maximum errors are smallest for the half-mass method so that this method is applied for evaluation of chromatograms.

Table S4.3: Determined distribution coefficients (K_d) of the different analytes at an injected concentration of 63 mg L^{-1} and 1 mM NaCl as eluent with column CNT1 (pH 6; 25 °C). Determined errors represent the maximum error estimated via error propagation from the standard deviation of three replicates.

analyte	K_d Apex [L kg^{-1}]	K_d Half-mass [L kg^{-1}]	K_d First moment [L kg^{-1}]
bromide	15.0 ± 2.1	15.3 ± 1.1	16.0 ± 2.7
nitrite	17.2 ± 3.7	18.1 ± 2.5	19.4 ± 3.7
nitrate	27.8 ± 3.6	29.8 ± 1.8	32.1 ± 2.2
iodide	44.9 ± 4.5	48.0 ± 4.0	51.7 ± 3.8

SI4.3 Comparison of different sorption models

Two different sorption isotherm models are compared in this study: the linear sorption model (equation S4.1) and the non-linear Freundlich model (equation S4.2). Sorption isotherms were determined with column CNT1. Determined regression factors are shown in table S4.4. Determination coefficients (R^2) are highest for the Freundlich model, while values of the linear model are lower. Consequently, the Freundlich model is used in this study to describe sorption isotherms.

$$c_{s,eq} = K_d \times c_{w,eq} + b \quad \text{(S4.1)}$$

$$c_{s,eq} = K_F \times c_{w,eq}^{n} \quad \text{(S4.2)}$$

Table S4.4: Comparison of regressions of the linear sorption model and the Freundlich model for bromide, nitrite, nitrate and iodide with 1 mM NaCl as eluent (pH 6; 25 °C). Injected concentrations range from 0.6 – 63 mg L^{-1}. K_d is the distribution coefficient [L kg^{-1}], b the y-intercept of the regression, R^2 the determination coefficient, K_f the Freundlich coefficient [(mg kg^{-1}) (mg L^{-1})$^{-n}$] and n the Freundlich exponent [-]. Errors shown in the table are the standard errors of the regression parameters.

	linear model			Freundlich model		
analyte	**K_d**	**b**	**R^2**	**K_f**	**n**	**R^2**
bromide	15.3 ± 0.1	0.3 ± 0.1	0.9998	15.7 ± 1.0	0.988 ± 0.005	0.9999
nitrite	18.0 ± 0.3	0.8 ± 0.6	0.9989	19.4 ± 1.0	0.974 ± 0.008	0.9997
nitrate	29.6 ± 0.7	1.5 ± 1.0	0.9977	32.6 ± 1.0	0.960 ± 0.012	0.9994
iodide	47.7 ± 0.9	1.3 ± 0.9	0.9985	50.9 ± 1.0	0.961 ± 0.008	0.9997

SI4.4 Comparison of ultrapure water with 1 mM NaCl as eluent

Chromatograms determined for the analytes with ultrapure water and 1 mM NaCl as eluent are shown in figure S4.1. Retention inside the column was stronger with ultrapure water as eluent compared to 1 mM NaCl as indicated by the higher retention time in the chromatogram. The general sequence of elution is similar in ultrapure water and 1 mM NaCl, but retention times are strongly reduced by the addition of NaCl indicating the competing effect between the analytes and chloride anions present in the eluent.

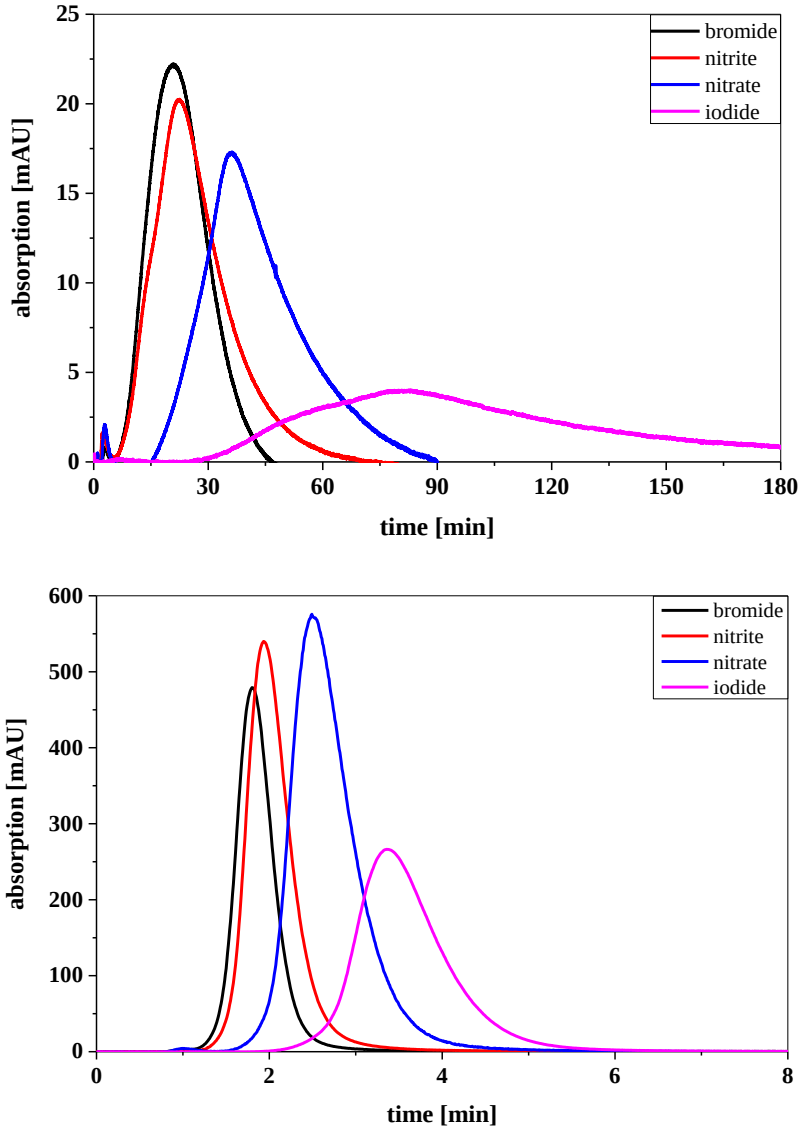

Figure S4.1: Comparison of chromatograms of the analytes measured with ultrapure water as eluent (top) to chromatograms measured with 1 mM NaCl as eluent (bottom) (pH 6; 25 °C). Injected concentration was in all cases 63 mg L^{-1}. Column CNT4 was used for measurements.

As the reproducibility of chromatograms was worse in ultrapure water as indicated in figure S4.2 for repeated injections of bromide, these data were not used to calculate distribution coefficients. Standard deviations would be very high. With 1 mM NaCl retention time of bromide and all other analytes was stable. This is shown for bromide in figure S4.3.

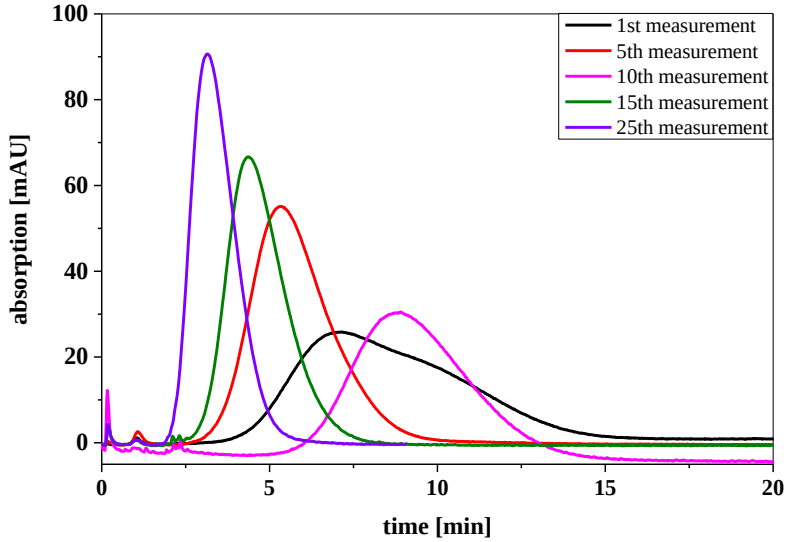

Figure S4.2: Chromatograms of repeated bromide injections with 63 mg L^{-1} injected concentration using column CNT1 and ultrapure water as eluent (pH 6; 25 °C).

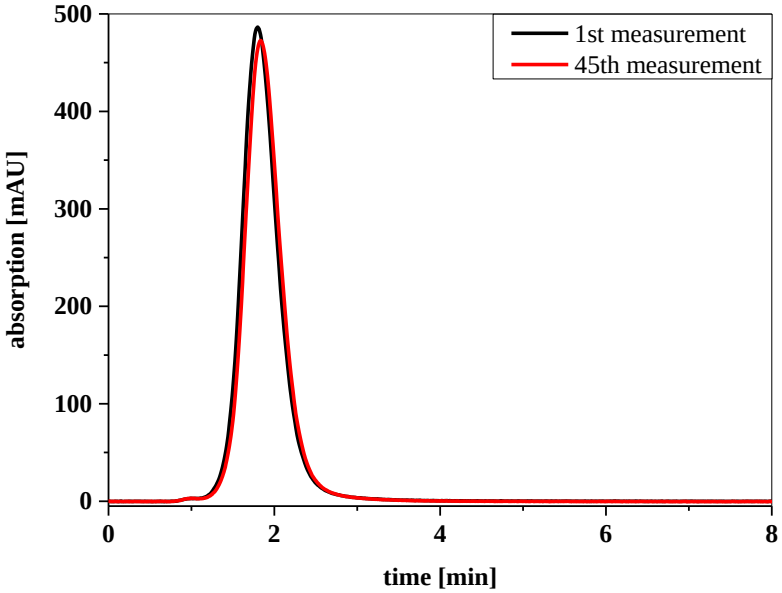

Figure S4.3: Chromatograms of repeated bromide injections with 63 mg L^{-1} injected concentration using column CNT1 and 1 mM NaCl as eluent (pH 6; 25 °C).

SI4.5 Sorption isotherms of analytes depending on the ionic strength

Figure S4.4 summarizes the sorption isotherms of the different sorbates determined with eluents of different ionic strength reached by the addition of 1 – 100 mM NaCl. Column CNT1 was used here. Bromide and nitrite at the highest concentration of 100 mM NaCl are not shown as no retention inside the column is observed. Determined Freundlich coefficients (K_f) and Freundlich exponents (n) are given in table S4.5.

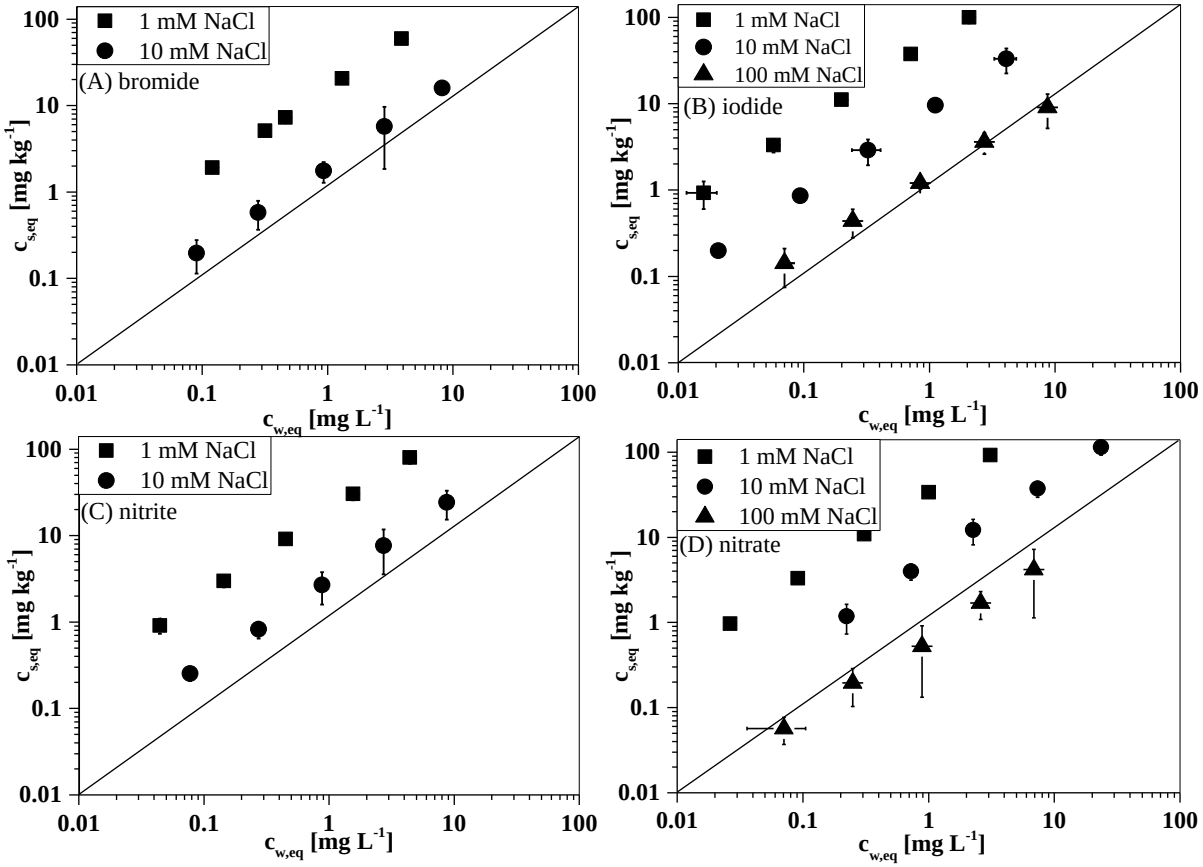

Figure S4.4: Sorption isotherms determined for bromide (A), iodide (B), nitrite (C) and Nitrate (D) at different ionic strengths / concentration of NaCl in the eluent ranging from 1 mM to 100 mM NaCl (pH 6; 25 °C). The straight line indicates a slope of 1.

Table S4.5: Logarithmic Freundlich coefficients (K_f) [(mg kg^{-1}) (mg $L^{-1})^{-n}$] and Freundlich exponents (n) [-] determined for the different isotherms of bromide, nitrite, nitrate and iodide with different concentrations of NaCl ranging from 1 mM to 100 mM NaCl in the eluent (pH 6; 25 °C) in combination with the corresponding determination coefficient (R^2). Errors represent the standard error of the regression parameters.

	1 mM NaCl			10 mM NaCl			100 mM NaCl		
analyte	**log K_f**	**n**	**R^2**	**log K_f**	**n**	**R^2**	**log K_f**	**n**	**R^2**
bromide	1.20 ± 0.01	0.988 ± 0.01	0.999	0.30 ± 0.01	0.978 ± 0.013	0.999	-	-	-
nitrite	1.28 ± 0.01	0.974 ± 0.01	0.999	0.47 ± 0.01	0.966 ± 0.007	0.999	-	-	-
nitrate	1.51 ± 0.01	0.960 ± 0.01	0.999	0.73 ± 0.01	0.979 ± 0.009	0.999	-0.17 ± 0.02	0.934 ± 0.025	0.997
iodide	1.71 ± 0.01	0.961 ± 0.01	0.999	0.93 ± 0.01	0.969 ± 0.01	0.999	0.16 ± 0.01	0.863 ± 0.01	0.999

SI4.6 Sorption isotherms of analytes depending on cation type

Figure S4.5 summarizes the sorption isotherms determined with 1 mM NaCl or 0.5 mM $CaCl_2$ as eluent. Column CNT2 was used for these measurements. Determined Freundlich coefficients (K_f) and Freundlich exponents (n) are given in table S4.6.

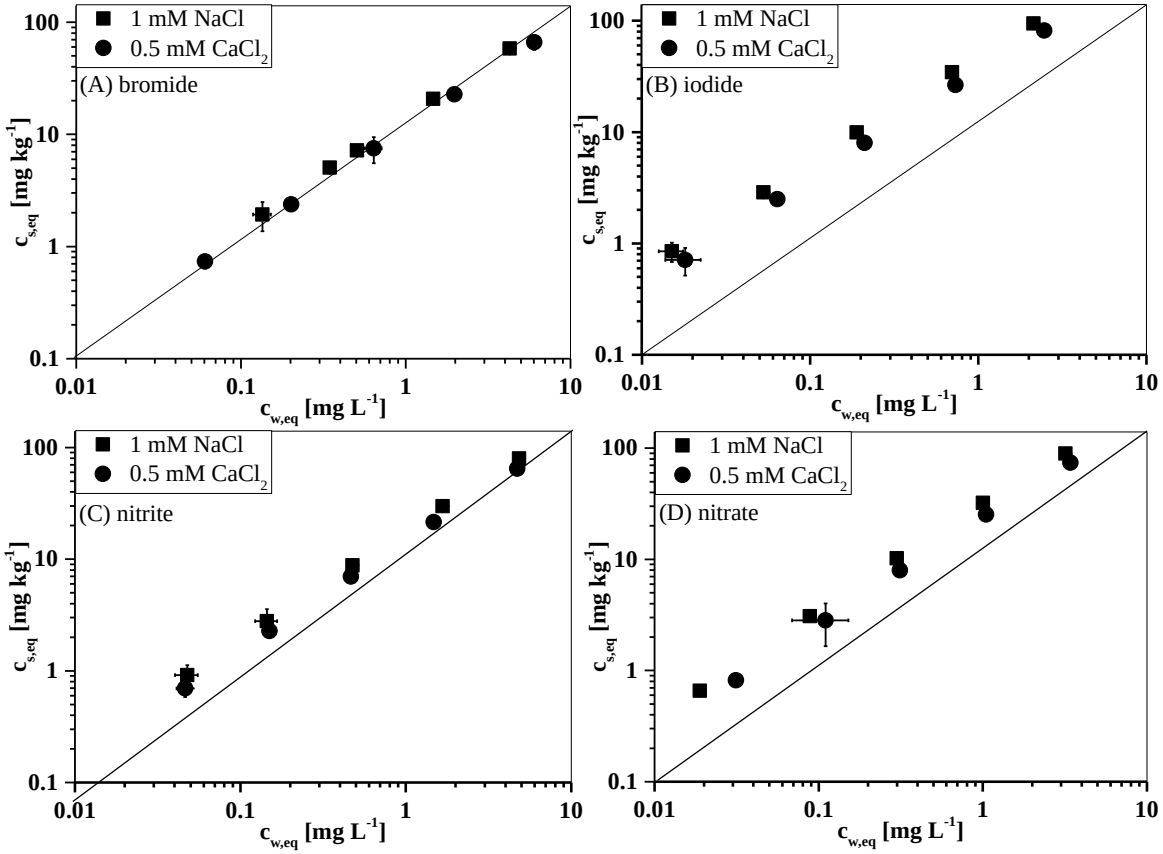

Figure S4.5: Sorption isotherms determined for bromide (A), iodide (B), nitrite (C), and nitrate (D) with 1 mM NaCl or 0.5 mM $CaCl_2$ as eluent (pH 6; 25 °C). The straight line indicates a slope of 1.

Table S4.6: Logarithmic Freundlich coefficients (K_f) [(mg kg^{-1}) (mg $L^{-1})^{-n}$] and Freundlich exponents (n) [-] determined for the different isotherms of bromide, nitrite, nitrate and iodide with 1 mM NaCl or 0.5 mM $CaCl_2$ as eluent (pH 6; 25 °C) in combination with the corresponding determination coefficient (R^2). Errors represent the standard error of the regression parameters.

	1 mM NaCl			0.5 mM $CaCl_2$		
analyte	**log K_f**	**n**	**R^2**	**log K_f**	**n**	**R^2**
bromide	1.14 ± 0.01	0.984 ± 0.01	0.9998	1.06 ± 0.01	0.981 ± 0.004	0.9999
nitrite	1.25 ± 0.01	0.968 ± 0.01	0.9998	1.16 ± 0.01	0.981 ± 0.01	0.9998
nitrate	1.49 ± 0.01	0.960 ± 0.01	0.9992	1.37 ± 0.01	0.963 ± 0.01	0.9995
iodide	1.68 ± 0.01	0.954 ± 0.01	0.9998	1.55 ± 0.01	0.965 ± 0.01	0.9997

Figure S4.6 shows the correlation between the ionic strength of the eluent and the determined distribution coefficient.

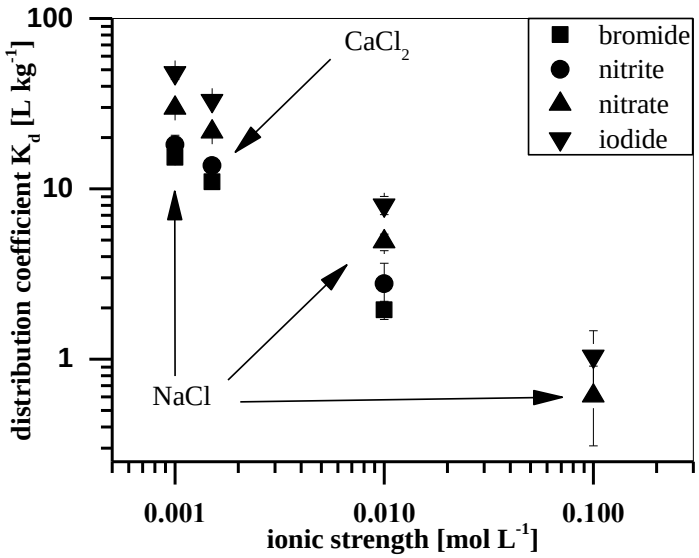

Figure S4.6: Correlation of K_d values of the different analytes determined using NaCl plotted against the corresponding ionic strength of the eluent in comparison to the K_d values of the analytes determined using 0.5 mM $CaCl_2$ at an ionic strength of 0.0015 (pH 6; 25 °C). The injected concentration was for all analytes 63 mg L^{-1}. Values of Br^- and NO_2^- at an ionic strength of 0.1 mol L^{-1} are left out as no sorption could be detected.

SI4.7 Sorption isotherms of iodide depending on anion type

Figure S4.7 summarizes the sorption isotherms determined with 1 mM NaCl or 1 mM NaBr as eluent (column CNT2), while figure S4.8 summarizes sorption isotherms determined with 1 mM HCl or 1 mM $HClO_4$ as eluent (column CNT5). Determined Freundlich coefficients (K_f) and Freundlich exponents (n) are given in table S4.7.

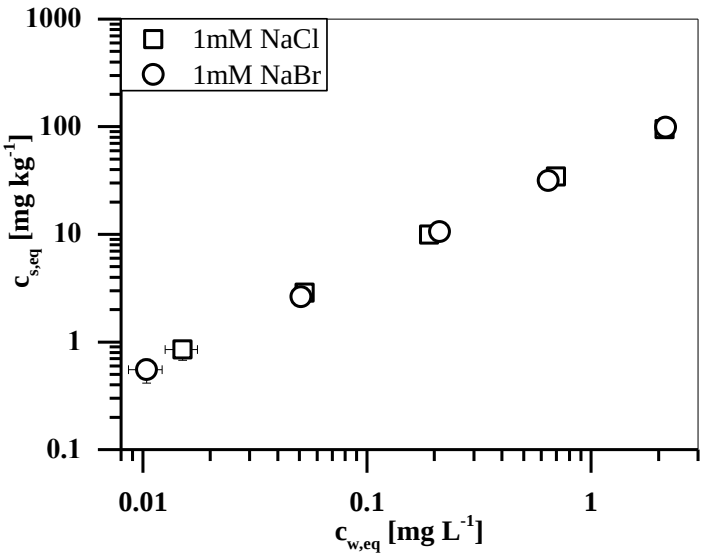

Figure S4.7: Sorption isotherms of iodide using 1 mM NaCl or 1 mM NaBr in the eluent (pH 6; 25 °C). Error bars represent the calculated maximum error.

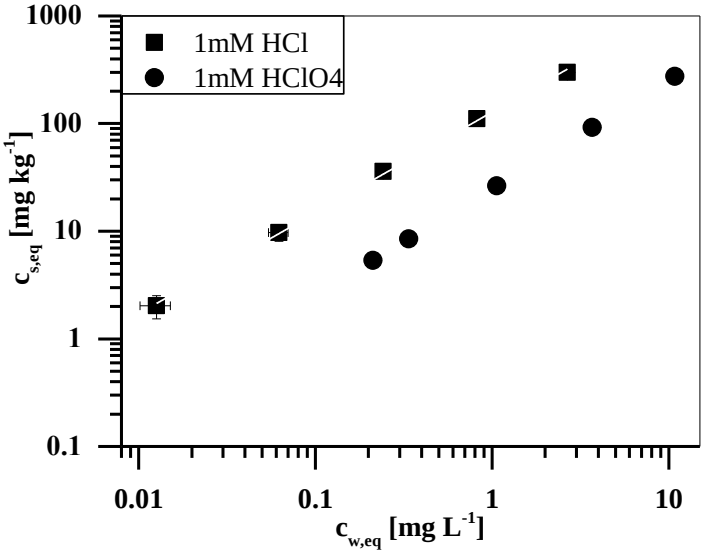

Figure S4.8: Sorption isotherms of iodide using 1 mM HCl or 1 mM $HClO_4$ in the eluent (pH 3; 25 °C). Error bars represent the calculated maximum error.

Table S4.7: Determined Freundlich coefficient (K_f), Freundlich exponent (n) and determination coefficient (R^2) of iodide isotherms determined using 1 mM NaCl or 1 mM NaBr (pH 6; 25 °C) and 1 mM HCl or 1 mM $HClO_4$ in the eluent (pH 3; 25 °C). K_f is given in (mg kg^{-1}) (mg L^{-1})$^{-n}$ and n is dimensionless. Error of K_f and n represent the standard errors of the regression coefficients.

	1 mM NaCl			1 mM NaBr		
analyte	**log K_f**	**n**	**R^2**	**log K_f**	**n**	**R^2**
iodide	1.67 ± 0.01	0.95 ± 0.01	0.999	1.68 ± 0.01	0.97 ± 0.01	0.999
	1 mM HCl			**1 mM $HClO_4$**		
analyte	**log K_f**	**n**	**R^2**	**log K_f**	**n**	**R^2**
iodide	2.11 ± 0.01	0.95 ± 0.02	0.999	1.40 ± 0.01	1.00 ± 0.01	0.999

SI4.8 Sorption isotherms of analytes depending on pH

Figure S4.9 summarizes the sorption isotherms of the different sorbates determined with eluents at pH 3, 6, and 9 at a constant ionic strength of 0.001 mol L^{-1}. Column CNT3 was used for these measurements. Determined Freundlich coefficients (K_f) and Freundlich exponents (n) are given in table S4.8. Nitrite at pH 3 was not measured as pH below pKs of nitrous acid of 3.3 may lead to the formation of nitrous gases.

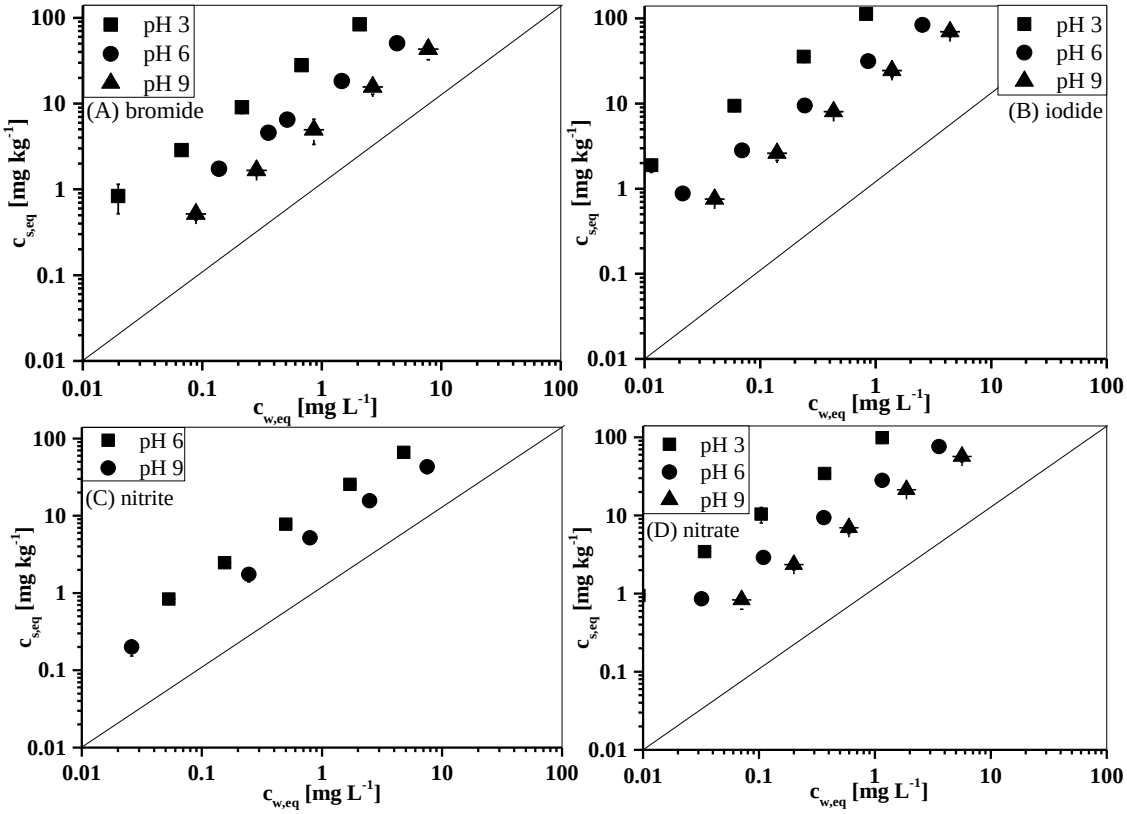

Figure S4.9: Sorption isotherms determined for bromide (A), iodide (B), nitrite (C) and Nitrate (D) with eluents at pH 3, 6, and 9 (constant ionic strength of 0.001 mol L^{-1}) (25 °C). The straight line indicates a slope of 1.

Table S4.8: Logarithmic Freundlich coefficients (K_f) [(mg kg^{-1}) (mg $L^{-1})^{-n}$] and Freundlich exponents (n) [-] determined with eluents at pH 3, 6, and 9 at a constant ionic strength of 0.001 mol L^{-1} (25 °C) in combination the corresponding determination coefficient (R^2). Errors represent the standard error of the regression parameters.

	pH 3			pH 6			pH 9		
analyte	**log K_f**	**n**	**R^2**	**log K_f**	**n**	**R^2**	**log K_f**	**n**	**R^2**
bromide	1.61 ± 0.01	0.990 ± 0.01	0.999	1.09 ± 0.01	0.981 ± 0.01	0.999	0.76 ± 0.01	0.991 ± 0.01	0.999
nitrite	-	-	-	1.17 ± 0.01	0.971 ± 0.01	0.999	0.81 ± 0.01	0.948 ± 0.01	0.999
nitrate	1.94 ± 0.01	0.962 ± 0.01	0.999	1.37 ± 0.01	0.955 ± 0.01	0.999	1.05 ± 0.01	0.970 ± 0.01	0.999
iodide	2.14 ± 0.01	0.956 ± 0.01	0.999	1.55 ± 0.01	0.956 ± 0.008	0.999	1.24 ± 0.01	0.968 ± 0.012	0.999

Figure S4.10 shows the isotherms of iodide determined at pH 3 using 1 mM HCl as eluent at different ionic strengths (conditions: 1 mM HCl; 1 mM HCl + 9 mM NaCl; 1 mM HCl + 99 mM NaCl). Column CNT5 was used for the measurements. Determined Freundlich coefficients (K_F) and Freundlich exponents (n) are given in table S4.9.

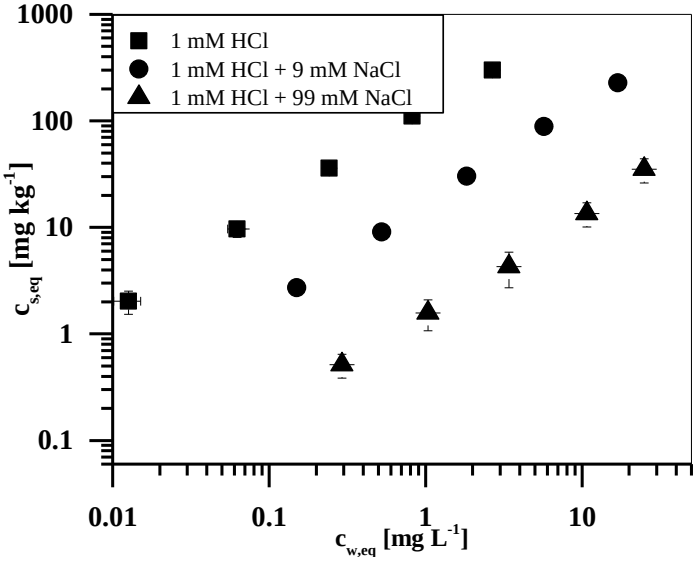

Figure S4.10: Sorption isotherms determined for iodide with eluents containing 1 mM HCl, 1 mM HCl + 9 mM NaCl or 1 mM HCl + 99 mM NaCl (pH 3, 25 °C).

Table S4.9: Determined Freundlich coefficient (K_f), Freundlich exponent (n), and determination coefficient (R^2) of iodide isotherms determined for iodide with eluents containing 1 mM HCl, 1 mM HCl + 9 mM NaCl or 1 mM HCl + 99 mM NaCl (pH 3, 25 °C). K_f is given in (mg kg^{-1}) (mg L^{-1})$^{-n}$ and n is dimensionless. Error of K_f and n represent the standard errors of the regression coefficients.

	1 mM HCl			1 mM HCl + 9 mM NaCl			1 mM HCl + 99 mM NaCl		
analyte	**log K_f**	**n**	**R^2**	**log K_f**	**n**	**R^2**	**log K_f**	**n**	**R^2**
iodide	2.11 ± 0.02	0.94 ± 0.02	0.999	1.22 ± 0.01	0.94 ± 0.01	0.999	0.19 ± 0.02	0.94 ± 0.03	0.996

Figures S4.11 and S4.12 summarize the results of the zeta-potential and XPS-measurements used to characterize the MWCNTs.

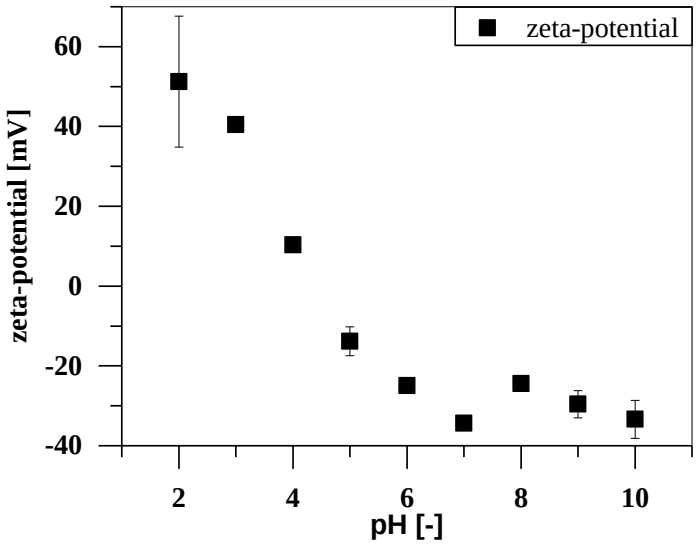

Figure S4.11: Determined zeta-potential of MWCNTs depending on the pH of the surrounding solution. Error bars represent the standard deviation of 5 replicates.

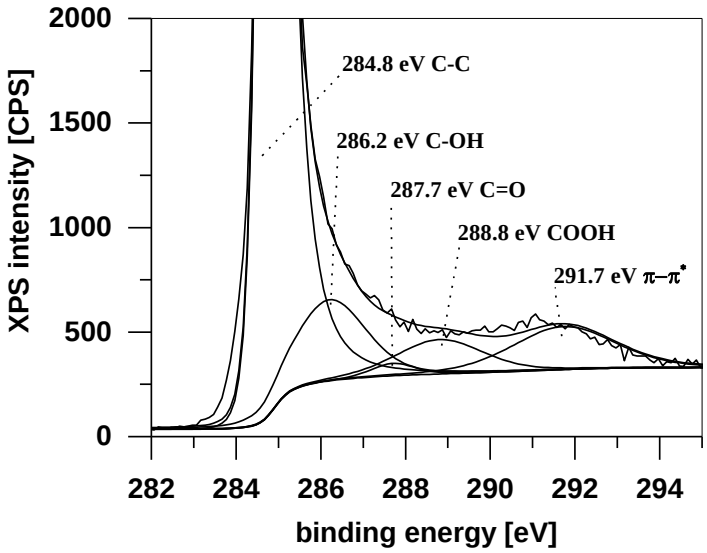

Figure S4.12: Deconvolution of the C1s peak of the XPS-measurement of MWCNTs ground to a particle size ≤ 63 µm.

References Appendix to Chapter 4

1. Bi, E. P.; Schmidt, T. C.; Haderlein, S. B. Practical issues relating to soil column chromatography for sorption parameter determination. *Chemosphere* **2010,** 80 (7), 787-793.

Chapter 5 - Influence of environmental conditions on sorption of organic compounds

Adapted from: Metzelder, F.; Funck, M.; Schmidt, T.C. Sorption of heterocyclic organic compounds to multiwalled carbon nanotubes. *Environmental Science & Technology*, **2018**, 52(9), 628 – 637.

5.1 Abstract

Sorption is an important natural and technical process. Sorption coefficients are typically determined in batch experiments, but this may be challenging for weakly sorbing compounds. A complementary method enabling analysis of those compounds is column chromatography. A column packed with the sorbent is used and sorption data are determined by relating sorbate retention to that of a non-retarded tracer.

In this study, column chromatography was applied for the first time to study sorption of previously hardly investigated heterocyclic organic compounds to multiwalled carbon nanotubes (MWCNTs). Sorption data for these compounds are very limited in literature and weak sorption is expected from prediction models. Deuterium oxide was used as non-retarded tracer.

Sorption isotherms were well described by the Freundlich model and data showed reasonable agreement with predicted values. Sorption was exothermic and physisorption was observed. H-bonding may contribute to overall sorption, which is supported by reduced sorption with increasing ionic strength due to blocking of functional groups. Lowering pH reduced sorption of ionizable compounds, due to electrostatic repulsion at pH 3 where sorbent as well as sorbates were positively charged. Overall, column chromatography was successfully used to study sorption of heterocyclic compounds to MWCNTs and could be further applied for other carbon-based sorbents.

5.2 Introduction

In the field of chemistry, research concerning carbon-based nanomaterials (CNMs) and carbon nanotubes (CNTs) as one class of CNMs often takes advantage of their strong sorption properties.[1-5] Strong sorption of different compound classes led to the application of for example multiwalled carbon nanotubes (MWCNTs) as solid phase extraction material for enrichment of organic[1, 4, 5] and inorganic compounds[2, 3] prior to analysis.

To characterize these sorption properties and study the influence of environmental conditions on sorption, batch experiments are typically conducted for organic[6-17] and inorganic compounds.[18-22] Batch experiments are simple to perform, but are accompanied by several drawbacks. First, the long equilibration time from hours[23] up to several weeks[6, 7] applied in literature in case of organic compounds makes experiments time intensive. This especially increases the time expenses to study the influence of environmental conditions on sorption if preliminary tests are necessary to adjust sorbent and sorbate amount needed to yield sufficient but not too strong / weak sorption. Second, the limited sorbent to solution ratio in batch experiments may reveal difficulties in the determination of reliable sorption data for highly soluble and weakly sorbing compounds (e.g. heterocyclic organic compounds like pyridine).[24] Third, a high amount of sorbent is necessary in case of weak sorption to investigate sorption, especially, when investigating the influence of environmental conditions on sorption in batch experiments. As an example, for sorption of perchlorate to MWCNTs in batch experiments, 37 mg sorbent were necessary when studying sorption at one pH value.[18] Using ten different pH values in triplicates would require more than one gram of sorbent. In case of more expensive sorbents like singlewalled carbon nanotubes or functionalized CNTs, one gram can cost up to 1000 euro. Finally, separation of CNMs from the water phase may be a challenging step, especially in case of dispersed materials[25, 26]. In this case, typically used techniques like filtration or sedimentation may be insufficient.[6] Additionally, the quantification of low concentrations of CNTs in matrices is challenging so that the efficiency of phase separation processes can be hardly quantified.[27] As consequence of these drawbacks, sorption models like poly-parameter linear free-energy relationships (ppLFERs) were developed for MWCNTs allowing the prediction of distribution coefficients (K_d) for organic compounds,[28, 29] without the necessity to perform additional sorption experiments for previously unknown compounds. However, these models are only valid for one setup of environmental conditions, which limits their applicability for varying environmental

conditions. It has been previously shown that pH[13, 15], ionic strength[30, 31] and temperature[32, 33] influence sorption properties of sorbates and CNMs.[34]

As complement to batch experiments, column experiments can be applied to study sorption, by determination of single K_d values as well as isotherms using the retardation of the sorbate in relation to a non-retarded tracer in a sorbent packed column. This experimental approach has been used successfully for sorption studies to soot particles,[35] soils[24, 36-45] or mineral surfaces,[46, 47]. The applicability of this methodology could also be shown in chapters 3 and 4 for sorption of inorganic anions and selected organic compounds to MWCNTs. Drawbacks of batch experiments can potentially be overcome by column experiments. The analysis of weakly sorbing and highly soluble compounds is possible because of higher sorbent to solution ratios without a simultaneous need of large amounts of sorbent material. Furthermore, changing the composition of the mobile phase regarding ionic strength, type of ions and pH or by changing the column temperature using a thermostat facilitates investigations of the influence of environmental conditions on sorption. Additionally, equilibration times can be significantly reduced. Additional equipment like centrifuges can be avoided, as the sorbent remains fixed in the column.

However, column experiments also may have disadvantages. Column clogging and too strong sorption can be serious problems, which lead to very high backpressure or cause long retention times and deterioration of the signal by peak broadening, respectively. Concomitant, backpressure and sorption can both be reduced by the dilution of the sorbent material with inert material like quartz[24, 40] or silicium carbide[37], which should not show any interaction with the sorbate. The dilution with inert material further reduces the sorbent demand and, consequently, costs to purchase those materials. An important disadvantage, potentially preventing the applicability of column experiments, is sorption hysteresis. Sorption hysteresis describes the incomplete desorption of a sorbate from the sorbent. Using a Dirac input (i.e. injection of a sorbate pulse instead of a continuous sorbate input) desorption is a prerequisite in column experiments, because otherwise no signal can be recorded. If sorbate molecules remain sorbed to the surface, changed interactions between the sorbent surface and sorbate molecules will be the consequence in consecutive measurements and this will result in potentially misleading sorption data. For the measurement of breakthrough curves, sorption hysteresis is less problematic, but each column could only be used for one compound and one introduced concentration. For further consecutive measurements the sorbent surface would not be pristine as sorbate molecules remain sorbed on the surface. Sorption hysteresis has already been shown for sorption of some organic compounds to CNMs in batch

experiments[48-50]. However, for inorganic anions and selected organic compounds, sorption hysteresis to MWCNTs was not observed in chapters 3 and 4.

Thus, the aim of this study was to investigate sorption of weakly sorbing organic compounds to MWCNTs using column chromatography and to identify the influence of environmental conditions like temperature, ionic strength and pH on sorption. Heterocyclic organic compounds were chosen as sorbates for this purpose, because only very limited sorption data are available in literature for this compound class and sorption data predicted using ppLFERs from literature[28] indicated only weak sorption that may preferably be analyzed using column chromatography instead of classical batch experiments.

5.3 Materials and Methods

5.3.1 Chemicals and Packing Materials

Chemicals used as sorbates in this study were heterocyclic organic compounds (furan, imidazole, oxazole, pyrazine, pyrazole, pyridazine, pyridine, pyrimidine, pyrrole, thiazole and thiophene). Detailed information on manufacturer and purity are given in section SI5.1 in chapter 5.6. Additional chemicals used in this study were hydrochloric acid (HCl) (37 %, analytical grade, Fisher Scientific), sodium hydroxide (NaOH) (1 mol L^{-1}, Bernd Kraft), calcium chloride ($CaCl_2 \times 2\ H_2O$) (≥ 99.5 %, AppliChem Panreac) and deuterium oxide (D_2O) (≥ 99.9 atom-%, Sigma-Aldrich). Eluents for high performance liquid chromatography (HPLC) were prepared with ultrapure water (18.2 MΩ cm^{-1} resistance, PURELAB Ultra, ELGA LabWater, Celle, Germany) and addition of appropriate amounts of salts, acid or base to reach the desired concentrations or pH value. Individual stock solutions of each sorbate and tracer were prepared in the respective eluent used for measurements and stored at 4 °C in the dark.

In this chapter, MWCNTs and quartz were used as packing materials like in the previous chapters. Detailed information on these materials can be found in chapter 3.3.1 in this thesis.

5.3.2 Apparatus

Detailed information on empty HPLC-columns and additional equipment used for column packing is mentioned in chapter 3.3.2. All experiments were conducted using the Knauer HPLC-system described also in chapter 3.3.2.

5.3.3 Column chromatography

The procedure for column packing developed in chapter 3 was applied also in this chapter for column packing. MWCNTs were diluted with quartz as inert material by a factor of 20 for all sorbates except thiophene, i.e. a MWCNT content of 5 % (wt/wt). Dilution with quartz increased both the stability of the packing material inside the column and reduced the backpressure. Even with this dilution, sorption was strong leading to measurement times of up to 90 minutes per measurement run in case of pyridine. For thiophene a dilution by a factor of 200, i.e. a MWCNT content of 0.5 % (wt/wt), was necessary as retention was too strong in columns containing 5 % MWCNTs. In 5 % MWCNT columns, measurement times of more than 150 minutes and a maximum absorption of only 60 mAU even for an almost saturated solution of thiophene were recorded because of a pronounced tailing. Maximum intensity in the chromatogram was much lower compared to the other sorbates, which was typically around 1500 mAU for the highest injected concentration. To reach a similar range in absorption, dilution of MWCNTs had to be increased.

The conservative tracer used in this study was D_2O. D_2O was diluted 1:9 with the respective eluent (vol.-%/vol.-%) and detected using the refractive index detector (RID). Retention times of sorbates and tracer used for calculation of the retardation factor (R) (equation 5.1) and K_d values (equation 5.2) were determined based on the half-mass point, i.e. the point at which the peak area is divided in two equal parts.[51] Peaks of sorbates in this study showed a pronounced tailing (e.g. asymmetry factors of peaks of pyridine determined at 10 % of the maximum intensity were up to 7.9). Standard deviations of R and K_d, determined by error propagation, were typically smallest for the half-mass method compared to other typically used approaches like the apex point of the eluting peak or the first moment approach[36, 37] (data not shown). Furthermore, the half-mass point has previously shown its applicability in sorption studies on soil or minerals,[24, 39, 40, 46] but also for MWCNTs as shown in the previous chapters.

$$R = (t_{R,sorb} - t_{0,sorb}) / (t_{R,tracer} - t_{0,tracer}) \quad (5.1)$$

$$R = 1 + \rho_b / \theta \times K_d \quad (5.2)$$

$t_{R,sorb}$ is the retention time of the sorbate while $t_{R,tracer}$ is the retention time of the tracer with column installed in the system. $t_{0,sorb}$ is the traveling time through injector and capillaries between autosampler and DAD without column, while $t_{0,tracer}$ is the traveling time from autosampler to the RID without column. Both detectors were connected in serial connection, which required different corrections for the retention time of sorbate and tracer. $t_{0,sorb}$ and $t_{0,tracer}$ were determined by repeated injections of sorbate and tracer without column installed in the system (n = 10). For measurements without column, capillaries were connected using a low dead volume stainless steel union (0.25mm bore, VICI Jour.). θ [-] and ρ_b [kg L^{-1}] are the porosity and the bulk density of the column used, respectively. Both were calculated according to equations 3.1 and 3.2 in chapter 3 of this thesis from repeated measurements of D_2O with and without column installed in the system (n = 10). Determined values for both characteristics of columns used in this study are given in chapter 5.6 (section SI5.2)**.** Recovery of D_2O was determined from peak areas with and without column and was found to be quantitative (90 to 105 %). Regular measurements of D_2O during sorption studies showed no significant shift of the retention time of D_2O for more than 200 injections (data not shown).

Wavelengths used to record chromatograms of the different sorbates are given in section SI5.1 in chapter 5.6. Interaction of the different sorbates with the inert material was checked in a column packed with exclusively quartz and was negligible (K_d calculated from the quartz column < 0.1 % of that calculated from the MWCNT column). K_d values for pyrazole, which was used as reference compound for each MWCNT-column, varied with a relative standard deviation of 6.2 % (ten columns), when injecting the same concentration in each column. This indicates an acceptable reproducibility for self-packed columns. Mass recovery of sorbates was calculated by comparison of peak areas of each sorbate from MWCNT-columns with those from measurements without column or a quartz column. Recoveries ranged between 80 and 120 % for all sorbates with exceptions for very low injected concentrations. In these cases, the measured absorption was very low and baseline noise became an issue because of peak broadening. Conclusively, sorption hysteresis was not observed in this study as recovery was quantitative. Error bars depicted in figures indicate the maximum error, which was derived from the individual standard deviations of retention times of sorbate and tracer with and without column via error propagation.

Columns were equilibrated for at least 12 hours by flushing at 0.1 mL min^{-1} with the respective eluent. Preliminary measurements were performed for each sorbate at 10 mM $CaCl_2$, pH 6 and 25 °C for different flow rates / pore water velocities to test the degree of non-equilibrium in the experiments. One concentration of each sorbate was separately

injected (concentrations are mentioned in section SI5.3 in chapter 5.6). Sorption was at or very close to equilibrium, because determined R values varied only slightly with maximum 8 % at different flow rates / velocities ranging from 0.015 – 0.1 mL min^{-1} or 0.33 – 2.2 cm min^{-1}, respectively (shown for selected compounds in section SI5.3 in chapter 5.6). Because of the small influence of the flow rate, 0.1 mL min^{-1} was used as flow rate for all experiments.

5.3.4 Isotherm determination

Isotherms of sorbates were determined using an eluent with 10 mM $CaCl_2$ at pH 6 and 25 °C controlled by the column thermostat, as these conditions were also applied in previous studies using the same type of MWCNTs.[28] Sorbates were injected separately in MWCNT columns with increasing concentration and three replicates with exception of pyridine, where two replicates were used due to long measurement times. Nine different concentrations were injected and used for isotherm generation of each sorbate. The injected concentrations of each sorbate are given in section SI5.4 in chapter 5.6.

Sorption isotherms of the sorbates investigated in this chapter were derived using the classical and alternative approach discussed in chapter 3.3.6 in this thesis. Calibrations of the different sorbates used for isotherm calculation are given in section SI5.5 in chapter 5.6. The Freundlich model was used to fit derived isotherm data as it was done in the previous chapters of this thesis. The similarity between both approaches was also evaluated for the sorbates investigated in this chapter, because applying the alternative approach reduces the time necessary for determination of an isotherm almost by a factor of ten compared to the classical approach in case of nine different concentrations used for isotherm construction. In chapter 3 the suitablility of this approach for other sorbates was already investigated, but differences due to the changed molecular structure may occur for sorbates in this chapter, which should be evaluated.

5.3.5 Influence of environmental conditions on sorption

To reduce the time expense in studying the influence of environmental conditions on sorption, a selection of heterocyclic compounds was chosen and only one concentration with three replicates per sorbate were injected. Evaluation was done based on the “alternative approach”. Compound selection was done according to the sorption strength / retention inside the column represented by the Freundlich-coefficient (K_f) of isotherms previously determined (see chapter 5.3.4), water-air distribution by the K_{wa}-value and the pK_a-value of the corresponding acid of the compound (section SI5.7 in chapter 5.6). A broad compound range

was represented by the selected compounds, as weakly to strongly sorbing compounds, compounds with low to high K_{wa}-values were present and compounds of which speciation is changed or remains the same by changing the pH value were used. Mean values of the three replicates of K_d as well as K_f and the Freundlich exponent (n) derived from chromatograms at varied environmental conditions are reported. Injected concentrations for the different conditions are given in chapter 5.6 (section SI5.7).

1) *Temperature:* Column CNT52 and CNT53; flow rate of 0.1 mL min^{-1}; 10 mM $CaCl_2$ in the mobile phase; pH 6; 25, 40 and 55 °C. CNT52 was used for the high concentrations of each compound, while CNT53 was used for the low concentrations.
2) *Ionic strength:* Column CNT54; flow rate of 0.1 mL min^{-1}; 25 °C; pH 6; 1, 10 or 100 mM $CaCl_2$ in the mobile phase.
3) *pH value:* Column CNT55; flow rate of 0.1 mL min^{-1}; 25 °C; pH 3, 6 or 9 using 10 mM $CaCl_2$. Ultrapure water with 10 mM $CaCl_2$ had the desired pH value of 6. NaOH was used to change the pH to 9. At pH 3, a concentration of 1 mM HCl was added to reach the desired pH value. For pH 3 and 9 the ionic strength was chanced by less than 5 % compared to pH 6 and was assumed to be constant.

   Variation of ionic strength at pH 3: Column CNT56; flow rate of 0.1 mL min^{-1}; 25 °C; pH 3; 1 mM $CaCl_2$ + 1 mM HCl, 10 mM $CaCl_2$ + 1 mM HCl or 100 mM $CaCl_2$ + 1 mM HCl in the mobile phase.

5.4 Results and Discussion

5.4.1 Determination of sorption isotherms

Different heterocyclic organic compounds were analyzed to determine sorption isotherms. With increasing injected concentration, the apex point of the peak increased in intensity and decreased in retention time. Selected chromatograms of pyrazole for different injected concentrations are shown in figure S5.2 in chapter 5.6 (section SI5.4). The same behavior was observed for the determined half-mass point and for all compounds investigated in this study.

Consequently, increasing injected concentration resulted in decreasing K_d values. In case of pyrazole, K_d decreased by more than a factor of five (111.8 L kg^{-1} for 15 mg L^{-1} injected concentration and 19.5 L kg^{-1} for 1000 mg L^{-1}). For the other compounds, the decrease was similar relative to the respective values. Decrease in K_d was much stronger compared to sorption of inorganic anions to MWCNTs in column experiments presented in chapter 4. For inorganic anions like iodide, the decrease was at maximum about 50 %, but in

most cases the decrease was only about 20 % or less, when increasing the injected concentration from 0.6 to 63 mg L^{-1}.

Strongly decreasing K_d values with increasing sorbate concentrations are a strong indicator for non-linear sorption. Sorption isotherms derived from chromatograms were calculated according to both methods mentioned in section 5.3.4 and fitted using the Freundlich model ($c_{s,eq} = K_f \times c_{w,eq}^n$), which is often used in batch experiments on sorption to CNTs.[10, 13, 15, 16, 28, 33, 52-54] Selected isotherms are also shown in an diagram in figure S5.3 in chapter 5.6. Values for K_f, n and correlation coefficients (R^2) of all sorbates are summarized in table 5.1.

Table 5.1: Determined Freundlich coefficients (K_f) [(mg kg^{-1}) (mg $L^{-1})^{-n}$], Freundlich exponents (n) [-] and correlation coefficients (R^2) [-] of isotherms of sorbates calculated based on the classical and the alternative approach. Uncertainties given in the table are the standard errors of the regression with K_f as y-intercept and n as slope of the regression for the classical approach and the standard deviation of the three replicates for the alternative approach.

	classical approach			alternative approach		
sorbate	K_f	n	R^2	K_f	n	R^2
furan	132.2 ± 2.3	0.60 ± 0.01	0.9995	154.8 ± 0.7	0.54 ± 0.01	0.9998 ± 0.0001
imidazole	39.3 ± 0.3	0.69 ± 0.01	0.9997	48.8 ± 0.6	0.60 ± 0.01	0.9998 ± 0.0001
oxazole	36.5 ± 0.8	0.77 ± 0.01	0.9978	47.9 ± 0.2	0.68 ± 0.01	0.9994 ± 0.0001
pyrazine	222.2 ± 5.2	0.58 ± 0.01	0.9967	231.7 ± 3.8	0.57 ± 0.01	0.9987 ± 0.0007
pyrazole	57.6 ± 2.9	0.71 ± 0.02	0.9920	73.3 ± 0.2	0.65 ± 0.01	0.9965 ± 0.0001
pyridazine	137.9 ± 0.4	0.64 ± 0.01	0.9999	144.9 ± 0.1	0.62 ± 0.01	0.9999 ± 0.0001
pyridine	243.1 ± 3.0	0.53 ± 0.01	0.9985	261.1 ± 2.9	0.50 ± 0.01	0.9994 ± 0.0001
pyrimidine	154.0 ± 4.9	0.67 ±0.01	0.9961	177.0 ± 2.9	0.62 ± 0.01	0.9996 ± 0.0001
pyrrole	65.2 ± 2.2	0.71 ± 0.02	0.9963	82.2 ± 0.1	0.62 ± 0.01	0.9997 ± 0.0001
thiazole	158.4 ± 3.3	0.59 ± 0.01	0.9978	187.9 ± 0.3	0.53 ± 0.01	0.9997 ± 0.0001
thiophene[a]	127.5 ± 0.8	0.74 ± 0.01	0.9999	234.2 ± 1.3	0.61 ± 0.01	0.9991 ± 0.0001

a: determined with a column containing only 0.5 % MWCNTs, which may result in slightly smaller values compared to the other compounds.

For both evaluation approaches, data were well fit by the Freundlich model as indicated by the high R^2 ($R^2 > 0.992$). Determined K_f values differed strongly between the different sorbates. The smallest value was determined for oxazole while an about six times higher value was determined for pyridine. The alternative approach gave generally higher values for K_f, but results were in all cases very similar to the classical approach with less than 30 % higher values for the alternative approach with exception of thiophene (84 % higher). The MWCNT content inside the column was lower for thiophene compared to the other sorbates, which led to a stronger increase in signal intensity with increasing injected concentration and a generally lower retention inside the column compared to the other sorbates (figure S5.4 and S5.5 in chapter 5.6). This results in a larger deviation between both approaches as the absorption used to calculate $c_{w,eq}$ in case of the alternative approach is much higher compared to the absorption used for the classical approach. Determined n values indicate that sorption of all sorbates was non-linear (0.50 – 0.75). Non-linearity was in all cases larger for the alternative approach, but deviation was less than 20 % for all compounds, which again shows the similarity of results obtained by both evaluation approaches. To further compare sorption isotherms, K_d values calculated based on the classical and alternative approach for 1 %, 0.1 % and 0.01 % of the maximum solubility in water of the respective compound (figures S5.6 – S5.8 in chapter 5.6 (section SI5.6)) agree well with each other with a deviation of less than 0.3 log units. Consequently, the alternative approach proved its suitability as K_f, n, and K_d values are similar to those of the classical approach, but it requires significantly reduced time.

Non-linear sorption to CNTs is commonly found in literature for organic[10, 13, 15, 16, 28, 33, 52-54] and inorganic compounds[18, 20, 21] in batch experiments. Only in rare cases, like for inorganic anions in chapter 4 or in a very low concentration range for PAHs[6], sorption to MWCNTs was found to be linear. When extending the concentration range also for PAHs[6] the sorption isotherms became non-linear. The non-linearity is attributed to the heterogeneous energy distribution of sorption sites becoming relevant when reaching higher concentrations. At low concentrations only high energy sorption sites like defects or functional groups are occupied, while at higher concentrations also sorption sites exhibiting a lower energy become relevant and sorption affinity decreases.[34]

Only for pyridine a sorption isotherm using MWCNTs as sorbent was found in literature, but experimental conditions were different.[55] Sorption experiments were done in batch experiments at pH 7 and 10, i.e. higher than the pH of 6 used in this study, which influences the speciation of pyridine. The fraction of positively charged pyridine drops from

15 % at pH 6 to 1.5 % at pH 7, which may also result in changing interactions between sorbent and sorbate due to charged sorbate molecules and sorbent surface. Sorption was found to be almost linear as n was with 0.94 close to unity.[55] Reason may be the small concentration range investigated. In a narrow concentration range, linearity may always approach one compared to a wider concentration range as already observed for PAHs.[6] K_f was found to be almost one order of magnitude higher in literature (2.5 x 10^3 (mg kg^{-1}) (mg L^{-1})$^{-n}$ (changed from unit (mmol kg^{-1}) (mmol L^{-1})$^{-n}$)).[55] These observations show substantial differences between both isotherms, which may be related to differences in the investigated concentration range, environmental conditions (pH, ionic strength), type of MWCNTs and sorbent to solution ratio limiting the comparability and resulting in large deviations. As further experimental sorption data for the other sorbates are missing, K_d values for all compounds were calculated from the respective isotherms and had to be compared to K_d values predicted using ppLFERs.[28]

ppLFERs were derived from batch isotherms using the exact same environmental conditions and sorbent material so that the experimental conditions are well comparable.[28] Solute descriptors are mentioned in section SI5.6 in chapter 5.6. The comparison of K_d values is shown for 1 %, 0.1 % and 0.01 % of the maximum solubility in water in figures S5.6 – S5.8 in chapter 5.6 (section SI5.6). For oxazole, pyrimidine, pyrrole and thiazole agreement of data calculated based on the isotherms of the classical and alternative approach with ppLFER data was good. Deviation was less than 0.3 log-units at all three concentrations levels, which is typically an acceptable deviation for predicted values. Higher deviations were observed for the other compounds of more than 0.5 log-units with exception of furan and pyrazole at 0.01 %. Maximum deviation was 0.9 log-units. For those compounds no general tendency could be observed, as predicted values were larger than measured values for furan, pyridine and thiophene, while for imidazole, pyrazole and pyridazine the opposite behavior was found. Regarding the relationship between structure and sorption of heterocyclic compounds it could be observed that sulfur atoms may enhance sorption. Thiazole has the heteroatoms in the same positions than imidazole and oxazole, but has a sulfur atom instead of oxygen or nitrogen. Thiazole showed much stronger sorption at the same relative concentration with regard to the calculated K_d values. Equally, thiophene containing sulfur had higher K_d values compared to furan containing oxygen and pyrrole containing nitrogen. For the ppLFER predictions it should be noted here, that predicted values are also connected with an uncertainty. First, solute descriptors used to set up the ppLFERs and predict K_d values are connected with an uncertainty. Second, mainly non-heterocyclic compounds were used to set up the ppLFERs

with the exception of larger heterocyclic compounds indole and benzofuran, which may result in deviations for the compounds analyzed in this study. Third, only non-ionic species were used to set up the ppLFERs.[28] Thus, pyridine and imidazole, which were partially charged at the environmental conditions used in this study, are compounds with limited suitability of the ppLFERs. This may also explain to some extent the larger deviations to predicted values for these two compounds.

In summary, column experiments proved suitable as fast technique to determine sorption isotherms for heterocyclic organic compounds. Additionally, much smaller amounts of approximately 8 mg sorbent material per sorbate and column were necessary because of the dilution with quartz and the possibility to use columns for several consecutive measurements applying different concentrations. Using batch experiments, the sorbent demand would have been much higher. More than one gram of the sorbent per isotherm of a sorbate would be necessary assuming triplicates and the sorbent demand used in case of sorption of trihalomethanes to MWCNTs.[33] The alternative approach in isotherm evaluation showed its applicability and reduces the time demand for isotherm measurement by almost a factor of ten. Consequently, for further experiments to evaluate the influence of environmental conditions on sorption the alternative approach was used. Thus, besides K_d values also isotherms could be derived using only one injected concentration measured in triplicates.

5.4.2 Influence of temperature

The influence of temperature on sorption is shown in figure 5.1. Sorption coefficients decreased with increasing temperature for all analytes. The sorption enthalpy (ΔH) was calculated using the van´t Hoff equation from the slope of the regression line in figure 5.1 according to equation 5.3.

$$\ln K_d = \Delta S/R_{const} - \Delta H/R_{const} \times 1/T \qquad (5.3)$$

Where ΔH is the sorption enthalpy [kJ mol^{-1}], ΔS the entropy change [kJ mol^{-1} K^{-1}], R_{const} the gas constant [8.3145×10^{-3} kJ mol^{-1} K^{-1}] and T the temperature [K].

The determined values for ΔH ranged between -20.6 and -27.1 kJ mol^{-1} (all values are shown in section SI5.8 in chapter 5.6). Consequently, sorption of these organic compounds is an exothermic process. In literature, sorption of different organic compounds like trihalomethanes,[33] atrazine,[32, 56] nitroaromatics,[57] phenols,[15, 58] oxaquindox,[59] ciprofloxacin[49] or toluene, m-xylene, ethylbenzene[23] to different CNTs was also found to be exothermic. Conversely, sorption of 1,2-dichlorobenzene,[13] sulfamethazine,[60] or dyes[14] to different CNTs was found to be endothermic or showed in case of dissolved organic matter to SWCNTs[61] no

temperature dependency. Consequently, there is no coherent thermodynamic basis for all compound classes reported in literature.

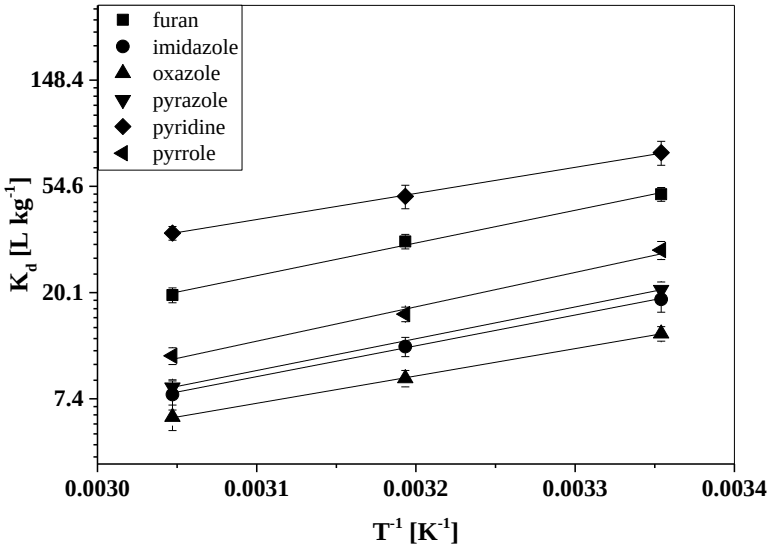

Figure 5.1: Determined K_d values of the analytes plotted against the reciprocal temperature at 10 mM $CaCl_2$ in the eluent at pH 6. Error bars indicate the maximum error estimated from standard deviation of retention times of sorbate and tracer via error propagation (n=3). Scale of K_d in the y-ordinate is set to the natural logarithm.

Covalent bonding like in case of chemisorption is absent in this study as determined values for ΔH were smaller than typically determined values in the range from -60 to -80 kJ mol^{-1} for organic compounds.[62] Consequently, physisorption seems to be the underlying mechanism. This was also concluded in other studies dealing with sorption to CNTs.[49, 57, 59] Additionally, this is supported by quantitative recovery and, consequently, fully reversible sorption, which is characteristic for physisorption. H-bonding (-10 – -40 kJ mol^{-1})[63] with functional groups located on the MWCNTs surface may be responsible for interactions between the analytes and sorbent. Functional groups offering this kind of interactions like -COOH, C=O and C-OH were present on the surface of MWCNTs as already shown in chapter 4. Additionally, also van-der-Waals (vdW) forces between sorbent and sorbates may be contributing due to the molecular structure of the sorbates, although typical ΔH-values are much smaller (vdW: -1 – -2 kJ mol^{-1})[64] when exclusively these forces contribute to sorption.

When the injected concentration of each analyte was reduced, the temperature effect on sorption was more pronounced for all analytes with exception of oxazole. Values for ΔH ranged at the lower injected concentration between -18.2 and -33.8 kJ mol^{-1} (all values are shown in section SI5.8 in chapter 5.6). Although the change in ΔH due to the lower concentration was relatively small, it was higher than the measurement uncertainty. A similar

trend regarding ΔH with increasing concentration was also observed for sorption of ciprofloxacin to SWCNTs[49] or various heterocyclic compounds including pyridine to reference soils.[40] The more pronounced temperature dependency is related to a reduced loading of the surface of MWCNTs with the consequence that energy distribution of sorption sites is less spread compared to the higher injected concentration. At the high concentration, energetically favorable and non-favorable sites are occupied, while at the lower concentration a similar number of favorable sites and less non-favorable sites are occupied.[34] This leads to more negative values for ΔH. This was also concluded in case of sorption to reference soils.[39]

Sorption isotherms derived from measurements at various temperatures showed that K_f decreased with increasing temperature while n only slightly increased (section SI5.8 in chapter 5.6). Decreasing K_f could be expected as sorption was generally reduced with increasing temperature. Sorption linearity expressed by n was not influenced by temperature. Similar observations regarding K_f and n were reported by Yan *et al.*[56].

5.4.3 Influence of ionic strength

The influence of ionic strength on sorption of the selected compounds is shown in figure 5.2. Determined K_d values reduced steadily, but in total it decreased only slightly with increasing ionic strength of the eluent for all compounds by 6 – 42 % with exception of imidazole and pyridine. For imidazole and pyridine, an overall tendency of reduced sorption with increasing ionic strength was also observed, but K_d at 10 mM $CaCl_2$ was even lower than those at 1 and 100 mM $CaCl_2$. Imidazole and pyridine are the only compounds that are partially positively charged (imidazole: ≈ 91 %; pyridine: 15 %) at the tested environmental conditions (pH 6), while the sorbent was negatively charged at these conditions as shown in chapter 4. Therefore, increased ionic strength would constantly and more pronounced reduce sorption if electrostatic attraction between charged sorbate molecules and the oppositely charged sorbent surface was significantly contributing to overall sorption. Consequently, electrostatic attraction seems to be less important in this case and is contributing at the most slightly to sorption of these two compounds, which may be related to the competition of positively charged sorbate molecules with Ca^{2+} present in solution. Ca^{2+} may interact preferably with the negatively charged sorbent surface shielding the negative charge of the surface visible to positively charged sorbate molecules so that electrostatic attraction of those is prevented.

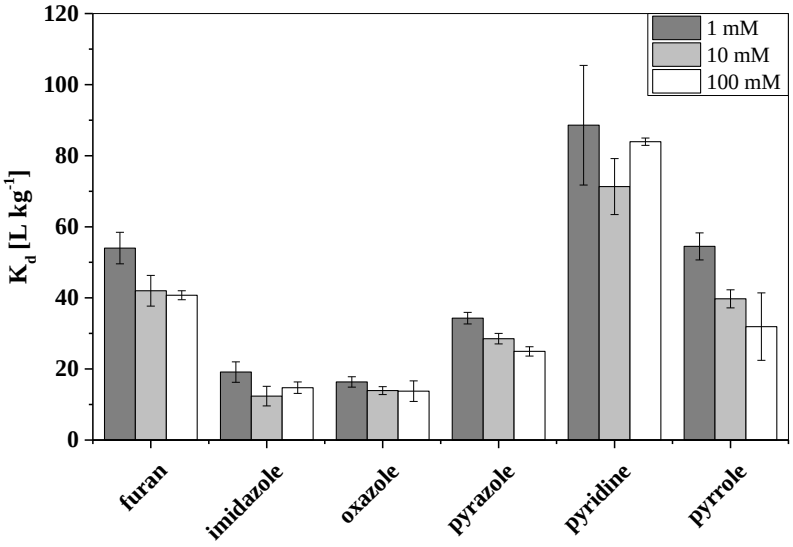

Figure 5.2: Determined K_d values of the different analytes for three different concentrations of $CaCl_2$ in the eluent (1, 10 and 100 mM). Error bars indicate the maximum error estimated from standard deviation of retention times of sorbate and tracer via error propagation (n=3).

Sorption isotherms derived from measurements showed that K_f and n remained almost constant or only slightly changed (section SI5.9 in chapter 5.6). This could be expected as K_d values were also only slightly influenced. K_f of pyridine reduced stronger, but this was a consequence of a spectral interference with the increasing chloride concentration, which is further discussed in chapter 5.6 (section SI5.9).

Reduced sorption to CNTs of chlorophenols with increasing concentration of sodium chloride (NaCl) was reported in literature, while in the same study increasing concentration of potassium chloride (KCl) showed no or only minimal reduction.[31] The authors assigned the difference to deviations in pi-cation interactions of Na^+ and K^+ between sorbents and sorbate. Also in case of roxarsone[30] increased ionic strength reduced sorption. Decreasing sorption was assigned to changes in CNT-aggregates reducing the available surface area and cations that interact with functional groups and therefore inhibit interactions between functional groups and sorbates. Also for inorganic anions shown in chapter 4 or cations[65] sorption decreased with increasing ionic strength of the eluent. Similar effects are expected in this study as increased concentrations of ions in solution may interfere H-bonding interactions of polar heterocyclic organic compounds with the sorbent as surface functional groups like COOH, C=O and C-OH may be blocked by ions from the liquid matrix accumulating at these locations.

5.4.4 Influence of pH

Finally, the influence of the pH value on sorption is shown in figure 5.3. Determined K_d values were almost constant for pyrazole, pyrrole, furan and oxazole, while K_d decreased strongly with decreasing pH for imidazole (54 %) and pyridine (79 %). In case of pyridine, decrease in K_d is sharp between pH 6 and 3. Speciation of the sorbates imidazole and pyridine is changed due to the pH value, while for the other compounds speciation remained unchanged (oxazole, pyrrole, furan) or was only changed very slightly (pyrazole). While at pH 3 more than 99 % of imidazole and pyridine are protonated and positively charged, only 15 % in case of pyridine and 92 % in case of imidazole are positively charged at pH 6. At pH 9 only 1 % or less of both compounds is present with a positive charge. Besides the speciation of the sorbates also the speciation of the sorbent is changed. At pH 3 the surface is positively charged, while at pH 6 and 9 the surface is negatively charged (compare chapter 4). Consequently, sorption of imidazole and pyridine may be reduced at pH 3 due to electrostatic repulsion occurring between the positively charged sorbent surface and the equally charged sorbate molecules. Contribution of electrostatic repulsion could be confirmed due to measurements at increased ionic strength at pH 3. At 100 mM $CaCl_2$ sorption of pyridine and imidazole increased compared to 10 mM $CaCl_2$ by 90 % and 50 %, respectively (figure S5.10 in chapter 5.6). Increased ionic strength results in reduction of the electrostatic repulsion of equal charges by shielding those with oppositely charged ions from the liquid matrix.

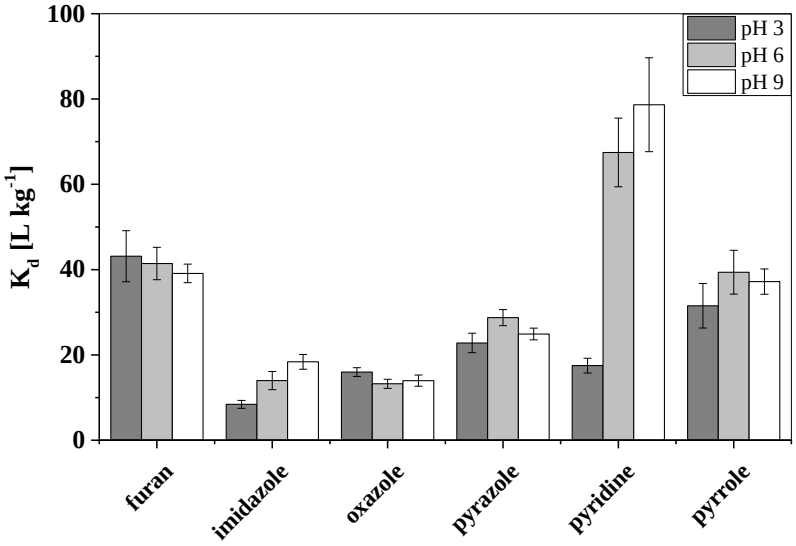

Figure 5.3: Determined K_d values of the different analytes for three different pH values of the eluent (3, 6 and 9). Error bars indicate the maximum error estimated from standard deviation of retention times of sorbate and tracer via error propagation (n=3).

Sorption isotherms derived from measurements showed that K_f of pyridine decreased strongly with decreasing pH as it was observed for K_d (section SI5.10 in chapter 5.6). In case of imidazole the change was less pronounced, but it was still visible. For the other compounds, no clear trend could be observed regarding K_f and sorption linearity expressed by n as it was also found for K_d.

Decreasing sorption to CNTs as consequence of electrostatic repulsion was also described in literature. In case of different anilines sorption decreased with decreasing pH due to electrostatic repulsion.[17] As an example, the pK_a-value of 4-chloroaniline is 4.15 indicating an increasing amount of the positively charged species with decreasing pH. Sorption reduced strongly when pH decreased below 6 when the fraction of the positively charged species started to increase. Similar observations were made for different phenol derivates[10, 16, 17, 31, 53, 58, 66], when pH was increased above the pK_a of the respective compound. As sorbents and sorbates were negatively charged, electrostatic repulsion occurred. No influence of pH on sorption for compounds of which speciation is not changed with changing pH was also reported in literature for naphthalene or 1,2-dichlorobenzene,[10] phenanthrene,[16] atrazine[54, 56] and m-xylene, toluene, or ethylbenzene.[23] This fits well to the results presented in this study.

Overall, column chromatography was used successfully for the first time to study sorption of heterocyclic organic compounds to MWCNTs and the influence of varying environmental conditions on their sorption. A fortitude of the column method is the fast and simple investigation of the influence of environmental conditions on sorption while concomitantly reducing the sorbent demand strongly. Trends and observations made with classical batch experiments regarding the influence of temperature, pH and ionic strength on sorption could also be observed using the column method presented here so that this method represents a promising alternative also for sorption studies regarding CNMs with the aim to investigate the influence of environmental conditions on sorption. This method is applicable for all UV-active organic compounds. Coupling to other detection techniques (e.g. mass spectrometry (MS)) would also allow the analysis of compounds with insufficient UV absorption. Depending on the type of compound, dilution of MWCNTs may have to be increased or decreased to be able to get sufficient and not too strong retention inside the column. The applicability of the method for other types of carbon-based sorbents will be shown in chapter 6 to compare sorption properties of these materials under similar conditions using column experiments.

5.5 References

1. Hüffer, T.; Osorio, X. L.; Jochmann, M. A.; Schilling, B.; Schmidt, T. C. Multi-walled carbon nanotubes as sorptive material for solventless in-tube microextraction (ITEX2) - a factorial design study. *Analytical and Bioanalytical Chemistry* **2013,** 405 (26), 8387-8395.
2. Duran, A.; Tuzen, M.; Soylak, M. Preconcentration of some trace elements via using multiwalled carbon nanotubes as solid phase extraction adsorbent. *Journal of Hazardous materials* **2009,** 169 (1-3), 466-471.
3. Gil, R. A.; Goyanes, S. N.; Polla, G.; Smichowski, P.; Olsina, R. A.; Martinez, L. D. Application of multi-walled carbon nanotubes as substrate for the on-line preconcentration, speciation and determination of vanadium by ETAAS. *Journal of Analytical Atomic Spectrometry* **2007,** 22 (10), 1290-1295.
4. Ma, J. P.; Lu, X.; Xia, Y.; Yan, F. L. Determination of pyrazole and pyrrole pesticides in environmental water samples by solid-phase extraction using multi-walled carbon nanotubes as adsorbent coupled with high-performance liquid chromatography. *Journal of Chromatographic Science* **2015,** 53 (2), 380-384.
5. Li, Q. L.; Yuan, D. X.; Lin, Q. M. Evaluation of multi-walled carbon nanotubes as an adsorbent for trapping volatile organic compounds from environmental samples. *Journal of Chromatography A* **2004,** 1026 (1-2), 283-288.
6. Kah, M.; Zhang, X. R.; Jonker, M. T. O.; Hofmann, T. Measuring and modelling adsorption of PAHs to carbon nanotubes over a six order of magnitude wide concentration range. *Environmental Science & Technology* **2011,** 45 (14), 6011-6017.
7. Chen, W.; Duan, L.; Zhu, D. Q. Adsorption of polar and nonpolar organic chemicals to carbon nanotubes. *Environmental Science & Technology* **2007,** 41 (24), 8295-8300.
8. Li, X. N.; Zhao, H. M.; Quan, X.; Chen, S. O.; Zhang, Y. B.; Yu, H. T. Adsorption of ionizable organic contaminants on multi-walled carbon nanotubes with different oxygen contents. *Journal of Hazardous materials* **2011,** 186 (1), 407-415.
9. Chen, J. Y.; Chen, W.; Zhu, D. Adsorption of nonionic aromatic compounds to single-walled carbon nanotubes: Effects of aqueous solution chemistry. *Environmental Science & Technology* **2008,** 42 (19), 7225-7230.
10. Chen, W.; Duan, L.; Wang, L. L.; Zhu, D. Q. Adsorption of hydroxyl- and amino-substituted aromatics to carbon nanotubes. *Environmental Science & Technology* **2008,** 42 (18), 6862-6868.
11. Tóth, A.; Torocsik, A.; Tombacz, E.; Olah, E.; Heggen, M.; Li, C. L.; Klumpp, E.; Geissler, E.; Laszlo, K. Interaction of phenol and dopamine with commercial MWCNTs. *Journal of Colloid and Interface Science* **2011,** 364 (2), 469-475.
12. Tóth, A.; Torocsik, A.; Tombacz, E.; Laszlo, K. Competitive adsorption of phenol and 3-chlorophenol on purified MWCNTs. *Journal of Colloid and Interface Science* **2012,** 387, 244-249.
13. Peng, X. J.; Li, Y. H.; Luan, Z. K.; Di, Z. C.; Wang, H. Y.; Tian, B. H.; Jia, Z. P. Adsorption of 1,2-dichlorobenzene from water to carbon nanotubes. *Chemical Physics Letters* **2003,** 376 (1-2), 154-158.
14. Kuo, C. Y.; Wu, C. H.; Wu, J. Y. Adsorption of direct dyes from aqueous solutions by carbon nanotubes: Determination of equilibrium, kinetics and thermodynamics parameters. *Journal of Colloid and Interface Science* **2008,** 327 (2), 308-315.
15. Sheng, G. D.; Shao, D. D.; Ren, X. M.; Wang, X. Q.; Li, J. X.; Chen, Y. X.; Wang, X. K. Kinetics and thermodynamics of adsorption of ionizable aromatic compounds from aqueous solutions by as-prepared and oxidized multiwalled carbon nanotubes. *Journal of Hazardous materials* **2010,** 178 (1-3), 505-516.

16. Zhang, S. J.; Shao, T.; Bekaroglu, S. S. K.; Karanfil, T. Adsorption of synthetic organic chemicals by carbon nanotubes: Effects of background solution chemistry. *Water Research* **2010,** 44 (6), 2067-2074.
17. Yang, K.; Wu, W. H.; Jing, Q. F.; Zhu, L. Z. Aqueous adsorption of aniline, phenol, and their substitutes by multi-walled carbon nanotubes. *Environmental Science & Technology* **2008,** 42 (21), 7931-7936.
18. Fang, Q. L.; Chen, B. L. Adsorption of perchlorate onto raw and oxidized carbon nanotubes in aqueous solution. *Carbon* **2012,** 50 (6), 2209-2219.
19. Mahdavi, S.; Akhzari, D. The removal of phosphate from aqueous solutions using two nano-structures: copper oxide and carbon tubes. *Clean Technologies and Environmental Policy* **2016,** 18 (3), 817-827.
20. Zong, E. M.; Wei, D.; Huan, Z. K.; Peng, D.; Wan, H. Q.; Zheng, S. R.; Xu, Z. Y. Adsorption of phosphate by zirconia functionalized multi-walled carbon nanotubes. *Chinese Journal of Inorganic Chemistry* **2013,** 29 (5), 965-972.
21. Ansari, M.; Kazemipour, M.; Dehghani, M. The defluoridation of drinking water using multi-walled carbon nanotubes. *Journal of Fluorine Chemistry* **2011,** 132 (8), 516-520.
22. Chen, P. H.; Hsu, C. F.; Tsai, D. D. W.; Lu, Y. M.; Huang, W. J. Adsorption of mercury from water by modified multi-walled carbon nanotubes: adsorption behaviour and interference resistance by coexisting anions. *Environmental Technology* **2014,** 35 (15), 1935-1944.
23. Yu, F.; Ma, J.; Wu, Y. Q. Adsorption of toluene, ethylbenzene and m-xylene on multi-walled carbon nanotubes with different oxygen contents from aqueous solutions. *Journal of Hazardous materials* **2011,** 192 (3), 1370-1379.
24. Bi, E.; Schmidt, T. C.; Haderlein, S. B. Sorption of heterocyclic organic compounds to reference soils: Column studies for process identification. *Environmental Science & Technology* **2006,** 40 (19), 5962-5970.
25. Hyung, H.; Kim, J. H. Natural organic matter (NOM) adsorption to multi-walled carbon nanotubes: Effect of NOM characteristics and water quality parameters. *Environmental Science & Technology* **2008,** 42 (12), 4416-4421.
26. Lin, D. H.; Liu, N.; Yang, K.; Xing, B. S.; Wu, F. C. Different stabilities of multiwalled carbon nanotubes in fresh surface water samples. *Environmental Pollution* **2010,** 158 (5), 1270-1274.
27. Petersen, E. J.; Flores-Cervantes, D. X.; Bucheli, T. D.; Elliott, L. C. C.; Fagan, J. A.; Gogos, A.; Hanna, S.; Kagi, R.; Mansfield, E.; Bustos, A. R. M.; Plata, D. L.; Reipa, V.; Westerhoff, P.; Winchester, M. R. Quantification of carbon nanotubes in environmental matrices: current capabilities, case studies, and future prospects. *Environmental Science & Technology* **2016,** 50 (9), 4587-4605.
28. Hüffer, T.; Endo, S.; Metzelder, F.; Schroth, S.; Schmidt, T. C. Prediction of sorption of aromatic and aliphatic organic compounds by carbon nanotubes using poly-parameter linear free-energy relationships. *Water Research* **2014,** 59, 295-303.
29. Apul, O. G.; Wang, Q. L.; Shao, T.; Rieck, J. R.; Karanfil, T. Predictive model development for adsorption of aromatic contaminants by multi-walled carbon nanotubes. *Environmental Science & Technology* **2013,** 47 (5), 2295-2303.
30. Hu, J. L.; Tong, Z. L.; Hu, Z. H.; Chen, G. W.; Chen, T. H. Adsorption of roxarsone from aqueous solution by multi-walled carbon nanotubes. *Journal of Colloid and Interface Science* **2012,** 377, 355-361.
31. Ding, H.; Li, X.; Wang, J.; Zhang, X. J.; Chen, C. Adsorption of chlorophenols from aqueous solutions by pristine and surface functionalized single-walled carbon nanotubes. *Journal of Environmental Sciences* **2016,** 43, 187-198.

32. Chen, G. C.; Shan, X. Q.; Zhou, Y. Q.; Shen, X. E.; Huang, H. L.; Khan, S. U. Adsorption kinetics, isotherms and thermodynamics of atrazine on surface oxidized multiwalled carbon nanotubes. *Journal of Hazardous materials* **2009,** 169 (1-3), 912-918.
33. Lu, C. S.; Chung, Y. L.; Chang, K. F. Adsorption thermodynamic and kinetic studies of trihalomethanes on multiwalled carbon nanotubes. *Journal of Hazardous materials* **2006,** 138 (2), 304-310.
34. Pan, B.; Xing, B. S. Adsorption mechanisms of organic chemicals on carbon nanotubes. *Environmental Science & Technology* **2008,** 42 (24), 9005-9013.
35. Bucheli, T. D.; Gustafsson, O. Soot sorption of non-ortho and ortho substituted PCBs. *Chemosphere* **2003,** 53 (5), 515-522.
36. Droge, S.; Goss, K. U. Effect of sodium and calcium cations on the ion-exchange affinity of organic cations for soil organic matter. *Environmental Science & Technology* **2012,** 46 (11), 5894-5901.
37. Schenzel, J.; Goss, K. U.; Schwarzenbach, R. P.; Bucheli, T. D.; Droge, S. T. J. Experimentally determined soil organic matter-water sorption coefficients for different classes of natural toxins and comparison with estimated numbers. *Environmental Science & Technology* **2012,** 46 (11), 6118-6126.
38. Altfelder, S.; Streck, T.; Maraqa, M. A.; Voice, T. C. Nonequilibrium sorption of dimethylphthalate - Compatibility of batch and column techniques. *Soil Science Society of America Journal* **2001,** 65 (1), 102-111.
39. Li, B. H.; Qian, Y. A.; Bi, E. P.; Chen, H. H.; Schmidt, T. C. Sorption behavior of phthalic acid esters on reference soils evaluated by soil column chromatography. *Clean-Soil Air Water* **2010,** 38 (5-6), 425-429.
40. Bi, E.; Schmidt, T. C.; Haderlein, S. B. Environmental factors influencing sorption of heterocyclic aromatic compounds to soil. *Environmental Science & Technology* **2007,** 41 (9), 3172-3178.
41. Das, B. S.; Lee, L. S.; Rao, P. S. C.; Hultgren, R. P. Sorption and degradation of steroid hormones in soils during transport: Column studies and model evaluation. *Environmental Science & Technology* **2004,** 38 (5), 1460-1470.
42. Fesch, C.; Simon, W.; Haderlein, S. B.; Reichert, P.; Schwarzenbach, R. P. Nonlinear sorption and nonequilibrium solute transport in aggregated porous media: Experiments, process identification and modeling. *Journal of Contaminant Hydrology* **1998,** 31 (3-4), 373-407.
43. Lee, L. S.; Rao, P. S. C.; Brusseau, M. L. Nonequilibrium sorption and transport of neutral and ionized chlorophenols. *Environmental Science & Technology* **1991,** 25 (4), 722-729.
44. Tülp, H. C.; Fenner, K.; Schwarzenbach, R. P.; Goss, K. U. pH-dependent sorption of acidic organic chemicals to soil organic matter. *Environmental Science & Technology* **2009,** 43 (24), 9189-9195.
45. Jolin, W. C.; Sullivan, J.; Vasudevan, D.; MacKay, A. K. Column chromatography to obtain organic cation sorption isotherms. *Environmental Science & Technology* **2016,** 50 (15), 8196-8204.
46. Qian, Y. Sorption of hydrophobic organic compounds (HOCs) to inorganic surfaces in aqueous solutions. Ph.D. disserstation, University Duisburg-Essen, Essen, Germany, 2010.
47. Mader, B. T.; Goss, K. U.; Eisenreich, S. J. Sorption of nonionic, hydrophobic organic chemicals to mineral surfaces. *Environmental Science & Technology* **1997,** 31 (4), 1079-1086.
48. Wu, W. H.; Jiang, W.; Zhang, W. D.; Lin, D. H.; Yang, K. Influence of functional groups on desorption of organic compounds from carbon nanotubes into water: Insight into desorption hysteresis. *Environmental Science & Technology* **2013,** 47 (15), 8373-8382.

49. Li, H. B.; Zhang, D.; Han, X. Z.; Xing, B. S. Adsorption of antibiotic ciprofloxacin on carbon nanotubes: pH dependence and thermodynamics. *Chemosphere* **2014,** 95, 150-155.
50. Wang, Z. Y.; Yu, X. D.; Pan, B.; Xing, B. S. Norfloxacin sorption and its thermodynamics on surface-modified carbon nanotubes. *Environmental Science & Technology* **2010,** 44 (3), 978-984.
51. Thomsen, A. B.; Henriksen, K.; Gron, C.; Moldrup, P. Sorption, transport, and degradation of quinoline in unsaturated soil. *Environmental Science & Technology* **1999,** 33 (17), 2891-2898.
52. Ji, L. L.; Chen, W.; Zheng, S. R.; Xu, Z. Y.; Zhu, D. Q. Adsorption of sulfonamide antibiotics to multiwalled carbon nanotubes. *Langmuir* **2009,** 25 (19), 11608-11613.
53. Lin, D. H.; Xing, B. S. Adsorption of phenolic compounds by carbon nanotubes: Role of aromaticity and substitution of hydroxyl groups. *Environmental Science & Technology* **2008,** 42 (19), 7254-7259.
54. Brooks, A. J.; Lim, H. N.; Kilduff, J. E. Adsorption uptake of synthetic organic chemicals by carbon nanotubes and activated carbons. *Nanotechnology* **2012,** 23 (29), 13.
55. Diaz-Flores, P. E.; Arcibar-Orozco, J. A.; Perez-Aguilar, N. V.; Rangel-Mendez, J. R.; Medina, V. M. O.; Alcala-Jauegui, J. A. Adsorption of organic compounds onto multiwall and nitrogen-doped carbon nanotubes: Insights into the adsorption mechanisms. *Water Air and Soil Pollution* **2017,** 228 (4), 13.
56. Yan, X. M.; Shi, B. Y.; Lu, J. J.; Feng, C. H.; Wang, D. S.; Tang, H. X. Adsorption and desorption of atrazine on carbon nanotubes. *Journal of Colloid and Interface Science* **2008,** 321 (1), 30-38.
57. Shen, X. E.; Shan, X. Q.; Dong, D. M.; Hua, X. Y.; Owens, G. Kinetics and thermodynamics of sorption of nitroaromatic compounds to as-grown and oxidized multiwalled carbon nanotubes. *Journal of Colloid and Interface Science* **2009,** 330 (1), 1-8.
58. Xu, L. H.; Wang, Z. M.; Ye, S. A.; Sui, X. Y. Removal of p-chlorophenol from aqueous solutions by carbon nanotube hybrid polymer adsorbents. *Chemical Engineering Research & Design* **2017,** 123, 76-83.
59. Zhang, L.; Xu, T. C.; Liu, X. Y.; Zhang, Y. Y.; Jin, H. J. Adsorption behavior of multi-walled carbon nanotubes for the removal of olaquindox from aqueous solutions. *Journal of Hazardous materials* **2011,** 197, 389-396.
60. Zhu, X.; Wang, J. L. Comparison of sulfamethazine adsorption by multi-walled carbon nanotubes (MWCNTs) and magnetic MWCNTs from aqueous solution. *Fresenius Environmental Bulletin* **2017,** 26 (1A), 579-589.
61. Engel, M.; Chefetz, B. Adsorption and desorption of dissolved organic matter by carbon nanotubes: Effects of solution chemistry. *Environmental Pollution* **2016,** 213, 90-98.
62. Delle Site, A. Factors affecting sorption of organic compounds in natural sorbent/water systems and sorption coefficients for selected pollutants. A review. *Journal of Physical and Chemical Reference Data* **2001,** 30 (1), 187-439.
63. Boutboul, A.; Lenfant, F.; Giampaoli, P.; Feigenbaum, A.; Ducruet, V. Use of inverse gas chromatography to determine thermodynamic parameters of aroma-starch interactions. *Journal of Chromatography A* **2002,** 969 (1-2), 9-16.
64. von Oepen, B.; Kordel, W.; Klein, W. Sorption of nonpolar and polar compounds to soils - Processes, measurements and experience with the applicability of the modified OECD-guideline 106. *Chemosphere* **1991,** 22 (3-4), 285-304.
65. Li, Y. H.; Ding, J.; Luan, Z. K.; Di, Z. C.; Zhu, Y. F.; Xu, C. L.; Wu, D. H.; Wei, B. Q. Competitive adsorption of Pb2+, Cu2+ and Cd2+ ions from aqueous solutions by multiwalled carbon nanotubes. *Carbon* **2003,** 41 (14), 2787-2792.
66. Kragulj, M.; Trickovic, J.; Kukovecz, A.; Jovic, B.; Molnar, J.; Roncevic, S.; Konya, Z.; Dalmacija, B. Adsorption of chlorinated phenols on multiwalled carbon nanotubes. *Rsc Advances* **2015,** 5 (32), 24920-24929.

5.6 Appendix to Chapter 5

SI5.1 Characteristics of compounds used as sorbates and MWCNTs used as sorbent

Table S5.1 summarizes characteristics of the compounds used in this study (CAS-Nr., manufacturer, purity, pKa-value and maximum solubility in water at pH 6 (c_{sat})) in combination with the wavelength (λ_{max}) used in HPLC measurements and determination of UV calibration curves. λ_{max} was self-determined using a UV-spectrophotometer.

Table S5.1: Characteristics (CAS-Nr, manufacturer, purity, pK_a, maximum solubility in water at pH 6 (c_{sat}), and wavelength used for measurements (λ_{max})) of compounds used in this study as sorbents. [a]: data from Scifinder for pH 6; [b]: pK_a-values refer to the acid species of the respective compound. λ_{max} was self-determined using a UV-spectrophotometer.

compound name	CAS-Nr.	manufacturer	purity [%]	pK_a [a,b] [-]	c_{sat} [g L^{-1}] pH 6[a]	λ_{max} [nm]
furan	110-00-9	Aldrich Chemicals	> 99	-	8.2	208
imidazole	288-32-4	Sigma-Aldrich	≥ 99	7.05	1000	206
oxazole	288-42-6	Alfa Aesar	98+	0.98	143	205
pyrazine	290-37-9	Alfa Aesar	99+	1.22	1000	261
pyrazole	288-13-1	Aldrich Chemicals	98	2.5	8.9	210
pyridazine	289-80-5	Alfa Aesar	98+	3.12	292	200
pyridine	110-86-1	Sigma-Aldrich	99.8	5.23	1000	200
pyrimidine	289-95-2	Alfa Aesar	99	1.78	1000	200
pyrrole	109-97-7	Aldrich Chemicals	98	17	17	205
thiazole	288-47-1	Alfa Aesar	99	2.72	18	232
thiophene	110-02-1	Aldrich Chemicals	≥ 99	-	2.9	216

SI5.2 Characteristics of columns

Table S5.2 summarizes characteristics of the columns used in sorption studies (dimensions, packing material composition, bulk density (ρ_b), porosity (θ) and the sorbate analyzed with the respective column).

Table S5.2: Summary of columns used in this study with their dimensions, packing material composition, (ρ_b), porosity (θ) and the respective sorbates.

column	dimension (L × ID) [mm]	packing material [w.-%]	bulk density ρ_b [kg L^{-1}]	porosity θ [-]	sorbate
Q22	14 × 3	100 % quartz	1.632	0.502	all
CNT36	14 × 3	95 % quartz / 5 % MWCNTs	1.314	0.617	pyrazole
CNT39	14 × 3	95 % quartz / 5 % MWCNTs	1.341	0.618	furan
CNT40	14 × 3	9 5% quartz / 5 % MWCNTs	1.334	0.617	pyrrole
CNT41	14 × 3	95 % quartz / 5 % MWCNTs	1.363	0.616	pyridazine
CNT42	14 × 3	95 % quartz / 5 % MWCNTs	1.326	0.612	pyrimidine
CNT43	14 × 3	9 5% quartz / 5 % MWCNTs	1.298	0.609	oxazole
CNT44	14 × 3	95 % quartz / 5 % MWCNTs	1.292	0.593	pyrazine
CNT45	14 × 3	95 % quartz / 5 % MWCNTs	1.243	0.606	thiazole
CNT46	14 × 3	95 % quartz / 5 % MWCNTs	1.312	0.627	imidazole
CNT47	14 × 3	95 % quartz / 5 % MWCNTs	1.302	0.631	pyridine
CNT49	14 × 3	99.5 % quartz / 0.5 % MWCNTs	1.528	0.542	thiophene
CNT52	14 × 3	95 % quartz / 5 % MWCNTs	1.235	0.587	furan, imidazole, oxazole, pyrazole, pyridine, pyrrole
CNT53	14 × 3	95 % quartz / 5 % MWCNTs	1.308	0.613	
CNT54	14 × 3	95 % quartz / 5 % MWCNTs	1.333	0.601	
CNT55	14 × 3	95 % quartz / 5 % MWCNTs	1.267	0.584	
CNT56	14 × 3	95 % quartz / 5 % MWCNTs	1.307	0.612	

SI5.3 Determination of local equilibrium

The injected concentration of each sorbate used for determination of sorption equilibrium is given in table S5.3.

Table S5.3: The injected concentration of the different sorbates used in this study for sorption equilibrium determination.

compound name	injected concentration [mg L^{-1}]
furan	1000
imidazole	110
oxazole	100
pyrazine	4000
pyrazole	150
pyridazine	560
pyridine	3000
pyrimidine	1000
pyrrole	95
thiazole	1000
thiophene	40

Figure S5.1 shows determined retardation factors of four selected sorbates at different flow rates. As the retardation factor showed no dependence on the flow rate, it was assumed that the system was in equilibrium.

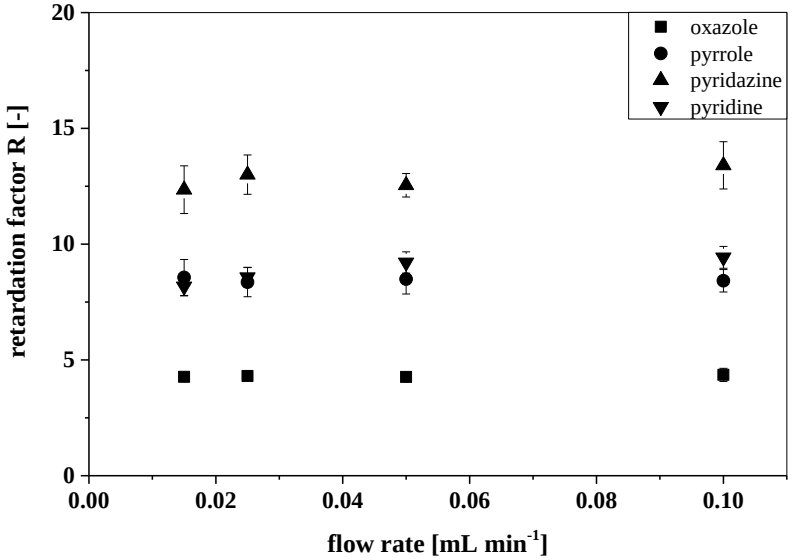

Figure S5.1: Calculated retardation factors R of oxazole, pyrrole, pyridazine and pyridine at different flow rates (0.015, 0.025, 0.050 or 0.100 mL min^{-1}). Error bars indicate the maximum error estimated from standard deviation of retention times of sorbate and tracer via error propagation (n=3).

SI5.4 Isotherm determination

Injected concentrations of each sorbate used for isotherm determination are given in table S5.4.

Table S5.4: Injected concentrations of the different sorbates used in this study for isotherm determination.

compound name	injected concentrations [mg L^{-1}]
furan	47, 84, 150, 265, 470, 845, 1000, 1200, 1500
imidazole	15, 26, 47, 84, 110, 150, 265, 350, 475
oxazole	10, 18, 32, 56, 100, 178, 240, 430, 562
pyrazine	178, 316, 562, 1000, 1333, 2000, 2500, 3000, 4000
pyrazole	15, 27, 47, 84, 150, 267, 474, 844, 1000
pyridazine	100, 177, 316, 562, 700, 1000, 1333, 1778, 2000
pyridine	562, 1000, 1333, 1778, 2000, 2500, 3000, 3500, 4000
pyrimidine	178, 316, 562, 1000, 1333, 1778, 2000, 2500, 3000
pyrrole	9, 17, 30, 53, 95, 169, 300, 534, 800
thiazole	56, 100, 178, 316, 562, 1000, 1333, 1778, 2000
thiophene	15, 30, 40, 75, 100, 170, 320, 450, 560

Figure S5.2 shows chromatograms recorded using pyrazole as sorbate. Concentration of pyrazole was varied between 45 and 1000 mg L^{-1}.

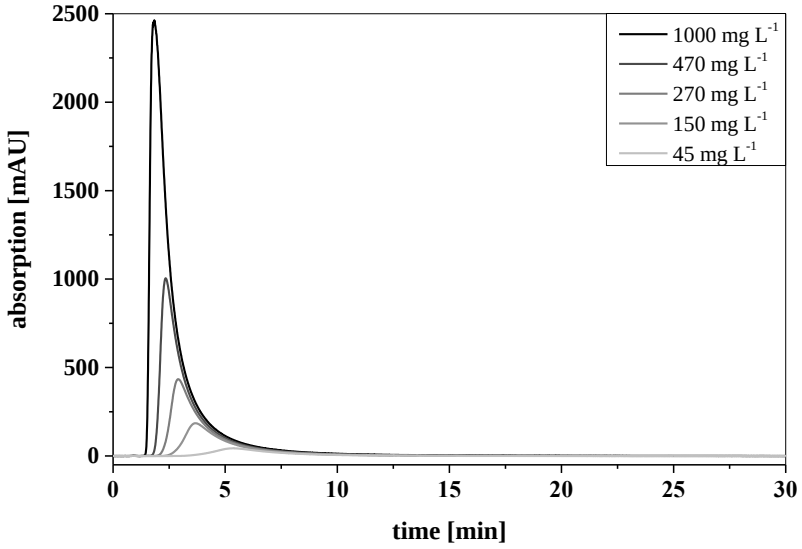

Figure S5.2: Selected chromatograms of consecutive runs of pyrazole with different injected concentrations ranging from 45 – 1000 mg L^{-1}.

Figure S5.3 shows selected isotherms of imidazole, pyrazole, furan and pyrimidine evaluated using the classical approach.

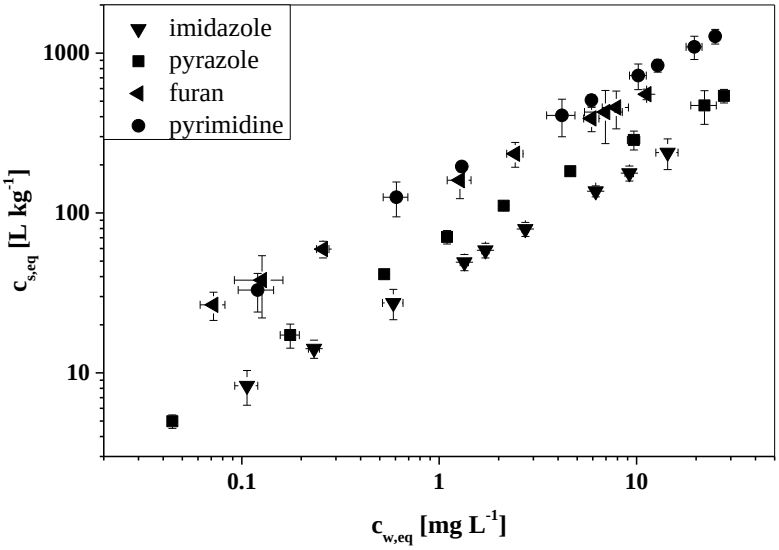

Figure S5.3: Selected isotherms of imidazole, pyrazole, furan and pyrimidine derived from chromatograms using the classical approach. Error bars indicate the maximum error estimated from standard deviation of retention times of sorbate and tracer via error propagation (n=3).

Figures S5.4 and S5.5 show chromatograms of pyrazine and thiophene for different injected concentrations, respectively. Increase in signal intensity with increasing injected concentration is stronger for thiophene compared to pyrazine. Tailing of the peaks is closer with increasing injected concentration for pyrazine, which explains the smaller deviation between the classical and alternative approach for isotherm determination.

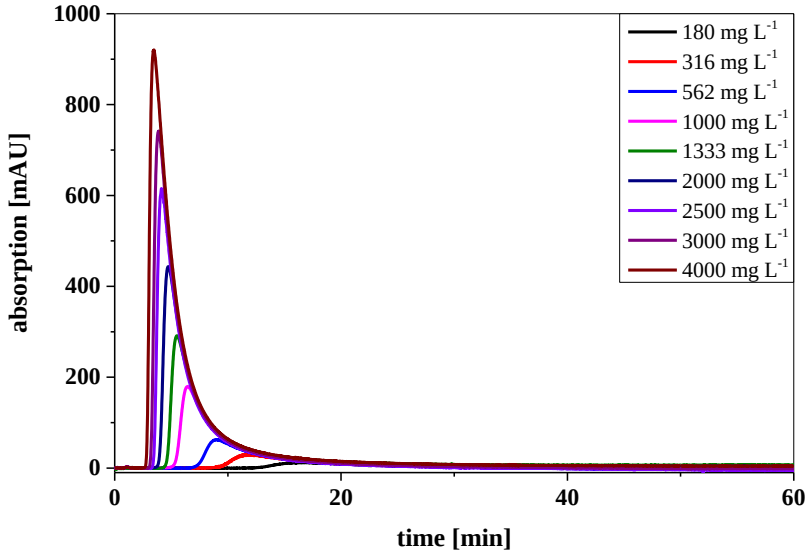

Figure S5.4: Chromatograms of pyrazine for different injected concentrations.

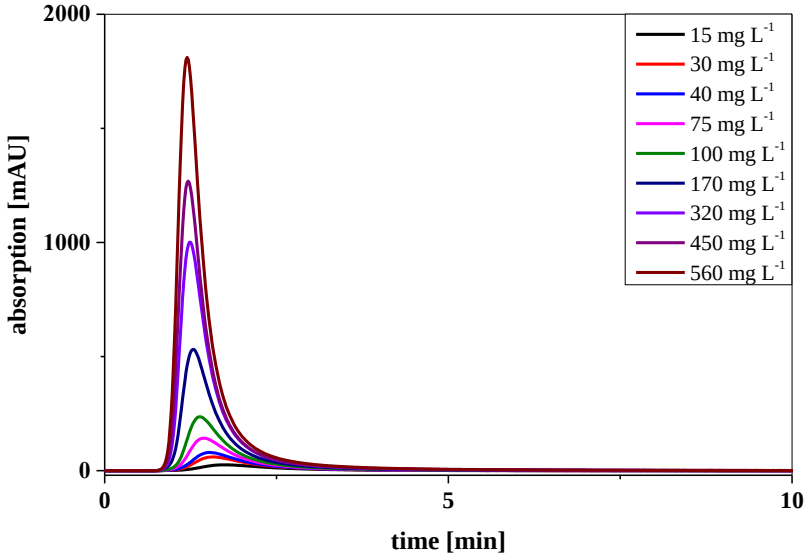

Figure S5.5: Chromatograms of thiophene for different injected concentrations.

SI5.5 UV-calibrations used for isotherm calculation

Table S5.5 gives calibration data for different sorbates, but the matrix was in this case 1 mM $CaCl_2$ at pH 6. They were also used for the calculation $c_{w,eq}$. The number of compounds in tables S5.5 and S5.7 is smaller compared to table S5.6 as calibration data of the other compounds were not necessary at 1 mM and 100 mM $CaCl_2$ in the eluent. Calibration curves determined with varied pH-value are not mentioned here as the UV-absorption did not change because of a varied pH-value. This was checked at pH 3, 6 and 9 with the same concentration.

Table S5.5: Calibrations of different sorbates used in this study to calculate dissolved liquid concentration in equilibrium ($c_{w,eq}$) for isotherm calculation (1 mM $CaCl_2$, pH 6).

compound name	slope [mAU L mg^{-1}]	y-intercept [mAU]	R^2 [-]
furan	70.4	1.5	0.9999
imidazole	100.3	-0.1	0.9999
oxazole	79.8	1.1	0.9999
pyrazole	89.0	-0.4	0.9999
pyridine	59.5	0.6	0.9999
pyrrole	119.6	1.0	0.9999

Table S5.6 summarizes UV-calibration curves used at 10 mM $CaCl_2$ at pH 6 as matrix in this study for the calculation of the dissolved liquid concentration in equilibrium ($c_{w,eq}$), which was necessary for isotherm calculation of each sorbate.

Table S5.6: Calibrations of different sorbates used in this study to calculate dissolved liquid concentration in equilibrium ($c_{w,eq}$) for isotherm calculation (10 mM $CaCl_2$, pH 6).

compound name	slope [mAU L mg^{-1}]	y-intercept [mAU]	R^2 [-]
furan	60.8	-0.4	0.9999
imidazole	83.1	-0.6	0.9999
oxazole	61.2	-0.4	0.9999
pyrazine	21.7	-2.3	0.9995
pyrazole	55.9	4.3	0.9999
pyridazine	81.9	0.6	0.9998
pyridine	50.9	1.6	0.9999
pyrimidine	39.6	4.4	0.9997
pyrrole	83.5	4.4	0.9999
thiazole	40.9	0.9	0.9999
thiophene	37.9	3.8	0.9999

Table S5.7 gives also calibration curves for different sorbates, but the matrix was in this case 100 mM $CaCl_2$ at pH 6. They were also used for the calculation $c_{w,eq}$.

Table S5.7: Calibrations of different sorbates used in this study to calculate dissolved liquid concentration in equilibrium ($c_{w,eq}$) for isotherm calculation (100 mM $CaCl_2$, pH 6).

compound name	slope [mAU L mg^{-1}]	y-intercept [mAU]	R^2 [-]
furan	47.7	-0.4	0.9999
imidazole	74.0	-4.8	0.9997
oxazole	60.5	-0.1	0.9999
pyrazole	56.4	-1.8	0.9999
pyridine	26.8	-1.2	0.9999
pyrrole	102.5	-1.5	0.9999

SI5.6 Prediction of K_d using ppLFER equations

Table S5.8 summarizes solute descriptors of the different sorbates used to predict sorption coefficients using poly-parameter linear free-energy relationships (ppLFERs) mentioned in literature.[1]

Table S5.8: Summary of solute descriptors of sorbates used in this study (E: excess molar refraction; S: polarizability; A: hydrogen-bond accepting properties; B: hydrogen-bond donating properties; V: McGowan molecular volume). Descriptors were taken from literature.[2]

compound name	E	S	A	B	V
furan	0.369	0.530	0.000	0.130	0.536
imidazole	0.710	0.850	0.420	0.780	0.536
oxazole	0.418	0.700	0.000	0.420	0.495
pyrazine	0.629	0.950	0.000	0.620	0.634
pyrazole	0.620	1.000	0.540	0.450	0.536
pyridazine	0.670	0.850	0.000	0.810	0.634
pyridine	0.631	0.840	0.000	0.520	0.675
pyrimidine	0.610	1.000	0.000	0.650	0.634
pyrrole	0.613	0.730	0.410	0.290	0.577
thiazole	0.800	0.800	0.000	0.450	0.600
thiophene	0.687	0.560	0.000	0.150	0.641

Figures S5.6, S5.7 and S5.8 show K_d values for 1 %, 0.1 % and 0.01 % of the maximum solubility in water on the one hand calculated using experimental isotherms of the classical and alternative approach or on the other hand predicted using ppLFERs from literature.[1]

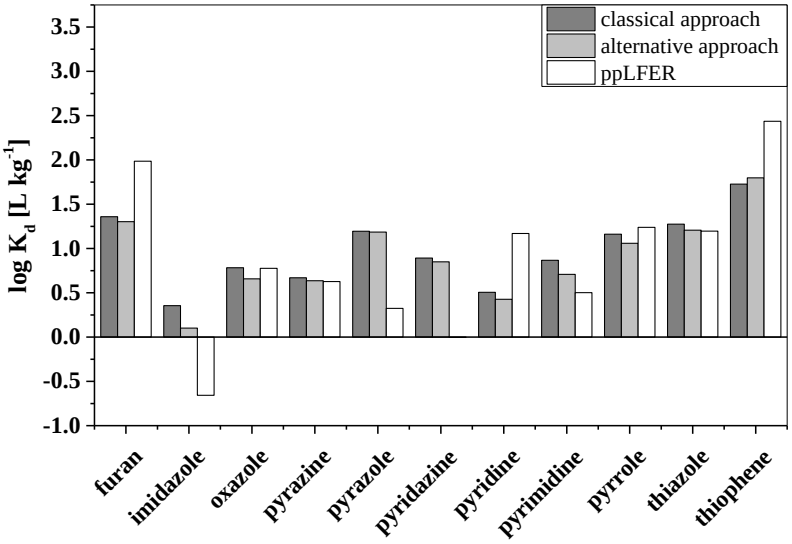

Figure S5.6: Comparison of calculated K_d values calculated from experimental isotherms and predicted values using a poly-parameter linear free-energy relationship (ppLFER) from literature[1] for a concentration of 1 % of the maximum solubility in water of the respective compound (see table S5.1).

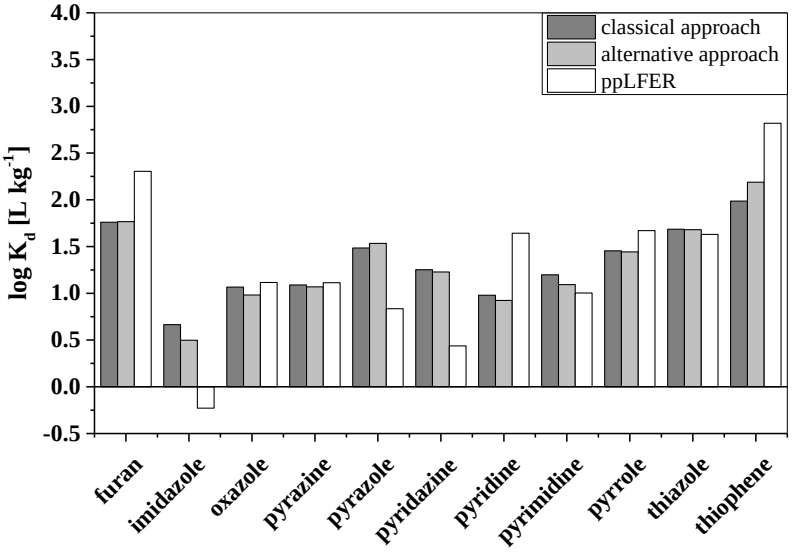

Figure S5.7: Comparison of K_d values calculated from experimental isotherms and predicted using a poly-parameter linear free-energy relationship (ppLFER) from literature[1] for a concentration of 0.1 % of the maximum solubility in water of the respective compound (see table S5.1).

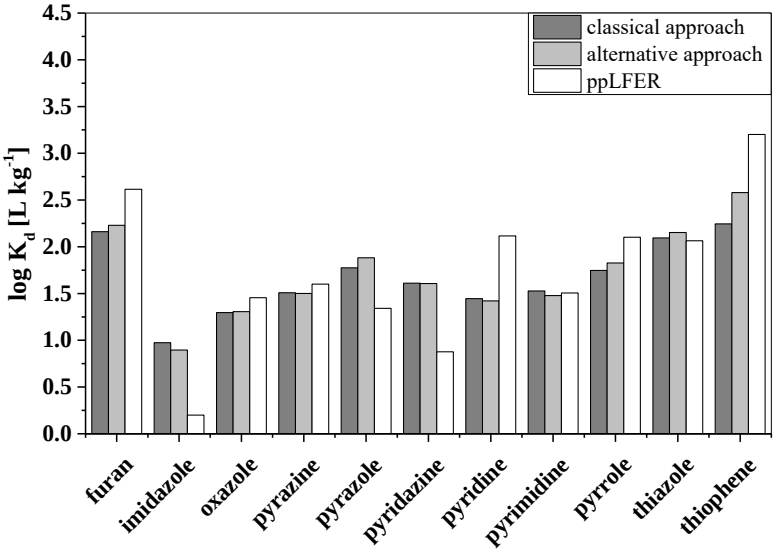

Figure S5.8: Comparison of K_d values calculated from experimental isotherms and predicted using a poly-parameter linear free-energy relationship (ppLFER) from literature[1] for a concentration of 0.01 % of the maximum solubility in water of the respective compound (see table S5.1).

SI5.7 Influence of environmental conditions on sorption

Table S5.9 summarizes values of the Freundlich coefficient K_f, log K_{wa} and the pK_a-values of the compounds used for investigation of the influence of environmental conditions on sorption. log K_{wa} values were determined using the LSER database of the Helmholtz Centre for environmental research (UFZ).[3] Table S5.10 summarizes the different injected concentrations used to investigate the influence of environmental conditions on sorption.

Table S5.9: Determined values for Freundlich coefficient K_f [(mg kg^{-1}) (mg L^{-1})$^{-n}$] based on the alternative approach, log K_{wa} [-] and the pK_a-values [-] of the corresponding acids of sorbates used for investigation of the influence of environmental conditions on sorption. [a]Data estimated using the LSER database of the Helmoltz Centre for environmental research[3] [b]Data taken from Scifinder. Mean values of three replicates of K_f and corresponding standard deviations are reported.

sorbate	K_f	log K_{wa}[a]	pK_a[b]
furan	154.8 ± 0.7	0.65	-
imidazole	48.8 ± 0.6	5.14 – 6.50	7
oxazole	47.9 ± 0.2	2.64	0.8
pyrazole	73.3 ± 0.2	5.69	2.5
pyridine	261.1 ± 2.9	3.21 – 3.50	5.23
pyrrole	82.2 ± 0.1	3.23 – 3.5	-

Table S5.10: The injected concentration of the different sorbates used in this study to investigate the influence of temperature, ion strength and pH.

compound name	temperature	ion strength	pH
	Injected concentration [mg L^{-1}]		
furan	400, 500	800	800
imidazole	150, 270	270	270
oxazole	200, 430	300	300
pyrazole	200, 470	350	350
pyridine	1200, 2500	2000	2000
pyrrole	150, 350	250	250

SI5.8 Influence of temperature

Table S5.11 summarizes sorption enthalpies (ΔH) calculated from van´t Hoff plot of sorption data measured with CNT-columns. Tables S5.12 to S5.14 summarize sorption isotherm characteristics (Freundlich coefficient K_f, Freundlich exponent n and the correlation coefficient R^2) of isotherms deduced from chromatograms of the high injected concentration using the alternative approach at three different temperatures of 25 °C (S5.12), 40 °C (S5.13) and 55 °C (S5.14). Displayed values are the mean values of three replicates and errors given show the standard deviation of these three measurements.

Table S5.11: Calculated sorption enthalpies (ΔH) determined when injecting the higher and the lower concentrations mentioned in section 5.2.5 in the paper.

sorbate	ΔH (high concentration) [kJ mol^{-1}]	ΔH (low concentration) [kJ mol^{-1}]
furan	-25.7	-27.3
imidazole	-24.3	-25.1
oxazole	-21.3	-18.2
pyrazole	-24.9	-31.9
pyridine	-20.6	-23.4
pyrrole	-27.1	-33.8

Table S5.12: Determined isotherm characteristics (Freundlich coefficient K_f [(mg kg^{-1}) (mg L^{-1})$^{-n}$], Freundlich exponent n [-] and corresponding correlation coefficient R^2 [-]) of the different sorbates determined at 25 °C (10 mM $CaCl_2$, pH 6). Mean values of three replicates and corresponding standard deviations are reported.

sorbate	K_f	n	R^2
furan	123.2 ± 1.1	0.53 ± 0.01	0.9998 ± 0.0001
imidazole	45.4 ± 0.9	0.58 ± 0.01	0.9988 ± 0.0001
oxazole	34.1 ± 0.3	0.73 ± 0.01	0.9994 ± 0.0001
pyrazole	55.6 ± 0.5	0.69 ± 0.01	0.9979 ± 0.0001
pyridine	225.9 ± 3.0	0.52 ± 0.01	0.9979 ± 0.0011
pyrrole	73.8 ± 0.7	0.61 ± 0.01	0.9997 ± 0.0001

Table S5.13: Determined isotherm characteristics (Freundlich coefficient K_f [(mg kg^{-1}) (mg L^{-1})$^{-n}$], Freundlich exponent n [-] and corresponding correlation coefficient R^2 [-]) of the different sorbates determined at 40 °C (10 mM $CaCl_2$, pH 6). Mean values of three replicates and corresponding standard deviations are reported. Pyrazole is not reported because of a wrong injected concentration.

sorbate	K_f	n	R^2
furan	92.4 ± 0.4	0.56 ± 0.01	0.9999 ± 0.0001
imidazole	33.4 ± 0.4	0.58 ± 0.01	0.9960 ± 0.0002
oxazole	24.3 ± 0.6	0.72 ± 0.01	0.9995 ± 0.0001
pyrazole	-	-	-
pyridine	158.6 ± 3.5	0.58 ± 0.01	0.9995 ± 0.0001
pyrrole	47.6 ± 0.1	0.64 ± 0.01	0.9999 ± 0.0001

Table S5.14: Determined isotherm characteristics (Freundlich coefficient K_f [(mg kg^{-1}) (mg L^{-1})$^{-n}$], Freundlich exponent n [-] and corresponding correlation coefficient R^2 [-]) of the different sorbates determined at 55 °C (10 mM $CaCl_2$, pH 6). Mean values of three replicates and corresponding standard deviations are reported.

sorbate	K_f	n	R^2
furan	61.9 ± 0.4	0.61 ± 0.01	0.9999 ± 0.0001
imidazole	23.7 ± 0.2	0.62 ± 0.01	0.9977 ± 0.0001
oxazole	18.8 ± 0.2	0.71 ± 0.01	0.9993 ± 0.0001
pyrazole	25.5 ± 0.1	0.72 ± 0.01	0.9998 ± 0.0001
pyridine	117.6 ± 0.7	0.58 ± 0.01	0.9995 ± 0.0001
pyrrole	33.4 ± 0.1	0.67 ± 0.01	0.9998 ± 0.0001

SI5.9 Influence of ionic strength

Tables S5.15 to S5.17 summarize sorption isotherm characteristics (Freundlich coefficient K_f, Freundlich exponent n and the correlation coefficient R^2) of isotherms deduced from chromatograms using the alternative approach with 1 mM $CaCl_2$ eluent (S5.15), 10 mM $CaCl_2$ eluent (S5.16) and 100 mM $CaCl_2$ eluent (S5.17). Displayed values are the mean values of three replicates and errors given show the standard deviation of these three measurements.

K_f and n remained almost constant or changed only slightly with exception of pyridine. For pyridine, K_f reduced strongly with increasing ionic strength while K_d was almost constant. This was most likely related to the increasing concentration of chloride in the eluent. Sensitivity of the DAD of the HPLC was significantly reduced with increasing chloride concentration at 200 nm causing interferences. This was also observed for the UV-calibrations measured at the external spectrophotometer, but the effect seems to be more pronounced for the DAD of the HPLC. For the higher wavelengths used for calibrations of the other sorbates the influence was less pronounced (tables S5.5 to S5.7). To further support this, Figure S5.9 shows chromatograms of pyridine at different ionic strengths of the eluent. The injected concentration was the same at all three conditions. The apex point of the peak as well as the determined half-mass point in the chromatogram did not change strongly in retention time, but the signal intensity was significantly reduced when changing the eluent from 10 mM to 100 mM $CaCl_2$. Therefore, values for K_f and n are marked red in table S5.18.

Table S5.15: Determined isotherm characteristics (Freundlich coefficient K_f [(mg kg^{-1}) (mg $L^{-1})^{-n}$], Freundlich exponent n [-] and corresponding correlation coefficient R^2 [-]) of the different sorbates determined at 1 mM $CaCl_2$ (25 °C, pH 6). Mean values of three replicates and corresponding standard deviations are reported.

sorbate	K_f	n	R^2
furan	138.1 ± 0.1	0.56 ± 0.01	0.9994 ± 0.0001
imidazole	41.8 ± 1.0	0.55 ± 0.01	0.9996 ± 0.0002
oxazole	34.9 ± 0.7	0.74 ± 0.01	0.9983 ± 0.0001
pyrazole	63.8 ± 0.1	0.63 ± 0.01	0.9991 ± 0.0001
pyridine	243.3 ± 6.8	0.46 ± 0.01	0.9980 ± 0.0016
pyrrole	73.2 ± 0.2	0.60 ± 0.01	0.9999 ± 0.0001

Table S5.16: Determined isotherm characteristics (Freundlich coefficient K_f [(mg kg^{-1}) (mg L^{-1})$^{-n}$], Freundlich exponent n [-] and corresponding correlation coefficient R^2 [-]) of the different sorbates determined at 10 mM $CaCl_2$ (25 °C, pH 6). Mean values of three replicates and corresponding standard deviations are reported.

sorbate	K_f	n	R^2
furan	133.8 ± 0.4	0.54 ± 0.01	0.9998 ± 0.0001
imidazole	33.8 ± 1.4	0.59 ± 0.01	0.9998 ± 0.0001
oxazole	30.5 ± 0.7	0.76 ± 0.01	0.9994 ± 0.0001
pyrazole	63.9 ± 0.1	0.66 ± 0.01	0.9988 ± 0.0001
pyridine	213.7 ± 6.5	0.51 ± 0.02	0.9979 ± 0.0015
pyrrole	73.4 ± 0.5	0.62 ± 0.01	0.9998 ± 0.0001

Table S5.17: Determined isotherm characteristics (Freundlich coefficient K_f [(mg kg^{-1}) (mg L^{-1})$^{-n}$], Freundlich exponent n [-] and corresponding correlation coefficient R^2 [-]) of the different sorbates determined at 100 mM $CaCl_2$ (25 °C, pH 6). Mean values of three replicates and corresponding standard deviations are reported.

sorbate	K_f	n	R^2
furan	139.5 ± 0.5	0.55 ± 0.01	0.9999 ± 0.0001
imidazole	37.6 ± 0.3	0.61 ± 0.01	0.9996 ± 0.0001
oxazole	31.7 ± 0.4	0.74 ± 0.01	0.9993 ± 0.0001
pyrazole	58.9 ± 0.3	0.65 ± 0.01	0.9998 ± 0.0001
pyridine	162.8 ± 2.2	0.52 ± 0.01	0.9983 ± 0.0003
pyrrole	60.1 ± .01	0.60 ± 0.01	0.9999 ± 0.0001

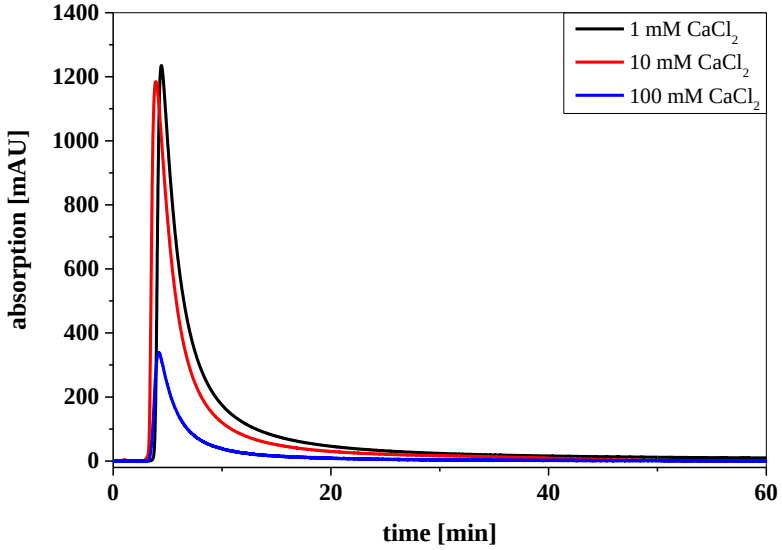

Figure S5.9: Chromatograms of pyridine at different concentrations of $CaCl_2$ in the eluent.

SI5.10 Influence of pH

Tables S5.18 to S5.20 summarize sorption isotherm characteristics (Freundlich coefficient K_f, Freundlich exponent n and the correlation coefficient R^2) of isotherms deduced from chromatograms using the alternative approach at pH 3 (S5.18), pH 6 (S5.19) and pH 9 (S5.20). Displayed values are the mean values of 3 replicates and errors given show the standard deviation of these three measurements.

Table S5.18: Determined isotherm characteristics (Freundlich coefficient K_f [(mg kg^{-1}) (mg L^{-1})$^{-n}$], Freundlich exponent n [-] and corresponding correlation coefficient R^2 [-]) of the different sorbates determined at pH 3 (10 mM $CaCl_2$, 25 °C). Mean values of three replicates and corresponding standard deviations are reported.

sorbate	K_f	n	R^2
furan	116.3 ± 1.5	0.58 ± 0.01	0.9997 ± 0.0003
imidazole	28.3 ± 0.3	0.52 ± 0.01	0.9985 ± 0.0002
oxazole	34.9 ± 0.3	0.73 ± 0.01	0.9997 ± 0.0001
pyrazole	52.6 ± 0.9	0.68 ± 0.01	0.9989 ± 0.0001
pyridine	83.4 ± 3.7	0.51 ± 0.02	0.9994 ± 0.0006
pyrrole	57.3 ± 0.4	0.66 ± 0.01	0.9997 ± 0.0001

Table S5.19: Determined isotherm characteristics (Freundlich coefficient K_f [(mg kg^{-1}) (mg L^{-1})$^{-n}$], Freundlich exponent n [-] and corresponding correlation coefficient R^2 [-]) of the different sorbates determined at pH 6 (10 mM $CaCl_2$, 25 °C). Mean values of three replicates and corresponding standard deviations are reported.

sorbate	K_f	n	R^2
furan	138.2 ± 1.3	0.54 ± 0.01	0.9999 ± 0.0001
imidazole	37.1 ± 0.8	0.59 ± 0.01	0.9998 ± 0.0001
oxazole	32.1 ± 0.5	0.73 ± 0.01	0.9993 ± 0.0001
pyrazole	65.9 ± 0.4	0.65 ± 0.01	0.9987 ± 0.0001
pyridine	210.8 ± 8.2	0.52 ± 0.02	0.9980 ± 0.0018
pyrrole	74.6 ± 0.6	0.62 ± 0.01	0.9996 ± 0.0001

Table S5.20: Determined isotherm characteristics (Freundlich coefficient K_f [(mg kg^{-1}) (mg L^{-1})$^{-n}$], Freundlich exponent n [-] and corresponding correlation coefficient R^2 [-]) of the different sorbates determined at pH 9 (10 mM $CaCl_2$, 25 °C). Mean values of three replicates and corresponding standard deviations are reported.

sorbate	K_f	n	R^2
furan	122.6 ± 0.5	0.54 ± 0.01	0.9999 ± 0.0001
imidazole	39.6 ± 0.2	0.64 ± 0.01	0.9999 ± 0.0001
oxazole	30.3 ± 0.4	0.76 ± 0.01	0.9994 ± 0.0001
pyrazole	55.6 ± 0.2	0.67 ± 0.01	0.9966 ± 0.0044
pyridine	213.5 ± 3.7	0.52 ± 0.02	0.9977 ± 0.0026
pyrrole	67.5 ± 0.1	0.62 ± 0.01	0.9998 ± 0.0001

Finally, the influence of the ionic strength at pH 3 on isotherm characteristics Freundlich coefficient K_f, Freundlich exponent n and the correlation coefficient R^2) derived from chromatograms using the alternative approach is shown in tables S5.21 to S5.23. Table S5.21 contains values determined with 1 mM $CaCl_2$ in the eluent, while Table S5.22 and S5.23 contain values determined with 10 mM or 100 mM $CaCl_2$ in the eluent, respectively.

Table S5.21: Determined isotherm characteristics (Freundlich coefficient K_f [(mg kg^{-1}) (mg L^{-1})$^{-n}$], Freundlich exponent n [-] and corresponding correlation coefficient R^2 [-]) of the different sorbates determined at 1 mM $CaCl_2$ (pH 3, 25 °C). Mean values of three replicates and corresponding standard deviations are reported.

sorbate	K_f	n	R^2
imidazole	28.2 ± 0.1	0.41 ± 0.01	0.9970 ± 0.0003
pyrazole	57.0 ± 0.2	0.66 ± 0.01	0.9982 ± 0.0006
pyridine	85.5 ± 0.8	0.43 ± 0.01	0.9987 ± 0.0003

Table S5.22: Determined isotherm characteristics (Freundlich coefficient K_f [(mg kg^{-1}) (mg L^{-1})$^{-n}$], Freundlich exponent n [-] and corresponding correlation coefficient R^2 [-]) of the different sorbates determined at 10 mM $CaCl_2$ (pH 3, 25 °C). Mean values of three replicates and corresponding standard deviations are reported.

sorbate	K_f	n	R^2
imidazole	28.2 ± 0.1	0.45 ± 0.01	0.9993 ± 0.0001
pyrazole	50.3 ± 0.2	0.70 ± 0.01	0.9982 ± 0.0001
pyridine	77.3 ± 0.3	0.48 ± 0.01	0.9995 ± 0.0001

Table S5.23: Determined isotherm characteristics (Freundlich coefficient K_f [(mg kg^{-1}) (mg L^{-1})$^{-n}$], Freundlich exponent n [-] and corresponding correlation coefficient R^2 [-]) of the different sorbates determined at 100 mM $CaCl_2$ (pH 3, 25 °C). Mean values of three replicates and corresponding standard deviations are reported.

sorbate	K_f	n	R^2
imidazole	31.9 ± 0.1	0.57 ± 0.01	0.9999 ± 0.0001
pyrazole	47.9 ± 0.4	0.68 ± 0.01	0.9998 ± 0.0001
pyridine	87.7 ± 2.2	0.60 ± 0.01	0.9976 ± 0.0012

Figure S5.10 shows K_d values determined for imidazole and pyridine for different concentrations of $CaCl_2$ in the eluent at pH 3 to determine the influence of electrostatic repulsion on determined distribution coefficients.

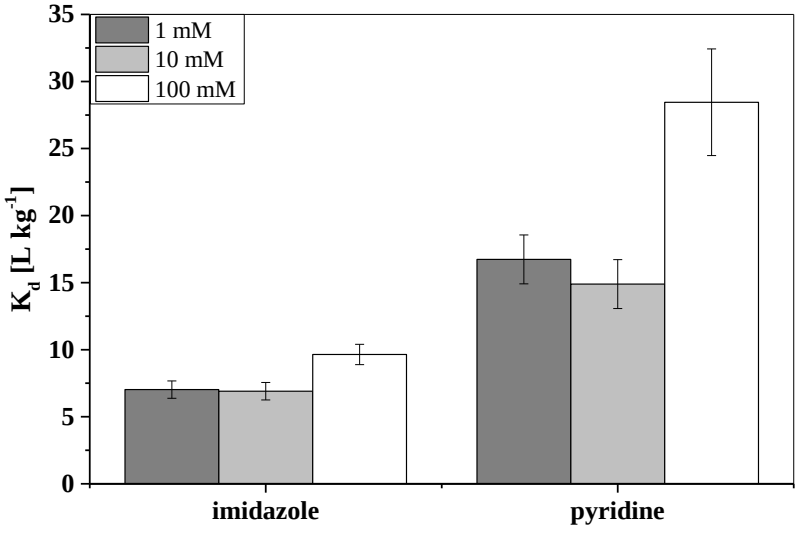

Figure S5.10: Determined K_d values of imidazole at the three different concentrations of $CaCl_2$ in the eluent (1, 10 and 100 mM) at pH 3. Error bars indicate the maximum error estimated from standard deviation of retention times of sorbate and tracer via error propagation (n=3).

References Appendix to Chapter 5

1. Hüffer, T.; Endo, S.; Metzelder, F.; Schroth, S.; Schmidt, T. C. Prediction of sorption of aromatic and aliphatic organic compounds by carbon nanotubes using poly-parameter linear free-energy relationships. *Water Research* **2014,** 59, 295-303.
2. Abraham, M. H.; Chadha, H. S.; Whiting, G. S.; Mitchell, R. C. Hydrogen bonding. 32. An analysis of water-octanol and water-alkane partitioning and the Δlog P parameter of seiler. *Journal of Pharmaceutical Sciences* **1994,** 83 (8), 1085-1100.
3. Ulrich, N.; Endo, S.; Brown, T. N.; Watanabe, N.; Bronner, G.; Abraham, M. H.; Goss, K. U., UFZ-LSER database v 3.2 [Internet], Leipzig, Germany, Helmholtz Centre for Environmental Research-UFZ. 2017 [accessed on 20.08.2017]. Available from http://www.ufz.de/lserd

Chapter 6 – Comparison of sorbent materials

Adapted from: Metzelder, F.; Funck, M.; Hüffer, T.; Schmidt, T.C. Comparison of sorption to carbon-based materials and nanomaterials using inverse liquid chromatography. *Environmental Science & Technology*, **2018**, submitted.

6.1 Abstract

Sorption studies for carbon-based materials and nanomaterials are typically conducted using batch experiments, but the analysis of weakly sorbing compounds may be challenging. Column chromatography represents a promising complement as higher sorbent to solution ratios can be applied. The sorbent is packed in a column and sorption data are calculated by relating sorbate retention times to that of a non-retarded tracer.

In this study, sorption of heterocyclic organic compounds (pyrazole, pyrrole, furan, thiophene) by carbon-based materials (activated carbon, biochar, graphite) and nanomaterials (functionalized carbon nanotubes, graphene platelets) was compared for the first time using column chromatography. D_2O was used as non-retarded tracer.

Sorption isotherms were non-linear and well described by the Freundlich model. Sorption differed between the materials regarding determined Freundlich coefficients (K_f) by more than two orders of magnitude for isotherms in a similar concentration range. Normalization of K_f with surface area of the sorbent significantly reduced the differences between the sorbents, but it did not remove it. Overall, column chromatography represents the opportunity to study sorption of weakly sorbing compounds to diverse carbon-based sorbent materials with a single experimental approach, which is challenging in batch experiments due to the very different sorption properties of some sorbent materials.

6.2 Introduction

The sorptive properties of carbon-based materials are used for many processes. For example in water treatment[1-3] and wastewater treatment[1, 4], activated carbon (AC) is used to remove contaminants from the water phase. In analytical chemistry, AC and also carbon nanomaterials (CNMs) are used as solid-phase extraction material for organic[5, 6] as well as inorganic compounds[7, 8] to enrich analytes prior to analysis.

To evaluate the sorption properties of a sorbent material, batch experiments are typically conducted, including carbon-based materials like AC[2, 9, 10], graphite[11, 12] and CNMs[10, 13, 14]. Additionally, the influence of material modifications by for example oxidation / etching of carbon nanotubes (CNTs) on sorption can be analyzed.[15, 16] Predominantly, organic compounds are used as sorbates comparing their sorption to different sorbent materials. The focus is often on highly hydrophobic compounds (e.g. phenanthrene,[10] benzene derivates[9]) and/or large molecules like pharmaceuticals (e.g. tetracycline,[16] norfloxacin,[17] sulfamethoxazole[18]). Sorption data for smaller compounds, which may also be of environmental concern like small heterocyclic organic compounds (e.g. pyrazole) to for example CNTs, are rare in literature. The limited availability of sorption data may be related to weak sorption of many heterocyclic organic compounds as indicated by prediction models for multiwalled carbon nanotubes (MWCNTs)[19] and AC,[20] which can be orders of magnitude lower compared to benzene derivates with regard to the predicted distribution coefficients (K_d). Weakly sorbing compounds or sorbent materials with low sorption capacity represent a challenge in batch experiments due to a limited sorbent to solution ratio. Although the sorption capacity of materials like graphite may be limited compared to AC, they might still have an impact on sorption in the environment that should be investigated. Weak sorption may result in just small deviations between the initial and equilibrium concentration in batch experiments making the determination of reliable sorption data difficult. Additional drawbacks of batch experiments are, first, the long equilibration time up to several weeks.[13, 21] Second, large amounts of sorbents may be required for weakly sorbing compounds. CNMs are, especially in case of functionalized materials, expensive and the application of high sorbent amounts should be avoided. Finally, the automation potential is low requiring many manual steps like weighing of sorbents, spiking of samples, and phase separation.

Column chromatography represents a complementary technique to overcome these drawbacks. Columns packed with the sorbent are used to determine sorption data like K_d values or isotherms. The retention of the sorbate in relation to a non-retarded tracer is used.

Consequently, a non-retarded tracer is an important prerequisite for this experimental approach. Weakly sorbing compounds can be analyzed as the sorbent to solution ratio is significantly higher compared to batch experiments, concomitantly, enabling a reduced sorbent demand, which is interesting for expensive sorbents or those with limited availability. Furthermore, equilibration times can be reduced and the automation potential is higher using an autosampler reducing the manual workload. However, column chromatography also has its limitations. Too strong sorption leads to long measurement times, but this disadvantage can be overcome using an inert material like quartz[22] or silicium carbide[23] for dilution of the sorbent. Additionally, column clogging, which was observed for clay containing soils,[22] is avoided using inert materials. The most challenging disadvantage may be sorption hysteresis (i.e. the incomplete desorption of the sorbate from the sorbent). Complete desorption is mandatory in case of an injection of a pulse of the sorbate instead of a continuous input. The properties of the sorbent surface would be altered by permanently attached sorbate molecules resulting in changed interactions for consecutive measurements. Consequently, each column could only be used for one sorbate and one concentration / setup of conditions diminishing the advantages of this experimental approach. Sorption hysteresis was observed for CNMs in batch experiments,[24, 25] but sorption was found to be fully reversible in case of MWCNTs in column experiments in chapters 3 – 5. The column method was successfully used for the determination of sorption data using soils,[22, 23, 26] minerals,[27, 28] but also soot particles[29] and previous studies using MWCNTs as shown in chapters 3 – 5. Comparison of different sorbents was done successfully using soils,[22] but comparison of carbon-based sorbents was not reported yet using column chromatography despite the advantages mentioned previously. So far, only batch experiments are the method of choice to compare for example AC with CNMs[17] or graphite.[30]

The aim of this work was to apply column chromatography as complementary technique to classical batch experiments for the comparison of sorbent materials like classical carbon-based materials (activated carbon, biochar, and graphite) and CNMs (functionalized MWCNTs (fMWCNTs), graphene platelets) regarding their sorption properties for polar heterocyclic organic compounds (pyrazole, furan, pyrrole, and thiophene). Additionally, sorption data for the sorbates to nonfunctionalized MWCNTs from chapter 5 were added for comparison.

6.3 Materials and Methods

6.3.1 Chemicals and Packing Materials

Chemicals used during this study were calcium chloride ($CaCl_2$) ($CaCl_2 \times 2\ H_2O$, ≥99.5 %, AppliChem Panreac), heavy water (D_2O) (≥99.9 atom-%, Sigma-Aldrich), pyrazole (98 %, Aldrich Chemicals), furan (>99 %, Aldrich Chemicals), pyrrole (98 %, Aldrich Chemicals), and thiophene (≥99 %, Aldrich Chemicals). Stock solutions and eluents were prepared using ultrapure water derived from an ELGA system (18.2 MΩ cm^{-1} resistance, PURELAB Ultra, ELGA LabWater, Celle, Germany). Sorbate stock solutions were stored at 4 °C in the dark.

Sorbent materials used in this study were biochar, graphite, graphene platelets, two types of activated carbon (AC1, AC2), and fMWCNTs. Details on manufacturer and treatment procedure during production of fMWCNTs are given in chapter 6.6 (section SI6.1). Additionally, quartz in a particle size <63 µm (≥99.7 %, Fluka) was used as inert material for dilution of sorbent materials during column preparation. All sorbents were ground and sieved to a particle size <63 µm and only those particles were used for experiments. Grinding as well as the additional oxidation to produce fMWCNTs before grinding had only small or negligible influence on the surface area determined by Brunauer-Emmett-Teller (BET) measurements (summarized in table S6.1 in the chapter 6.6 with other specifications of sorbent materials).

6.3.2 Devices

Detailed information on empty HPLC-columns and additional equipment used for column packing is mentioned in chapter 3.3.2. The Knauer HPLC-system from chapter 3 was used also in this chapter for all sorbent materials investigated in this chapter except for fMWCNTs. For fMWCNTs, an Agilent HPLC-system was used, which is listed chapter 6.6 (section SI6.1). Devices used in this study were equipped with a diode-array detector (DAD) in case of the Knauer device or UV detector (UVD) in case of the Agilent device and refractive index detector (RID) for both devices. The DAD or UVD and RID were connected in series connection passing first the DAD or UVD. The DAD or UVD was used for detection of sorbates while the RID was mandatory for the detection of D_2O, which was used as non-retarded tracer for all materials. As shown in chapter 3 and 4, sorption of other typically used tracers like bromide to MWCNTs was observed, which made D_2O necessary. For the other materials in the respective dilutions used in experiments, also bromide would be applicable as non-retarded tracer. Sorption data calculated with bromide as non-retarded tracer were equal

to those calculated with D_2O (data not shown). The material dilution was an important factor as for AC1 with a content of 5 % (wt/wt) diluted with quartz in the column a substantial retention of bromide inside the column could be observed (data not shown). Connecting capillaries were kept as short as possible and had an inner diameter of 0.13 mm. Injection was done using an injection-loop-valve with an injection volume of 5 µL. The UV spectrophotometer used for determination of UV calibrations for isotherm calculations was a Shimadzu UV-1650PC (Shimadzu Europe GmbH, Duisburg, Germany).

6.3.3 Column chromatography

The packing procedure developed in chapter 3 was adapted in this chapter. Although other sorbent materials were used, the procedure could be used as previously described. Only changes in dilution of the sorbent material with quartz and column length were necessary because of too strong (e.g. in case of AC) or too weak sorption (e.g. in case of graphite). Details regarding applied dilution of sorbent materials and column dimensions are mentioned in table S6.3 in chapter 6.6.

The non-retarded tracer D_2O was diluted 1:9 with the respective eluent (vol.-%/vol.-%). The half-mass point, i.e. the point at which the peak area is divided in two equal parts,[31] was applied to determine retention times of sorbates and tracer necessary to calculate the retardation factor (R) (equation 6.1) and K_d values (equation 6.2). In chromatograms recorded during experiments peaks of sorbates showed an extensive tailing (e.g. asymmetry factors of peaks of thiophene determined at 10 % of the maximum intensity were around 10.9 using AC1 as sorbent material). The half-mass point has previously shown its applicability in sorption studies on soils or minerals,[22, 27, 32, 33] but also for MWCNTs in the previous chapters of this thesis.

$$R = (t_{R,sorb} - t_{0,sorb}) / (t_{R,tracer} - t_{0,tracer}) \quad (6.1)$$

$$R = 1 + \rho_b / \theta \times K_d \quad (6.2)$$

where $t_{R,sorb}$ is the retention time of the sorbates, while $t_{R,tracer}$ is the retention time of the tracer in measurements with column installed in the HPLC system. $t_{0,sorb}$ is the traveling time through injector and capillaries between autosampler and DAD or UVD without column, while $t_{0,tracer}$ is the traveling time from autosampler to the RI-detector without column. Different corrections for the retention time of sorbates and tracer were required, because both detectors were connected in serial connection. Repeated injections of sorbates as well as tracer without column installed in the system (n = 10) were used to determine $t_{0,sorb}$ and $t_{0,tracer}$.

Capillaries were connected using a low dead volume stainless steel union (0.25mm bore, VICI Jour.) for measurements without column. θ [-] and ρ_b [kg L^{-1}] are the porosity and the bulk density of the column used, respectively and calculated according to equations 3.1 and 3.2 from chapter 3 of this thesis. Determined values for these parameters in combination with the sorbent content and column dimensions are given in table S6.3 in chapter 6.6**.** Wavelengths used for detection of the sorbates were 210 nm (pyrazole), 205 nm (pyrrole), 208 nm (furan), and 216 nm (thiophene). Interaction of the different sorbates with quartz as inert material was checked in a column packed with exclusively quartz. No interaction was observed so that quartz was suitable as inert material for all sorbates (K_d calculated from the quartz column < 0.1 % of that calculated from the sorbent containing columns) (data not shown). Mass recovery of sorbates and tracer was calculated by comparison of peak areas from measurements with column and without column. Quantitative recovery and absence of hysteresis for all investigated sorbent materials was observed as recovery ranged between 80 and 120 % for the tracer and all sorbates with stable retention times. Exceptions regarding recovery were observed for injections of solutions containing only low concentrations of the sorbates and baseline noise became an issue.

Columns were equilibrated for at least 12 hours by flushing at 0.1 mL min^{-1} with the eluent containing 10 mM $CaCl_2$ in ultrapure water at pH 6. For each sorbate with each sorbent preliminary measurements were conducted with a column temperature of 25 °C applying different flow rates / pore water velocities to test the degree of non-equilibrium in the experiments. One solution with a defined concentration of the sorbate was injected (concentrations are mentioned in table S6.4 in chapter 6.6). Sorption was at or close to equilibrium, because determined R values varied only slightly with maximum 8 % at different flow rates / velocities ranging from 0.010 – 0.1 mL min^{-1} or 0.25 – 2.7 cm min^{-1}, respectively. In case of AC, the increase in R was up to 25 %, which was higher compared to the other sorbent materials. However, applying lower flow rates (e.g. 0.010 mL min^{-1}) would have caused measurement times of up to 30 hours per measurement run in case of thiophene, which is not practicable. As result of the relatively small influence of the flow rate, 0.1 mL min^{-1} was used for all experiments yielding acceptable measurement times of still up to 3 hours as in case of thiophene with AC1 as sorbent.

A distinctly different behavior was observed for biochar. Measurements using biochar as packing material resulted in strongly increasing R values with decreasing flow rate. R values increased by 500 % when decreasing the flow rate from 0.1 to 0.025 mL min^{-1} in case of pyrazole (shown in figure S6.1 in chapter 6.6 compared to other sorbent materials).

Additionally, increasing tailing and decreasing maximum intensity of the peak with decreasing flow rate were observed (figure S6.2 in chapter 6.6). For the other sorbent materials, peak shape and signal intensity were similar with decreasing flow rate. Consequently, local equilibrium could not be assumed for biochar in contrast to the other sorbent materials and determination of sorption isotherms was not possible. A reason for the different behavior may be the very heterogeneous structure of biochar compared to the other sorbents of this study. Biochar is composed of carbonized and noncarbonized material fractions containing different surface functionalities,[34, 35] while the other sorbents of this study are almost exclusively composed of carbonized material. Additionally, absorption into noncarbonized fractions of biochar[36] may be stronger influenced by the flow rate than adsorption to the carbonized surface of the other sorbents, which was shown previously to be the dominant sorption mechanism for MWCNTs.[37]

6.3.4 Isotherm determination

Isotherms of sorbates were determined using an eluent with 10 mM $CaCl_2$ at pH 6 and 25 °C column temperature, as these conditions were also applied in previous studies for batch experiments[19] and chapter 3 and 5 of this thesis using the same type of MWCNTs for organic sorbates. Sorbates were injected separately in columns containing the sorbent material. The concentration of the sorbate in the injected solution was increased stepwise with three replicates for each concentration. Only in case of thiophene using AC1 two replicates were used due to long measurement times. Nine different solutions of each sorbate were injected. The concentrations of the solutions of each sorbate used for the different sorbents are given in table S6.5 in chapter 6.6.

Isotherms of the sorbates for the different sorbent materials were again calculated according the classical and alternative approach mentioned in chapter 3.3.6 and the suitability / comparability of the approaches was evaluated for the different sorbent materials. UV calibrations used for calculations are mentioned in table S6.6 in chapter 6.6. Sorption isotherms were fitted using the Freundlich model with the Freundlich coefficient (K_f) and the Freundlich exponent (n).

6.4 Results and Discussion

6.4.1 Determination of sorption isotherms

Sorption isotherms determined for the sorbates in this study and those determined for MWCNTs in chapter 5 are summarized in table 6.1. Only the values derived with the alternative approach described in section 3.3.6 are shown here while values of the classical approach are shown in chapter 6.6 in table S6.7. Additionally, isotherms derived with both evaluation approaches are shown for pyrazole in figures S6.3 and S6.4 in chapter 6.6. Nonlinearity of isotherms was confirmed by fitting the data using a linear sorption isotherm, which resulted in lower values for R^2 and increased errors of the regression parameters (exemplarily shown for pyrazole in table S6.9). Sorption data from both evaluation approaches were well fitted by the Freundlich model indicated by R^2 values > 0.98. The alternative approach showed its applicability compared to the classical approach already for MWCNTs in chapters 3 and 5 as calculated K_d values for different aqueous concentrations of the sorbates based on the isotherm characteristics K_f and n were very similar. Calculated K_d values for the isotherms of this study showed acceptable deviations between both evaluation approaches in most cases below 0.3 log units although K_f and n of both evaluation approaches showed in some cases strong deviations (figures S6.7 – S6.9 in chapter 6.6). Only for the lowest calculated concentration (0.01 % of the maximum aqueous solubility) and AC1 and AC2 as sorbent material larger deviations of up to 0.6 log units were observed. Trends observed for each sorbent and between the different sorbents were also similar for both approaches. A further discussion of the two evaluation approaches is shown in chapter 6.6 in section SI6.4. In conclusion, the alternative approach proved its suitability also for the sorbent materials of this study.

Table 6.1: Isotherm characteristics (Freundlich coefficient (K_f) [(mg kg^{-1}) (mg L^{-1})$^{-n}$], Freundlich exponent (n) [-] and the correlation coefficient (R^2) [-]) of the alternative approach for the different sorbents and sorbates. Values for MWCNTs were taken from chapter 5. Uncertainties given in the table are the standard deviations of each parameter of three replicates.

sorbate	sorbent	K_f	n	R^2
furan	MWCNTs	$(1.55 \pm 0.01) \times 10^2$	0.57 ± 0.01	0.9999
	fMWCNTs	$(3.12 \pm 0.03) \times 10^1$	0.54 ± 0.01	0.9995
	graphene	$(6.59 \pm 0.01) \times 10^1$	0.48 ± 0.01	0.9993
	graphite	$(8.10 \pm 0.10) \times 10^{-1}$	0.74 ± 0.01	0.9993
	AC1	$(5.34 \pm 0.06) \times 10^3$	0.40 ± 0.01	0.9929
	AC2	$(4.10 \pm 0.02) \times 10^3$	0.39 ± 0.01	0.9954
pyrazole	MWCNTs	$(7.33 \pm 0.02) \times 10^1$	0.65 ± 0.01	0.9965
	fMWCNTs	$(4.27 \pm 0.01) \times 10^1$	0.60 ± 0.01	0.9992
	graphene	$(3.05 \pm 0.01) \times 10^1$	0.58 ± 0.01	0.9977
	graphite	$(5.50 \pm 0.10) \times 10^{-1}$	0.76 ± 0.01	0.9981
	AC1	$(2.03 \pm 0.05) \times 10^3$	0.43 ± 0.01	0.9861
	AC2	$(1.57 \pm 0.08) \times 10^3$	0.45 ± 0.01	0.9901
pyrrole	MWCNTs	$(8.22 \pm 0.01) \times 10^1$	0.62 ± 0.01	0.9997
	fMWCNTs	$(2.67 \pm 0.01) \times 10^1$	0.62 ± 0.01	0.9992
	graphene	$(3.88 \pm 0.02) \times 10^1$	0.54 ± 0.01	0.9977
	graphite	$(5.20 \pm 0.10) \times 10^{-1}$	0.78 ± 0.01	0.9986
	AC1	$(2.91 \pm 0.50) \times 10^3$	0.43 ± 0.01	0.9861
	AC2	$(2.02 \pm 0.02) \times 10^3$	0.41 ± 0.01	0.9893
thiophene	MWCNTs	$(2.34 \pm 0.01) \times 10^2$	0.61 ± 0.01	0.9991
	fMWCNTs	$(7.71 \pm 0.02) \times 10^1$	0.56 ± 0.01	0.9997
	graphene	$(1.88 \pm 0.06) \times 10^2$	0.45 ± 0.01	0.9967
	graphite	$(3.18 \pm 0.02) \times 10^0$	0.67 ± 0.01	0.9988
	AC1	$(1.81 \pm 0.01) \times 10^4$	0.37 ± 0.01	0.9829
	AC2	$(1.29 \pm 0.01) \times 10^4$	0.38 ± 0.01	0.9874

6.4.2 Comparison of sorption linearity expressed by n

For each sorbent, n was for the different sorbates in a very similar range. Sorption of the sorbates determined applying the classical and alternative evaluation approach to all sorbent materials in this study was nonlinear. Only in case of the classical approach with graphite as sorbent material and furan, pyrazole, or pyrrole as sorbates, sorption was only slightly nonlinear (n = 0.91 – 0.96). The extent of nonlinearity differed between the sorbent materials and evaluation approaches. For the classical approach, n values of all sorbent materials and sorbates despite the already mentioned deviations for graphite were in a similar range. Differences in n values were related to deviations between the evaluation approaches resulting in a more nonlinear sorption for the alternative evaluation approach. The tailing of the sorbate peak in the chromatogram has more influence on isotherms calculated according to the alternative approach than for the classical approach. This is discussed in detail in section SI6.4 in chapter 6.6. For the alternative evaluation approach, three sorbent groups could be observed when comparing the calculated n values. Group 1 comprised the two AC materials that showed the strongest non-linearity (n = 0.39 – 0.43). Group 2 included the two types of MWCNTs and graphene, which had slightly higher linearities (n = 0.45 – 0.65). Finally, graphite with the highest values (n = 0.67 – 0.78).

Nonlinearity of sorption is related to the heterogenous energy distribution of sorption sites located on the sorbent surface. This distribution becomes more relevant the broader the investigated concentration range is. In a narrow and/or low concentration range, sorption sites exhibiting a similar and high sorption energy like defects or functional groups are occupied[38] resulting in linear sorption (e.g. sorption of polycyclic aromatic hydrocarbons (PAHs) to MWCNTs in a low concentration range).[13] Over a broad and/or in a high concentration range, sorption sites exhibiting strongly different sorption energies are occupied[38] leading to nonlinear sorption (e.g. PAHs to MWCNTs over a six orders of magnitude concentration range).[13] This heterogenous energy distribution of sorption sites may also be the reason for the observed differences in linearity among the sorbent materials according to the alternative approach. Compared to the other materials, the surface of AC is very irregular and heterogeneous in its structure potentially offering sorption sites of very different sorption energies. MWCNTs, fMWCNTs and graphene platelets are more regular and controlled in their structure increasing potentially the linearity, but aggregates of the materials contain different sized and accessible pores resulting in sorption sites of different energies. Graphite, exhibiting the most linear sorption, is a non-porous material and has, consequently, the most

regular structure and similarity in sorption sites. A similar interpretation was given comparing sorption of naphthalene and nitrobenzenes to singlewalled carbon nanotubes (SWCNTs) and graphite, which was more nonlinear for SWCNTs.[39]

Nonlinear sorption was also described in literature for these sorbent materials using various sorbates (e.g. sulfamethoxazole to graphite and graphene oxide,[18] atrazine to MWCNTs and AC,[9] or nitroaromatic compounds to MWCNTs and fMWCNTs[40]). However, contrary to the results of this study almost linear sorption of naphthalene to AC[30] was reported. This may also be related to the small investigated concentration range of less than one log unit.[30] Furthermore, a consistent trend of sorption linearity when comparing sorbent materials like those in this study was not found in literature. On the one hand, naphthalene sorption to AC was linear while sorption to MWCNTs was strongly nonlinear,[30] which is the opposite of the tendency observed in this study. On the other hand, sorption of benzene to graphite was more linear than to SWCNTs,[41] which agrees with the trend observed for graphite and CNTs of this study. Sorption linearity of sorbates to MWCNTs and fMWCNTs in this study was similar and not influenced by functionalization. Similar observations were reported in literature comparing SWCNTs and MWCNTs in functionalized and pristine form.[15, 17, 40, 42, 43] For example, Cho *et al*.[43] observed a very similar linearity for sorption of naphthalene with increasing content of oxygen on MWCNTs. This indicated that sorption linearity was not affected by surface oxidation. In some cases it was also reported that sorption linearity changed with functionalization of CNTs.[44] For different PAHs like naphthalene or pyrene sorption linearity increased from about 0.42 up to 0.90 with increasing oxidation, while sorption linearity decreased for benzene and toluene with increasing oxidation.[44] Additionally, self-conducted batch experiments comparing MWCNTs and fMWCNTs using sorbates like benzene derivates, naphthalene, or ethers showed an increasing or decreasing value when comparing MWCNTs and fMWCNTs contrary to the results of the column methodology presented in this study (data and applied procedure shown in section SI6.5 in chapter 6.6). For own batch experiments other sorbates were used as the available amount of fMWCNTs was insufficient for sorption studies using the sorbates presented here in column experiments. Consequently, there are no strict dependencies in literature regarding sorption linearity of different sorbates to different sorbent materials and no general rankings in sorption linearity are possible comparing different sorbent materials. The combination of sorbate and sorbent material is important and cannot be generally transferred from for example one type of activated carbon to another type or from MWCNTs to fMWCNTs without possible differences regarding sorption linearity. However, the column method was

suitable to derive data that show comparable trends to data presented in literature using batch experiments although data in literature show in some cases strong deviations with each other.

6.4.3 Comparison of sorption affinity expressed by K_f

For all sorbent materials except fMWCNTs, determined K_f values followed the order pyrazole < pyrrole < furan < thiophene. For graphite, K_f of pyrrole was slightly smaller than K_f of pyrazole, but the deviation was only about 5 %. For fMWCNTs, the order changed to pyrrole < furan < pyrazole < thiophene. Reason for the changes in sorption affinity might be the difference in the material characteristics / interaction mechanisms between sorbate and sorbent preferring other sorbates. fMWCNTs contained an increased amount of oxygen determined by measurements of the elemental composition. Content of oxygen increased from <1 % for MWCNTs to 7.8 % for fMWCNTs (table S6.1 in chapter 6.6). Consequently, the relative abundance of functional groups increased, which was shown by X-ray photoelectron spectroscopy measurements, while the content of graphitic carbon decreased for fMWCNTs compared to MWCNTs (table S6.2 in chapter 6.6). Interactions between surface functional groups on the sorbent and sorbate molecules like H-bonds may result in preferred interaction with pyrazole compared to pyrrole and furan. Solute descriptors for the H-bond accepting (A) and H-bond donating abilities (B)[45] of pyrazole are higher compared to pyrrole and furan supporting this hypothesis. However, H-bonding may not explain completely differences observed regarding K_f as it can also be shown using the solute descriptors. Values for A and B are higher for pyrrole compared to furan, but sorption of pyrrole was weaker than furan. Consequently, other interactions mechanisms contributed to sorption and may be differently affected by the surface modification of fMWCNTs compared to MWCNTs. For the other materials, interaction mechanisms between sorbent and sorbate contributing to overall sorption seemed to be similar as the order in sorption affinity of different sorbates was similar. It must be mentioned here that K_f values of isotherms may be influenced by the investigated concentration range. As the concentration ranges of isotherms for all sorbates using the different sorbents were similar (table S6.8 in chapter 6.6), also K_f values are comparable. Only K_f values of the alternative evaluation approach are discussed in detail as trends for the classical approach were similar, although the K_f values of the classical approach were lower (Table S6.7 in chapter 6.6).

Calculating the ratio of K_f determined for thiophene to the K_f determined for furan, the ratios for the different sorbent materials were in a similar range (figure 6.1). Only the ratio

calculated for MWCNTs was lower, which may be related to the different dilution of MWCNTs in columns used for measurements with 0.5 % (wt/wt) for thiophene and 5 % (wt/wt) in case of furan. The influence on dilution of sorbent material on K_f determined by column experiments is discussed in section SI6.4 in chapter 6.6. Furthermore, the ratio of K_f determined for thiophene to the K_f determined for pyrrole was also for all sorbent materials relatively similar (figure 6.1). The direct comparison to literature data is difficult as sorption data for the same combination of sorbates and sorbents as in this study were not found in literature. Data for sorption of thiophene and pyrrole were found in literature for sorption to reference soil materials.[22] Sorption of pyrrole was very low and could only be detected for two of five soils.[22] The ratio of K_d of thiophene to the K_d of pyrrole was similar to those determined in the present study.[22] K_d was chosen for comparison as linear sorption was assumed and no K_f value was available in this reference.[22] Non-specific interactions were dominant for sorption of thiophene and pyrrole to soil, which may also be the case for the present study as the ratios were similar. Sorption of benzothiophene, benzofuran, and indole to soils was also dominated by non-specific interactions.[22] These sorbates are structurally similar to thiophene, furan and pyrrole used in the present study, but they contained an additional benzene ring. Ratios of K_d values determined for benzothiophene to benzofuran or indole, were in a similar range than the ratios of K_f values of the structurally similar sorbates in the present study (also shown in figure 6.1).

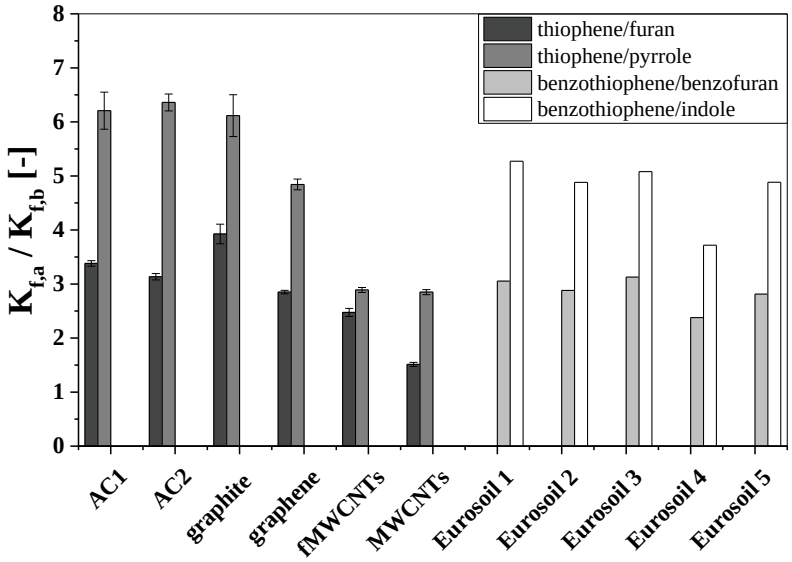

Figure 6.1: Comparison of ratios of K_f values ($K_{f,a}$ / $K_{f,b}$) determined for the sorbent materials of this study for thiophene (a) to furan (b) and thiophene (a) to pyrrole (b) to ratios of K_d values from literature for sorption to reference soils (Eurosoil 1 – 5) for benzothiophene (a) to benzofuran (b) and benzothiophene (a) to indole (b). Indices a and b mentioned after the compound names were used to clarify the ratio shown on the y-axis.

For all sorbates the order of K_f was graphite < fMWCNTs < graphene < MWCNTs < AC2 < AC1. Only exception is pyrazole where fMWCNTs and graphene changed their order. In total, determined K_f values differed strongly among the sorbent materials of up to a factor of 6000 between the highest and smallest K_f value (e.g. ratio of K_f values determined for thiophene regarding sorption to AC1 and graphite). This shows a strong deviation in sorption affinity for all sorbates between the different sorbent materials in this study (as shown in figure 6.2 for all sorbates as relative difference between the highest and lowest K_f determined for one sorbate with the different sorbent materials). This indicates generally similar sorption mechanisms, but different sorption affinities among sorbent materials.

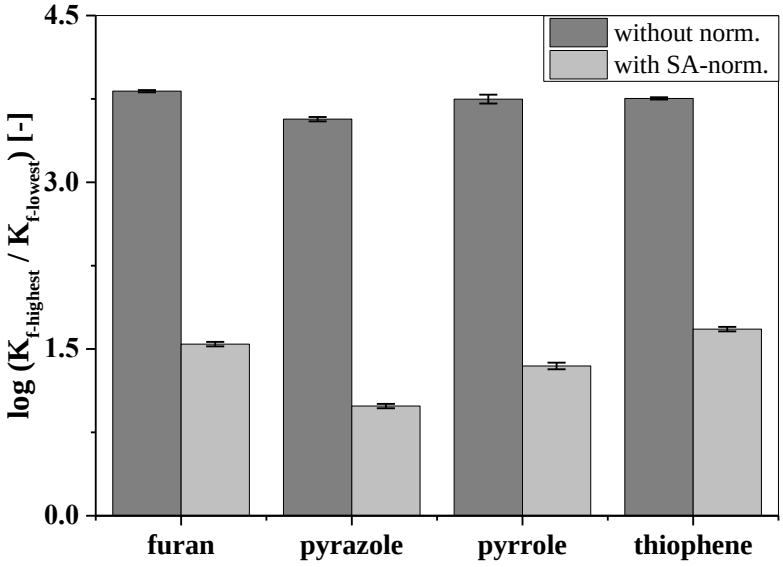

Figure 6.2: Logarithmic relative deviation of the highest K_f value determined for a sorbent material to the lowest K_f value determined for a sorbent material with each sorbate (grey) and after normalization of K_f with the corresponding surface area (SA) (white). Values of K_f taken from table 6.1. Values for the SA of the sorbent materials taken from table S6.1 in chapter 6.6. Error bars represent the maximum error estimated via error propagation.

To the best of our knowledge, nowhere in literature a comparison of all sorbent materials used in this study was reported. Thus, different studies must be combined. Sorption of organic compounds to AC resulted in higher K_f values compared to MWCNTs[17] or graphene nanosheets.[10] Sorption of benzene derivates to SWCNTs[39] or tetracycline to SWCNTs and MWCNTs[46] resulted in higher K_f values compared to graphite. These trends meet those observed in this study. However, sorption of phenanthrene or biphenyl to graphene nanosheets was also described to yield higher K_f values compared to MWCNTs,[10] which is the opposite order of the one in the present study. Consequently, as for the discussion of n, different trends were reported and may partially depend on the combination of sorbent and sorbate investigated as well as sorbent characteristics.

The influence of the functionalization of CNTs on sorption affinity was often reported in literature. In this study, fMWCNTs showed for all sorbates a reduction of K_f values between 50 and 80 % compared to MWCNTs. Reduced sorption due to functionalization was also observed in batch experiments with the materials of this study as shown in chapter 6.6 for other sorbates than investigated using the column method (section SI6.5). Reduction of K_f was with up to factor 50 much stronger in batch experiments than for the column method. In literature, reduced sorption with increasing functionalization was reported for MWCNTs[43, 47-49] as well as SWCNTs.[15, 42] For example, K_f values describing sorption of different benzene derivates to SWCNTs were reduced by about 30 % from pristine to functionalized material.[42] Furthermore, for aromatic compounds K_f values to SWCNTs in pristine, weakly and strongly oxidized form, were reduced by about 50 %.[15] Consequently, reduction of K_f in this study determined using the column method was comparable to results of the batch experiments from literature. Reduced sorption may be attributed to a more hydrophilic sorbent surface due to the increased content of functional groups. This leads to the enhanced formation of water clusters at the sorbent surface resulting in a reduced availability and accessibility of sorption sites.[38, 43, 47, 50, 51] Furthermore, functional groups may themselves reduce the accessibility of pores and sorption sites within CNT aggregates due to steric hinderance preventing optimal electron donor-acceptor interactions between sorbent and sorbate.[42] In this study, the surface area (SA) was not responsible for weaker sorption to fMWCNTs as the surface area measured for fMWCNTs by BET measurements was almost identical for fMWCNTs with 251 $m^2\ g^{-1}$ compared to 228 $m^2\ g^{-1}$ for MWCNTs, respectively (table S6.1 in chapter 6.6). Consequently, trends observed for the influence of functionalization of CNTs regarding K_f can also be observed using the column methodology presented in this study.

The large deviations in K_f observed between the sorbent materials in this study may be related to the available SA of the material. This is shown in figure 6.3 plotting the determined K_f values of the different sorbates against the corresponding SA of the sorbent material. Additionally, the carbon content of the sorbent materials may influence sorption and explain partially the deviations as it was shown for the comparison of different CNTs and AC.[9] For the sorbent materials of this study, SA and carbon content were different as summarized in table S6.1 in chapter 6.6. SA was up to 1170 $m^2\ g^{-1}$ for AC1 having the highest K_f values and only 2.2 $m^2\ g^{-1}$ for graphite having the lowest K_f values. The carbon content differed only slightly between 87 % for AC2 and 99 % in case of graphite.

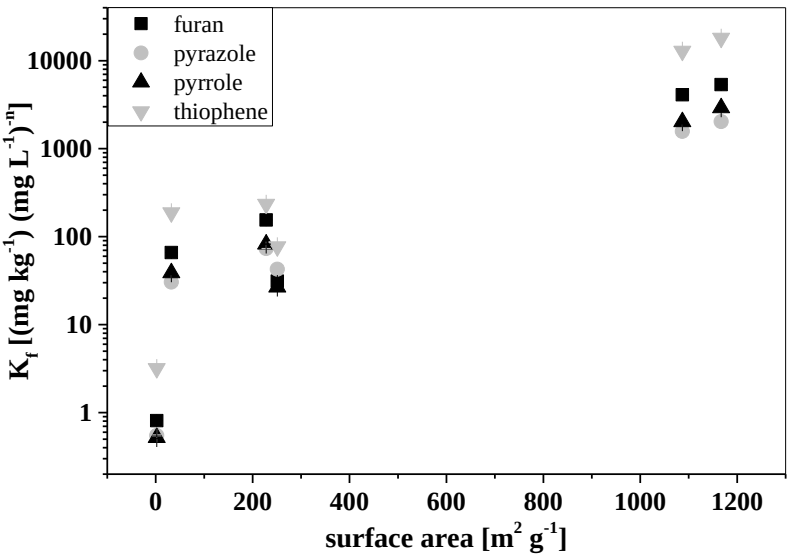

Figure 6.3: Determined Freundlich coefficients (K_f) against the corresponding surface area of the sorbent material used in experiments.

The relative differences between the largest K_f to the smallest K_f determined for one sorbate with the different sorbent materials without and with SA normalization are shown in figure 6.2. Only the normalization using the SA of the sorbent materials is shown in figure 6.2 as the influence of the carbon content on the relative difference between the different sorbent materials was low. Deviation between the sorbent materials could only be slightly reduced using the carbon content (about 10 %, which is in the range of the overall experimental error estimated via error propagation). SA normalization reduced K_f deviation by more than two log units. Consequently, SA was the dominant factor for differences in sorption between the different materials, but other factors like surface functional groups or accessibility of surface area also contribute to the calculated differences. The low contribution of the carbon content could be expected as the content was relatively similar in contrast to the surface area that differed strongly. For sorbent materials with a strongly different carbon content (e.g. soils) the carbon content may also account for differences in sorption.

Similar observations regarding the influence of SA normalization are reported in literature. For the comparison of AC with SWCNTs and MWCNTs, normalization with SA strongly reduced differences observed between the sorbent materials.[9] The effect of SA was also more pronounced than the effect of the carbon content normalization[9] as it could also derived from data in the present study. It was concluded that SA and carbon content are characteristics that account for main differences between the sorbent materials.[9] However, still a deviation between the sorbent materials was observed that could not be completely removed.[9] For sorption of naphthalene, 1,3-dichlorobenzene and 2,4-dichlorophenol

normalization using the SA reduced the deviation between different types of SWCNTs and graphite almost completely.[15] For 2-naphthol and 1-naphthylamine deviations between the materials were still observed after normalization although they were reduced.[15] These observations could be supported with the results of the present study as sorption of the different sorbates still showed differences after normalization.

Remaining differences in sorption between the sorbent materials of the present study may be related to differences in the accessible surface area and effects originating from the surface chemistry of sorbent materials.[9, 15] The SA measured using N_2 or CO_2 adsorption is not ideal for all sorbates as N_2 or CO_2 are smaller in molecule size compared to those sorbates used in literature and sorbates used in the present study. Consequently, N_2 or CO_2 may be able to reach regions where the surface area is inaccessible for the sorbates because of their size or pores are additionally blocked by functional groups.[9] Furthermore, N_2 or CO_2 surface area is measured at dry conditions while sorption studies were conducted in aqueous solution reducing the available surface area due to the presence of water. In this context, the pore size distribution of sorbent materials may differ and result in differences between materials. Influences on the accessible surface area were discussed for norfloxacin sorption to AC or CNTs.[17] The SA of AC was up to six times higher than the SA of CNTs. When comparing data on the unit surface basis, sorption to CNTs was stronger than AC while on mass unit basis the opposite tendency was observed.[17] One potential reason mentioned by the authors was that N_2 molecules were able to reach smaller pores than norfloxacin because of the reduced size compared to norfloxacin.[17] The influence of surface chemistry / functionalities was shown for sorption of 2-naphthol and 1-naphthylamine compared to 1,3-dichlorobenzene, 2,4-dichlorophenole, and naphthalene.[15] After SA normalization, isotherms of 2-naphthol and 1-naphthylamine still differed between SWCNTs and graphite and the authors concluded that differences in surface functionalities of sorbent materials may cause differences depending on the sorbate selection.[15]

Overall, the presented column approach was proven suitable to study and compare sorption of polar compounds like heterocyclic organic compounds to different carbon-based materials. Variation of the sorbent material content inside the column and variation of column dimensions enabled the analysis of very different carbon-based sorbent materials like graphite and activated carbon using the same experimental approach. Sorption to AC was strong compared to the other sorbent materials as only 0.1 % (wt/wt) of AC was present inside the column enabling sorption studies on these materials with the here investigated sorbates in batch experiments. Differences in the experimental approaches between batch and column

experiments may cause deviations in K_f and n that diminish or change observed trends. Therefore, comparison of all sorbent materials with the same experimental procedure is favorable. Sorption studies including the effect of environmental conditions could be done in the future in combination with the alternative approach for the sorbent materials of this study, significantly reducing the manual workload and time demand compared to batch experiments as it was shown for MWCNTs in chapters 4 and 5. Generating a large data set for different sorbent materials using different sorbates and changing environmental conditions would enable setting up of prediction models considering the influence of environmental conditions on sorption. This would be very useful in environmental modeling as speciation of sorbates as well as sorbent materials affect sorption in the environment.

6.5 References

1. Kim, S. D.; Cho, J.; Kim, I. S.; Vanderford, B. J.; Snyder, S. A. Occurrence and removal of pharmaceuticals and endocrine disruptors in South Korean surface, drinking, and waste waters. *Water Research* **2007,** 41 (5), 1013-1021.
2. Ternes, T. A.; Meisenheimer, M.; McDowell, D.; Sacher, F.; Brauch, H. J.; Gulde, B. H.; Preuss, G.; Wilme, U.; Seibert, N. Z. Removal of pharmaceuticals during drinking water treatment. *Environmental Science & Technology* **2002,** 36 (17), 3855-3863.
3. Westerhoff, P.; Yoon, Y.; Snyder, S.; Wert, E. Fate of endocrine-disruptor, pharmaceutical, and personal care product chemicals during simulated drinking water treatment processes. *Environmental Science & Technology* **2005,** 39 (17), 6649-6663.
4. Snyder, S. A.; Adham, S.; Redding, A. M.; Cannon, F. S.; DeCarolis, J.; Oppenheimer, J.; Wert, E. C.; Yoon, Y. Role of membranes and activated carbon in the removal of endocrine disruptors and pharmaceuticals. *Desalination* **2007,** 202 (1-3), 156-181.
5. Hüffer, T.; Osorio, X. L.; Jochmann, M. A.; Schilling, B.; Schmidt, T. C. Multi-walled carbon nanotubes as sorptive material for solventless in-tube microextraction (ITEX2) - a factorial design study. *Analytical and Bioanalytical Chemistry* **2013,** 405 (26), 8387-8395.
6. Ma, J. P.; Lu, X.; Xia, Y.; Yan, F. L. Determination of pyrazole and pyrrole pesticides in environmental water samples by solid-phase extraction using multi-walled carbon nanotubes as adsorbent coupled with high-performance liquid chromatography. *Journal of Chromatographic Science* **2015,** 53 (2), 380-384.
7. Gil, R. A.; Goyanes, S. N.; Polla, G.; Smichowski, P.; Olsina, R. A.; Martinez, L. D. Application of multi-walled carbon nanotubes as substrate for the on-line preconcentration, speciation and determination of vanadium by ETAAS. *Journal of Analytical Atomic Spectrometry* **2007,** 22 (10), 1290-1295.
8. Duran, A.; Tuzen, M.; Soylak, M. Preconcentration of some trace elements via using multiwalled carbon nanotubes as solid phase extraction adsorbent. *Journal of Hazardous materials* **2009,** 169 (1-3), 466-471.
9. Brooks, A. J.; Lim, H. N.; Kilduff, J. E. Adsorption uptake of synthetic organic chemicals by carbon nanotubes and activated carbons. *Nanotechnology* **2012,** 23 (29), 13.
10. Apul, O. G.; Wang, Q. L.; Zhou, Y.; Karanfil, T. Adsorption of aromatic organic contaminants by graphene nanosheets: Comparison with carbon nanotubes and activated carbon. *Water Research* **2013,** 47 (4), 1648-1654.

11. Guo, H. Y.; Li, H.; Liang, N.; Chen, F. Y.; Liao, S. H.; Zhang, D.; Wu, M.; Pan, B. Structural benefits of bisphenol S and its analogs resulting in their high sorption on carbon nanotubes and graphite. *Environmental Science and Pollution Research* **2016,** 23 (9), 8976-8984.
12. Wang, C.; Ma, L. X.; Liu, B.; Zhang, D.; Pan, B. Co-contaminant effects on ofloxacin adsorption onto activated carbon, graphite, and humic acid. *Environmental Science and Pollution Research* **2017,** 24 (30), 23834-23842.
13. Kah, M.; Zhang, X. R.; Jonker, M. T. O.; Hofmann, T. Measuring and modelling adsorption of PAHs to carbon nanotubes over a six order of magnitude wide concentration range. *Environmental Science & Technology* **2011,** 45 (14), 6011-6017.
14. Yang, K.; Wu, W. H.; Jing, Q. F.; Zhu, L. Z. Aqueous adsorption of aniline, phenol, and their substitutes by multi-walled carbon nanotubes. *Environmental Science & Technology* **2008,** 42 (21), 7931-7936.
15. Chen, W.; Duan, L.; Wang, L. L.; Zhu, D. Q. Adsorption of hydroxyl- and amino-substituted aromatics to carbon nanotubes. *Environmental Science & Technology* **2008,** 42 (18), 6862-6868.
16. Ji, L. L.; Shao, Y.; Xu, Z. Y.; Zheng, S. R.; Zhu, D. Q. Adsorption of monoaromatic compounds and pharmaceutical antibiotics on carbon nanotubes activated by KOH etching. *Environmental Science & Technology* **2010,** 44 (16), 6429-6436.
17. Wang, Z. Y.; Yu, X. D.; Pan, B.; Xing, B. S. Norfloxacin sorption and its thermodynamics on surface-modified carbon nanotubes. *Environmental Science & Technology* **2010,** 44 (3), 978-984.
18. Wang, C.; Li, H.; Liao, S. H.; Zheng, H.; Wang, Z. Y.; Pan, B.; Xing, B. S. Coadsorption, desorption hysteresis and sorption thermodynamics of sulfamethoxazole and carbamazepine on graphene oxide and graphite. *Carbon* **2013,** 65, 243-251.
19. Hüffer, T.; Endo, S.; Metzelder, F.; Schroth, S.; Schmidt, T. C. Prediction of sorption of aromatic and aliphatic organic compounds by carbon nanotubes using poly-parameter linear free-energy relationships. *Water Research* **2014,** 59, 295-303.
20. Shih, Y. H.; Gschwend, P. M. Evaluating activated carbon-water sorption coefficients of organic compounds using a linear solvation energy relationship approach and sorbate chemical activities. *Environmental Science & Technology* **2009,** 43 (3), 851-857.
21. Chen, W.; Duan, L.; Zhu, D. Q. Adsorption of polar and nonpolar organic chemicals to carbon nanotubes. *Environmental Science & Technology* **2007,** 41 (24), 8295-8300.
22. Bi, E.; Schmidt, T. C.; Haderlein, S. B. Sorption of heterocyclic organic compounds to reference soils: Column studies for process identification. *Environmental Science & Technology* **2006,** 40 (19), 5962-5970.
23. Schenzel, J.; Goss, K. U.; Schwarzenbach, R. P.; Bucheli, T. D.; Droge, S. T. J. Experimentally determined soil organic matter-water sorption coefficients for different classes of natural toxins and comparison with estimated numbers. *Environmental Science & Technology* **2012,** 46 (11), 6118-6126.
24. Wu, W. H.; Jiang, W.; Zhang, W. D.; Lin, D. H.; Yang, K. Influence of functional groups on desorption of organic compounds from carbon nanotubes into water: Insight into desorption hysteresis. *Environmental Science & Technology* **2013,** 47 (15), 8373-8382.
25. Li, H. B.; Zhang, D.; Han, X. Z.; Xing, B. S. Adsorption of antibiotic ciprofloxacin on carbon nanotubes: pH dependence and thermodynamics. *Chemosphere* **2014,** 95, 150-155.
26. Droge, S.; Goss, K. U. Effect of sodium and calcium cations on the ion-exchange affinity of organic cations for soil organic matter. *Environmental Science & Technology* **2012,** 46 (11), 5894-5901.
27. Qian, Y. Sorption of hydrophobic organic compounds (HOCs) to inorganic surfaces in aqueous solutions. Ph.D. disserstation, University Duisburg-Essen, Essen, Germany, 2010.

28. Mader, B. T.; Goss, K. U.; Eisenreich, S. J. Sorption of nonionic, hydrophobic organic chemicals to mineral surfaces. *Environmental Science & Technology* **1997,** 31 (4), 1079-1086.
29. Bucheli, T. D.; Gustafsson, O. Soot sorption of non-ortho and ortho substituted PCBs. *Chemosphere* **2003,** 53 (5), 515-522.
30. Ji, L. L.; Chen, W.; Duan, L.; Zhu, D. Q. Mechanisms for strong adsorption of tetracycline to carbon nanotubes: A comparative study using activated carbon and graphite as adsorbents. *Environmental Science & Technology* **2009,** 43 (7), 2322-2327.
31. Thomsen, A. B.; Henriksen, K.; Gron, C.; Moldrup, P. Sorption, transport, and degradation of quinoline in unsaturated soil. *Environmental Science & Technology* **1999,** 33 (17), 2891-2898.
32. Bi, E.; Schmidt, T. C.; Haderlein, S. B. Environmental factors influencing sorption of heterocyclic aromatic compounds to soil. *Environmental Science & Technology* **2007,** 41 (9), 3172-3178.
33. Li, B. H.; Qian, Y. A.; Bi, E. P.; Chen, H. H.; Schmidt, T. C. Sorption behavior of phthalic acid esters on reference soils evaluated by soil column chromatography. *Clean-Soil Air Water* **2010,** 38 (5-6), 425-429.
34. Sigmund, G.; Sun, H. C.; Hofmann, T.; Kah, M. Predicting the sorption of aromatic acids to noncarbonized and carbonized sorbents. *Environmental Science & Technology* **2016,** 50 (7), 3641-3648.
35. Kah, M.; Sigmund, G.; Xiao, F.; Hofmann, T. Sorption of ionizable and ionic organic compounds to biochar, activated carbon and other carbonaceous materials. *Water Research* **2017,** 124, 673-692.
36. Sigmund, G.; Huffer, T.; Hofmann, T.; Kah, M. Biochar total surface area and total pore volume determined by N_2 and CO_2 physisorption are strongly influenced by degassing temperature. *Science of the Total Environment* **2017,** 580, 770-775.
37. Hüffer, T.; Schroth, S.; Schmidt, T. C. Influence of humic acids on sorption of alkanes by carbon nanotubes - Implications for the dominant sorption mode. *Chemosphere* **2015,** 119, 1169-75.
38. Pan, B.; Xing, B. S. Adsorption mechanisms of organic chemicals on carbon nanotubes. *Environmental Science & Technology* **2008,** 42 (24), 9005-9013.
39. Chen, J. Y.; Chen, W.; Zhu, D. Adsorption of nonionic aromatic compounds to single-walled carbon nanotubes: Effects of aqueous solution chemistry. *Environmental Science & Technology* **2008,** 42 (19), 7225-7230.
40. Shen, X. E.; Shan, X. Q.; Dong, D. M.; Hua, X. Y.; Owens, G. Kinetics and thermodynamics of sorption of nitroaromatic compounds to as-grown and oxidized multiwalled carbon nanotubes. *Journal of Colloid and Interface Science* **2009,** 330 (1), 1-8.
41. Wang, L. L.; Zhu, D. Q.; Duan, L.; Chen, W. Adsorption of single-ringed N- and S-heterocyclic aromatics on carbon nanotubes. *Carbon* **2010,** 48 (13), 3906-3915.
42. Chin, C. J. M.; Shih, M. W.; Tsai, H. J. Adsorption of nonpolar benzene derivatives on single-walled carbon nanotubes. *Applied Surface Science* **2010,** 256 (20), 6035-6039.
43. Cho, H. H.; Smith, B. A.; Wnuk, J. D.; Fairbrother, D. H.; Ball, W. P. Influence of surface oxides on the adsorption of naphthalene onto multiwalled carbon nanotubes. *Environmental Science & Technology* **2008,** 42 (8), 2899-2905.
44. Kragulj, M.; Trickovic, J.; Dalmacija, B.; Kukovecz, A.; Konya, Z.; Molnar, J.; Roncevic, S. Molecular interactions between organic compounds and functionally modified multiwalled carbon nanotubes. *Chemical Engineering Journal* **2013,** 225, 144-152.
45. Abraham, M. H.; Chadha, H. S.; Whiting, G. S.; Mitchell, R. C. Hydrogen bonding. 32. An analysis of water-octanol and water-alkane partitioning and the Δlog P parameter of seiler. *Journal of Pharmaceutical Sciences* **1994,** 83 (8), 1085-1100.

46. Ji, L. L.; Chen, W.; Bi, J.; Zheng, S. R.; Xu, Z. Y.; Zhu, D. Q.; Alvarez, P. J. Adsorption of tetracycline on single-walled and multi-walled carbon nanotubes as affected by aqueous solution chemistry. *Environmental Toxicology and Chemistry* **2010,** 29 (12), 2713-2719.
47. Li, X. N.; Zhao, H. M.; Quan, X.; Chen, S. O.; Zhang, Y. B.; Yu, H. T. Adsorption of ionizable organic contaminants on multi-walled carbon nanotubes with different oxygen contents. *Journal of Hazardous materials* **2011,** 186 (1), 407-415.
48. Wang, X. L.; Liu, Y.; Tao, S.; Xing, B. S. Relative importance of multiple mechanisms in sorption of organic compounds by multiwalled carbon nanotubes. *Carbon* **2010,** 48 (13), 3721-3728.
49. Cho, H. H.; Huang, H.; Schwab, K. Effects of solution chemistry on the adsorption of ibuprofen and triclosan onto carbon nanotubes. *Langmuir* **2011,** 27 (21), 12960-12967.
50. Wu, W. H.; Chen, W.; Lin, D. H.; Yang, K. Influence of surface oxidation of multiwalled carbon nanotubes on the adsorption affinity and capacity of polar and nonpolar organic compounds in aqueous phase. *Environmental Science & Technology* **2012,** 46 (10), 5446-5454.
51. Chen, G. C.; Shan, X. Q.; Wang, Y. S.; Pei, Z. G.; Shen, X. E.; Wen, B.; Owens, G. Effects of copper, lead, and cadmium on the sorption and desorption of atrazine onto and from carbon nanotubes. *Environmental Science & Technology* **2008,** 42 (22), 8297-8302.

6.6. Appendix to chapter 6

SI6.1 Addition to materials and methods

Sorption studies on fMWCNTs were done using an Agilent 1100 system consisting of the following parts: quaternary pump (G1211A), degasser (G1379A), autosampler (G1313), column oven (G1316A), variable wavelength detector (G1314A), and a RID (G1362A).

Sorbent materials used in this study were biochar (SWP700, UK biochar research centre, The University of Edinburgh, School of GeoSciences, Edinburgh, Scotland), graphite (99.99 % trace metal basis, <150 µm, Aldrich Chemicals), graphene platelets (99.5 %, 11 – 15 nm, CP-0068-HP-0050, IOLITEC Ionic Liquids Technologies GmbH, Heilbronn, Germany), two types of activated carbons (AC1: Norit GAC 830 (Cabot Corporation, Norit Nederland B.V., Amersfoort, Netherlands), AC2: Chemviron HPC Maxx 830 (Chemviron, Feluy, Belgium)), and fMWCNTs produced from MWCNTs (C150HP, Bayer Material Science, Leverkusen, Germany) as base material according to a procedure from literature.[1] In brief, MWCNTs were heated to 350 °C for 1 h to remove amorphous carbon according to literature, which proved the removal via transmission electron microscopy.[2] Second, nitric acid was used to oxidize MWCNTs yielding fMWCNTs with functional groups on the surface.[1]

The tables in this section are further additions to materials and methods section. Table S6.1 shows the determined surface area of different sorbent materials in unground and ground state in combination with the carbon and oxygen content of the respective sorbent material. Table S6.2 summarizes the results of X-ray photoelectron spectroscopy measurements of MWCNTs and fMWCNTs. Table S6.3 summarizes the characteristics of all columns used this study. Column dimension, packing material composition, bulk density (ρ_b), porosity (θ) and sorbate measured with the respective column are given. ρ_b and θ were determined by repeated measurements of D_2O (n = 10) with and without column installed in the system.

Table S6.1: Summary of surface area of the native and ground sorbent materials measured by Brunauer-Emmett-Teller method with N_2 sorption isotherms with the corresponding standard deviation (n=3) together with the carbon and oxygen content determined by elemental analysis.

sorbent material	surface area unground [m^2 g^{-1}]	surface area ground [m^2 g^{-1}]	carbon content [%]	oxygen content [%]
MWCNTs	211 ± 1.5	228 ± 1.7	98.4	<1
fMWCNTs	229 ± 0.6	251 ± 2.0	90.7	7.8
graphite	2.10 ± 0.06	2.20 ± 0.14	99	<1
graphene	29.5 ± 0.5	32.3 ± 0.4	96	3.2
AC1	1100 ± 0.4	1167 ± 3.8	94	5.3
AC2	883 ± 5.4	1087 ± 0.2	87	11.6
biochar	173	182	91.5	6.6

Table S6.2: Determined content of functional groups for MWCNTs and fMWCNTs of this study. Relative content of functional groups under the C1s-peak were determined by X-ray photoelectron spectroscopy measurements.

	MWCNTs	fMWCNTs
C−C content [%]	74.9	72.8
C−O− content [%]	10.7	17.8
C=O content [%]	1.0	0
COOH content [%]	5.4	3.4
π-π* content [%]	8.0	6.0

Table S6.3: Summary of columns used in this study with their dimensions, packing material composition, bulk density (ρ_b), porosity (θ) and the respective sorbates.

column	dimension (L × ID) [mm]	packing material [w.-%]	bulk density ρ_b [kg L^{-1}]	porosity θ [-]	sorbate
Q22	14 × 3	100 % quartz	1.632	0.502	all
B3	14 × 3	95 % quartz / 5 % biochar	1.422	0.503	pyrazole
CNTF2	14 × 3	95 % quartz / 5 % fMWCNTs	1.395	0.559	pyrazole
CNTF8	14 × 3	95 % quartz / 5 % fMWCNTs	1.435	0.549	furan
CNTF6	14 × 3	95 % quartz / 5 % fMWCNTs	1.414	0.546	pyrrole
CNTF7	14 × 3	95 % quartz / 5 % fMWCNTs	1.443	0.520	thiophene
G4	53 × 3	40 % quartz / 60 % graphene	1.114	0.546	all
Gf1	14 × 3	85 % quartz / 15 % graphene	1.217	0.639	pyrazole
Gf3	14 × 3	85 % quartz / 15 % graphene	1.222	0.651	furan
Gf2	14 × 3	85 % quartz / 15 % graphene	1.254	0.621	pyrrole
Gf4	14 × 3	95 % quartz / 5 % graphene	1.353	0.603	thiophene
AC1.3	14 × 3	99.9 % quartz / 0.1 % AC1	1.508	0.502	pyrazole
AC1.6	14 × 3	99.9 % quartz / 0.1 % AC1	1.470	0.508	furan
AC1.5	14 × 3	99.9 % quartz / 0.1 % AC1	1.502	0.513	pyrrole
AC1.4	14 × 3	99.9 % quartz / 0.1 % AC1	1.520	0.487	thiophene
AC2.1	14 × 3	99.9 % quartz / 0.1 % AC2	1.523	0.515	pyrazole
AC2.2	14 × 3	99.9 % quartz / 0.1 % AC2	1.556	0.527	furan
AC2.3	14 × 3	99.9 % quartz / 0.1 % AC2	1.592	0.515	pyrrole
AC2.4	14 × 3	99.9 % quartz / 0.1 % AC2	1.531	0.532	thiophene

SI6.2 Determination of equilibrium

Figure S6.1 summarizes retardation factors (R) of pyrazole determined for the different sorbent materials of this study using different flow rates. The concentration of the solution of each sorbate injected for determination of the local equilibrium is mentioned in table S6.4. For all sorbent materials despite biochar no increasing trend of R with decreasing flow rate could be observed. For biochar, R strongly increased. Additionally, the peak shape changed strongly when decreasing the flow rate in case of biochar (figure S6.2). Signal intensity of the apex point strongly decreased and tailing increased with decreasing flow rate. These observations were not made for the other sorbent materials. Consequently, local equilibrium inside the columns could be assumed for all sorbent materials despite biochar. Sorption isotherms were determined for those sorbent materials local equilibrium inside the column could be achieved.

Table S6.4: Summary of concentrations of solutions for each sorbate with the different sorbents injected in columns during determination of equilibrium.

	pyrazole	**pyrrole**	**furan**	**thiophene**
sorbent	**mg L^{-1}**			
MWCNTs	150	100	1000	40
fMWCNTs	100	100	100	500
graphite	100	50	50	500
graphene	125	100	300	1000
AC1	100	150	200	750
AC2	125	150	175	1500
biochar	400	-	-	-

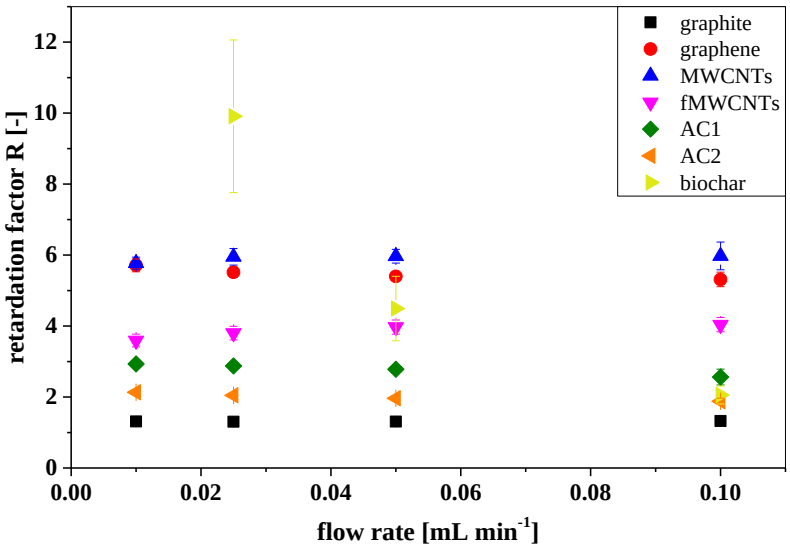

Figure S6.1: Comparison of retardation factors (R) determined using pyrazole as sorbate at different flow rates (0.01 – 0.10 mL min^{-1}) for all sorbent materials used in this study. Concentrations used for the different sorbent materials are shown in table S6.4.

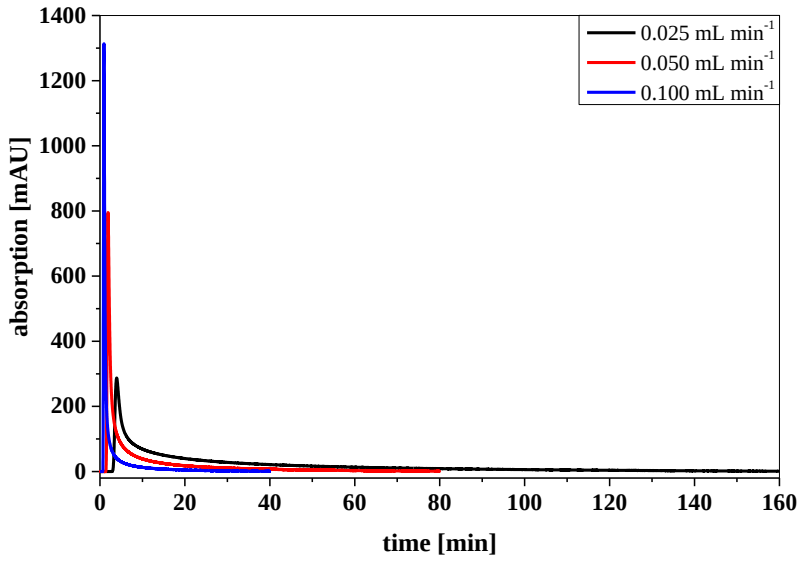

Figure S6.2: Chromatograms of pyrazole recorded with a column B3 containing 5 % biochar applying different flow rates (0.025 – 0.100 mL min^{-1}).

SI6.3 Isotherm determination

Table S6.5: Summary of concentrations of solutions for each sorbate with the different sorbents injected in columns during determination of isotherms.

	pyrazole	pyrrole	furan	thiophene
sorbent	**mg L^{-1}**			
MWCNTs	1000, 840, 470, 270, 150, 84, 47, 26, 15	800, 534, 300, 170, 95, 53, 30, 17, 9	1500, 1200, 1000, 840, 470 ,270, 150, 84, 47	560, 450, 320, 170, 100, 75, 40, 30, 15
fMWCNTs	600, 470, 350, 270, 150, 84, 47, 26, 13	300, 200, 150, 100, 75, 60, 25, 15, 10	400, 300, 200, 100, 80, 60, 40, 25, 15	1250, 1000, 750, 500, 250, 150, 80, 60
graphite	250, 175, 150, 125, 80, 50, 30, 20, 10	175, 125, 75, 50, 25, 15, 10, 7, 5	400, 300, 200, 150, 100, 50, 30, 20, 10	1350, 1000, 875, 750, 500, 350, 200, 150, 100
graphene	1000, 750, 500, 400, 300, 150, 100, 80, 60	850, 650, 500, 325, 150, 175, 100, 75, 50	1500, 1200, 1000, 800, 600, 450, 325, 225, 150	1750, 1500, 1250, 1050, 750, 600, 500, 350, 200
AC1	500, 400, 300, 200, 125, 80, 50, 30, 20	800, 400, 325, 250, 175, 100, 75, 50, 25	1200, 1000, 850, 650, 500, 325, 250, 125, 90	3250, 2500, 2000, 1500, 1000, 750, 500, 350, 200
AC2	500, 400, 250, 200, 125, 80, 50, 30, 20	400, 325, 200, 175, 150, 125, 75, 40, 25	900, 750, 600, 450, 350, 250, 175, 100, 80	3250, 2400, 2000, 150, 1250, 1000, 750, 500, 350

Table S6.6: Calibrations of different sorbates used in this study to calculate dissolved liquid concentration in equilibrium ($c_{w,eq}$) for isotherm calculation (10 mM $CaCl_2$, pH 6).

compound name	Slope [mAU L mg^{-1}]	y-intercept [mAU]	R^2 [-]
furan	60.8	-0.4	0.9999
pyrazole	55.9	4.3	0.9999
pyrrole	83.5	4.4	0.9999
thiophene	37.9	3.8	0.9999

SI6.4 Comparison of classical and alternative evaluation approach

Calculated values for the Freundlich coefficient (K_f) and the Freundlich exponent (n) of the classical and alternative approach are compared in table S6.7 while the isotherms of pyrazole with the different sorbent materials are shown in figure S6.3 (classical approach) and S6.4 (alternative approach). The concentration ranges used for isotherm fitting are summarized in table S6.8. Fitting parameters using a linear fit to describe sorption isotherms are shown in table S6.9, which had lower R^2 values and higher errors of the regression parameters than the Freundlich isotherms shown in table S6.7 showing the better applicability of the Freundlich model.

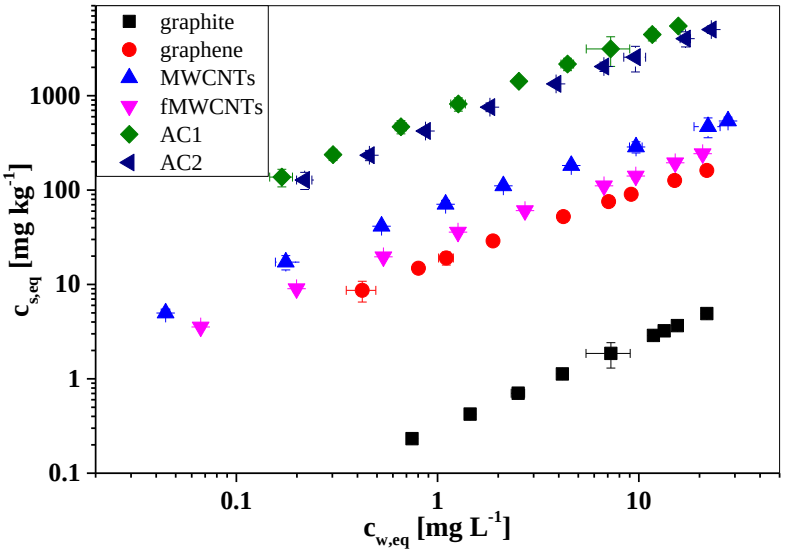

Figure S6.3: Isotherms of pyrazole determined with the different sorbent materials of this study according to the classical approach. Error bars represent the maximum error determined via error propagation.

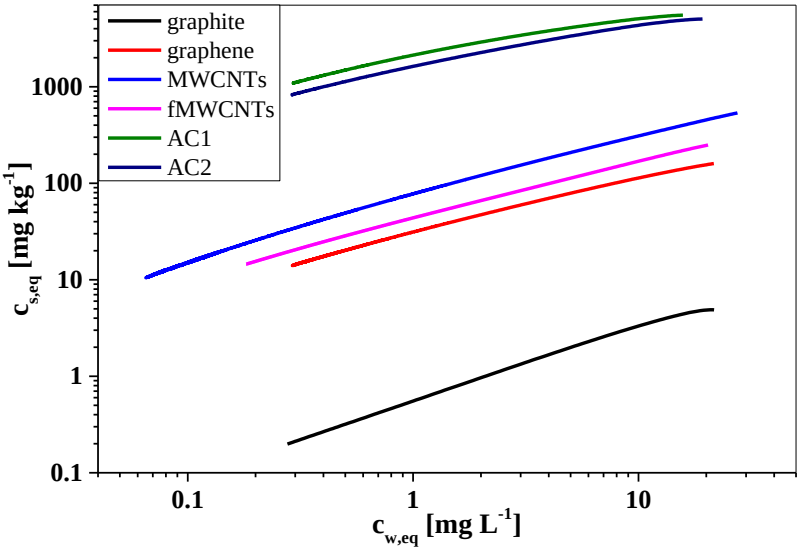

Figure S6.4: Isotherms of pyrazole determined with the different sorbent materials of this study according to the alternative approach. No error bars are given as one of the three recorded replicates is shown.

K_f values of the alternative approach were for all sorbent materials larger than the classical approach while for n the opposite trend was observed. While for MWCNTs, fMWCNTs, graphene, and graphite the deviation in K_f between the two evaluation approaches was less than a factor of two, larger deviations of up to about factor four were found for the two activated carbon materials. Reason for the deviations in K_f were related to the differences in intensity used for isotherm calculation. Intensity used for the calculation of $c_{w,eq}$ was higher using the alternative approach at the same retention time in the chromatogram yielding finally higher K_f values for the alternative approach because of the evaluation steps. The larger deviation for activated carbons was related to higher dilution of the sorbent material compared to the other sorbent materials. This relationship to the dilution of sorbent material was shown previously in chapter 5 and can be seen for thiophene with MWCNTs as sorbent material in table 6.1. Thiophene was analyzed in columns containing only 0.5 % MWCNTs (wt/wt) while the other sorbates were analyzed in column containing 5 % MWCNTs (wt/wt) in chapter 5. The lower content of MWCNTs resulted in a lower retention inside the column and a stronger increasing signal intensity with increasing concentration of the injected solution. The same reason will result in the larger deviation for K_f for AC1 and AC2 (exemplarily shown for thiophene with AC1 in figure S6.5 compared to pyrazine in figure S6.6 (taken from chapter 5). While the tailing of pyrazine measurement of solutions injected with different concentrations overlapped strongly (figure S6.6), more deviations in the recorded peaks were recognized for thiophene (figure S6.5). The K_f values determined for pyrazine were with 222.2 for the classical and 231.7 for the alternative approach almost identical (compare table 5.1 in chapter 5).

The K_f value of thiophene with MWCNTs as sorbent material taken from a previous study may also be too low compared to the other sorbates measured with MWCNTs as sorbent material because of the increased dilution of MWCNTs for thiophene compared to the other sorbates. Thiophene could not be measured in columns containing 5 % MWCNTs (wt/wt) as the signal intensity was too low and retention inside the column too strong. The detection of the other sorbates was possible without problems caused by high retention and low signal intensity. Therefore, the deviation of K_f determined for thiophene (234.2) to the K_f values of the other sorbates (73.3 – 154.8) could be expected to be larger as the dilution of MWCNTs was increased by factor ten to 0.5 % MWCNTs (wt/wt) (table 5.1 in chapter 5). This may then finally result in the reduced ratio of the K_f determined for thiophene to the K_f determined for furan compared to the other sorbent materials as mentioned in the main paper.

The non-linearity expressed by n increased for all sorbent materials using the alternative approach. For example, sorption to graphite was almost linear (0.91 – 0.96 for furan, pyrazole and pyrrole) using the classical approach. However, n reduced applying the alternative approach to 0.74 – 0.78 for the same sorbates. For the activated carbons the reduction of n was even stronger (0.67 – 0.81 for the classical and 0.37 – 0.43 for the alternative approach). n was smaller for the alternative approach because the tailing of the peak in the chromatogram influenced the derived isotherm in the alternative approach more than in the classical approach. The slow decrease in the absorption in the chromatogram (figure S6.5) and corresponding $c_{w,eq}$, which was directly calculated from the absorption, with proceeding measurement time increased nonlinearity of the derived isotherm based on the alternative approach, because the corresponding K_d value and, consequently, $c_{s,eq}$ belonging to $c_{w,eq}$ changed stronger. For the classical approach, decrease of absorption and $c_{w,eq}$ is stronger and the tailing is not reflected that strong. Consequently, the linearity of isotherms derived with the classical approach was higher.

Similar to the procedure in chapter 5 using only MWCNTs as sorbent showing the comparability of both evaluation approaches, the calculated K_d values for all sorbents with both approaches for 1 %, 0.1 % and 0.01 % of the aqueous solubility in water of each sorbate agreed well with an deviation of maximum 0.3 log units (exemplarily shown in figures S6.7 to S6.9 for AC1, graphene and fMWCNTs for the different solubility levels). Only for the activated carbon materials deviation increased to maximum 0.6 log units at 0.01 % of the aqueous solubility while at the higher concentrations deviation was within 0.3 log units. This shows that the alternative evaluation approach was also suitable for different carbon-based sorbents of this study and deviation of up to factor four in determined K_f values between both approaches resulted in relatively small deviations in K_d as the changed linearity of the isotherms expressed by n seemed to partially compensate that deviation. A deviation of 0.3 log units is an acceptable deviation especially when considering the reduced time demand for isotherm determination using the alternative evaluation approach of up to factor ten when using nine concentrations for the classical approach. Trends were similar for both evaluation approaches and the alternative approach proved its suitability also for other sorbent materials than MWCNTs.

Table S6.7: Comparison of isotherm characteristics (Freundlich coefficient (K_f) [(mg kg^{-1}) (mg L^{-1})$^{-n}$], Freundlich exponent (n) [-], and the correlation coefficient (R^2) [-]) of the classical and alternative approach for the different sorbates. Values for MWCNTs were taken from chapter 5. Uncertainties given in the table are the standard errors of the regression with K_f as y-intercept and n as slope of the regression for the classical and the standard deviation of the three replicates for the alternative approach.

		classical approach			alternative approach		
sorbate	**sorbent**	**K_f**	**n**	**R^2**	**K_f**	**n**	**R^2**
furan	**MWCNTs**	$(1.32 \pm 0.02) \times 10^2$	0.60 ± 0.01	0.9995	$(1.55 \pm 0.01) \times 10^2$	0.57 ± 0.01	0.9999
	fMWCNTs	$(1.63 \pm 0.1) \times 10^1$	0.75 ± 0.01	0.9995	$(3.12 \pm 0.03) \times 10^1$	0.54 ± 0.01	0.9995
	graphene	$(4.43 \pm 0.02) \times 10^1$	0.60 ± 0.01	0.9999	$(6.59 \pm 0.01) \times 10^1$	0.48 ± 0.01	0.9993
	graphite	$(4.30 \pm 0.10) \times 10^{-1}$	0.91 ± 0.01	0.9996	$(8.10 \pm 0.10) \times 10^{-1}$	0.74 ± 0.01	0.9993
	AC1	$(1.80 \pm 0.01) \times 10^3$	0.72 ± 0.01	0.9997	$(5.34 \pm 0.06) \times 10^3$	0.40 ± 0.01	0.9929
	AC2	$(1.45 \pm 0.01) \times 10^3$	0.69 ± 0.01	0.9997	$(4.10 \pm 0.02) \times 10^3$	0.39 ± 0.01	0.9954
pyrazole	**MWCNTs**	$(5.76 \pm 0.03) \times 10^1$	0.71 ± 0.02	0.9930	$(7.33 \pm 0.02) \times 10^1$	0.65 ± 0.01	0.9965
	fMWCNTs	$(2.82 \pm 0.07) \times 10^1$	0.72 ± 0.01	0.9981	$(4.27 \pm 0.01) \times 10^1$	0.60 ± 0.01	0.9992
	graphene	$(1.74 \pm 0.03) \times 10^1$	0.74 ± 0.01	0.9988	$(3.05 \pm 0.01) \times 10^1$	0.58 ± 0.01	0.9977
	graphite	$(3.00 \pm 0.01) \times 10^{-1}$	0.91 ± 0.01	0.9999	$(5.50 \pm 0.10) \times 10^{-1}$	0.76 ± 0.01	0.9981
	AC1	$(6.32 \pm 0.01) \times 10^2$	0.81 ± 0.01	0.9983	$(2.03 \pm 0.05) \times 10^3$	0.43 ± 0.01	0.9861
	AC2	$(4.47 \pm 0.09) \times 10^2$	0.78 ± 0.01	0.9989	$(1.57 \pm 0.08) \times 10^3$	0.45 ± 0.01	0.9901
pyrrole	**MWCNTs**	$(6.52 \pm 0.02) \times 10^1$	0.71 ± 0.01	0.9968	$(8.22 \pm 0.01) \times 10^1$	0.62 ± 0.01	0.9997
	fMWCNTs	$(1.61 \pm 0.02) \times 10^1$	0.76 ± 0.01	0.9994	$(2.67 \pm 0.01) \times 10^1$	0.62 ± 0.01	0.9992
	graphene	$(2.43 \pm 0.05) \times 10^1$	0.70 ± 0.01	0.9989	$(3.88 \pm 0.02) \times 10^1$	0.54 ± 0.01	0.9977
	graphite	$(2.80 \pm 0.02) \times 10^{-1}$	0.96 ± 0.01	0.9999	$(5.20 \pm 0.10) \times 10^{-1}$	0.78 ± 0.01	0.9986
	AC1	$(1.09 \pm 0.03) \times 10^3$	0.78 ± 0.01	0.9995	$(2.91 \pm 0.50) \times 10^3$	0.43 ± 0.01	0.9861
	AC2	$(8.14 \pm 0.02) \times 10^2$	0.74 ± 0.01	0.9995	$(2.02 \pm 0.02) \times 10^3$	0.41 ± 0.01	0.9893
thiophene	**MWCNTs**	$(1.28 \pm 0.08) \times 10^2$	0.74 ± 0.01	0.9999	$(2.34 \pm 0.01) \times 10^2$	0.61 ± 0.01	0.9991
	fMWCNTs	$(4.95 \pm 0.05) \times 10^1$	0.69 ± 0.01	0.9995	$(7.71 \pm 0.02) \times 10^1$	0.56 ± 0.01	0.9997
	graphene	$(1.10 \pm 0.01) \times 10^2$	0.60 ± 0.01	0.9995	$(1.88 \pm 0.06) \times 10^2$	0.45 ± 0.01	0.9967
	graphite	$(2.53 \pm 0.03) \times 10^0$	0.72 ± 0.01	0.9996	$(3.18 \pm 0.02) \times 10^0$	0.67 ± 0.01	0.9988
	AC1	$(7.69 \pm 0.27) \times 10^3$	0.67 ± 0.01	0.9933	$(1.81 \pm 0.01) \times 10^4$	0.37 ± 0.01	0.9829
	AC2	$(6.48 \pm 0.12) \times 10^3$	0.55 ± 0.01	0.9977	$(1.29 \pm 0.01) \times 10^4$	0.38 ± 0.01	0.9874

Table S6.8: Concentration ranges of the aqueous concentration in equilibrium ($c_{w,eq}$) of the isotherms derived from column measurements according to the classical and alternative evaluation approach.

		$c_{w,eq}$ range of the determined isotherm [mg L^{-1}]	
sorbate	**sorbent**	**classical approach**	**alternative approach**
furan	**MWCNTs**	0.10 – 18.8	0.21 – 8.5
	fMWCNTs	0.32 – 23.4	0.18 – 24.1
	graphene	0.86 – 17.5	0.42 – 17.5
	graphite	0.48 – 27.0	0.20 – 27.4
	AC1	0.56 – 18.8	0.43 – 18.8
	AC2	0.46 – 19.2	0.43 – 19.2
pyrazole	**MWCNTs**	0.10 – 27.7	0.10 – 27.2
	fMWCNTs	0.11 – 20.7	0.18 – 20.5
	graphene	0.42 – 21.8	0.31 – 21.7
	graphite	0.75 – 21.8	0.27 – 22.2
	AC1	0.17 – 15.7	0.29 – 15.7
	AC2	0.22 – 22.9	0.29 – 22.6
pyrrole	**MWCNTs**	0.10 – 18.7	0.17 – 18.8
	fMWCNTs	0.25 – 17.8	0.12 – 17.8
	graphene	0.25 – 13.4	0.26 – 13.5
	graphite	0.44 – 16.4	0.16 – 16.9
	AC1	0.16 – 11.4	0.27 – 11.9
	AC2	0.14 – 10.8	0.25 – 10.7
thiophene	**MWCNTs**	0.40 – 39.0	0.44 – 39.1
	fMWCNTs	0.17 – 20.3	0.28 – 20.1
	graphene	0.68 – 24.7	0.42 – 25.4
	graphite	1.56 – 31.0	0.43 – 31.5
	AC1	0.10 – 14.0	0.45 – 14.0
	AC2	0.46 – 23.9	0.43 – 24.5

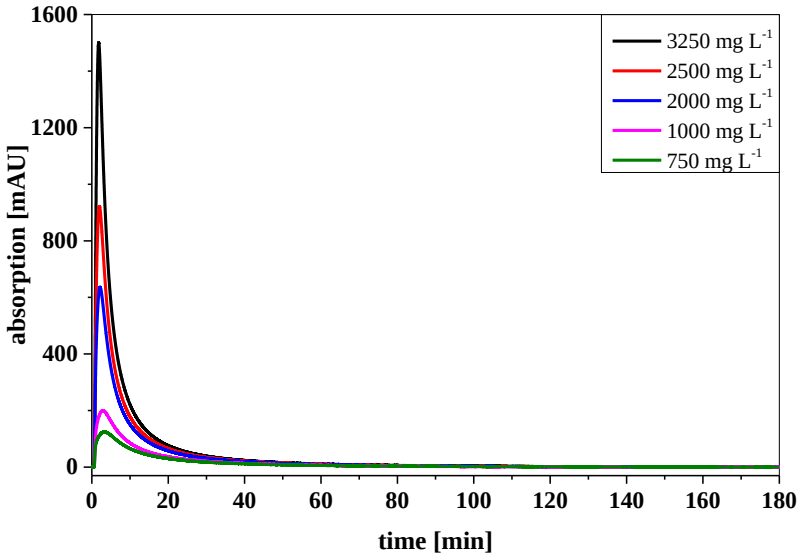

Figure S6.5: Chromatograms of thiophene for injected solutions having different concentrations using AC1 as sorbent material.

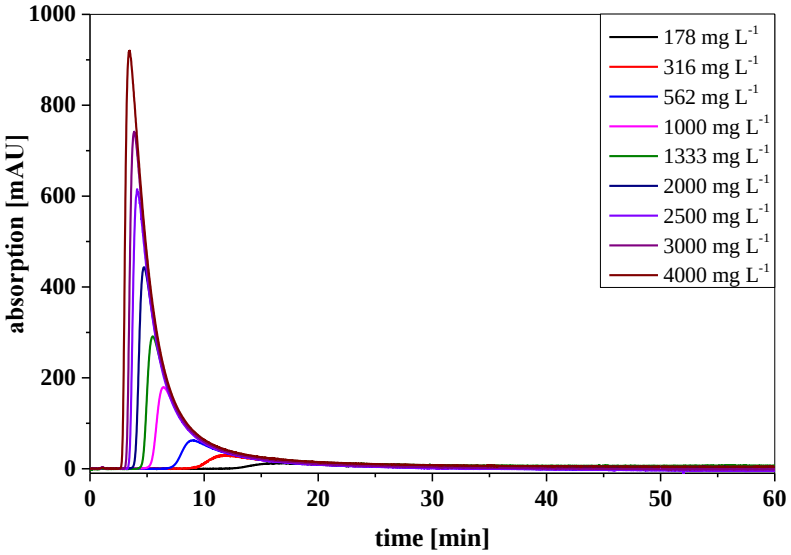

Figure S6.6: Chromatograms of pyrazine for injected solutions having different concentrations using MWCNTs as sorbent material from chapter 5.

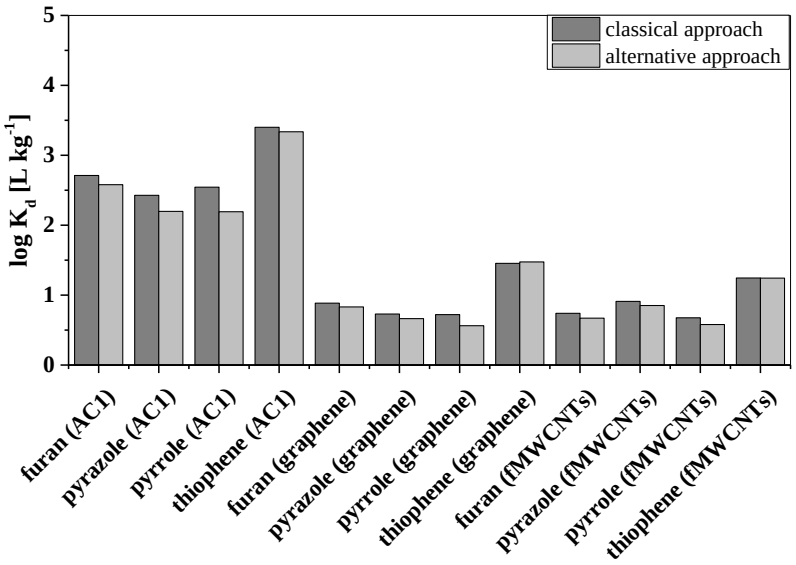

Figure S6.7: Comparison of K_d values calculated based on classical and the alternative approach using the Freundlich coefficients (K_f) and Freundlich exponents (n) listed in table S6.7 for an aqueous concentration of 1 % of the maximum solubility of the respective sorbate (furan: 8200 mg L^{-1}; pyrazole: 8900 mg L^{-1}; pyrrole: 17000 mg L^{-1}; thiophene: 2900 mg L^{-1}).

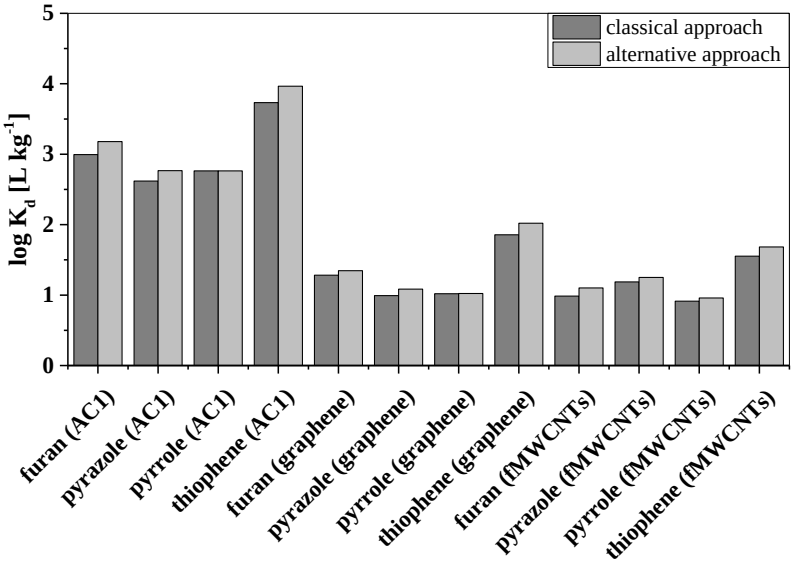

Figure S6.8: Comparison of K_d values calculated based on classical and the alternative approach using the Freundlich coefficients (K_f) and Freundlich exponents (n) listed in table S6.7 for an aqueous concentration of 0.1 % of the maximum solubility of the respective sorbate (furan: 8200 mg L^{-1}; pyrazole: 8900 mg L^{-1}; pyrrole: 17000 mg L^{-1}; thiophene: 2900 mg L^{-1}).

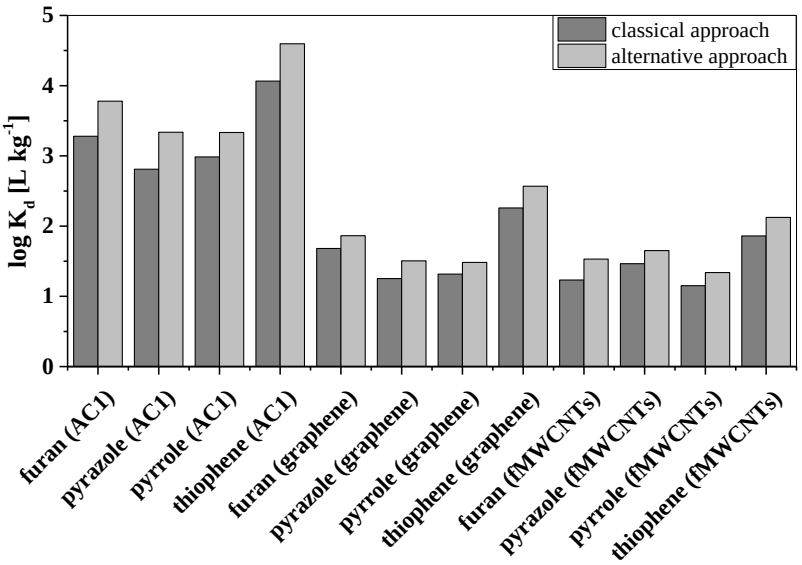

Figure S6.9: Comparison of K_d values calculated based on classical and the alternative approach using the Freundlich coefficients (K_f) and Freundlich exponents (n) listed in table S6.7 for an aqueous concentration of 0.01 % of the maximum solubility of the respective sorbate (furan: 8200 mg L^{-1}; pyrazole: 8900 mg L^{-1}; pyrrole: 17000 mg L^{-1}; thiophene: 2900 mg L^{-1}).

Table S6.9: Comparison of linear regression results (slope (m) [(mg kg^{-1}) (mg L^{-1})$^{-1}$], y-intercept (b) [mg kg^{-1}], and the correlation coefficient (R^2) [-]) of isotherms derived according to the classical and alternative approach exemplarily for the pyrazole. Values for MWCNTs derived with data from chapter 5. Errors given in the table are the standard errors of the regression related to m and b.

		data of classical approach			data of alternative approach		
sorbate	**sorbent**	m	b	R^2	m	b	R^2
pyrazole	**MWCNTs**	$(1.89 \pm 0.13) \times 10^{1}$	$(4.90 \pm 1.61) \times 10^{1}$	0.9631	$(2.27 \pm 0.02) \times 10^{1}$	$(4.45 \pm 0.10) \times 10^{1}$	0.9282
	fMWCNTs	$(1.15 \pm 0.06) \times 10^{1}$	$(1.80 \pm 0.56) \times 10^{1}$	0.9790	$(1.33 \pm 0.01) \times 10^{1}$	$(2.74 \pm 0.03) \times 10^{1}$	0.9477
	graphene	$(7.18 \pm 0.39) \times 10^{0}$	$(1.50 \pm 0.38) \times 10^{1}$	0.9766	$(8.07 \pm 0.08) \times 10^{0}$	$(2.44 \pm 0.04) \times 10^{1}$	0.9309
	graphite	$(2.20 \pm 0.10) \times 10^{-1}$	$(1.50 \pm 0.40) \times 10^{-1}$	0.9976	$(2.47 \pm 0.04) \times 10^{-1}$	$(4.17 \pm 0.31) \times 10^{-1}$	0.9665
	AC1	$(3.45 \pm 0.16) \times 10^{2}$	$(3.47 \pm 1.12) \times 10^{2}$	0.9838	$(3.59 \pm 0.06) \times 10^{2}$	$(1.68 \pm 0.03) \times 10^{3}$	0.8362
	AC2	$(2.15 \pm 0.09) \times 10^{2}$	$(3.21 \pm 0.92) \times 10^{2}$	0.9865	$(2.50 \pm 0.05) \times 10^{2}$	$(1.37 \pm 0.03) \times 10^{3}$	0.8316

SI6.5 Batch sorption experiments using MWCNTs and fMWCNTs

Table S6.10 shows sorption isotherms using MWCNTs or fMWCNTs as sorbent materials in batch experiments. A three-phase system was used. The sorbent was phase 1, the aqueous solution was phase 2, and a gaseous phase was phase 3. All three phases were present in a 20 mL headspace screw vial. The aqueous phase contained 10 mM $CaCl_2$ at pH 6 to regulate the ionic strength and vials were incubated at 25 °C. Consequently, the experimental conditions were identical to the column experiments presented in the main paper. The vial was spiked with the sorbate and equilibrated for 24 hours on a horizontal shaker at 250 rounds per minute. Preliminary experiments using toluene and trichloro ethylene indicated an equilibration within 10 hours. After equilibration and prior to analysis, vials were placed on the laboratory bench for at least one hour to equilibrate gaseous and aqueous phase. The concentration of the sorbate in the gas phase was determined with a gas chromatograph (GC) (Trace GC Ultra, Thermo Electron Corporation, Austin, Texas, United States) coupled to a mass spectrometer (MS) (DSQ Quadrupole MS; Thermo Electron Corporation, Austin, Texas, United States) equipped with a PAL Autosampler with headspace option (PAL COMBI-Xt, CTC Analytics AG, Zwingen, Switzerland) using headspace injection of 1 mL. The injector of the GC was operated in split mode with a split ratio of 1:10. The column inside the GC system was a HP5 (length: 30 m; inner diameter: 0.32 mm; film thickness: 0.25 µm; J&W Scientific, Waldbronn, Germany). Helium was used as carrier gas with a flow rate of 1.5 mL min^{-1}. Temperature of ion source inside the MS was 220 °C while the transfer line was set to 250 °C. Column temperature and used m/z-ratios for quantification are summarized in table S6.11. The sorbed concentration in equilibrium ($c_{s,eq}$) was calculated using a mass balance. First, the equilibrium concentration of the sorbate in the gaseous phase ($c_{a,eq}$) was determined using an external calibration measured prior to measurement of sorption samples (equation S6.1). Using the known Henry constant (K_H) of the different sorbates (mentioned in table S6.10) and $c_{a,eq}$, the equilibrium concentration in the aqueous phase ($c_{w,eq}$) was determined (equation S6.2). Knowing the volume of the gaseous (V_a) and aqueous phase (V_w), the mass of the sorbate in both phases (m_a: mass in gaseous phase; m_w: mass in aqueous phase) was calculated and subtracted from the initially spiked mass of the sorbate (m_0) yielding the sorbed mass of the sorbate (m_s) (equation S6.3). $c_{s,eq}$ was then calculated by dividing the sorbed mass of the sorbate by the amount of sorbent in the system ($m_{sorbent}$) (equation S6.4). $c_{w,eq}$ and $c_{s,eq}$ were fitted using the Freundlich model. For each sorbate and sorbent combination measurements were performed as duplicate.

$c_{a,eq}$ = (measured peak area – y-intercept of calibration) / slope of calibration (S6.1)

$$c_{w,eq} = c_{a,eq} / K_H \quad \text{(S6.2)}$$

$$m_s = m_0 - m_a - m_w = m_0 - V_a \times c_{a,eq} - V_w \times c_{w,eq} \quad \text{(S6.3)}$$

$$c_{s,eq} = m_s / m_{sorbent} \quad \text{(S6.4)}$$

Table S6.10: Comparison of isotherm characteristics (Freundlich coefficient (K_f) [(µg kg^{-1}) (µg L^{-1})$^{-n}$], Freundlich exponent (n) [-], and the correlation coefficient (R^2) [-]) determined using multiwalled carbon nanotubes (MWCNTs) or functionalized multiwalled carbon nanotubes (fMWCNTs). Uncertainties given in the table are the standard errors of the regression with K_f as y-intercept and n as slope of the regression.

	MWCNTs			fMWCNTs		
sorbate	**log K_f**	**n**	**R^2**	**log K_f**	**n**	**R^2**
benzene	4.70 ± 0.04	0.53 ± 0.02	0.95	3.11 ± 0.08	0.92 ± 0.03	0.95
toluene	5.49 ± 0.04	0.33 ± 0.02	0.96	3.93 ± 0.06	0.67 ± 0.03	0.95
propyl benzene	5.89 ± 0.04	0.36 ± 0.02	0.94	4.36 ± 0.03	0.60 ± 0.01	0.98
naphthalene	7.81 ± 0.02	0.55 ± 0.03	0.96	7.70 ± 0.03	0.62 ± 0.05	0.94
perchloro ethylene	5.56 ± 0.04	0.43 ± 0.01	0.99	4.39 ± 0.36	0.48 ± 0.05	0.90
trichloro ethylene	4.94 ± 0.07	0.53 ± 0.03	0.97	4.04 ± 0.10	0.64 ± 0.04	0.92
methyl *tert*-butyl ether	5.02 ± 0.05	0.93 ± 0.02	0.99	3.36 ± 0.12	0.82 ± 0.05	0.91
di-n-butyl ether	5.85 ± 0.04	0.30 ± 0.03	0.99	4.13 ± 0.03	0.51 ± 0.02	0.98
di-n-propyl ether	5.06 ± 0.06	0.49 ± 0.03	0.94	3.66 ± 0.14	0.78 ± 0.07	0.88

Table S6.11: Summary of Henry constants (K_H)[3] used for the different sorbates, applied oven temperature [°C] at the GC-MS and recorded m/z-ratios for evaluation.

sorbate	log K_H [-][3]	oven temperature [°C]	m/z
benzene	-0.65	80	78
toluene	-0.60	100	65, 91, 92
propyl benzene	-0.40	150	91, 120
naphthalene	-1.74	160	128
perchloro ethylene	0.08	131	94, 131, 164
trichloro ethylene	-0.31	90	90 – 140
methyl *tert*-butyl ether	-1.54	70	53, 73
di-n-butyl ether	-0.69	130	57, 87
di-n-propyl ether	-0.97	70	43, 73, 102

References Appendix to Chapter 6

1. Wepasnick, K. A.; Smith, B. A.; Schrote, K. E.; Wilson, H. K.; Diegelmann, S. R.; Fairbrother, D. H. Surface and structural characterization of multi-walled carbon nanotubes following different oxidative treatments. *Carbon* **2011,** 49 (1), 24-36.
2. Lu, C. Y.; Chiu, H. S. Adsorption of zinc(II) from water with purified carbon nanotubes. *Chemical Engineering Science* **2006,** 61 (4), 1138-1145.
3. Schwarzenbach, R. P.; Gschwend, P. M.; Imboden, D. M., *Environmental Organic Chemistry*. John Wiley and Sons: Hoboken, NJ, USA, 2003.

Chapter 7 - General Conclusion and Outlook

7.1 General conclusion

In this thesis, column chromatography was shown to be a suitable complementary methodology in sorption studies on carbon-based materials and nanomaterials that so far solely focused on batch experiments. The applied sorbent material variety in literature using column chromatography hitherto was predominantly limited to soils[1-5] and minerals.[6, 7] Applications for purely or predominantly carbon-based materials with the aim to determine sorption data like K_d values were rarely found in literature (e.g. soot[8]) and this study extends the applied sorbent material variety substantially to other purely carbon-based materials like MWCNTs, fMWCNTs, or graphene. Sorbates like for example PAHs[9] or PCBs[10] typically studied for their sorption to carbon-based sorbent materials can be easily studied with batch experiments as sorption is strong, but column chromatography extends the analyzable sorbate range to less sorbing compounds like heterocyclic organic compounds previously hardly studied in literature as shown in **Chapters 5 and 6**.

Identification of a non-retarded tracer was more challenging than expected as typically used tracers like inorganic anions[11] or THS[1] used in literature as tracers for other materials showed strong sorption to MWCNTs depending on the applied environmental conditions. D_2O was suitable as shown in **Chapter 3,** but the detection requires a refractive index detector (RID), which is today not commonly available in laboratories. Utilizing the findings of **Chapter 4**, also inorganic anions like bromide could potentially be used as tracer applying high ionic strengths to suppress sorption to the sorbent (e.g. MWCNTs). This would enable the application of inorganic anions as non-retarded tracers using more common UV detection available in almost every laboratory. On the one hand, this increases the applicability of the method presented in this thesis as most likely existing equipment can be used without the need for further equipment. On the other hand, application of high ionic strengths limits the opportunity to analyze the influence of the ionic strength on sorption. Furthermore, inorganic anions were retarded differently in the columns as shown in **Chapter 3 and 4**, which indicates that columns containing MWCNTs could be potentially used for separation purposes in ion chromatography, but separations were outside the scope of this thesis.

Full reversibility of sorption to the sorbent materials used within this thesis was shown, which disagrees with others observing hysteresis for sorption to CNMs.[12, 13] Differences may be related to the sorbates studied as hysteresis was observed for larger molecules. Reversibility of sorption and absence of hysteresis indicates that carbon-based materials can potentially act as transport vehicles for environmental contaminants and

influence their distribution. While at high concentrations the availability of contaminants can be decreased by sorption, release of sorbed contaminants by desorption may result in long-term presence of those in the environment. Additionally, when contaminated sorbent materials are transported to previously uncontaminated areas, a contamination of these areas is possible, but the mobility of the materials investigated in this study in the environment cannot be deduced from this thesis and was outside the scope of this thesis.

Advantages of column chromatography could be successfully used to study the influence of environmental conditions on sorption to MWCNTs as shown in **Chapters 4 and 5**. Experiments yielded comparable results to batch experiments from literature regarding the influence of pH[14-16] or ionic strength[17-20] with reduced time and sorbent demand for previously hardly investigated sorbates. Especially, application of the alternative evaluation approach for organic sorbates deriving the sorption isotherm directly from the peak of the sorbate in the chromatogram allows the fast determination of sorption isotherms. By varying column dimensions and sorbent material content inside the column, column chromatography could also be used for the comparison of different sorbent materials comprising weak (e.g. by graphite) to strong sorption (e.g. by AC) (**Chapter 6**) with one experimental approach.

7.2 Outlook

After successful evaluation of the suitability of column chromatography for CNMs and other carbon-based sorbent materials, the variety of sorbates for different sorbent materials of this study can now be widened immediately. Additional ionizable and ionic compounds can be studied for their sorption behavior to different sorbent materials and data regarding the influence of environmental conditions can be generated. In combination with design of experiment approaches, already used in analytical method development,[21] prediction models can be derived allowing the prediction of sorption data for various environmental conditions. Up to now, sorption models used for prediction of sorption data to MWCNTs[22] or AC[23] mainly focus on non-ionic sorbates and are only valid for defined environmental conditions. Thus, these models cannot include changes in sorbate speciation or changes of the sorbent material properties (e.g. surface charge), which may also be changed due to environmental conditions. As electrostatic interactions were shown in literature[14-16] as well as this thesis to influence sorption of organic as well as inorganic compounds, models also covering these influences would be very useful in predicting sorption data in environmental sciences. First approaches dealing with models for organic cations in soils were already mentioned in literature.[24]

Column chromatography should be used more frequently in the future as the necessary equipment used is mainly a classical HPLC system, which is already available in most laboratories today. Additionally, sorption of compounds without chromophores could be analyzed using a mass spectrometer (MS) as detector increasing the detectable compound range. However, measurements using high ionic strengths of the eluent by the addition of sodium chloride or calcium chloride may cause difficulties using MS and other compounds to adjust the ionic strength (e.g. ammonium formiate) must be used and the effect of the changed reagents must be evaluated. Advantages of this technique like for example the high degree of automation make it very useful as research projects require more and more data and an at least partially automated determination of those data would be very useful. It could be implemented as technique for fast screening of sorption properties of newly developed materials or materials with very limited availability. Micro-sized plastic materials, which are relatively close to the sorbent materials of this study, can be an interesting research field in the future as they are of high environmental relevance. These materials are and will be a major issue in environmental sciences as they are thought to potentially impact transport and fate of contaminants in the environment.[25] Consequently, column chromatography could be used to study and model sorption of environmental contaminants to microplastics in the aquatic environment, using only plastic and inert material as packing material. Furthermore, in the terrestrial environment the impact of plastic materials on sorption can also be studied using mixtures of plastic materials and soil as packing materials. First experiments on the influence of plastic materials on contaminant transport in plastic contaminated soils are already started in cooperation with the university of Vienna using knowledge and expertise acquired during this study.[26]

Besides the determination of sorption isotherms and influence of environmental conditions using column chromatography, applications of packed columns using MWCNTs as packing material are possible in analytical chemistry. Applications of MWCNTs were already reported as solid-phase extraction material used for preconcentration and extraction of analytes prior to analysis.[27] The developed packing procedure finally yielded stable columns. In combination with the reversibility of sorption and strong sorption of polar compounds determined for MWCNTs, these columns could be used as precolumns in liquid chromatography measurements. A focusing effect for polar analytes, which are typically hardly retarded in commercially available HPLC columns, using MWCNTs in precolumns at the beginning of chromatographic separations could improve their detectability as the recorded signal is often deteriorated by peak broadening. Here, the applicability and stability

of the packed columns needs to be evaluated as the packing materials might behave differently using organic solvents instead of fully aqueous eluents.

7.3 References

1. Bi, E.; Schmidt, T. C.; Haderlein, S. B. Sorption of heterocyclic organic compounds to reference soils: Column studies for process identification. *Environmental Science & Technology* **2006,** 40 (19), 5962-5970.
2. Bi, E.; Schmidt, T. C.; Haderlein, S. B. Environmental factors influencing sorption of heterocyclic aromatic compounds to soil. *Environmental Science & Technology* **2007,** 41 (9), 3172-3178.
3. Schenzel, J.; Goss, K. U.; Schwarzenbach, R. P.; Bucheli, T. D.; Droge, S. T. J. Experimentally determined soil organic matter-water sorption coefficients for different classes of natural toxins and comparison with estimated numbers. *Environmental Science & Technology* **2012,** 46 (11), 6118-6126.
4. Droge, S.; Goss, K. U. Effect of sodium and calcium cations on the ion-exchange affinity of organic cations for soil organic matter. *Environmental Science & Technology* **2012,** 46 (11), 5894-5901.
5. Li, B. H.; Qian, Y. A.; Bi, E. P.; Chen, H. H.; Schmidt, T. C. Sorption behavior of phthalic acid esters on reference soils evaluated by soil column chromatography. *Clean-Soil Air Water* **2010,** 38 (5-6), 425-429.
6. Qian, Y. Sorption of hydrophobic organic compounds (HOCs) to inorganic surfaces in aqueous solutions. Ph.D. disserstation, University Duisburg-Essen, Essen, Germany, 2010.
7. Mader, B. T.; Goss, K. U.; Eisenreich, S. J. Sorption of nonionic, hydrophobic organic chemicals to mineral surfaces. *Environmental Science & Technology* **1997,** 31 (4), 1079-1086.
8. Bucheli, T. D.; Gustafsson, O. Soot sorption of non-ortho and ortho substituted PCBs. *Chemosphere* **2003,** 53 (5), 515-522.
9. Kah, M.; Zhang, X. R.; Hofmann, T. Sorption behavior of carbon nanotubes: Changes induced by functionalization, sonication and natural organic matter. *Science of the Total Environment* **2014,** 497, 133-138.
10. Velzeboer, I.; Kwadijk, C.; Koelmans, A. A. Strong sorption of PCBs to nanoplastics, microplastics, carbon nanotubes, and fullerenes. *Environmental Science & Technology* **2014,** 48 (9), 4869-4876.
11. Das, B. S.; Lee, L. S.; Rao, P. S. C.; Hultgren, R. P. Sorption and degradation of steroid hormones in soils during transport: Column studies and model evaluation. *Environmental Science & Technology* **2004,** 38 (5), 1460-1470.
12. Wu, W. H.; Jiang, W.; Zhang, W. D.; Lin, D. H.; Yang, K. Influence of functional groups on desorption of organic compounds from carbon nanotubes into water: Insight into desorption hysteresis. *Environmental Science & Technology* **2013,** 47 (15), 8373-8382.
13. Wang, Z. Y.; Yu, X. D.; Pan, B.; Xing, B. S. Norfloxacin sorption and its thermodynamics on surface-modified carbon nanotubes. *Environmental Science & Technology* **2010,** 44 (3), 978-984.
14. Zhang, S. J.; Shao, T.; Bekaroglu, S. S. K.; Karanfil, T. Adsorption of synthetic organic chemicals by carbon nanotubes: Effects of background solution chemistry. *Water Research* **2010,** 44 (6), 2067-2074.
15. Yang, K.; Wu, W. H.; Jing, Q. F.; Zhu, L. Z. Aqueous adsorption of aniline, phenol, and their substitutes by multi-walled carbon nanotubes. *Environmental Science & Technology* **2008,** 42 (21), 7931-7936.

16. Zong, E. M.; Wei, D.; Huan, Z. K.; Peng, D.; Wan, H. Q.; Zheng, S. R.; Xu, Z. Y. Adsorption of phosphate by zirconia functionalized multi-walled carbon nanotubes. *Chinese Journal of Inorganic Chemistry* **2013,** 29 (5), 965-972.
17. Hu, J. L.; Tong, Z. L.; Hu, Z. H.; Chen, G. W.; Chen, T. H. Adsorption of roxarsone from aqueous solution by multi-walled carbon nanotubes. *Journal of Colloid and Interface Science* **2012,** 377, 355-361.
18. Ding, H.; Li, X.; Wang, J.; Zhang, X. J.; Chen, C. Adsorption of chlorophenols from aqueous solutions by pristine and surface functionalized single-walled carbon nanotubes. *Journal of Environmental Sciences* **2016,** 43, 187-198.
19. Fang, Q. L.; Chen, B. L. Adsorption of perchlorate onto raw and oxidized carbon nanotubes in aqueous solution. *Carbon* **2012,** 50 (6), 2209-2219.
20. Ansari, M.; Kazemipour, M.; Dehghani, M. The defluoridation of drinking water using multi-walled carbon nanotubes. *Journal of Fluorine Chemistry* **2011,** 132 (8), 516-520.
21. Hüffer, T.; Osorio, X. L.; Jochmann, M. A.; Schilling, B.; Schmidt, T. C. Multi-walled carbon nanotubes as sorptive material for solventless in-tube microextraction (ITEX2) - a factorial design study. *Analytical and Bioanalytical Chemistry* **2013,** 405 (26), 8387-8395.
22. Hüffer, T.; Endo, S.; Metzelder, F.; Schroth, S.; Schmidt, T. C. Prediction of sorption of aromatic and aliphatic organic compounds by carbon nanotubes using poly-parameter linear free-energy relationships. *Water Research* **2014,** 59, 295-303.
23. Shih, Y. H.; Gschwend, P. M. Evaluating activated carbon-water sorption coefficients of organic compounds using a linear solvation energy relationship approach and sorbate chemical activities. *Environmental Science & Technology* **2009,** 43 (3), 851-857.
24. Droge, S. T. J.; Goss, K. U. Development and evaluation of a new sorption model for organic cations in soil: Contributions from organic matter and clay minerals. *Environmental Science & Technology* **2013,** 47 (24), 14233-14241.
25. Rochman, C. M.; Manzano, C.; Hentschel, B. T.; Simonich, S. L. M.; Hoh, E. Polystyrene plastic: A source and sink for polycyclic aromatic hydrocarbons in the marine environment. *Environmental Science & Technology* **2013,** 47 (24), 13976-13984.
26. Hüffer, T.; Slawek, S.; Metzelder, F.; Sigmund, G.; Schmidt, T. C.; Hofmann, T., Einfluss von Polyethylen Mikroplastik auf den Transport organischer Schadstoffe. In *Wasser 2018 - Jahrestagung der Wasserchemischen Gesellschaft*, Papenburg, 2018.
27. Ma, J. P.; Lu, X.; Xia, Y.; Yan, F. L. Determination of pyrazole and pyrrole pesticides in environmental water samples by solid-phase extraction using multi-walled carbon nanotubes as adsorbent coupled with high-performance liquid chromatography. *Journal of Chromatographic Science* **2015,** 53 (2), 380-384.

Chapter 8 - Appendix

8.1 List of figures

8.2 List of tables

8.3 List of abbreviations and symbols

AC	activated carbon
BET	Brunauer-Emmett-Teller
Br^-	bromide
c_0	initial concentration of the sorbate
C_{60}	fullerenes
$c_{a,eq}$	concentration of the sorbate in the gaseous phase
$CaCl_2$	calcium chloride
ClO_4^-	perchlorate
CNMs	carbon nanomaterials
CNTs	carbon nanotubes
c_{sat}	saturation concetration of the compound in water
$c_{s,eq}$	solid phase concentration of the sorbate in equilibrium
$c_{w,eq}$	aqueous phase concentration of the sorbate in equilibrium
CVD	chemical vapor deposition
D_2O	heavy water
DAD	diode-array detector
DWCNTs	doublewalled carbon nanotubes
F^-	fluoride
fMWCNTs	functionalized multiwalled carbon nanotubes
GC	gas chromatography
H_2O	water
HCl	hydrochloric acid
HPLC	high performance liquid chromatography
I^-	iodide
ICP-MS	inductively coupled plasma mass spectrometry
KCl	potassium iodide
K_d	distribution coefficient
K_f	Freundlich coefficient
K_H	Henry constant
K_{HW}	hexadecane / water distribution coefficient
K_L	Langmuir affinity
K_{ow}	octanol / water distribution coefficient
m_0	initial mass of the sorbate
m_a	mass of the sorbate in the gaseous phase
$m_{col,equip}$	mass of the supplementary equipment of the column (sieves, …)
$m_{col,tot}$	mass of the column filled with packing material and water
m_s	sorbed mass of the sorbate
MS	mass spectrometry
$m_{sorbent}$	mass of sorbent
m_{water}	mass of water inside the column
MWCNTs	multiwalled carbon nanotubes
n	Freundlich exponent
NaBr	sodium bromide
NaCl	sodium chloride
NaI	sodium iodide
$NaNO_2$	sodium nitrite
$NaNO_3$	sodium nitrate
NO_2^-	nitrite
NO_3^-	nitrate

NaOH	sodium hydroxide
NOM	natural organic matter
PAHs	polycyclic aromatic hydrocarbons
PCBs	polychlorinated biphenyls
pH_{pzc}	pH value with a neutral surface charge of a sorbent
pK_s	logarithmic acidity constant
PO_4^{3-}	phosphate
ppLFERs	polyparameter linear free-energy relationships
PTFE	polytetrafluoroethylene
Q_{max}	maximum sorption capacity
R	retardation factor
R^2	correlation coefficient
R_{const}	universal gas constant
RID	refractive index detector
SA	surface area
SWCNTs	singlewalled carbon nanotubes
T	temperature
t_0	retention time of the tracer with column
$t_{0,sorb}$	retention time of the sorbate without column
$t_{0,tracer}$	retention time of the tracer without column
t´	retention time of tracer and sorbate without column
$t_{R,sorb}$	retention time of the sorbate with column
$t_{R,tracer}$	retention time of the tracer with column
$t_{R,wc}$	retention time of the tracer with column
$t_{R,woc}$	retention time of the tracer without column
THS	thiourea
t_R	retention time of the sorbate with column
UV	ultraviolett
UVD	UV-detector
v*	flow rate of the eluent
V_a	volume of the gaseous phase
vdW	van-der-Waals
V_w	volume of the water phase
WP	work package
XPS	x-ray photoelectron spectroscopy
θ	porosity
ρ_b	bulk density
ΔH	enthalpy change
ΔS	entropy change
λ_{max}	maximum absorption wavelength

8.4 List of publications

Publications in peer-reviewed journals

Hüffer, T.; Endo, S.; Metzelder, F.; Schroth, S.; Schmidt, T.C. Prediction of sorption of aromatic and aliphatic organic compounds by carbon nanotubes using poly-parameter linear free-energy relationships. *Water Research*, **2014**, 59, 295 – 303.

Metzelder, F.; Schmidt, T.C. Environmental conditions influencing sorption of inorganic anions to multiwalled carbon nanotubes studied by column chromatography. *Environmental Science & Technology*, **2017**, 51 (9), 2928 – 2935.

Metzelder, F.; Funck, M.; Schmidt, T.C. Sorption of heterocyclic organic compounds to multiwalled carbon nanotubes. *Environmental Science & Technology*, **2018**, 52 (9), 628 – 637.

Metzelder, F.; Funck, M.; Hüffer, T.; Schmidt, T.C. Comparison of sorption to carbon-based materials and nanomaterials using inverse liquid chromatography. *Environmental Science & Technology*, **2018**, submitted.

Publications in non-peer-reviewed journals

Metzelder, F.; Funck, M.; Schmidt, T.C. Untersuchung der Sorption an Kohlenstoffnanomaterialien mittels inverser Flüssigkeitschromatographie. Mitteilungen der Fachgruppe Umweltchemie und Ökotoxikologie, **2018**, 1, 6 – 9.

Oral presentations

Metzelder, F.; Schmidt, T.C. Characterization of sorption properties of carbon nanomaterials (CNM) using packed columns and inverse liquid chromatography. *Workshop: Innovations around adsorption*, **2016**, 14. June 2016, Duisburg, Germany.

Metzelder, F.; Schmidt, T.C. Sorption of organic and inorganic compounds to carbon nanomaterials studied using inverse liquid chromatography. *Neujahrskolloquium der Fakultät Chemie der Universität Duisburg-Essen*, **2018**, 10. January 2018, Essen, Germany.

Poster presentations

Metzelder, F.; Schmidt, T.C. Charakterisierung der Sorptionseigenschaften von Kohlenstoffnanomaterialien mittels gepackter Säulen und inverser Flüssigkeitschromatographie. *Jahrestagung der Wasserschemischen Gesellschaft*, **2015**, 11. – 13. May 2015, Schwerin, Germany.

Metzelder, F.; Schmidt, T.C. Characterization of sorption properties of carbon nanomaterials (CNM) using packed columns and inverse liquid chromatography. *10th International Conference on the Environmental Effects of Nanoparticles and Nanomaterials*, **2015**, 6. – 10. September, Vienna, Austria.

Metzelder, F.; Schmidt, T.C. Charakterisierung der Sorptionseigenschaften von Kohlenstoffnanomaterialien mittels gepackter Säulen und inverser Flüssigkeitschromatographie. Phase 2: Untersuchung des Einflusses von Umweltbedingungen. *Jahrestagung der Wasserschemischen Gesellschaft*, **2016**, 2. – 4. Mai 2016, Bamberg, Germany.

Metzelder, F.; Schmidt, T.C. Kohlenstoffnanoröhren zur chromatographischen Trennung anorganischer Anionen – Konzeptionelle Untersuchung des Materials. *2. Wasseranalytisches Seminar (MWAS)*, **2016**, 14. – 15. September 2016, Mülheim, Germany.

Metzelder, F.; Funck, M.; Schmidt, T.C. Charakterisierung der Sorptionseigenschaften von Kohlenstoffnanomaterialien mittels gepackter Säulen und inverser Flüssigkeitschromatographie. *Jahrestagung der Wasserschemischen Gesellschaft*, **2017**, 22. – 24. Mai 2017, Donaueschingen, Germany.

8.5 Curriculum Vitae

Der Lebenslauf ist in der Online-Version aus Gründen des Datenschutzes nicht enthalten.

8.6 Erklärung

Hiermit versichere ich, dass ich die vorliegende Arbeit mit dem Titel

„Investigation of sorption properties of carbon nanomaterials using packed columns and inverse liquid chromatography"

selbst verfasst, keine außer den angegebenen Hilfsmitteln und Quellen benutzt habe, alle wörtlich oder inhaltlich übernommenen Stellen als solche gekennzeichnet sind und die Arbeit in dieser oder ähnlicher Form noch bei keiner anderen Universität eingereicht wurde.

Essen, im April 2018

_____
Florian Metzelder